University of Southampton

Palynology, palynofacies and hydrocarbon potential of the Cretaceous rocks of northern Egypt

By

Amr Said Deaf

This thesis is submitted for Doctor of Philosophy

Faculty of Engineering, Science and Mathematics
School of Ocean and Earth Sciences

December 2009

UNIVERSITY OF SOUTHAMPTON

ABSTRACT

FACULTY OF ENGINEERING, SCIENCE AND MATHEMATICS

SCHOOL OF OCEAN AND EARTH SCIENCES

Doctor of Philosophy

Palynology, Palynofacies and Hydrocarbon Potential of the Cretaceous Rocks of Northern Egypt

By Amr Deaf

Recent hydrocarbon exploration in the Egyptian northern Western Desert and the Gulf of Suez have revealed relatively rich hydrocarbon accumulations, mainly of gas, and demonstrates promising future prospects. In order to improve our understanding of these areas and to provide a biostratigraphic framework for the poorly-dated Lower Cretaceous successions palynological analyses were carried out on 134 ditch cutting samples from the Abu Tunis 1x drilled in the northern Western Desert, and 78 samples from the BB80-1 borehole in the Gulf of Suez area.

Palynostratigraphic investigations focussed on the lower parts of the borehole successions as earlier studies have largely ignored these Cretaceous sediments. A central objective was therefore to construct a biostratigraphic scheme, for both boreholes. Analysis of the Abu Tunis 1x samples enabled the identification of eight palynozones largely defined by first occurrences of spores, gymnosperm and angiosperm pollen and dinoflagellate cysts. Three new palynostratigraphically defined age divisions are described for the lower part of the Abu Tunis 1x succession, and a more refined biostratigraphy is made for the upper part of the sequence. In contrast, the Gulf of Suez BB80-1 borehole samples proved palynologically lean and provided less information for age dating. It was only possible to define two palynozones of lower age-resolution than that for Abu Tunis 1x. Spore and pollen grains recovered from both boreholes show characteristics of the Cretaceous Phytogeographic Provinces of northern Africa-northern South America. Sporomorphs of the pre-Albian *Dicheiropollis/Afropollis* Province were recognised from the lower part of the Abu Tunis 1x borehole and sporomorphs characteristic of Albian-Cenomanian Elaterate Province identified from both. No

spore and pollen grains of the Senonian Palmae Province have been recognised due to the complete marine nature of the early Santonian sediments of the Abu Tunis 1x borehole.

In order to understand the palaeoenvironmental conditions prevailing in the two boreholes during the deposition of the clastic and carbonate sediments, quantitative palynological data was combined with geophysical wireline data and cuttings lithologies. The quantitative distribution of certain terrestrial palynomorphs with known botanical affinities and palaeoenvironmental significance have been used as proxy indicators for identifying palaeoclimatic and palaeoceanographic conditions in both borehole regions.

In general, the lower part of the Abu Tunis 1x succession (consisting of shale and sandstones) was deposited in deltaic settings during a regressive cycle with sediments of the upper Alam El Buieb Formation and the Alamein Formation representing the late Barremian-Aptian transgression cycle, during which shallow marine settings prevailed. Clastics of the Dahab and Kharita formations represent another regression in marine sedimentation, where fine silts and a few shale horizons of the latter formations were deposited in a delta channel system that prograded through time over prodelta sediments as a response to sea level fall. Mixed clastic and carbonate sediments of the upper Kharita and lower Bahariya represent more distal marine deposition as a response to a second minor rise in sea level, where a partially marine isolated, brackish lagoonal depositional system developed that was subjected to occasional marine incursions. Integration of the same datasets demonstrate that the upper carbonate-dominated part of the Abu Tunis 1x succession (the upper Bahariya, Abu Roash, and Khoman B formations) was deposited mainly in deeper marine settings interpreted as outer shallow marine, during a major transgressive cycle. The upper part of the BB80-1 borehole also shows this late Cretaceous marine transgression, represented by high concentrations of phytoplankton-rich carbonate sequences. The lower part of this Gulf of Suez sequence is of latest early Cretaceous age, and appears to have been deposited in a continental basin, far from source vegetation, possibly in alluvial settings, which witnessed occasional marine incursions represented by deposition of a few organic-rich marine shale intercalations that are interpreted as shallow

marginal marine in origin. These environmental fluctuations are related to global sea level fluctuations and global tectonic processes, such as the breakup of Western Gondwana during the opening of the Southern Atlantic Ocean.

Investigation of the hydrocarbon potential of the Abu Tunis 1x and BB8-1 shows that the first borehole has source rock potential, with the second of no potential due to its organic-poor lithology. The lower part of the Abu Tunis 1x borehole represented by the Alam El Bueib Formation sediments is regarded as a non commercial gas-prone source rock; this is indicated from visual kerogen study and vitrinite reflectance investigations of its thermal maturation. A burial history reconstruction for the Abu Tunis 1x borehole sequence indicates that the lower part of the Alam El Bueib source rock entered the early stage of thermal maturation during the Oligocene and is currently at the early mature stage. By investigating the organic matter quality and conducting maturity analyses such as vitrinite reflectance studies, the overlying clastics of the Dahab, Kharita and lower Bahariya, and the carbonates of the upper Bahariya, Abu Roash and Khoman formations are shown also to contain relatively high amounts of oil-prone organic matter, but it is immature, and thus they are not active source rocks in the region of the Abu Tunis 1x borehole. The BB80-1 borehole is made of a thick organic-poor, porous sandstone unit of the Malha and lower Raha formations that are intercalated by a few organic-rich shale horizons. This sandstone lithology is regarded as having no hydrocarbon potential.

ACKNOWLEDGEMENTS

All gratitude is due to almighty **ALLAH** who guided me to bring-forth this thesis to light. I am greatly indebted to Dr. **Ian C. Harding** and Prof. **John Marshall** for their supervision, guidance, valuable discussions, encouragement, and sincere support in addition to critically revising the manuscript of the present work. The author wishes to thank the Egyptian General Petroleum Corporation Authorities namely, Exploration Manager and the Geologists for providing well logs and samples of the Abu Tunis 1x borehole and to also thanks my friend Dr. Maher I. El-Sougheir for providing the samples and well log of the second borehole BB80-1 used in this work. I would like to thank Shir Akbari for his endless supports in the laboratory.

A special word of gratitude and thanks are due to the Egyptian authority represented by the **Ministry of Higher Education** and my institute the **Geology Department**, **Faculty of Science**, **Assiut University** for granting me the current PhD scholarship.

Finally I would like to give special thanks to my mother and all my family for their unfailing support and encouragement during my study.

GRADUATE SCHOOL OF THE SOUTHAMPTON OCEANOGRAPHY

This PhD dissertation by

Amr Said Deaf

has been produced under the supervision of the following persons;

Supervisor/s

Dr. Ian C. Harding

Prof. John Marshall

Chair of Advisory Panel

Prof. Alan Kemp

DECLARATION

This thesis is the result of work done wholly while under registered postgraduate candidature.

CONTENTS

LIST OF FIGURES

LIST OF TABLES

INTRODUCTION

1.1 Background and aims

Recently, significant new hydrocarbon discoveries have been documented in the northern Western Desert of Egypt, the second most important oil-producing area in Egypt. Natural gases comprise the largest constituent of these hydrocarbons. During 2005, Egyptian gas production was about 4,870 thousand cubic feet/day (mcf/d) with a proven gas reserve of 62 trillion cubic feet (tcf) and a probable future rise up to 120 tcf (Ford, 2005), making the northern Western Desert the major gas province in Egyptian territory. The Cretaceous and Jurassic sandstone reservoirs have proved to be the most prolific gas and oil producing horizons in the Western Desert, where large reserves of gas and condensates have been found (APS Review Oil Market Trends, 2006). Therefore, in addition to the known basal Bahariya oil producing horizon (middle Cretaceous), the lower part of the lower Cretaceous succession (Neocomian-Barremian) has recently been considered as the new target for oil and gas explorations. The Western Desert is therefore considered to be the future of the Egyptian gas and oil industry. However, the sediments of this geological interval (i.e. lower Cretaceous) have not been subject to detailed biostratigraphic study or lithostratigraphic correlation. Even the basic separation of the different time-rock units is poorly known, as all operating companies have described this part of the succession on their logs with the term “no information”. The operators are now looking to carry out large-scale and detailed biostratigraphic and lithostratigraphic correlations.

The Gulf of Suez region is regarded as the first major oil-producing area in Egypt, where the upper Cretaceous (Campanian-Maastrichtian) and the Miocene oil-producing horizons (Vanderbeek, 1994) have been the subject of the majority of the

geological investigations. However, the Nubian Sandstone reservoir in the Gulf of Suez Basin, ranging in age from Cambrian to early Cretaceous has been less studied stratigraphically (Schütz, 1994), despite the fact that the lower Cretaceous "Nubia A" unit represents one of the important oil-producing horizons. Accordingly, integrated analyses are also needed of the lower Cretaceous subsurface succession in the Gulf of Suez area, which possesses a more complex geological structure than the northern Western Desert. This PhD project therefore seeks to complete applied micropalaeontological investigations of borehole successions from these two regions which will provide a significant contribution to these problems. This project aims to:

1. Integrate lithostratigraphic and biostratigraphic schemes for the two studied boreholes.
2. Provide independent age control for the studied intervals by means of other micropalaeontological studies, such as the fossil nannoplankton, especially for the upper Cretaceous succession (mainly carbonate).
3. Produce micropalaeontologically defined palaeoenvironmental interpretations of individual subsurface lithostratigraphic units.
4. Correlate both biostratigraphic and palaeoenvironmental results with those in other palaeogeographically related areas, such as the African and South American (ASA) phytogeoprovince for spore and pollen grains, and the Tethyan Realm for the dinoflagellate cysts.
5. Complete a taxonomic study for all of the recorded taxa, with emphasis on the regional and global stratigraphic distribution of stratigraphically significant forms.
6. Reconstruct the burial history of the boreholes and determine the hydrocarbon potential of the subsurface units investigated.

1.2 Objectives

In order to achieve the aims of this project the following analyses and investigations were carried out:

1. Standard acid maceration palynological preparation techniques were applied to selected samples in order to extract palynomorphs (i.e. spores, pollen grains, dinoflagellate cysts, microforaminiferal test linings, etc.) for systematic, biostratigraphic and other investigations.
2. Taxonomic identification and analysis of the vertical distribution of the palynomorphs recovered from the two boreholes was undertaken in order to establish a biostratigraphy for each of the two borehole successions.
3. The chronostratigraphic units which have been proposed by the original operating company have been revised, and age determination for the undifferentiated parts of the successions using the palynological investigations has been conducted.
4. The palaeoenvironmental and palaeoclimatic settings prevailing during the deposition of the studied sections have been determined, through study of the palynomorphs and palynofacies analyses.
5. Source rock analyses (i.e. TOC analysis) have been used to determine source rocks potential for hydrocarbon generation, in addition to the determination of the different kerogen types in order to evaluate the hydrocarbon potential and quality of source rocks.
6. Thermal maturity of the studied sequence has been deduced by using both qualitative spore colour analysis and vitrinite reflectivity, followed by reconstruction of the burial history using BasinModTM software.

1.3 Study area

The material selected for this project was collected from two different and distinct geologic areas: namely the Western Desert of Egypt (the Abu Tunis 1x borehole) and the offshore Gulf of Suez (the BB 80-1 borehole), from which subsurface Cretaceous samples have been taken from the boreholes, respectively (Fig. 1.1).

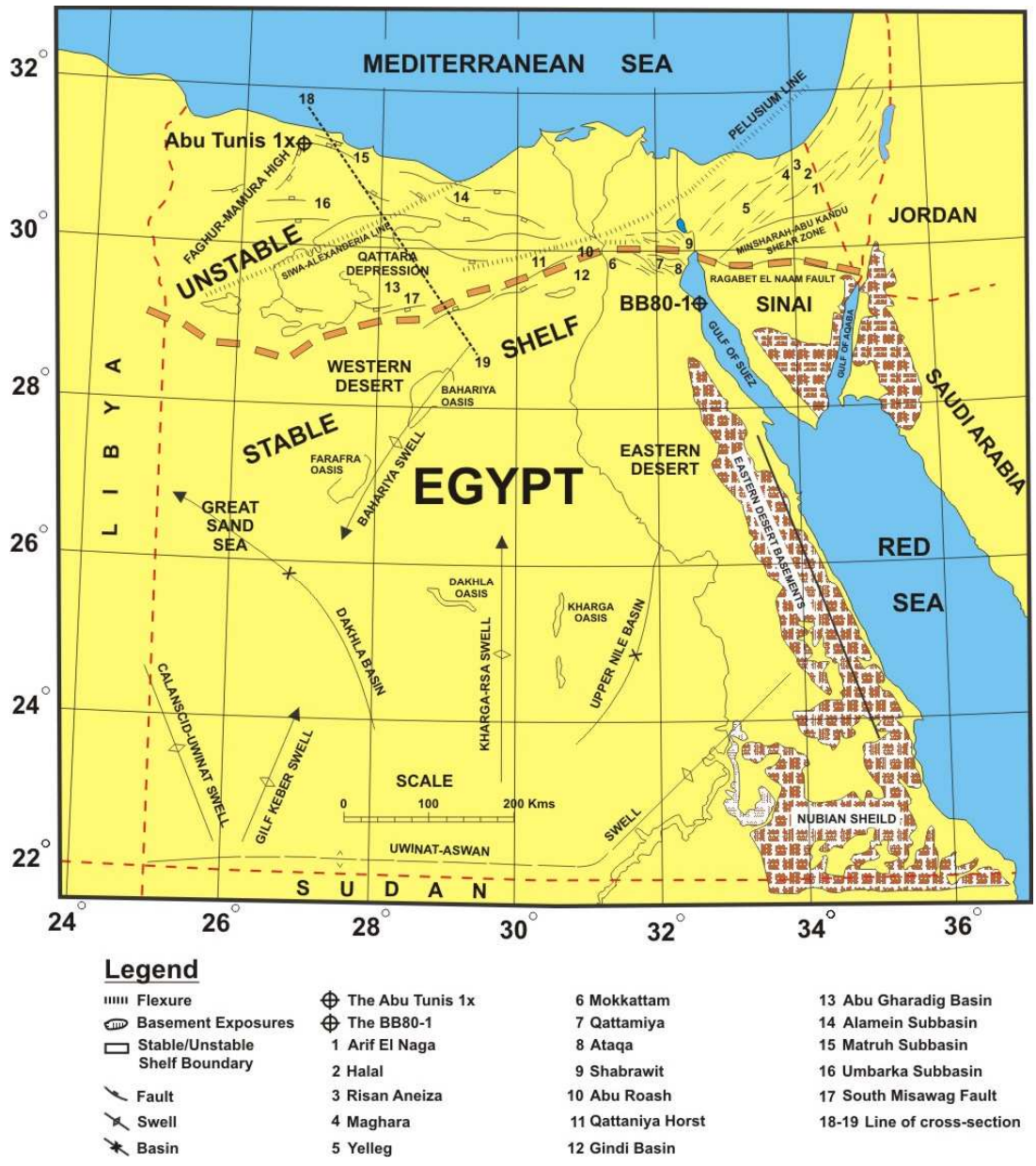

Figure 1.1 Structural map of Egypt showing the boundary between the Stable and Unstable Shelves, and distribution of different Mesozoic tectonic elements (after Kerdany & Cherif, 1990).

1.3.1 Geological setting and tectonic evolution

Said (1962) divided the Egyptian continental mass into two main provinces. The Stable Shelf is represented by the southern Western Desert bordering the Nubian Shield, the Eastern Desert as far as the northern eastern margin of the South Galala Plateau, and southern Sinai (Fig. 1.1). The Unstable Shelf lies to the north of the Stable Shelf with a Western Subprovince (i.e. the northern Western Desert), an Eastern Subprovince (i.e. northern Sinai), and the northern Eastern Desert as a transitional zone between the Eastern and Western Subprovinces. The northern Gulf of Suez, bordered at its southernmost boundary by the SE-facing Wadi Araba Monocline to the northeast of the South Galala Plateau (Fig. 1.3), also belongs to the Unstable Shelf (Patton et al., 1994; Moustafa & Khalil, 1995).

The Egyptian northern Western Desert area is characterized by a simple featureless surface, despite its intricate subsurface structures. This northern part of the African Platform (Fig. 1.1) is made up of a thick sedimentary sequence, gently sloping seaward, and encounters rocks ranging in age from Cambrian to Recent (Fig. 1.2). The sequence reaches its maximum thickness in the Abu Gharadig Basin (8-9 km deep), while to the north it may reach only 3 to 6 km (Hantar, 1990).

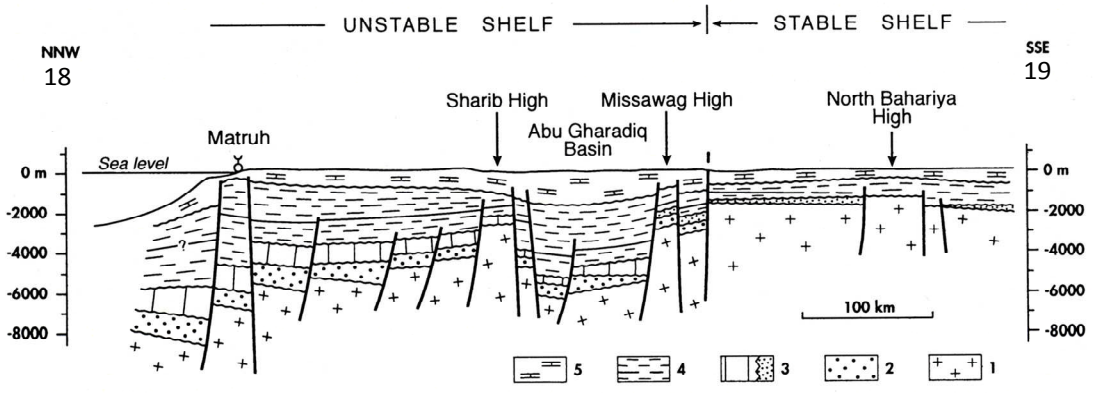

Figure 1.2 Generalized geological cross-section across the northern Western Desert of Egypt. 1. Pan-African basement, 2. Paleozoic, 3. Jurassic, 4. Cretaceous, 5. Cenozoic (after Guiraud & Bosworth, 1999). See Fig. 1.1 for section location (18-19).

In contrast, the Gulf of Suez region is one of the most structurally complex areas in the world (Fig. 1.3), with different parts of the region having very different geological histories. The relationship of different fault blocks and their associated sedimentary successions are variable (Fig. 1.4); consequently, no one area in the Gulf can be representative of stratigraphy or the structure of the whole Gulf of Suez domain (Said, 1962).

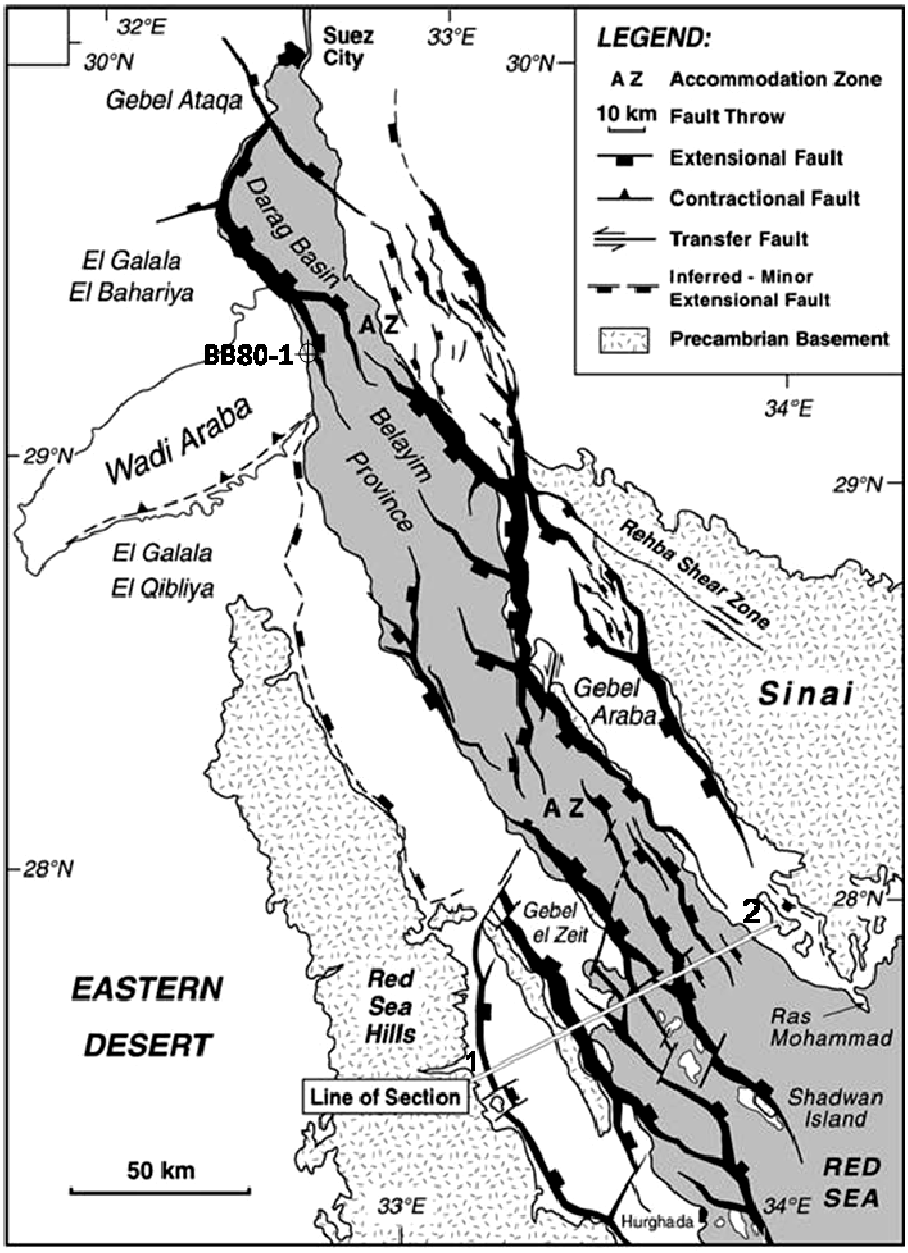

Figure 1.3. Structural map of the Gulf of Suez region showing the main basement faults, with line width proportional to throw (after Khalil, 1998; Bosworth & McClay, 2001).

The Gulf of Suez is an intra-cratonic basin oriented in a northwest-southeast direction, spanning about 300 km in length, and ranging in width from about 50 km at its northern part to 90 km at its southern part (Fig. 1.3). The Gulf of Suez extends between latitude 27° N to 30° N and lies nearly between longitude 32° 15′ E to 34° 15′ E (Said, 1962; Bosworth & McClay, 2001). The Gulf of Suez is bounded by a zigzag fault system (Fig. 1.3) with N-S, NNE-SSW, E-W and NW-SE orientations (e.g. Jarrige et al., 1986; Meshref, 1990; Moustafa, 1993; Patton et al., 1994; McClay et al., 1998; Bosworth & McClay, 2001). The Gulf of Suez Basin is structurally divided into three large asymmetric half-graben sub-basins, generally bordered by a NW-SE fault system: the Abu Darag Basin in the north, the Belayim Province in the centre, and the Amal-Zeit Province in the south (Fig. 1.3). These three sub-basins are linked together by a complex strike-slip fault system (i.e. accommodation zones), and within each sub-basin the stratal dips show alternating patterns of NE dip in the central basin and SW dip in the northern and southern basins (Moustafa, 1976; Bosworth, 1985; Coffield & Schamel, 1989).

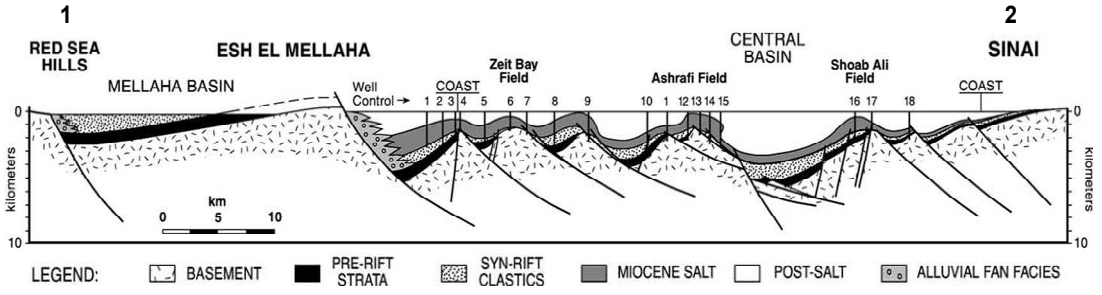

Figure 1.4. Section across the southern Gulf of Suez, illustrating rotated faulted block geometry (after Bosworth, 1994). See Fig. 1.3 for section location.

During the Mesozoic, Egypt was part of the northern African plate, which was affected by three main regional tectonic events. The first event was during the mid Jurassic, as the Apulian "Turkish" microplate separated from the Egyptian continental mass, rifting northward (Fig. 1.5). This was related to the formation of the Neotethyan Ocean and the closure of the Palaeotethyan Ocean by the mid Jurassic.

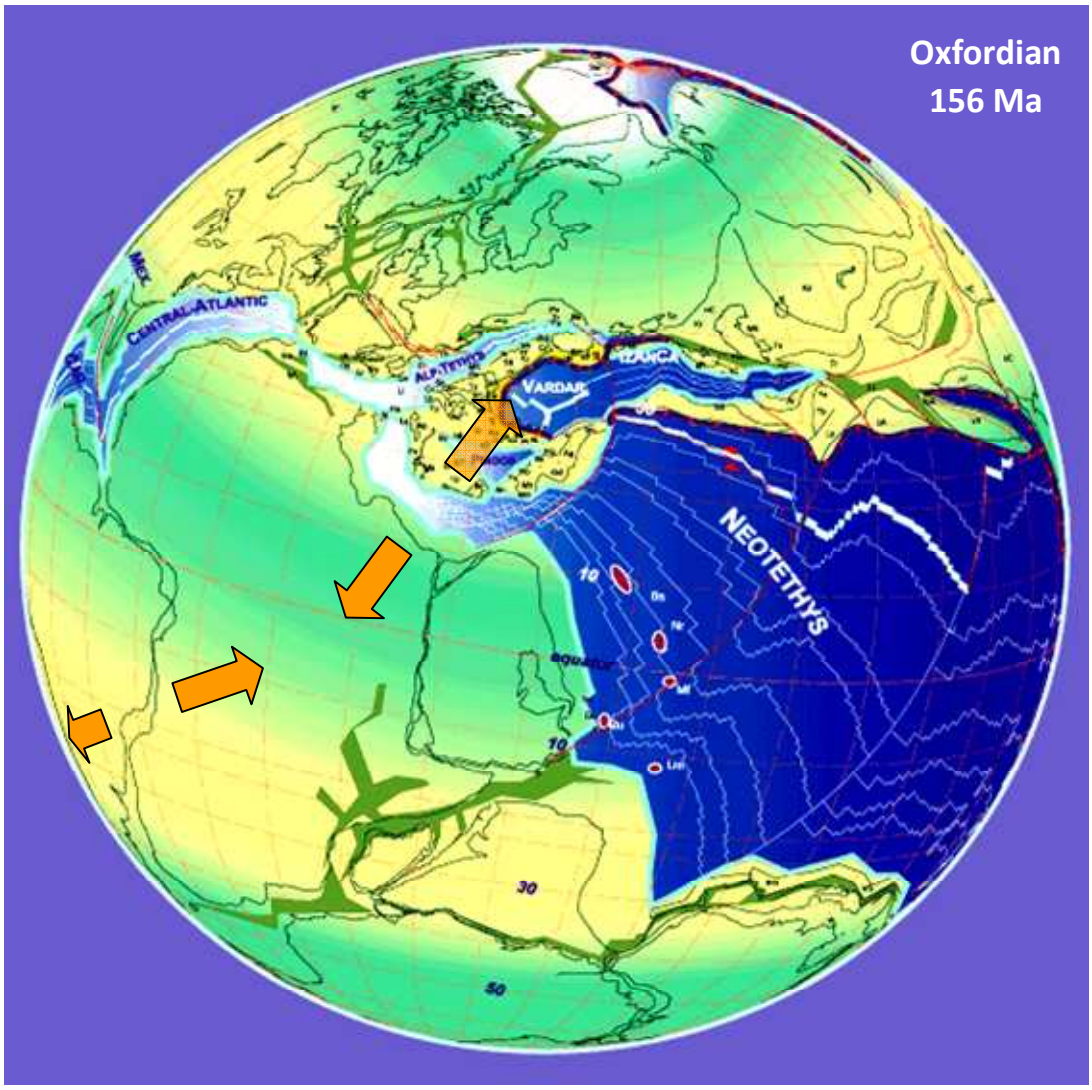

Figure 1.5. Reconstruction of the late Jurassic break-up of western Gondwana and evolution of the Neotethys (after Stampfli & Borel, 2002).

At the same time, the African plate was also moving eastward with respect to the European plate as the Atlantic Ocean opened (Kerdany & Cherif, 1990, Bumby & Guiraud, 2005). The second important tectonic event occurred during the late Cretaceous-early Tertiary (Fig. 1.6), when the northern African plate moved towards Europe, producing compressional stresses which resulted in a series of ENE-WSW folds (Syrian Arc System) and faults (Hantar, 1990; Guiraud & Bosworth, 1997; Bumby & Guiraud, 2005; Guiraud et al., 2005).

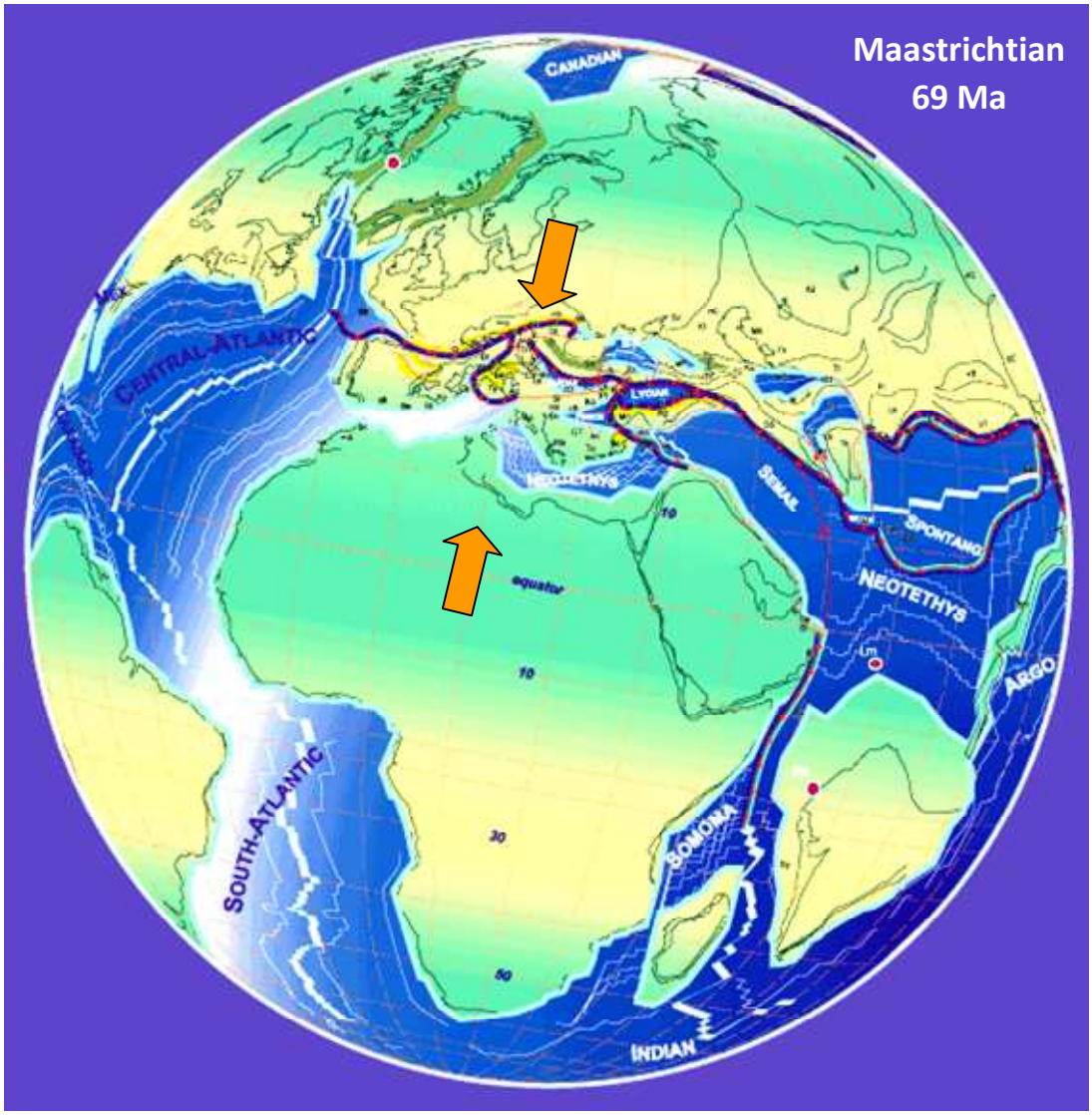

Figure 1.6. Reconstruction of the late Cretaceous break-up of Gondwana, evolution of the Neotethys and closure of the Palaeotethys (after Stampfli & Borel, 2002).

1.3.2 Structural and stratigraphic history

Mesozoic rocks outcrop in southern Egypt and in northern Sinai (Fig. 1.7) where an almost complete sequence from the Triassic to the Cretaceous has been described (Kerdany & Cherif, 1990). However, in the northern Western Desert Mesozoic rocks are buried beneath younger Neogene sediments (Fig. 1.7), and are only known from the subsurface (Kerdany & Cherif, 1990).

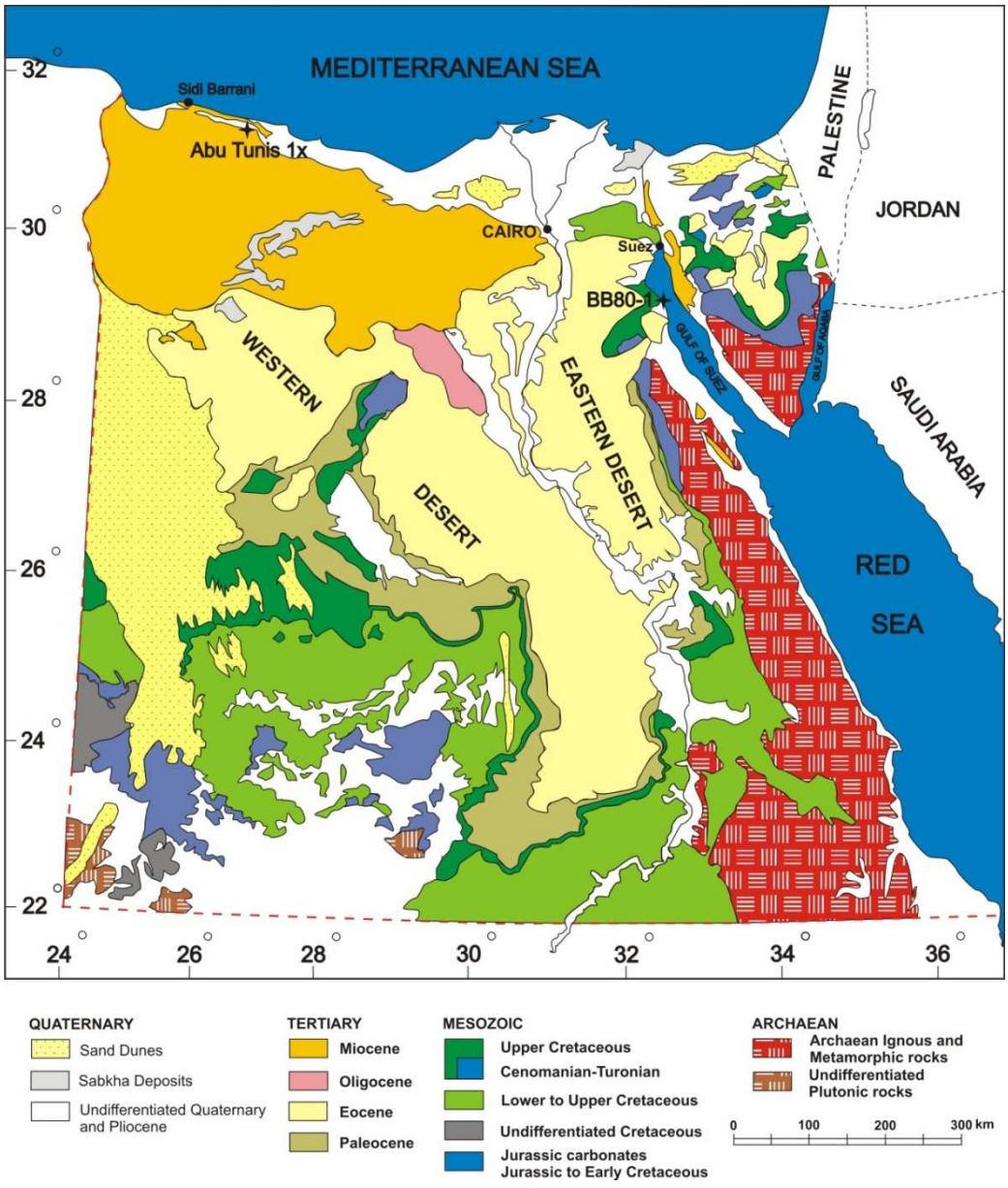

Figure 1.7. Geological map of Egypt showing the distribution of sedimentary (Mesozoic and Cenozoic) and igneous rocks (after Egyptian Geological Survey, 1991).

Mesozoic rocks are poorly exposed in the Gulf of Suez region. However there are rare exposures, on the western coast: the Permo-Triassic rocks at the Abu Darag area, the Jurassic rocks of the North Galala Plateau, and the Cretaceous rocks of the Gebel Shabrawet and the South Galala Plateau. Mesozoic rocks are also found on the eastern coast: the Cretaceous rocks of Wadi Sudr. Work on exposures on the eastern side of the Gulf of Suez (e.g. Khalil & McClay, 1998) together with the offshore Gulf of Suez boreholes (e.g. Moustafa & Khalil, 1995) has enabled a complete composite stratigraphic sequence of Mesozoic rocks to be established.

The late Jurassic-early Cretaceous eastward movement of the African plate along sinistral strike-slip faults - as a result of the opening of the Atlantic Ocean - resulted in two main tectonic structures in the northern Western Desert: WNW folding associated with thrusting, and ENE trending strike-slip faults with left lateral movement (Meshref, 1990). At the same time Neotethyan rifting and the development of the eastern and southern margins of the Mediterranean Sea resulted in faulting and uplifting with a E-W trend across the northern Gulf of Suez, the development of the NW-SE trending Suez Arc parallel to the present day western margin of the Gulf of Suez, and a reactivation of the Kharga-Aswan-Red Sea High (Van Houten et al., 1984; Patton et al., 1994). The Kharga and Suez arcs intersected in the northern Red Sea and southern Gulf of Suez resulting in a basement uplift, which persisted throughout the Mesozoic and the early Tertiary (Van Houten et al., 1984).

In general the early Cretaceous sedimentation in the northern Western Desert in general indicates a major regressive phase, demonstrated by the deposition of marginal marine sandstones and shales with rare carbonate streaks of the Alam El Bueib Formation (Neocomian-Barremian). Subsequently this formation was greatly affected by the WNW folding system (Kerdany & Cherif, 1990; Said,

1990). In the extreme north western part of Egypt (Fig. 1.8) a dark brown to dark grey shale unit (the Matruh Shale) rests conformably over the Sidi Barrani Formation of late Jurassic age (Hantar, 1990). Aptian rocks were deposited during a transgressive episode that brought the northern Western Desert area under the influence of a shallow sea, where a carbonate unit (made up of light brown dolomite with a few thin shale interbeds), the Alamein Formation, was deposited. The Albian is represented by another regressive phase in which a large part of the Western Desert was occupied by a shallow marine basin that received the fluvial detritus of rivers coming from the eroded elevated massif to the south, resulting in the deposition of fine to coarse-grained sandstones of the Kharita Formation. In the extreme north around the Matruh Basin, carbonates form a dominant part of the sequence (Said, 1990).

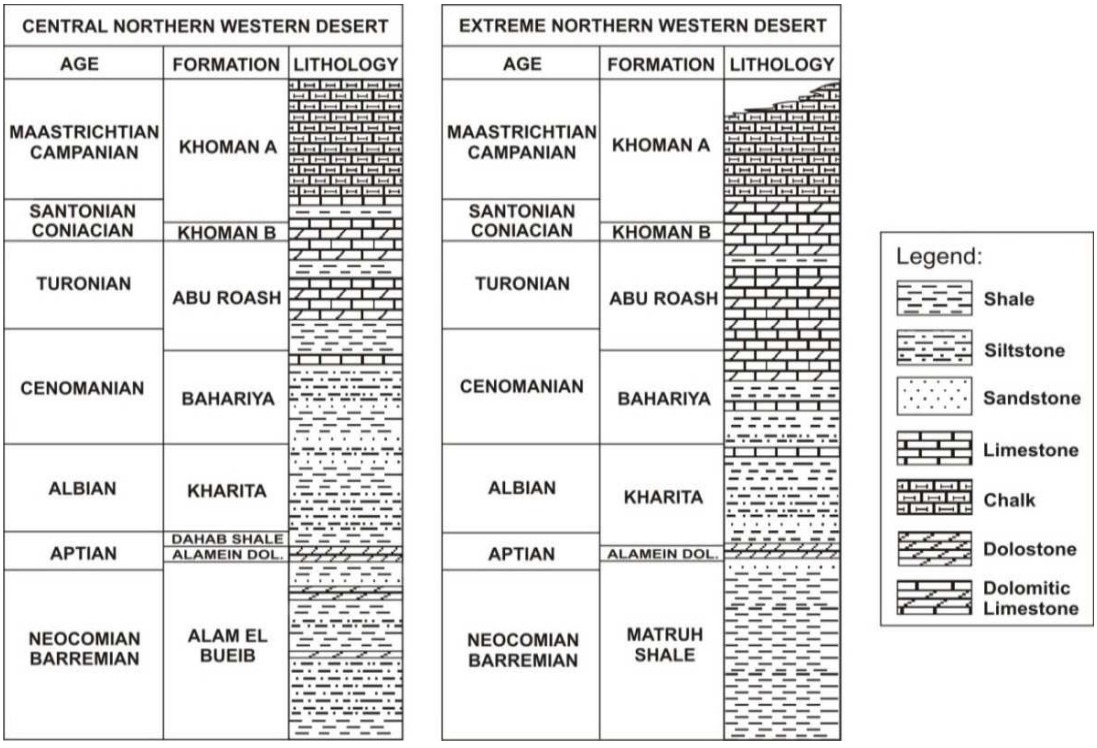

Figure 1.8. Composite lithological successions showing variations in different Cretaceous lithostratigraphic units, compiled from reference boreholes for the extreme northern Western Desert section (Mersa Matruh-1 & Siqeifa-1x wells), and for the central northern Western Desert section (Betty-1 & Abu Gharadig-1 wells). (After Said, 1962). See Fig. 2.1 for well locations.

In the northern part of the Gulf of Suez area at Abu Darag, the late Jurassic-early Cretaceous uplift resulted in an hiatus in the geological record (Fig. 1.9). During the Aptian time, sedimentation renewed and alluvial sediments of the Malha Formation (Aptian-Albian) were deposited over rocks ranging in age from the Precambrian to Jurassic (Soliman & Amer, 1972; Garfunkel & Bartov, 1977; Van Houten et al., 1984; Patton et al., 1994).

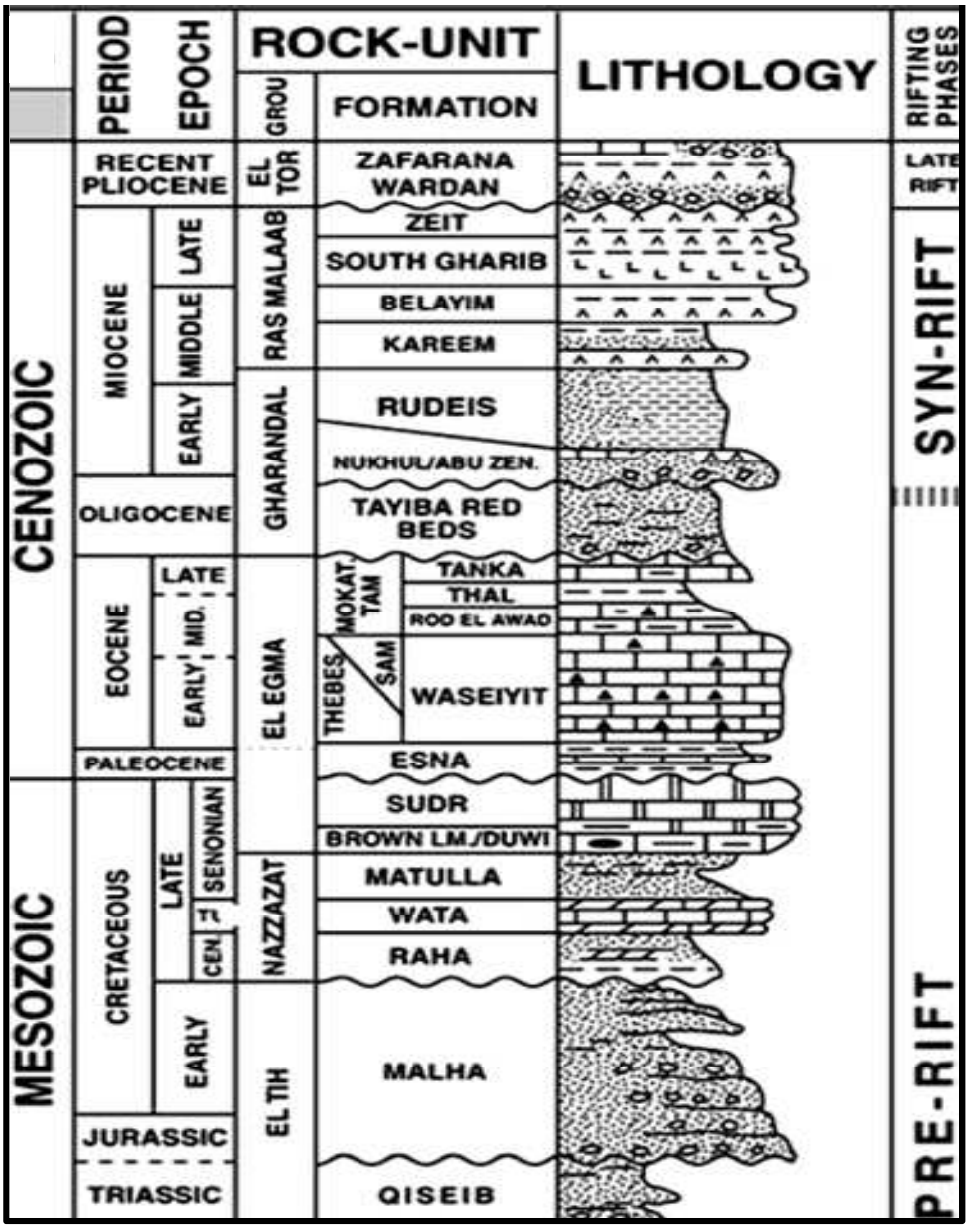

Figure 1.9. Detailed (Mesozoic-Cenozoic) composite stratigraphic section of the Gulf of Suez (after Darwish & El Araby, 1993; Bosworth & McClay, 2001).

Late Cenomanian time witnessed regional subsidence across the northern African margin related to Neotethyan rifting. By the late Santonian a right lateral movement between Africa and Laurasia (e.g. Meshref, 1990) due to the opening of the North Atlantic resulted in NW-directed compressive forces across the north eastern margin of the African plate. These compressive forces in turn resulted in a series of N-W folds associated with thrust faults, WNW dextral strike-slip faults across the northern Western Desert, and a ENE-WSW fold system across northern Gulf of Suez - the so called the Syrian Arc System (Meshref, 1990; Patton et al., 1994). During the Campanian-Maastrichtian, extension and subsidence dominated northern Eastern African tectonics, for example, the Abu Gharadig Basin in the Western Desert, while local folding and uplifting took place, for example, in the northern Eastern Desert on the western side of the Gulf of Suez at Wadi Araba (Guiraud & Bosworth, 1999; Guiraud et al., 2001).

Upper Cretaceous sediments in the northern Western Desert and the Gulf of Suez region indicate a major transgressive phase. During the late Cenomanian a regional subsidence related to Neotethyan rifting took place across the northern African margin, and a marine transgression covered the entire northern African plate, including the Gulf of Suez. As a result, fluvio-marine deposits of the Bahariya Formation accumulated in the Western Desert (Fig. 1.8). During the Turonian, marine conditions generally persisted across most of the Western Desert, where a thick carbonate succession in the extreme northern Western Desert (e.g. in the Mersa Matruh-1 & the Seqiefa-1 wells) gave way southward (e.g. in the Betty-1 & the Abu Gharadig-1 wells) to carbonate and shallow marine clastics of the Abu Roash Formation (Said, 1962, 1990). However, the late Turonian Laramide tectonic event caused uplift and basin inversion of the Sidi Barrani Sub-basin, the Qattara Ridge and the Bahariya Arc (Said, 1990). But by Coniacian times most of the northern Western Desert was again covered by another marine transgression,

during which another carbonate succession, known as the Khoman “B” Formation was deposited (Said, 1990). During the Santonian yet another regression took place, where continuing carbonate deposition of the lower part of the Khoman “B” Formation changed southward to marine clastic sedimentation across the Western Desert (Fig. 1.8). During Campanian-Maastrichtian time, most of the Western Desert was again covered by deep marine waters as a result of a major transgressive cycle, resulting in the deposition of a thick sequence of chalky limestone known as the Khoman “A” Formation (Said, 1990).

The Gulf of Suez area also witnessed the Cenomanian transgressive cycle, where shallow marine shale, sandstone and marl of the Raha Formation (Fig. 1.9) was overlain by the Turonian limestones of the Wata Formation (Kerdany & Cherif, 1990; Said, 1990; Guiraud et al., 2001; Bosworth et al., 2005). During the Coniacian-Santonian period regression took place and as a result, the shales and sandstones of the Matulla Formation were deposited (Said, 1990; Guiraud et al., 2001). The major Campanian-Maastrichtian transgressive cycle also resulted in the deposition of thick carbonate successions (Fig. 1.9), comprised of phosphatic cherty limestones and organic-rich brown limestones of the Duwi Formation, and the snow-white chalky limestone of the Sudr Formation, both lying comformably over the Matulla Formation (Said, 1990; Guiraud et al., 2001).

MATERIAL AND METHODS

2.1 Material

Material was collected from two boreholes in northern Egypt: the Abu Tunis 1x and the BB 80-1. A summary of the palynological samples used with their depth and palynological status are shown in Appendix 1.

2.1.1 The Abu Tunis 1x borehole

The material collected from the Abu Tunis 1x borehole covers most of the Cretaceous sequence of the northern Western Desert of Egypt, represented by 134 ditch cutting samples. The Abu Tunis 1x borehole was drilled in the Faghur area at the northern Western Desert of Egypt in 1968 by the Western Desert Operating Petroleum Company (WEPCO). The Abu Tunis 1x borehole is located at geographic coordinates Lat. 31° 16′ 08″ N, and Long. 26° 50′ 41″ E (Fig. 2.1), and attained a total depth of 12487 ft (3806 m), covering a geologic interval from the lower Eocene to the upper Jurassic.

The Faghur area is located to the east of the Faghur-Maamura High, west of the Matruh Subbasin, and north of the Umbarka Subbasin (Fig. 2.1), where the Cretaceous succession, represented by the Alam El Bueib, Alamein, Kharita, Bahariya, and Abu Roash Formations, was penetrated by the Abu Tunis 1x borehole (Fig. 2.2).

In the past, the Alam El Bueib Formation has been given different names, for example: the Matruh Group, the Aptian clastics, the Alamein shale, or the Dawabis, the Umbarka and the Maamura Formations and has also been given some operational names, for example: units A, B, C, D1, D2, E, and F1 (Hantar, 1990). This lithostratigraphic unit was introduced by Norton (1967) as a member of the

Burg El Arab Formation. However, Ghorab et al. (1971) raised it to formational rank (Fig. 2.3). The Alam El Bueib Formation is mainly composed of sandstone with frequent shale interbeds in its lower part and occasional limestone beds in its upper part (Fig. 2.2). The limestone beds become thicker and especially abundant to the northwest.

Figure 2.1 Simple structural map of Egypt showing the location of the studied boreholes (Abu Tunis-1x and BB 80-1) and the location of the type locality of the Cretaceous formations of the northern Western Desert (after Kerdany & Cherif, 1990).

The type locality is the interval from 3927 to 4297 m of the Alam El Bueib-1 well (Fig. 2.1). This unit is believed to range in age from Barremian to Aptian (Fig. 2.3), and the environment of deposition has been described as shallow marine, with a more continental influence toward the south (Hantar, 1990; Kerdany & Cherif, 1990).

The Alamein Formation was also proposed by Norton (1967) as a member of Burg El Arab Formation; however, Ghorab et al. (1971) also raised this unit to formational rank. This formation is widely distributed, and is well-known all over North Africa and Arabia. It is composed of light brown, hard microcrystalline dolomite with vuggy porosity (Fig. 2.2). The type section of the Alamein Formation is the interval between 2489 to 2573 m of the Alamein-1 well (Fig. 2.1). Its thickness ranges from 20 to 80 m over most of the area except in the north where a maximum thickness (97 m) is reported in the Kanayis-1 borehole (Hantar, 1990). The Alamein Formation has been attributed to an Aptian age, and seems to have been deposited in a shallow marine, low to moderate energy environment (Kerdany & Cherif, 1990).

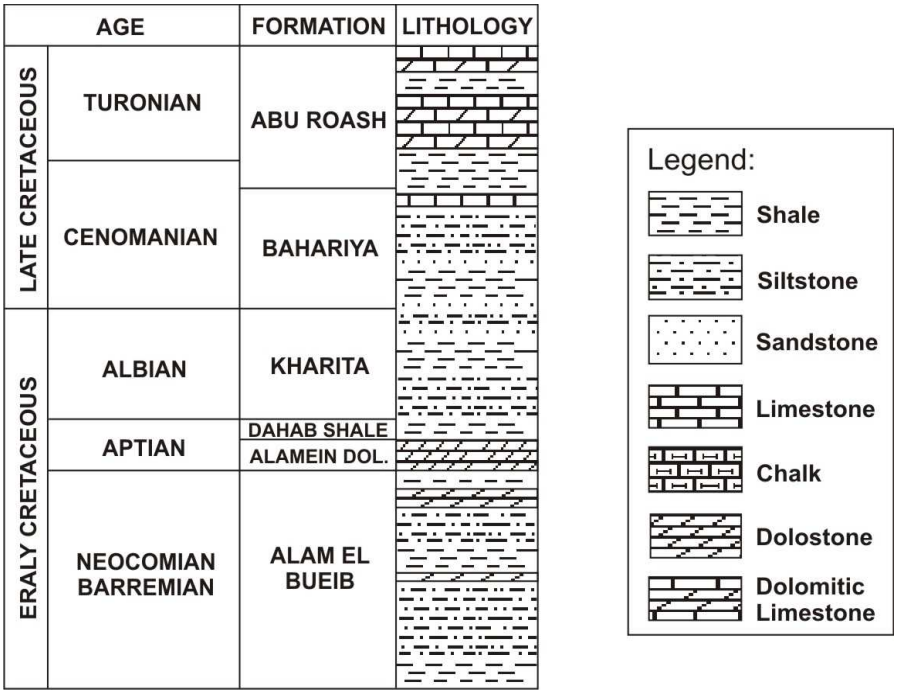

Figure 2.2. Cretaceous stratigraphic subdivisions of the Abu Tunis 1x borehole, northern Western Desert, Egypt (present study).

The Kharita Formation was also introduced by Norton (1967) as a member of the Burg El Arab Formation, with Ghorab et al. (1971) raising it to a formational rank. It is composed of fine to coarse grained sandstones with subordinate shale and carbonate interbeds (Fig. 2.2). The type section is the interval between 2501 to 2890 m of the Kharita-1 well (Fig. 2.1). The Kharita Formation is attributed an Albian age, and it is believed to be deposited in a high-energy shallow marine environment. In the extreme north, the Kharita Formation seems to be deposited in deeper waters, while in the south the unit has continental indications (Hantar, 1990; Kerdany & Cherif, 1990).

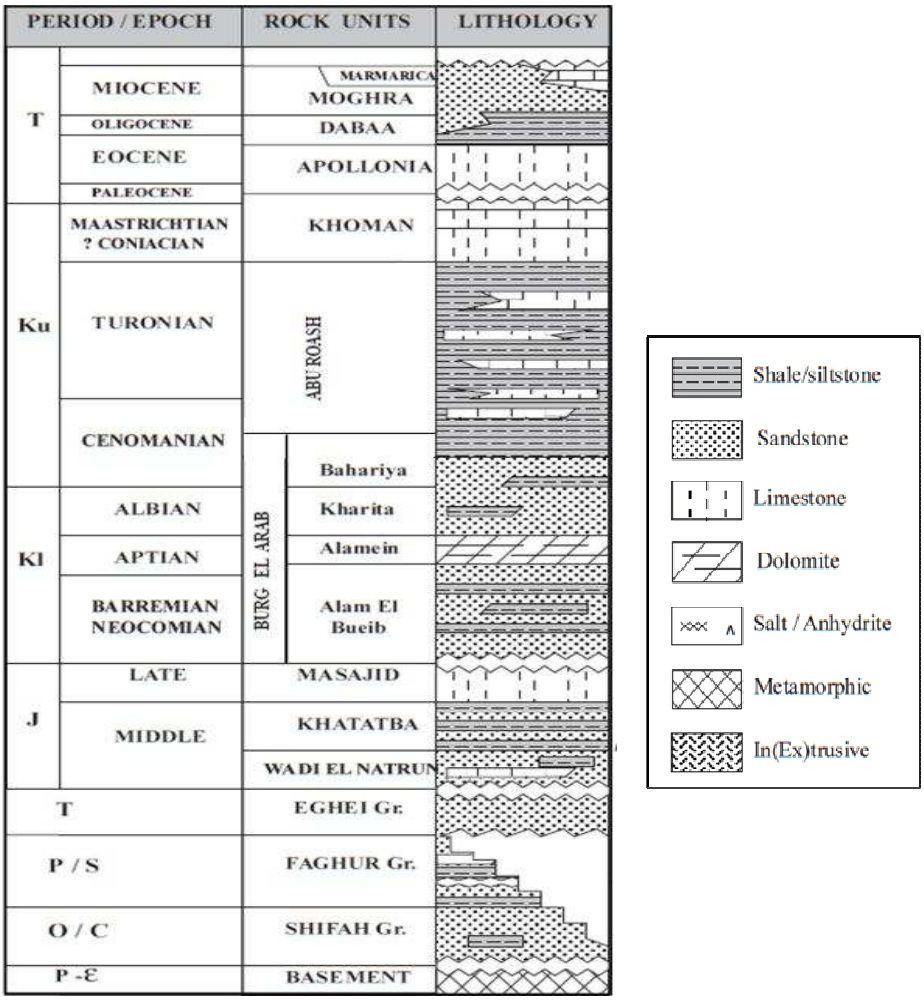

Figure 2.3. Generalized stratigraphic section of the northern Western Desert of Egypt (after Wever, 2000).

The Bahariya Formation was described by Akkad & Issawi (1963) and given a formational name by Norton (1967). The Bahariya Formation is composed of three members: the Gebel Ghorabi Member at the base, made up of non-fossiliferous cross-bedded sandstones of fluvial origin (Dominick, 1985), the Gebel Dist Member deposited under estuarine conditions (Dominick, 1985), made up of fine-grained ferruginous clastic sediments containing vertebrate (i.e. dinosaur) and invertebrate (e.g. bivalve) fossils, and the El Heiz Member deposited under lagoonal conditions (Dominick, 1985) and made up of fossiliferous dolostone (Hantar, 1990). The Bahariya Formation is of Cenomanian age, its type locality is in the base and the scarps of the Bahariya Oasis (Fig. 2.1), represented by a 170 m exposed section (Norton, 1967). This unit shows maximum thickness of 1143 m in the Kattaniya-1 well and varies in other areas from 50 to 500 m (Hantar, 1990). This rock unit has also been given some operational names, for example: the Razzak sand, the Meleiha sand or the Medeiwar Member of the Abu Subeiha Formation (Hantar, 1990).

The Abu Roash Formation was described by Beadnell (1902), and named by Norton (1967). It is mainly composed of a limestone sequence with interbeds of shale and sandstone (Fig. 2.2). This unit is subdivided into seven members designated from bottom to top as: G, F, E, D, C, B and A. The lowermost “G” member is probably coeval with the El Heiz Member of the Bahariya Formation. The type locality of this unit is the classic Abu Roash area to the north of the Giza pyramids (Fig. 2.1). The Abu Roash Formation ranges in age from late Cenomanian to Turonian and it is believed to have been deposited in an open shallow marine shelf, except for unit “G” of inferred lagoonal origin in the south. This unit has varying thicknesses: 1814 m in the Ghourab-1 well in the Betty Basin, more than 1000 m in the Abu Gharadig Basin, and it varies in other areas from 250 to 750 m (Hantar, 1990).

2.1.2 The BB80-1 borehole

The material collected from the BB 80-1 borehole covers the Cretaceous of the offshore Gulf of Suez, represented by 78 ditch cutting samples. The BB 80-1 borehole was drilled on the Zafarana Platform, in the offshore Gulf of Suez by the Suez Oil Company (SUCO) in 1980. The BB 80-1 borehole is located at Lat. 29° 16′ 10″ N, and Long. 32° 38′ 8″ E (Fig. 2.4),

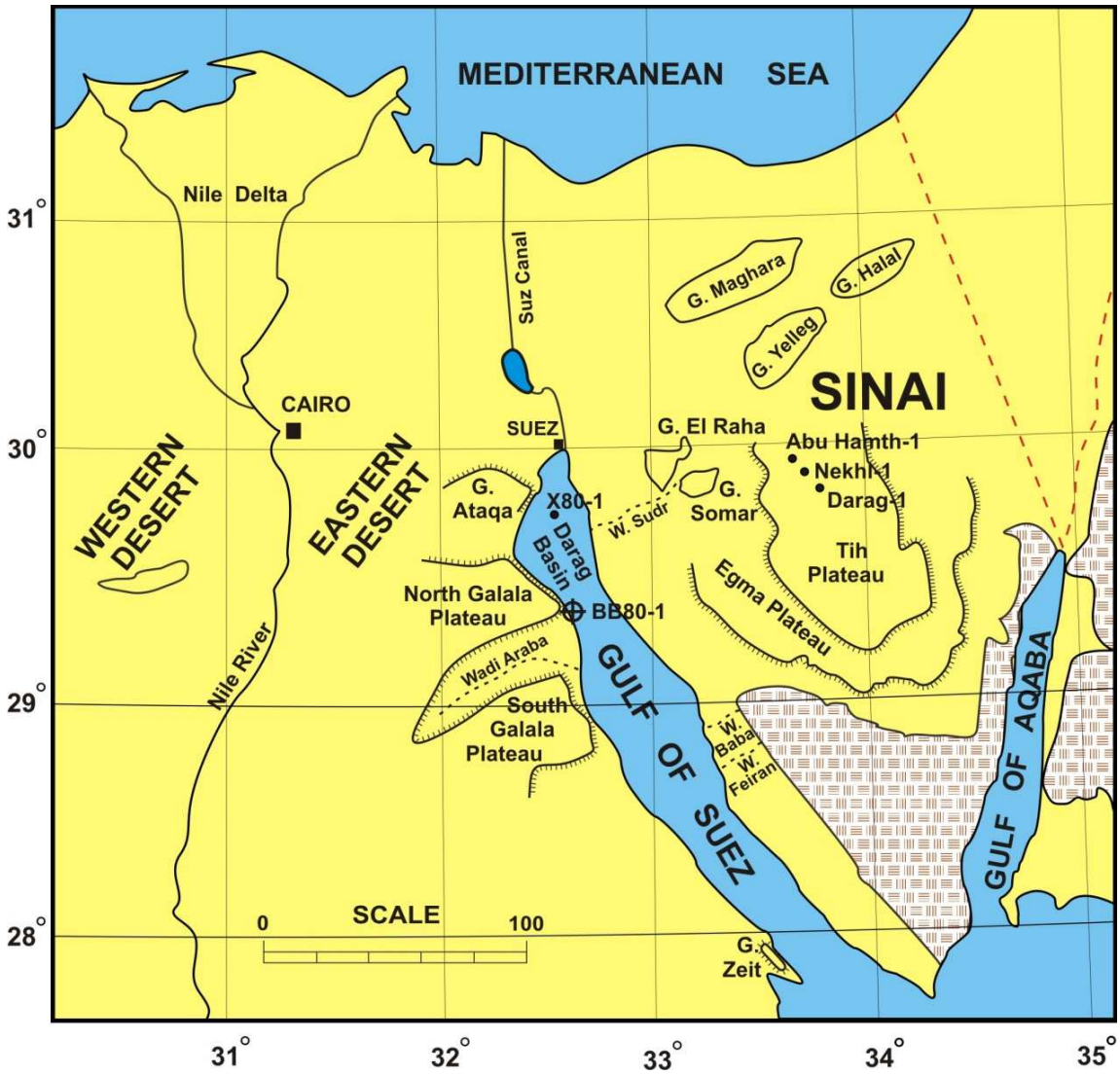

Figure 2.4. Geological map of Sinai and the western Gulf of Suez showing the location of the BB 80-1 and the location of the type localities of the Cretaceous formations of the Gulf of Suez and Sinai (after Khalil & McClay, 1998).

The BB-80-1 borehole attained a total depth of 6658 ft (2029 m), covering the Neogene, Cretaceous, Jurassic, and Precambrian, with a major hiatus, as the Palaeogene, Triassic and the whole Palaeozoic is missing. The subsurface Cretaceous is represented by the Malha and the Raha Formation (Fig. 2.5).

The Malha Formation exposed at the surface, is a sandstone unit that was described by Abdallah et al. (1963), and is the equivalent to the offshore Nubia "A" sandstone unit (Moustafa & Khalil, 1995). The Malha Formation is composed of coarse, medium to fine-grained sandstones and siltstones with occasional shales of fluviatile origin (Kerdany & Cherif, 1990; Schütz, 1994). The Malha Formation is of a palynologically defined Albian to Aptian age (Schütz, 1994), and shows significant variations in thickness. It ranges from 30-100 m in the offshore Gulf of Suez wells; 880 m inshore, east of Gulf of Suez at Wadi Feiran, 500 m at Wadi Baba from 398 m and 245 m in onshore central Sinai (Fig. 2.4) in the Abu Hamth and the Nekhl wells, respectively (Kerdany & Cherif, 1990; Schütz, 1994). The type locality is the Wadi Malha in the south eastern cliffs of the Northern Galala Plateau, where this formation ranges in thickness form 70 to 130 m (Fig. 2.4).

The Raha Formation was described by Ghorab (1961) and is composed at its type locality (Gebel Raha, western Sinai; Fig. 2.4) of a 70-120 m thick clastic and carbonate sequence (Fig. 2.5).

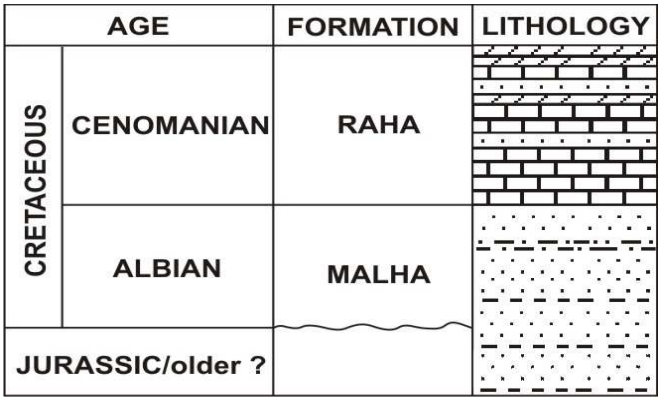

Figure 2.5. Cretaceous stratigraphic subdivisions of the BB 80-1 borehole, offshore Gulf of Suez, Egypt (present study). See Fig. 2.2 for legend.

This sedimentary sequence is made up of sandstone, dolostone, massive fossiliferous limestone, marls and glauconitic shales, and contains ammonites, gastropods, echinoids, and the well-marked oyster beds (Kerdany & Cherif, 1990; Schütz, 1994). The Raha Formation is of Cenomanian age, and is believed to have been deposited in a shallow marine environment during the major Cenomanian transgression (Kerdany & Cherif, 1990; Schütz, 1994). The Raha Formation shows a northward increase in thickness (Schütz, 1994), ranging from 20 m in the south at Gebel Zeit, 170 m in central Gulf of Suez and 280 m in the northern Gulf of Suez (X80-1 well). In the Darag, Nekhl, and Abu Hamth wells in central Sinai the Raha Formation has a thickness of 310 m, 316 m, and 326 m respectively (Kerdany & Cherif, 1990). Equivalents to the Raha Formation are the Halal Formation (Said, 1971) made up of dolomite, marls and fossiliferous limestone at its type locality in northern Sinai at the Gebel Halal (Fig. 2.4); the Galala Formation (Abdallah et al., 1963) made up of marls, shales, and sandstone interbeds overlain by a carbonate sequence at its type locality the Galala Plateau, and the Bahariya Formation in the Western Desert (Kerdany & Cherif, 1990; Schütz, 1994).

2.2 Preparation techniques and methods of study

Reliable qualitative and quantitative palynological investigations, and hence secure interpretations, require that rigid protocols are adhered to throughout sample collection, processing and analysis. Funkhouser (1969) described the factors that can make samples unreliable, such as: laboratory contamination, assemblages mixing in nature, and misplacing of samples through human error. For laboratory preparations employed for this study, the samples were crushed using a simple traditional method (agate mortar), in order to avoid any possible contamination that might have come from using mechanical crushing devices. The mortar was cleaned thoroughly after each sample was crushed. Laboratory contamination might also come from using ordinary tap water which contains modern pollen, spores, diatoms, etc.. However, modern palynomorphs are easily distinguishable from fossil material, and so, deionised water was used in the final stages of processing, especially in the extraction and concentration of the organic residues.

Natural assemblage mixing (stratigraphic leakage) and misplacing of samples through shipping and storing represent errors outside the researcher's control. Both have the same effect of mixing material from different depths, so palynologists must have an appropriate knowledge of the fossil material in order to detect any reworking, caving, or other mixing due to human interference (Traverse, 2007). As the present samples were collected from a deep borehole, possible contamination by modern material is not to be expected.

2.2.1 Palynological processing and methods

The samples are mainly composed of siliciclastic rocks intercalated with a few carbonate horizons, and therefore standard palynological techniques (e.g. Phipps & Playford, 1984; Wood et al., 1996; Green, 2001), with some modifications, have been employed in the processing of these samples as follows:

1. 5 grams of each sample were weighed, crushed and then placed in labelled plastic beakers and placed in a fume cupboard.
2. 15-25 ml of commercial grade 36% hydrochloric acid (HCl) was added to each sample in order to dissolve the carbonate minerals, left for 24 hours, and stirred every 1-2 hours. The time was increased for samples which had higher carbonate content.
3. When no reaction could be detected and settling of the residue had taken place, the samples were washed by decantation several times (usually 4-6) with deionised water until neutralization was reached.
4. About 15-20ml of 60% hydrofluoric acid (HF) was added to the samples and left for approximately about 2 days, with stirring (usually 2-3 times) in order to dissolve silicate minerals.
5. An exotic spike was added to the samples after the first HF decanting, where 1 tablet of a known quantity (12,542 grains/tablet with V ± 3.3 %) of modern *Lycopodium* spores was (made by Department of Quaternary Geology, Lund University, batch no. 124961) added to each sample for absolute abundance analysis.
6. The samples were again washed several times (5-6) with deionised water, sieved at 15 micron mesh and then boiled in 15ml of 36% HCL for 1-2 minutes to remove neo-formed fluorides.
7. The samples were then decanted and washed again several times (4-5) with deionised water until neutralized.
8. Sieving was carried out using a nylon mesh screen (10 μm), to concentrate the organic residue and to retain any small acritarchs and angiosperm pollen specimens.

9. Finally, two permanent slides were prepared for light microscopic investigation, where three drops of the residue were mounted as strews on cover slips, left to dry and were then mounted on glass slides using Elvacite 2044 as a mounting medium.

Palynological slides, organic residue stored in sealed vials, and rock samples are stored in the Geological Museum, Geology Department, Faculty of Science, Assiut University, Egypt.

A. Qualitative (light microscopic) investigations

Qualitative palynological investigations are based on the light microscopic description of the total composition of the organic residue using an Olympus (BX41) transmitted-light microscope (serial no. 8B25715). Scanning of the microfossil grains was made at lower magnifications of x100 and x250, while higher magnifications of x400 and x1000 (oil) were only used for the rare species and for species of very small size, and when investigating detailed morphological features of some dinoflagellate cysts species:

The taxonomic identifications of spores, pollen grains, dinoflagellate cysts, freshwater algae, etc. have been made to generic and specific levels. Two slides were counted for each sample, in order to document any rare palynomorphs, and to guarantee getting a representative record of the palynomorphs present.

Qualitative palynofacies analysis of the organic debris, which involves the determination of the different organic macerals (i.e. phytoclasts and palynomorphs) and their state of preservation, has also been conducted.

B. Semi-quantitative palynomorph analysis

The percentage frequency distribution (i.e. relative abundance) of the main terrestrial elements (sporomorphs, spores, gymnosperm and angiosperm pollen),

and the marine elements (dinoflagellate cysts and microforaminiferal test linings) has been calculated. This was done simply by dividing the number of the fossils counted in each sample by the total count (250 particles) and multiplied by 100 to obtain the percentage.

The relative abundance variations of sporomorphs to phytoplankton have been widely used to determine the relative proximity of the source vegetation to the depositional site (Batten, 1979, Lister & Batten, 1988, Tyson, 1993) . Furthermore, the frequency distributions of sporomorphs have also been used to show the most dominant plant groups, and in particular those known to show environmental or climatic preferences, which assists in the interpretation of the palaeoenvironmental settings (Tyson, 1993; 1995).

C. Quantitative palynomorph analysis

The quantitative method used in the present work involved spiking the samples with one tablet of a known number of modern *Lycopodium* spores during processing. The absolute abundance of each fossil category counted (i.e. spores, gymnosperm pollen, etc.) has been made with reference to the actual number of *Lycopodium* spores counted in the sample and to the original weight of the sample. The concentration (grains/gram) of each fossil category can be calculated by applying in the absolute abundance formula of Stockmarr (1971) as follows:

$$\text{Absolute abundance} = \frac{\text{No. of specimens counted}}{\text{No. of } \textit{Lycopodium} \text{ counted}} \times \frac{\text{Total } \textit{Lycopodium} \text{ added}}{\text{Sample weight}} \quad (1)$$

Several quantitative methods have been proposed by different authors to find a more accurate method to reflect a representative count of palynomorphs. Wilson (1959) attempted to determine the representative number of palynomorphs that should be counted in such palynological material, by plotting the rarefaction curve i.e. the numbers of specimens against the number of species identified until the curve flattened (i.e. become asymptotic), after this point few new species would be counted, whatever the total number of specimens counted. Wilson (1959) found that the number of specimens that should be counted depends on the type of lithology investigated. However, Tschudy (1969) found that the first 200-500 counts would be appropriate, followed by scanning of the remainder of the slide for any rare species not included in the count.

Another factor that may also have a strong impact on the number of specimens to be counted in a given spiked sample, is the error associated with the counting process due to the addition of *Lycopodium* tablets. Stockmarr (1971) found a 3% error in the quoted number of *Lycopodium* spores in each tablet, in addition to the resulting errors in the number of specimens counted. The actual number of *Lycopodium* counted should also be taken into consideration. Stockmarr (1971) calculated the total errors, and constructed curves which showed the relation between the number of specimens counted, the number of *Lycopodium* spores counted, and the expected total resulting error (Fig. 2.6).

In this context, for the current work, the first 250 specimens have been chosen for the counting process, where this number provides a total maximum error of 7% according to the Stockmarr (1971) curve. Further scanning of the rest of each slide was made to detect any rare, out of count species.

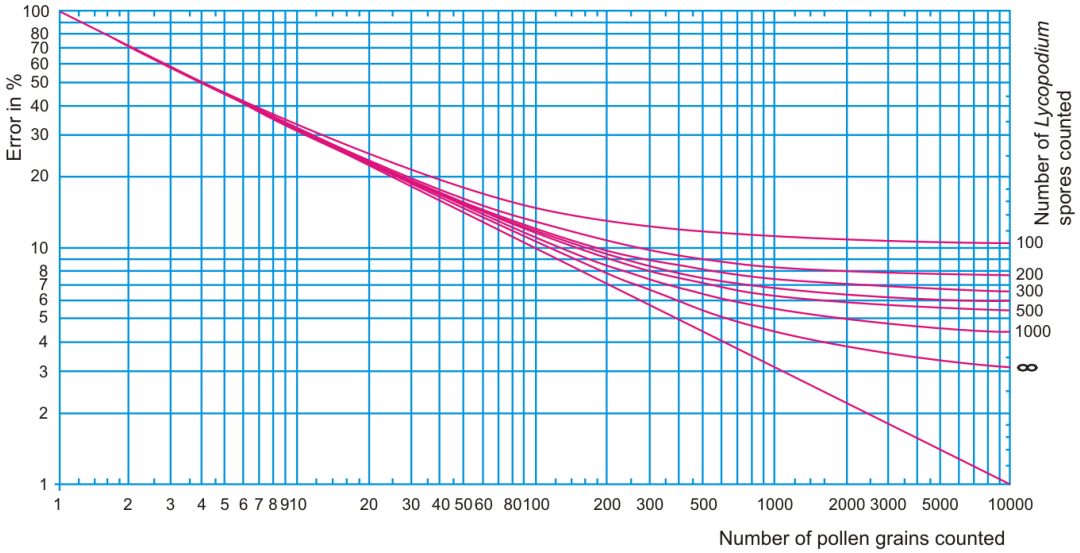

Figure 2.6 Stockmarr's (1971) chart showing the estimated total error (curves) in % when error in the pollen counts (horizontal lines), error on the tablets, and error in the *Lycopodium* spores are taken into account.

D. Quantitative palynofacies analysis

The quantitative analysis of the bulk organic composition (palynofacies) of these samples has been calculated with the same absolute abundance formula (1) mentioned above. All particulate components of the organic residue have been taken into consideration such as the phytoclasts (tracheids, black wood, cuticles, membranous tissues, etc.), the marine elements (dinoflagellate cysts and microforaminiferal test linings), and selected terrestrial palynomorph groups (pteridophyte spores, saccate pollen, *Classopollis* pollen, *Ephedripites* pollen and angiosperm pollen). The conventional count of the first 250 particles was also applied to these samples.

2.2.2 Vitrinite

The petrographic examination of vitrinite is exclusively carried out under reflected light microscopy. This type of study was initially used in coal petrology to evaluate the rank of the coal by measuring the vitrinite reflectivity, as the adsorption index of the vitrinite rises in coal with increasing rank (Stach et al., 1982). This

study requires the preparation of polished surfaces of coal particles embedded in resin moulds. Hillier & Marshall (1988) noted that this method was adopted from the preparation techniques of Stach et al., (1975), American Society for Testing and Materials (1978), and British Standards Institute (1982). Other preparation techniques have been described by Bostick & Alpern (1977), Baskin (1979), Davies & Avery (1984), and Bertrand et al., (1985) to study the petrographic properties of the organic matter concentrate on thin polished sections which has been recovered from the rock samples by the standard HCl/HF technique. Hillier & Marshall (1988) described a simple preparation technique for thin polished sections to study organic matter concentrates, which takes less time with minimum polishing, and requires only a small amount of the organic concentrate, and is therefore suitable for samples with low concentrations of organic contents, or for small samples. In this study the Hillier & Marshall (1988) preparation technique has been employed as follows:

1. After the recovery of the organic matter from the rock samples by the standard HCl/HF preparation technique, the concentrates of seventeen non-oxidized organic residues known to be rich in phytoclasts with a 300 foot (91.44 m) interval between each sample were selected for the preparation of thin polished sections.
2. Sixteen standard cover slips (22 x 22 mm) were coated on one side with the releasing agent polytetrafluoroethylene (PTFE), and left for few minutes until the carrier evaporated.
3. A small quantity of the organic matter concentrate of each sample was pipetted onto the coated surface of the cover slips, and then left to dry in a closed fume cupboard to eliminate airborne contamination.
4. A crystal pen was used to mark the edges on the unfrosted surfaces of the frosted microscope slides.

5. One drop of resin was placed in the centre of the frosted side of the slides. Then the slide was held in contact over the cover slip, the resin allowed to spread. The slides were then quickly placed in a horizontal position to allow the resin to spread uniformly beneath the residue. The slides were left for 2-3 days to set.
6. After the complete setting of the resin, the cover slips were prised off using a razor blade, the organic matter remaining embedded in the thin layer of resin on the slide.
7. Finally, the resin embedded-organics were polished on an emery paper selvyt cloth lap for 40 seconds clockwise and 40 seconds anticlockwise. The slides were successively polished with two fine grade 320 and 520 alumina powder each for 30 seconds at 150 rpm, with washing of the slides between each polishing step. After the completion of the polishing, the slides were dried and buffed on a selvyt cloth lap.

Vitrinite reflectivity measurements were carried out using a Zeiss Universal Microspectrophotometer (UMSP 50) in the School of Ocean and Earth Science, University of Southampton. This equipment is composed of three main units: the Zeiss Universal Microspectrophotometer 50 itself, a microscope photometer control unit (MPC 64), and a desktop computer. The vitrinite reflectance measurements were carried out using halogen light (Hal 100, 12V 100W), with a Zeiss epi-condenser II P condenser, and a standard H-Pl-Pol Zeiss reflected light prism. An ANTIFLEX Zeiss EPIPLAN 40/0.85 Pol oil objective was used with immersion oil of n_e= 1.518 ± 0.0004 at 23 ºC. The technique depends on measuring the intensity of light reflected from the surface of the investigated sample, which is compared to a standard where the reflected light intensity is measured by a photomultiplier (HTVR 928) which converts the reflected light rays into electrical signals and processes

them. The data from the photometer is then processed using a reflectance measuring programme, SLAP, written by S. J. Hillier (Ecolé Normal, Paris).

Calibration of the photometer using an artificial 3G garnet (gadolinium gallium garnet) with a known standard reflectance (RI = 0.919) was carried out before taking any measurements. Five reflectance measurements of the standard before and after measurements of each investigated sample were also made, in order to estimate the relative errors for each investigated sample. During the measurement process several measurements for each unknown sample were taken (48-87) from different parts of the vitrinite particles. Where particles contained inclusions or pyrite crystals, these were avoided. Scratches on the surface of the polished vitrinite particles were also avoided during the measurement process. Finally, correction for error of average reflectance measurements of each sample was made as follows:

$$\text{corr Rv} = (\text{avg Rv} * \text{act Std})/\text{avg Stds} \qquad (2)$$

Where;

corr Rv = corrected average measurement of each sample

avg Rv = average reflectance measurements of each sample

avg Stds = average reflectance measurements of the standard

act Std = actual reflectance known of the standard

2.2.3 Total organic carbon (TOC) analysis

Samples selected to undergo total organic carbon analysis were prepared for elemental analysis as follows:

1. 2 grams of each sample was crushed into fine powder using an agate mortar, and split into two halves.
2. The first half of each sample was labelled for total carbon determination as `$C_b$` , with its corresponding borehole name and depth, and oven dried at 160 ºC for 3 days, before being placed in desiccator before elemental analysis.
3. The other split of each sample was labelled `$C_a$`, for acid treatment, where dilute 36% HCl analar was added to samples to dissolve mineral carbon present in the form of calcium carbonate.
4. Each C_a sample then washed several times with deionised water to remove any remaining acid traces, and the organic residue then concentrated using a 10 µm nylon mesh screen.
5. The concentrate of each acid treated-sample was dried in an oven at 160 ºC for 3 days, and then placed in a desiccator before elemental analysis.
6. Approximately 3 mg of both the acid-treated and untreated splits of each sample were weighed into tin capsules. These capsules were sealed to force out any trapped air, and then placed in the analyser sample chamber.

Elemental analyses were carried out using a Carlo Erba CHNS-O, EA1108 elemental analyser, running with Carlo Erba software EAGER 100. The technique depends on the oxidation of samples at about 1200 ºC under a mixture of oxygen and helium gases to convert C, H, and N into oxides. These oxides then undergo reduction and gas chromatographic separation (GC). Each organic element induces electric charges detected by a thermal conductivity detector, and produces a

spectrum (time sec versus mv) characteristic for each compound (CO_2, H_2O, and NO_2). The EAGER 100 software then processes these data and produces the calculated wt% of each element. The elemental analyser was calibrated before running any analysis using the standard compound sulphanilamide ($C_6H_8N_2O_2S$) of known carbon content (41.84%). Stability of the analyser was assessed by analyzing the sulphanilamide standard after the analysis of five unknowns, and to estimate the relative errors.

As this elemental analyser cannot determine the organic carbon apart from mineral carbon within calcium carbonate, each sample (C_b and C_a) was analysed separately in order to calculate total organic carbon (TOC). The equation of Wilkinson (1991) was used to calculate the TOC as follows:

$$C = 100\ C_a\ (1\text{-}0.0833\ C_b)/\ (100\text{-}8.33\ C_a) \qquad (3)$$

Where;

C = total organic carbon (TOC) wt%

C_a = C wt% in acid treated sample

C_b = C wt% in untreated sample

PREVIOUS PALYNOLOGICAL WORK

3.1 Survey of palynological work on the Cretaceous of Northern Gondwana

This survey will focus on some of the important palynological results which are directly related to Egyptian material. In a phytogeographic context, Egypt was located in the northern part of Gondwana during the Cretaceous, where a regional terrestrial floral province covered northern Africa and northern South America (e.g. Abdel-Kireem et al., 1996). As Egypt also occupied a part of the main marine Tethyan Realm at this time, it is also necessary to examine marine palynological studies carried out on Tethyan successions. The identification of taxa of biostratigraphic importance from these studies will allow a revision of the local biostratigraphy, and those taxa of palaeoenvironmental significance can then be utilised to interpret local palaeoenvironmental conditions.

3.1.1 The African-South American Phytogeographic Provinces

Regional geographic areas showing different distinct microfloral assemblages with the Cretaceous stages in Africa and South America have been assigned by several authors to different phytogeographic provinces. The characteristics of these phytogeographic provinces along with the previous palynological work carried out on these provinces are summarised as below:

A. The *Dicheiropollis etruscus*/*Afropollis* Province

Originally known variously as the Northern Gondwana Province of Brenner (1976), Phytogeoprovince III of Srivastava (1978), or the West African-South American (WASA) Province of Herngreen & Chlonova (1981). This province was later emended by Herngreen et al. (1996) to include northern and eastern Africa and

renamed the *Dicheiropollis etruscus*/*Afropollis* Province (Fig. 3.1) and represents the pre-Albian early Cretaceous equatorial palynoprovince.

The *Dicheiropollis etruscus*/*Afropollis* Province is characterised (from older to younger sporomorphs) by *Dicheiropollis etruscus*, *Tucanopollis crisopolensis*, *Afropollis* spp., *Complicatisaccus cearensis* and *Sergipea* spp. The high abundance (up to 80%) of *Classopollis*, low to moderate abundance (20-25%) of gymnosperm taxa *Exesipollenites*, *Araucariacites*, and *Inaperturopollenites* also characterize the province.

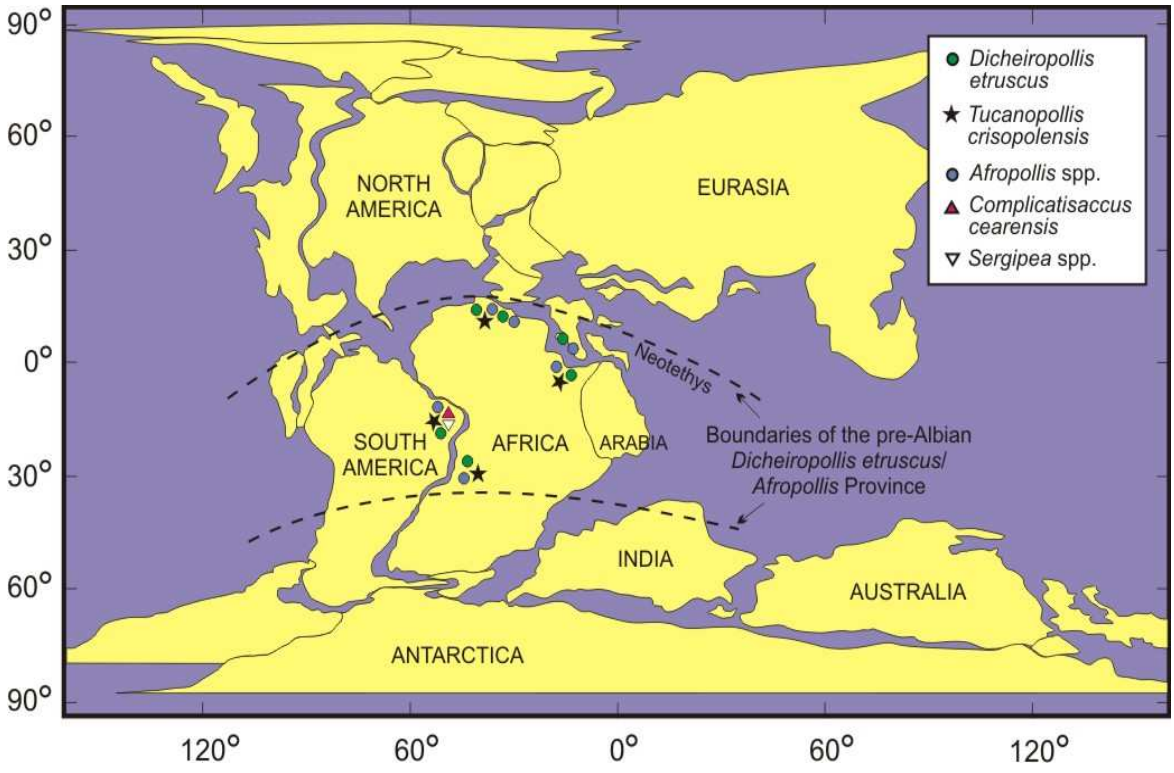

Figure 3.1. Palaeogeographic reconstruction at 125 Ma simplified after Hay et al., (1999), showing the pre-Albian *Dicheiropollis/Afropollis* Phytogeographic Province and distribution of the most important pollen and spore species characteristic of the province. Map based on selected palynological studies as follows: North Africa: Egypt (Schrank, 1992; Ibrahim & Schrank, 1996; Schrank & Mahmoud, 1998, 2002), Sudan (Schrank, 1992; Awad, 1994), Libya (Thusu & van der Eem, 1985; Thusu et al., 1988; Uwins & Batten, 1988), Algeria (Jardiné et al., 1974), Morocco (Gübeli et al., 1984; Bettar & Courtinat, 1987); West Africa: Gabon & Congo (Doyle et al., 1977); south Switzerland & north Italy: (Hochuli, 1981); South America: NE Brazil (Müller, 1966; Regali et al., 1974; Arai et al., 1989; Regali & Viana, 1989).

The low abundance of the xerophytic gymnosperm pollen *Ephedripites*/*Gnetaceaepollenites*, rare occurrence (3-15%) of bisaccate pollen (e.g. *Alisporites*, *Cedripites*, *Complicatisaccus* and *Vitreisporites*) are also found in the province. The rare occurrence of *Eucommiidites* (2-5%) along with the occurrence of smooth trilete spores (mainly *Concavisporites*, *Gleicheniidites* and *Cyathidites*) and the presence of schizaeacean (i.e. *Cicatricosisporites*) and *Aequitriradites* spores are also characteristic of the province (Herngreen et al., 1996).

B. The Albian-Cenomanian Elaterates Province

Another microfloral province was proposed for the mid Cretaceous (Albian-Cenomanian) of Africa and South America and named the African-South American (ASA) Province by Herngreen (1974a), equating to the Northern Gondwanan Province of Brenner (1976), the *Galeacornea* phytogeoprovince of Srivastava (1978) and the *Elaterosporites* province of Srivastava (1981). Herngreen et al. (1996) revised this phytogeoprovince concept and renamed this collection of provinces as the Albian-Cenomanian Elaterates Province (Fig. 3.2). Herngreen et al., (1996) suggested that the eastern border of this province should be extended to include China and Papua-New Guinea, as new palynological records with the same characteristic elaterate pollen were recorded from these regions.

The Albian-Cenomanian Elaterates Province is characterised (from older to younger sporomorphs) by *Afropollis jardinus*, *Crybelosporites pannuceus* (as *Perotrilites pannuceus*), *Elateropollenites jardinei*, *Elaterosporites klaszii*, *Elaterocolpites castelainii*, *Cretacaeiporites polygonalis*, *Elateroplicites africaensis*, *Galeacornea causea*, *Sofrepites legouxiae* and *Senegalosporites petrobrasi*. The moderate diversification of the angiosperm pollen and polyplicate gymnosperm pollen (*Ephedripites*, *Equisetosporites*, *Gnetaceaepollenites* and *Steevesipollenites*) and the scarcity of the pteridophyte spores along with the absence of bi- and

trisaccate gymnosperm pollen are also characteristic of the province. The angiosperm pollen *Hexaporotricolpites*, *Triorites*, *Psilatricolporites*, *Tetradites* and *Retitricolpites* also characterise the province (Herngreen et al., 1996).

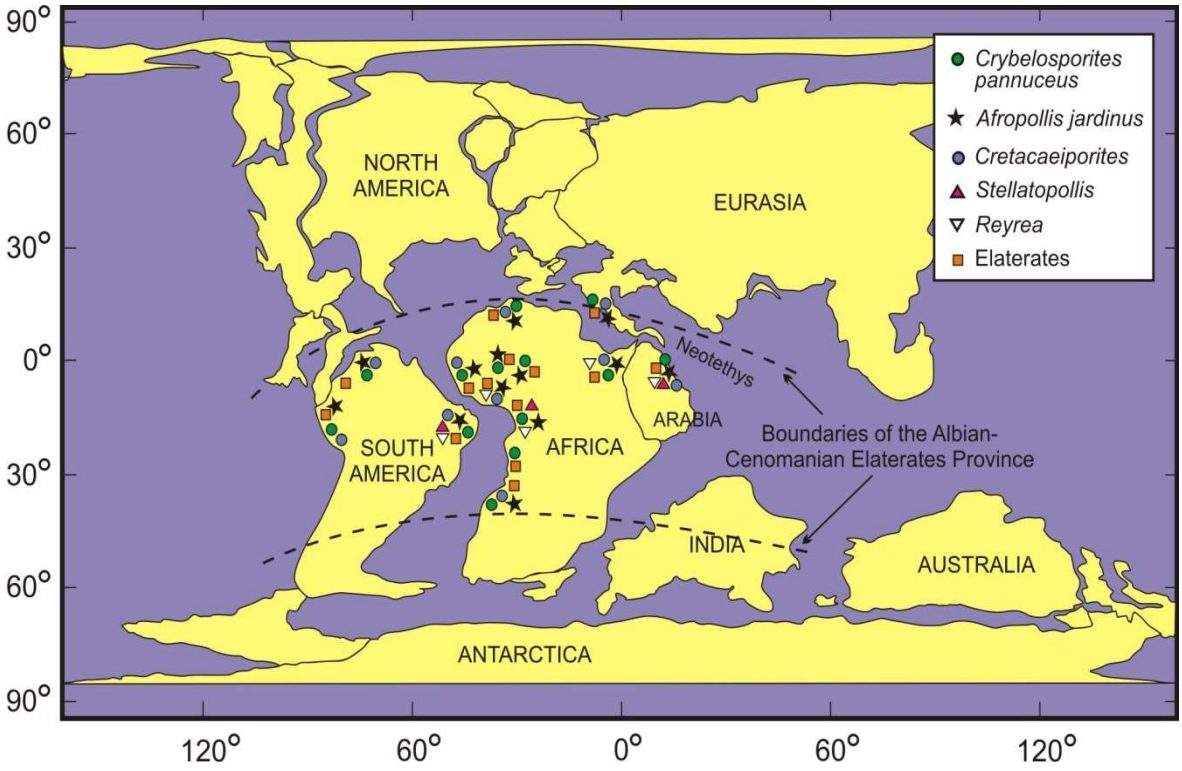

Figure 3.2. Palaeogeographic reconstruction at 100 Ma simplified after Hay et al., (1999), showing the Albian-Cenomanian Elaterates Phytogeographic Province and distribution of the most important pollen and spore species characteristic of the province. Map based on selected palynological work as follows: Arabian Gulf area (Srivastava, 1984; El-Beialy & Al-Hitmi, 1994; Ibrahim et al., 2000); North Africa: Egypt (Schrank, 1991; El-Beialy, 1993; Schrank & Ibrahim, 1995; Ibrahim, 1996), Sudan (Awad, 1994), Libya (Batten & Uwins, 1985; Uwins & Batten, 1988), Morocco (Bettar & Méon, 2001, 2006); West Africa: Ghana (Atta-Peters & Salami, 2006), Senegal & Ivory Coast (Jardiné & Magloire, 1965), Angola basin & Nigeria (Lawal & Moullade, 1986; Abubakar et al., 2006), Intertropical Africa (Salard-Cheboldaeff, 1990); south Switzerland & north Italy: (Hochuli, 1981); South America: NE Brazil (Regali et al., 1974; Herngreen, 1974a; Regali, 1989; Dino et al., 1999), Colombia (Herngreen & Jimenez, 1990), Peru (Brenner, 1968), Ecuador (Dino et al., 1999).

C. The Senonian Palmae Province

The Turonian microfloras of Africa and South America have been assigned - with some reservation, due to scarcity of data - to the Senonian Palmae Province by Herngreen et al. (1996). The Senonian Palmae Province of Herngreen and Chlonova (1981) originally proposed by Herngreen (1980) as the Late Cretaceous Palmae Province corresponds to *Buttinia* African-South American Province of Graus-Cavagnetto (1978) and the *Constantinisporis* phytogeoprovince of Srivastava (1978, 1981).

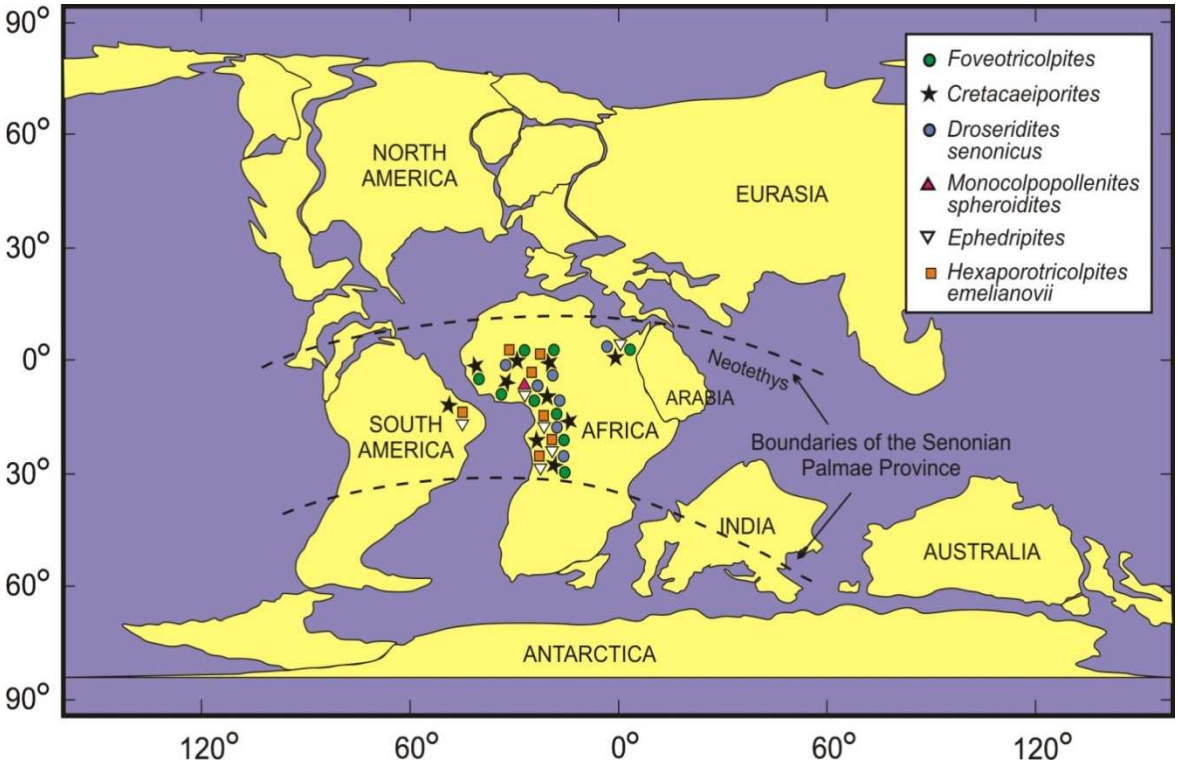

Figure 3.3. Palaeogeographic reconstruction at 90 Ma simplified after Hay et al., (1999), showing the Senonian Palmae Phytogeographic Province and distribution of the most important pollen and spore species characteristic of the province. Map based on selected palynological work as follows: North Africa: Egypt (Schrank & Ibrahim, 1995; Ibrahim, 1996), Nigeria (Jan du Chêne et al., 1978; Lawal & Moullade, 1986), Senegal & Ivory Coast (Jardiné & Magloire, 1965), Intertropical Africa (Salard-Cheboldaeff, 1990), South America: NE Brazil (Herngreen, 1974a, 1974b, 1975).

Herngreen and Chlonova (1981) identified two slightly different regions within the Palmae Province: the northern basins (northernmost part of South America, offshore Suriname, the Senegal Basin, Sahara and Egypt) and the southern basins (Rio de Janeiro Platform and Angola Basin). The northern region is characterised by *Foveotricolpites giganteus*, *Foveotricolpites gigantoreticulatus*, *Cretacaeiporites*, *Droseridites senonicus* and *Monocolpopollenites spheroidites*. The Turonian microflora is also characterised by *Ephedripites*, *Hexaporotricolpites emelianovii*, the disappearance of elaterate pollen and *Classopollis*, a decline in the triporate pollen *Triorites*, and the general dominance of angiosperms and rare occurrence of spores (Herngreen & Chlonova, 1981; Herngreen et al., 1996).

The Senonian Palmae Province is characterised by the sharp decline of *Hexaporotricolpites*, *Cretacaeiporites* and polyplicate pollen, and an increase in monocolpate pollen (*Psilamonocolpites*, *Retimonocolpites* and *Longapertites*) and palm pollen (*Spinizonocolpites echinatus*, *Proxapertites* spp. and *Mauritiidites franciscoi*). The appearance of triporate forms (*Echitriporites trianguliformis*, *Scabratriporites* spp. and *Proteacidites* spp.), syncolp(or)ate pollen (*Cupanieidites* spp., *Syncolporites* spp., *Auriculiidites reticulatus*, *Buttinia andreevii* and *Retidiporites magdalenensis*) together with an increase in spores of aquatic plants (*Zlivisporis blanensis* and *Ariadnaesporites* spp.) is also characteristic of the Palmae Province (Herngreen & Chlonova, 1981; Herngreen et al., 1996).

3.1.2 Tethyan Realm

The palynological study carried out by Millioud (1967) on the Valanginian and the Hauterivian stratotype sections in southeast France and Switzerland, and the subsequent study of the Berriasian to the lower Aptian stratotype sections carried out by Millioud (1969) represent the first studies of dinoflagellate assemblages from the Tethyan Realm. These studies were continued by Davey &

Verdier (1973; 1974) on the Aptian and Albian-Cenomanian stratotype sections. The independently age dated-palynological work carried out by Habib (1975) on the lower and the middle Cretaceous of the Western North Atlantic, introduced the first formal dinoflagellate zonation for the Neocomian-Barremian of the Tethyan Realm. This zonation was later revised by Habib (1977) and extended in to the Cenomanian (Fig. 3.4). Other palynological work, which was mainly taxonomic, was carried out on subsurface Cretaceous successions of the southern Tethyan Realm (e.g. Below, 1981, 1982a, 1982b, 1984). The palynological work of Wilpshaar (1995) and Leereveld (1997a, 1997b) represent a continuation of palynological studies carried out on the lower Cretaceous stratotype sections and nearby areas. Leereveld's work (1997a, 1997b) on the lower Cretaceous of southern Spain and southern France, resulted in the identification of the most comprehensive micropalaeontologically calibrated-dinoflagellate zonation for the lower Cretaceous of the Tethyan Realm in Western Europe (Figs. 3.5 and 3.6).

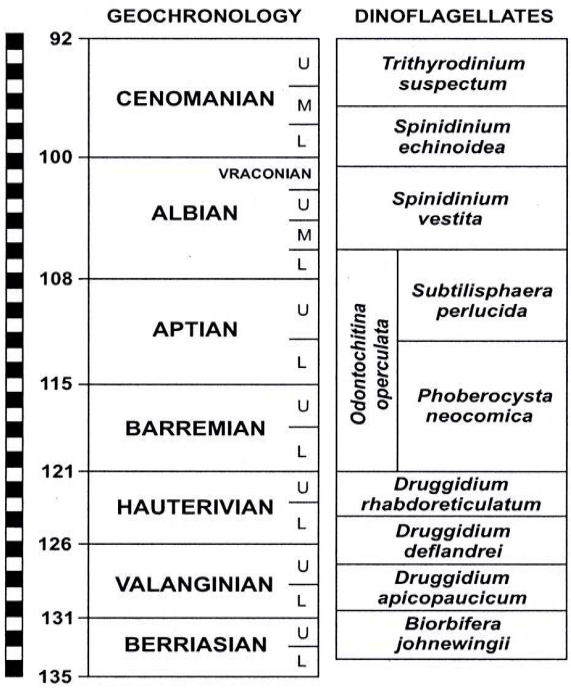

Figure 3.4. Early Cretaceous dinoflagellate zonation for the Tethyan Realm (Habib, 1975; 1977).

STAGES	SUBSTAGES	AMMONITE ZONATION		CALPIONELLID ZONATIONS	DINOCYST ZONATION	
		ZONES	SUBZONES (* HORIZON)		ZONES	SUBZONES
VALANGINIAN	UPPER	N. pachydicranus			Cva (pp)	Sent (pp)
			* N. callidiscus			Lame
			H. trinodosum			
		S. verrucosum			Spi	Tama
	LOWER	B. campylotoxus				Pare
		T. pertransiens		darderi (E)		Cive
		T. otopeta		hungarica (D3)		
BERRIASIAN	UPPER	F. boissieri	T. alpillensis		Ppe	Diho
			B. picteti	oblonga (D2)		Prol
			M. paramimounum	simplex (D1)		
	MIDDLE	T. occitanica	D. dalmasi	elliptica (C)	Bjo (pp)	
			B. privasensis			
			T. subalpina			
	LO.	B. jacobi		remaniella (B)		

Figure 3.5. Micropalaeontologically calibrated dinoflagellate zonation for the Berriasian-Valanginian of the European Tethys (Leereveld, 1997a).

STAGES	SUBSTAGES	AMMONITE (SUB)ZONES	DINOCYST ZONES	DINOCYST SUBZONES	PL. FORAM ZONES	CALC.NANNO ZONES
BARREMIAN	UPPER	M. sarasini	Oop pp		G. blowi pp	*
		I. giraudi				M. hoschulzii
		H. feraudianus				
		H. sartousiana				
		A. vandenheckii			H. similis – H. kuznetsovae	
	LOWER	H.caillaudianus	Ssc			
		S.nicklesi				
		S. hugii	Spe		H. sigali – H. delrioensis	M. obtusus
HAUTERIVIAN	UPPER	P. angulicostata				
		B. balearis	Aei			N. bucheri
		P. ligatus		Capi		
		S. sayni	Lst	Flin		N. bollii
	LOWER	L. nodosoplicatum		Kiok		
			Mst	Catr		C. oblongata pp
		C. loryi		Hiou		
				Bour		
		A. radiatus	Cva pp			

Figure 3.6. Micropalaeontologically calibrated dinoflagellate zonation for the Hauterivian-Barremian of the European Tethys (Leereveld, 1997b).

The palynological work of Torricelli (2000, 2006) on the lower Cretaceous (Fig. 3.7) and Torricelli and Amore (2003) on the upper Cretaceous of Italy (Fig. 3.8) represent the most recent palynological studies carried out with independent age control in the European Tethyan Realm.

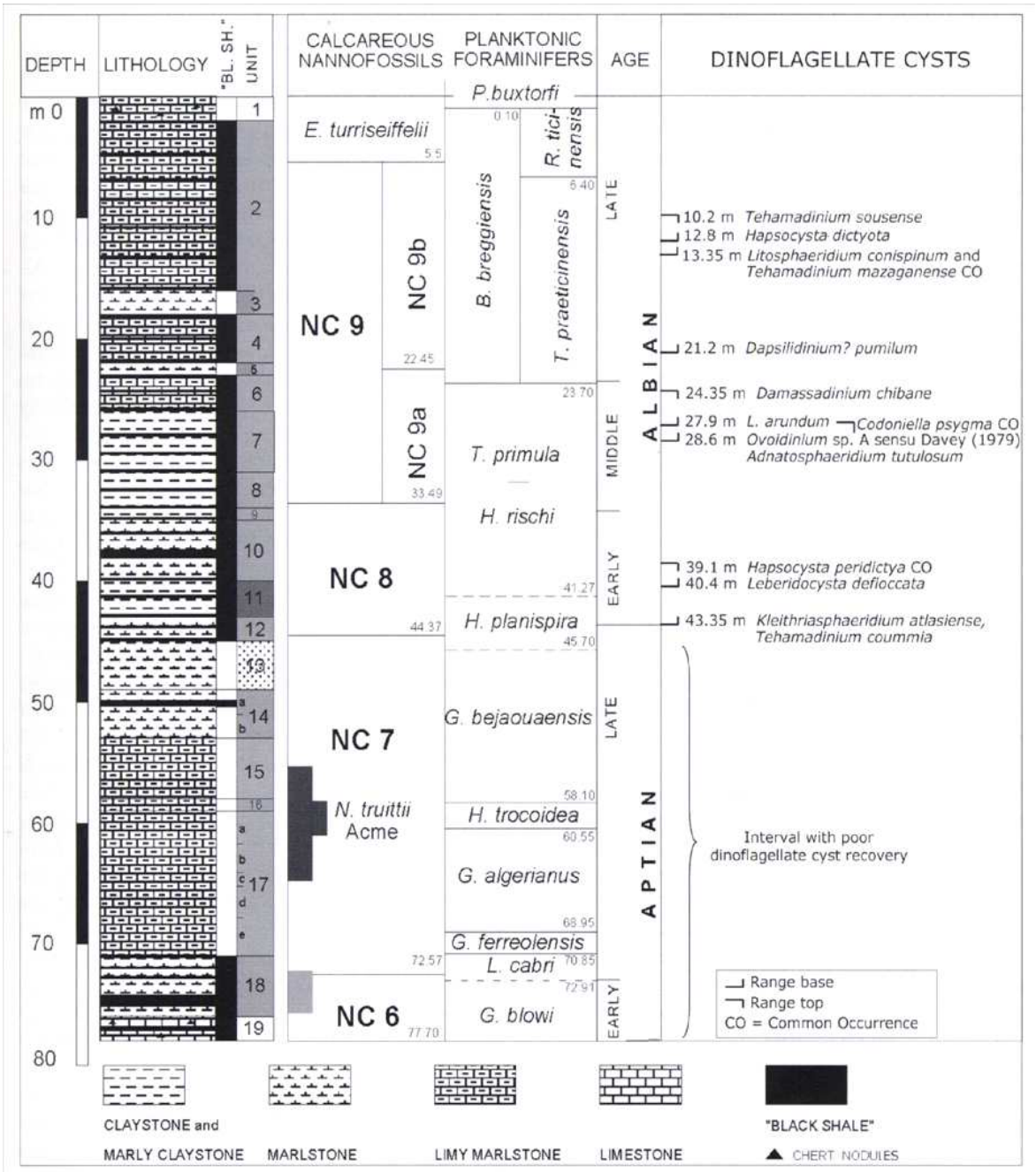

Figure 3.7. Micropalaeontologically calibrated dinoflagellate events for the Aptian-Albian of the European Tethys (Torricelli, 2006).

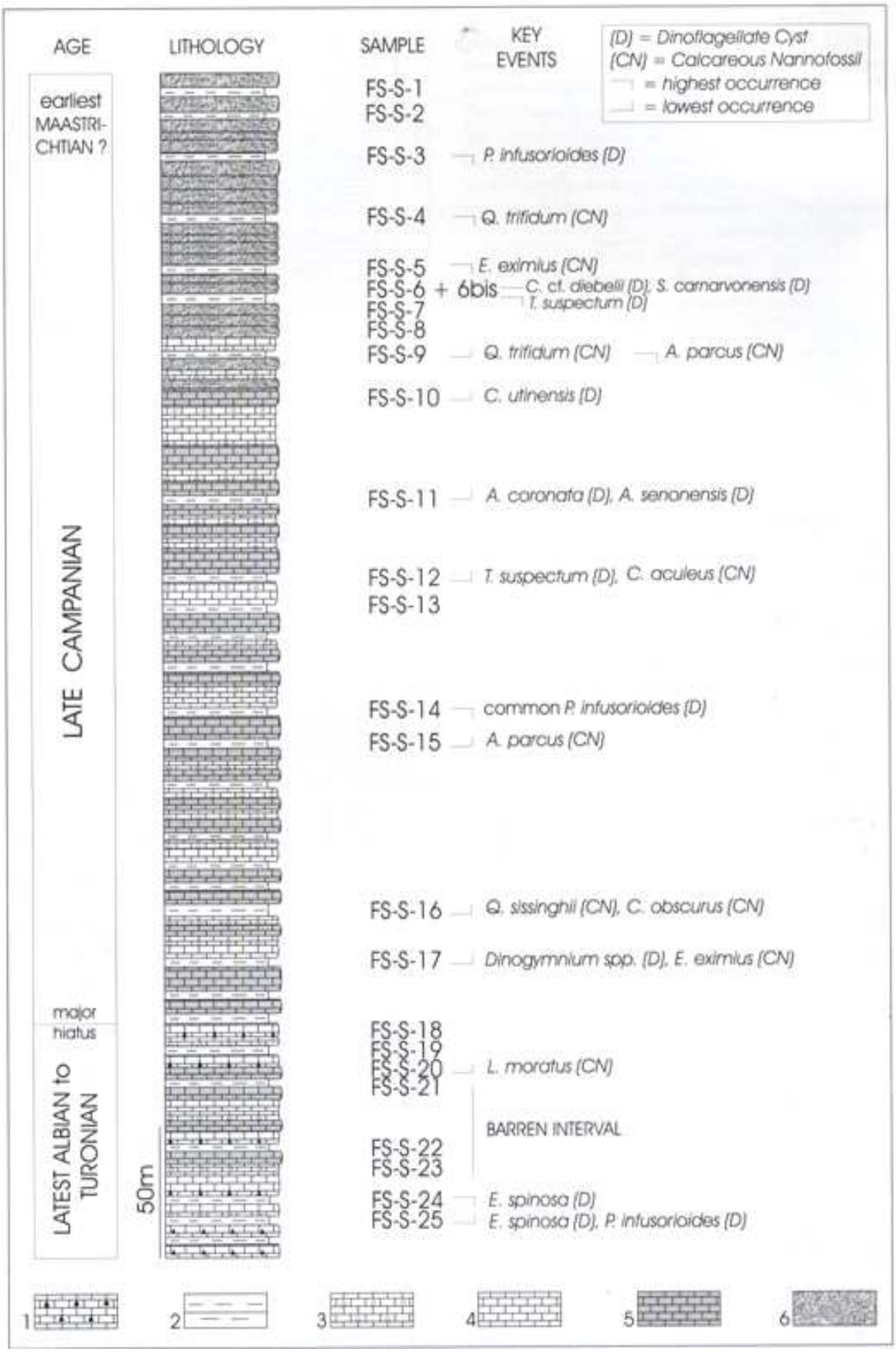

Figure 3.8. Micropalaeontologically calibrated dinoflagellate events for the Albian-Maastrichtian of the European Tethys (Torricelli & Amore, 2003).

SYSTEMATIC PALYNOLOGY

4.1 Introduction

This chapter deals with the taxonomic description of the fossil palynomorphs that are different from the original description, especially those of biostratigraphic and/or palaeoenvironmental importance. All descriptions provided are abridged original and/or modified descriptions followed by taxonomic remarks, based on the material studied herein.

The taxonomic identification of the spores and pollen grains has mainly been made with reference to the original descriptions and diagnoses of these species in their original published articles. The TAXON electronic database of Ravn (1998, http://www.palydisks.palynology.org/), in addition to the *Genera File of Fossil Spores and Pollen* of Jansonius and Hills (1976 and subsequent supplements) have been used as additional sources for identification and resolution of taxonomic problems. An alphabetical list of the identified spores and pollen grains arranged by major palynological category (i.e. spores, gymnosperm pollen and angiosperm pollen) where morphologically similar forms are grouprd together is presented. The rationale for not using the traditional and widely used classifications of such authors as Iversen & Troels-Smith (1950), Potonié, (1956), and Dettmann (1963) for spores and pollen grains is that they are informal arbitary, do not comply with the rules of the International Code of Botanical Nomenclature (ICBN; McNeill et al., 2006) and lack the rule of priority (Traverse, 2007). The Glossary of Pollen and Spore Terminology of Punt et al., (2007) for morphological spore/pollen terminology has been followed.

The generic and specific identification of dinoflagellate species has also been based on the original descriptions and diagnoses of these species in the

original articles, in addition to the Eisenack Catalog of Fossil Dinoflagellates (Fensome et al., 1995, 1996). The Lentin and Williams Index of Fossil Dinoflagellates (Fensome & Williams, 2004) along with the updated electronic database DINOFLAJ2, Version 1 (Fensome et al., 2008, http://dinoflaj.smu.ca/wiki/Main_Page) has been followed to ensure that correct generic assignments have been employed. The classification of Fensome et al. (1993) for modern and fossil dinoflagellates has also been used.

References dealing with the following systematic text will not be acknowledged in the reference list. Alphabetical list of all recovered taxa with reference to their position in the quantitative charts below as follows:

4.2 Alphabetic list of palynomorph

Numbers in the parentheses refer to position of taxa on the quantitative chart, the first number is for the Abu Tunis 1x borehole, and the second number is for the BB-80-1 borehole, with the empty parentheses denoting absence of a taxon in a borehole.

Spores

Aequitriradites norrissii Backhouse, 1988 (40).

Aequitriradites spinulosus (Cookson & Dettmann) Cookson & Dettmann, 1961 (29).

Aequitriradites verrucosus (Cookson & Dettmann) Cookson & Dettmann, 1961 (47).

Appendicisporites erdtmanii Pocock, 1964 (50).

Appendicisporites sp. (34).

Auritulinasporites intrastriatus Nilsson, 1958 (55).

Auritulinasporites scanicus Nilsson, 1958 (53).

Balmeisporites cf. *holodictyus* Cookson & Dettmann, 1958 (9).

Balmeisporites longirimosus Kondinskaya, 1966 (20).

Biretisporites potoniaei Delcourt & Sprumont, 1955 (30).

Balmeisporites spp. (25), (4).

Cibotiidites cf. *tuberculiformis* (Cookson) Srivastava, 1977 (57).

Cibotiumspora jurienensis (Balme) Filatoff, 1975 (37).

Cicatricosisporites orbiculatus Singh, 1964 (4), (1).

Cicatricosisporites sinuosus Hunt, 1985 (13).

Cicatricosisporites spp. (7), (6).

Concavisporites spp. (19).

Concavissimisporites punctatus (Delcourt & Sprumont) Brenner, 1963 (10).

Concavissimisporites variverrucatus Singh, 1964 (58).

Concavissimisporites spp. (11).

Crybelosporites brenneri Playford, 1971 (32).

Crybelosporites pannuceus (Brenner) Srivastava, 1977 (2), (2).

Crybelosporites striatus (Cookson & Dettmann) Dettmann, 1963 (46).

Deltoidospora australis (Couper) Pocock, 1970 (38).

Deltoidospora concavus Bolkhovotina, 1956 (49).

Deltoidospora crassexina (Nilsson) Lund, 1977 (23).

Deltoidospora hallii Miner, 1935 (5).

Deltoidospora minor (Couper) Pocock, 1970 (26).

Deltoidospora psilostomata Rouse, 1959 (33).

Deltoidospora toralis (Leschik) Lund, 1977 (16).

Deltoidospora spp. (1), (3).

Dictyophyllidits harrisii Couper, 1958 (28).

Dictyophyllidits sp. (36).

Echinatisporis varispinosus (Pocock) Srivastava, 1977 (54).

Gemmatrilites sp. (41).

Gleicheniidites feronensis (Delcourt & Sprumont) Delcourt & Sprumont, 1959 (39).

Gleicheniidites rasilis Bolkhovitina, 1968 (44).

Gleicheniidites senonicus Ross, 1949 (15).

Impardecispora apiverrucata (Couper) Venkatachala et al., 1969 (61).

Impardecispora uralensis (Bolkhovitina) Venkatachala et al., 1969 (60).

Ischyosporites areolatus (Singh) Fensome, 1987 (59).

Ischyosporites sp. (51).

Januasporites sp. (42).

Kyrtomisporis spp. (27).

Leptolepidites major Couper, 1958 (43).

Leptolepidites psarosus Norris, 1969 (45).

Matonisporites spp. (24).

Microfoveolatosporites skottsbergii (Selling) Srivastava, 1971 (22).

Murospora cf. *kosankei* Somers, 1952 (21).

Murospora cf. *mesozoica* Pocock, 1961 (35).

Murospora florida (Balme) Pocock, 1961 (17).

Murospora sp. 1 (18).

Murospora spp. (48), (7).

Pilosisporites trichopapillosus (Thiergart) Delcourt & Sprumont, 1955 (56).

Todisporites major Couper, 1958 (31).

Todisporites minor Couper, 1958 (14).

Trilobosporites hannonicus (Delcourt & Sprumont) Potonié, 1956 (52).

Trilobosporites laevigatus El-Beialy, 1994 (6), (8).

Triplanosporites sp. (3), (5).

Triporoletes reticulatus (Pocock) Playford, 1971 (12).

Verrucosisproites obscurilaesuratus Pocock, 1962 (8).

Gymnosperm pollen

Alisporites cf. *grandis* (Cookson) Dettmann, 1963 (62).

Arucariacites australis Cookson ex Couper, 1953 (69).

Balmeiopsis limbatus (Balme) Archangelsky, 1979 (63).

Callialasporites trilobatus (Balme) Sukh Dev, 1961 (82).

Callialasporites turbatus Schülz, 1967 (85).

Classopollis brasiliensis Herngreen, 1975 (---), (14).

Classopollis classoides Pflug, 1953 (64), (13).

Classopollis spp. (68).

Cycadopites carpentieri (Delcourt & Sprumont) Singh, 1964 (80).

Cycadopites fragilis Singh, 1964 (86).

Cycadopites cf. *fragilis* Singh, 1964 (87).

Cycadopites nitudus Norris, 1969 (90).

Cycadopites cf. *ovatus* Rouse, 1959 (88).

Cycadopites spp. (67).

Dicheiropollis etruscus Trevisan, 1972 (89).

Elaterocolpites castelainii Jardiné & Magloire, 1965 (70), (11).

Elateroplicites africaensis Herngreen, 1973 (---), (12).

Elaterosporites acuminatus (Stover) Jardiné, 1967 (73).

Elaterosporites klaszii (Jardiné & Magloire) Jardiné, 1967 (66), (9).

Elaterosporites protensus (Stover) Jardiné, 1967 (74).

Elaterosporites verrucatus (Jardiné & Magloire) Jardiné, 1967 (72).

Ephedripites irregularis Herngreen, 1973 (78).

Ephedripites spp. (65), (10).

Eucommidites treodsonii (Erdtman) Potonié, 1958 (79).

Exesipollenites sp. (83).

Galeacornea causea Stover, 1963 (76).

Gnetaceaepollenitess cf. *clathratus* Stover, 1964 (75).

Inaperturopollenites undulatus Weyland & Greifeld, 1953 (77).

Reyrea polymorpha Herngreen, 1974 (81).

Sofrepites legouxiae Jardiné, 1967 (71).

Taxacites sahariensis Reyre, 1973 (84).

Angiosperm pollen

Afropollis jardinus Doyle et al., 1982 (92), (15).

Afropollis aff. *jardinus* Doyle et al., 1982 (122).

Afropollis kahramanensis Ibrahim & Schrank 1995 (98), (20).

Afropollis operculatus Doyle et al., 1982 (126).

Afropollis zonatus Doyle et al., 1982 (128).

Afropollis aff. *zonatus* Doyle et al., 1982 (127).

Afropollis sp. B Doyle et al., 1982 (130).

Arecipites microfoveolatus Ibrahim, 2002a (140).

Cretacaeiporites densimurus Schrank & Ibrahim, 1995 (94), (19).

Cretacaeiporites mullerii Herngreen, 1973 (101).

Cretacaeiporites polygonalis (Jardiné & Magloire) Herngreen, 1973 (108).

Dichastopollenites ghazalatensis Ibrahim, 1996 (111).

Foveotricolpites gigantoreticulatus (Jardiné & Magloire) Schrank, 1987a (92).

*Papillopollis vancampoae K*edves & Pittau, 1979 (96).

Proteacidites cf. africaensis (Jardiné & Magloire) Schrank & Ibrahim, 1995 (91).

Retiacolpites columellatus Schrank in Schrank & Mahmoud, 2002 (134).

Retimonocolpites bueibensis Ibrahim, 2002a (135).

Retimonocolpites ghazalii Ibrahim, 2002a (115).

Retimonocolpites matruhensis Penny, 1986 (131).

Retimonocolpites matruhensis-Retimonocolpites ghazalii complex (132)

Retimonocolpites pennyi Schrank & Mahmoud, 2002 (136).

Retimonocolpites variplicatus Schrank & Mahmoud, 1998 (97), (18).

Retimonocolpites textus (Norris) Singh, 1983 (105).

Retimonocolpites sp. 1 Schrank & Mahmoud, 2002 (139).

Retimonocolpites sp. 1 (138).

Retimonocolpites sp. (---), (22).

Rousea brenneri Singh, 1983 (106).

Rousea delicipollis Srivastava, 1977 (100).

Rousea cf. *miculipollis S*rivastava, 1975 (103).

Rousea sp. (---), (23).

Stellatopollis barghoornii Doyle in Doyle et al., 1976 (117).

Stellatopollis bituberensis Penny, 1986 (137).

Stellatopollis dejaxii Ibrahim, 2002a (120).

Stellatopollis densiornatus (Lima) Ward, 1986 (118).

Stellatopollis doylei Ibrahim, 2002a (125).

Stellatopollis hughesii Penny, 1986 (129).

Stellatopollis limai Ibrahim, 2002a (121).

Stellatopollis spp. (124), (17).

Stephanocolpites sp. (116).

Striatopollis cf. *trochuensis (*Srivastava) Ward, 1986 (119).

Tetracolpites sp. (123).

Tetraporopollenites sp. (95).

Tricolpites cf. *crassimurus* (Groot & Penny) Singh, 1971 (112).

Tricolpites micromunus (Groot & Penny) Singh, 1971 (110).

Tricolpites parvus Stanley, 1965 (107).

Tricolpites sagax Norris, 1967 (114).

*Tricolpites vulgaris (*Pierce) Srivastava, 1969 (104).

Tricolpites spp. (93), (16).

Tricolporopollenites sp. (99), (21).

Triporites spp. (102), (24).

Triporopollenites spp. (109).

Tucanopollis annulatus Schrank in Schrank & Mahmoud, 2002 (133).

Pollen tetrads

Classopollis sp. (144).

Cretacaeiporites densimurus Schrank & Ibrahim, 1995 (141).

Droseridites baculites Ibrahim, 1996 (142).

Droseridites senonicus Jardiné & Magloire, 1965 (143).

Freshwater algae

Botryococcus sp. (147), (27).

Chomotriletes minor (Kedves) Pocock, 1970 (148).

Ovoidites parvus (Cookson & Dettmann) Nakoman, 1966 (145), (26).

Pediastrum sp. (149), (25).

Fungal fruiting body (146), (28).

Dinoflagellate cysts

Aptea polymorpha Eisenack, 1958a (193).

Canningia senonica Clarke & Verdier, 1967 (152).

Cannosphaeropsis utinensis Wetzel, 1933b (169).

Chatangiella madura Lentin & Williams, 1976 (154).

Chlamydophorella discreta Clarke & Verdier, 1967 (164).

Circulodinium brevispinatum (Millioud) Fauconnier in Fauconnier & Masure, 2004 (202).

Circulodinium brevispinosum (Pocock) Jansonius, 1986 (205).

Circulodinium cf. *brevispinosum* (Pocock) Jansonius, 1986 (213).

Circulodinim distinctum (Deflandre & Cookson) Jansonius, 1986 (173).

Circulodinium cf. *attadalicum* (Cookson & Eisenack) Helby, 1987 (210).

Circulodinium spp. (204), (38).

Coronifera albertii Millioud, 1969 (174), (36).

Coronifera oceanica Cookson & Eisenak, 1958 (170), (43).

Coronifera tubulosa Cookson & Eisenak, 1974 (177), (35).

Coronifera spp. (186).

Cribroperidinium edwardsii (Cookson & Eisenack) Davey, 1969 (181).

Cribroperidenium sp. (183), (45).

Cyclonephelium vannophorum Davey, 1969 (212).

Cyclonephelium cf. *vannophorum* Davey, 1969 (211).

Dinogymnium denticulatum (Alberti) Evitt et al., 1967 (162).

Dinogymnium spp. (155).

Dinopterygium tuberculatum (Eisenack & Cookson) Stover & Evitt, 1978 (---), (33).

Downiesphaeridium sp. (165).

Eucladinium gambangense (Cookson & Eisenack) Stover & Evitt, 1978 (166).

Exochosphaeridium bifidum (Clarke & Verdier) Clarke et al., 1968 (153).

Florentinia berran Below, 1982 (171), (31).

Florentinia clavigera (Deflandre) Davey & Verdier, 1973 (---), (40).

Florentinia cooksoniae (Singh) Duxbury, 1980 (201).

Florentinia laciniata Davey & Verdier, 1973 (176), (44).

Florentinia mantellii (Davey & Williams) Davey & Verdier, 1973 (172), (34).

Florentinia radiculata (Davey & Williams) Davey & Verdier, 1973 (---), (48).

Florentinia spp. (167), (29).

Isabelidinium acuminatum (Cookson & Eisenack) Stover & Evitt, 1978 (163).

Litosphaeridium siphoniphorum (Cookson & Eisenack) Davey & Williams, 1966b (159).

Muderongia aequicorna Århus in Århus et al., 1990 (216).

Muderongia pariata Duxbury, 1983 (198).

Muderongia tomaszowensis Alberti, 1961 (203).

Muderongia spp. (206), (49).

Odontochitina ancala Bint, 1986 (200).

Odontochitina operculata (Wetzel) Deflandre & Cookson, 1955 (151), (37).

Odontochitina costata Alberti, 1961 (156).

Odontochitina porifera Cookson, 1956 (157).

Odontochitina spp. (209), (46).

Oligosphaeridium albertense (Pocock) Davey & Williams, 1969 (178).

Oligosphaeridium asterigerum (Gocht) Davey & Williams, 1969 (196), (47).

Oligosphaeridium complex (White) Davey & Williams, 1966 (179).

Oligosphaeridium diluculum Davey, 1982 (197).

Oligosphaeridium patulum Riding & Thomas, 1988 (218).

Oligosphaeridium poculum Jain, 1977 (180).

Oligosphaeridium pulcherrimum (Deflandre & Cookson) Davey & Williams, 1966 (195).

Oligosphaeridium spp. (214).

Palaeoperidinium cretaceum (Pocock) Lentin & Williams, 1976 (187).

Phoberocysta neocomica (Gocht) Millioud, 1969 (217).

Phoberocysta spp. (215).

Pseudoceratium almohadense (Below) Lentin & Williams, 1989 (208).

Pseudoceratium anaphrissum (Sarjeant) Bint, 1986 (184).

Pseduoceratium expolitum Brideaux, 1971 (189).

Pseudoceratium pelliferum Gocht, 1957 (207).

Pseduoceratium retusum Brideaux, 1977 (190).

Pseudoceratium securigerum (Davey & Verdier) Bint, 1986 (185).

Pterodinium sp. (175).

Senegalinium aenigmaticum (Boltenhagen) Lentin & Williams, 1981 (158), (39).

Spinifereites spp. (150), (30).

Subtilisphaera perlucida (Alberti) Jain & Millepied, 1973 (188).

Subtilisphaera scabrata Jain & Millepied, 1973 (192).

Subtilisphaera senegalensis Jain & Millepied, 1973 (182).

Subtilisphaera terrula (Davey) Lentin & Williams, 1976 (194).

Subtilisphaera spp. (191), (32).

Surculosphaeridium cf. *longifurcatum* (Firtion) Davey et al., 1966 (161).

Tenua sp. (199).

Trichodinium castanea Deflandre, 1935 (160), (41).

Xiphophoridium alatum (Cookson & Eisenack) Sarjeant, 1966b (168), (42).

Acritarchs

Baltisphaeridium spp. (219).

Micrhystridium stellatum Deflandre, 1945a (223), (50).

Micrhystridium spp. (220), (52).

Veryhachium collectum Wall, 1965 (221), (51).

Veryhachium metum Davey, 1970 (222).

Veryhachium reductum (Deunff) Downie & Sarjeant, 1965 (225).

Veryhachium valiente Cramer, 1964 (224).

Microforaminiferal test linings (226), (53).

4.3 Taxonomy

4.3.1 Spores

Genus: ***Deltoidospora*** Miner, 1935 emend. Van Buggenum, 1985

Type species: *Deltoidospora hallii* Miner, 1935, p. 618, pl. 24, fig. 7.

Deltoidospora hallii Miner, 1935

(pl. 1, fig. 7; pl. 2, fig. 5)

Diagnosis: Potonié (1956) provided diagnosis of the type species as follows: 33-39 µm, sides straight or slightly concave; rays Y mark 2/3 diameter or more; exine smooth.

Emendation: Danzé-Corsin & Laveine (1963) extended the description as follows: Trilete spores, ambitus concavely triangular to sub-circular; trilete mark distinct, rays at least 2/3 spore radius; exine two-layered, smooth or infrapunctate, with or without exinal folds (± kyrtome) along the tilete mark; 25-80 µm.

Remarks (1): Miner (1935) proposed the genus *Deltoidospora* to accommodate smooth deltoid or sub-deltoid spores without assigning a type species; later Potonié (1956) assigned *Deltoidospora hallii* as the type species. Similarly, Naumova (1939) proposed the genus *Leiotriletes* to accommodate smooth trilete spores without assigning a type species, where Potonié & Kremp (1954) emended the genus to encompass smooth trilete spores with concave or convex sides and designated *Leiotriletes sphaerotriangulus* (Loose) Potonié & Kremp, 1954 as the type species. Couper (1953) proposed the valid genus *Cyathidites* to accommodate smooth trilete spores with more or less concave ambs. Pocock (1970) suggested that the genera *Leiotriletes* and *Cyathidites* are very similar regardless of the difference in grain size, and therefore the genera *Leiotriletes* and *Cyathidites* are synonyms. Srivastava (1977) argued that the differentiation between *Deltoidospora* and *Cyathidites* based on striate or concave ambs (e.g. Delcourt et al., 1963; Dettmann, 1963) or on differences in exine thickness (e.g. Singh, 1964) is

unjustified and the genera *Deltoidospora* and *Cyathidites* should be viewed as synonyms. As *Deltoidospora* was proposed before the nomenclatural rules of the ICBN 1958, the name *Deltoidospora* is conserved as the senior synonym of *Cyathidites* and *Leiotriletes* based on the rule of priority (Pocock, 1970; Srivastava, 1977), which will be followed in the present study. *Deltoidospora hallii* is distinguished from *Deltoidospora psilostomata* by its smaller size 30-40 µm.

Remarks (2): *Deltoidospora psilostomata* is found here to be very similar to *Deltoidospora australis* and is just larger in size than *Deltoidospora minor*. This suggests that all the three species may be synonyms, and this may be due to the difficulty in the early 1940's to 1960's where scientific communication among the palynostratigraphers and publication availablity were limited, which led to a wide spectrum of identification of similar if not the same species of *Deltoidospora*. This shows the need for a great refinement of all similar species. Until then and from a practical point of view, it is suggested to group all similar forms as *Deltoidospora* spp., as the majority of the *Deltoidospora* species have a long range and thus they are of no biostratigraphic significance.

Dimension: Maximum diameter (8 specimens) 38 (41) 45 µm.

Deltoidospora australis (Couper) Pocock, 1970

(pl. 1, fig. 9; pl. 2, fig. 1)

1953: *Cyathidites australis* Couper, p. 27, pl. 2, fig. 11.

1970: *Deltoidospora australis* (Couper) Pocock, p. 28, pl. 5, fig. 38.

Description: Trilete spore, amb triangular with slightly concave sides. Exine smooth to weakly punctuate punctate, 1.5-2 µm thick. Laesura at least 2/3 spore radius.

Dimension: Maximum equatorial diameter (5 specimens) 53 (57) 62 µm.

Deltoidospora crassexina (Nilsson) Lund, 1977

(pl. 4, fig. 4)

1958: *Concavisporites crassexinus* Nilsson, p. 35, pl. 1, fig. 11.

1977: *Deltoidospora crassexina* (Nilsson) Lund, p. 51, pl. 1, fig. 4; pl. 12, fig. 8.

Description: Trilete spore, amb triangular with concave sides. Exine smooth to weakly scabrate, 1.5-2 µm thick. Laesura distinct almost reaching equator with raised lips, trilete mark rays delineated with thick strongly concave 3.5-4 µm labra gaping from each other at the centre of the trilete mark and becoming closer to each other and nearly disappearing near the apices.

Dimension: Maximum diameter (2 specimens) 35 (42.5) 50 µm.

Deltoidospora concavus Bolkhovotina, 1956

(pl. 2, fig. 3)

Description: Trilete spore, amb triangular concave with pointed convex apices. Exine smooth to weakly punctuate, 1.5-2.5 µm thick. Laesura simple slit reaching the equator.

Dimension: Maximum diameter (2 specimens) 54 (74) 90 µm.

Deltoidospora minor (Couper) Pocock, 1970

(pl. 3, fig. 3)

1953: *Cyathidites minor* Couper, p. 28, pl. 2, fig. 13.

1970: *Deltoidospora minor* (Couper) Pocock, p. 28, pl. 5, fig. 3.

Description: Trilete spore, amb triangular with straight to slightly concave sides. Exine smooth to weakly punctuate, 1-2 µm thick. Laesura simple, 2/3 spore radius.

Remarks: *Deltoidospora minor* is distinguished from *Deltoidospora australis* by its smaller size (25-45 µm).

Dimension: Maximum diameter (4 specimens) 38 (40) 42 µm.

Deltoidospora psilostomata Rouse, 1959

(pl. 2, figs. 2, 4, 12)

Description: Trilete spore, amb triangular with straight to slightly concave sides. Exine smooth to weakly punctuate, 2-3 µm thick. Laesura simple slit reaching the equator.

Dimension: Maximum diameter (5 specimens) 40 (49) 58 µm.

Deltoidospora toralis (Leschik) Lund, 1977

(pl. 1, fig. 5; pl. 2, fig. 9; pl. 4, figs. 2, 3)

1955: *Laevigatosporites toralis* Leschik, p. 12, pl. 1, fig. 9.

1977: *Deltoidospora toralis* (Leschik) Lund, p. 49, pl. 1, figs. 2, 3.

Description: Trilete spore, amb triangular, sides straight to slightly concave. Exine smooth, 1-1.5 µm thick. Laesura distinct, almost reaching equator with raised lips, trilete mark rays delineated with concave labra very close to centre of the trilete mark, thicken in the interradial area (4-5 µm), becoming thinner (1.5-2 µm) and broader near the apices to continue around the whole apex.

Dimension: Maximum diameter (6 specimens) 34 (41) 45 µm.

Genus: ***Dictyophyllidites*** Couper, 1958 emend. Dettmann, 1963

Type species: *Dictyophyllidites harrisii* Couper, 1958, p. 140, pl. 21, figs. 5, 6.

Dictyophyllidites harrisii Couper, 1958

(pl. 1, fig. 1)

Description: Trilete spore, amb triangular with slightly concave sides. Exine smooth 1.5-2 µm thick. Laesura distinct, reaching the equator with raised lips bounded by parallel labra.

Remarks: *Dictyophyllidites* is distinguished from *Deltoidospora* by laesura enclosed within membranous elevated lips (Dettmann, 1963).

Dimensions: Maximum diameter (5 specimens) 42 (44.5) 47 µm.

Genus: ***Auritulinasporites*** Burger, 1966

Type species: *Auritulinasporites scanicus* Nilsson, 1958, p. 35, pl. 1, fig. 16.

Auritulinasporites scanicus Nilsson, 1958

(pl. 1, fig. 4)

Description: Trilete spore, amb triangular, sides straight to slightly convex. Exine smooth, 0.5-1.5 µm thick. Laesura distinct, at least 2/3 spore radius with raised lips, trilete mark rays delineated with thick strongly concave, 3.5-4 µm labra, usually projecting at apices.

Remarks: *Auritulinasporites* is distinguished from *Gleicheniidites* by thick labra enclosing trilete mark rays, and lack of exinal thickening on distal face.

Dimension: Maximum diameter (4 specimens) 28 (38.5) 53 µm.

Auritulinasporites intrastriatus Nilsson, 1958

(pl. 2, fig. 8)

Remarks: *Auritulinasporites intrastriatus* differs from *Auritulinasporites scanicus* in having thicker exine 2-3 µm and thicker labra (5-6 µm) delineating the trilete mark rays.

Dimension: Maximum diameter (2 specimens) 37 (41) 45 µm.

Genus: ***Gleicheniidites*** Ross, 1949 ex Delcourt & Sprumont, 1955

emend. Dettmann, 1963

Type species: *Gleicheniidites senonicus* Ross, 1949, p. 31, pl. 1, fig. 3.

Gleicheniidites senonicus Ross, 1949

(pl. 3, fig. 2; pl. 5, fig. 9)

Description: Trilete spore, amb triangular, sides slightly concave. Exine smooth, 2-2.5 µm thick at corners increasing to 3.5-4 µm at sides. Laesura distinct, reaching equator with raised lips. Proximal face shows exinal thickenings which delineate trilete mark rays and disappear at corners, distal face shows strong concave exinal thickening without interruption at corners.

Remarks: *Gleicheniidites* is distinguished form *Concavisporites* by more variation in wall thickness, as the spore exine in equatorial regions is usually of unequal thickness (Krutzsch, 1959), and is also distinguished by having exinal thickenings on the distal face.

Dimension: Maximum diameter (4 specimens) 50 (54.5) 60 µm.

Gleicheniidites feronensis (Delcourt & Sprumont) Delcourt & Sprumont, 1959

(pl. 3, figs. 1, 4)

1957: *Triremisporites feronensis* Delcourt & Sprumont, p. 61, pl. 2, fig. 9; pl. 3, figs. 15, 23-25; non pl. 3, figs. 14a, b.

1959: *Gleicheniidites feronensis* (Delcourt & Sprumont) Delcourt & Sprumont, p. 34.

Remarks: *Gleicheniidites feronensis* differs from *Gleicheniidites senonicus* in having a more irregularly triangular amb with strongly undulating concave sides, protruding corners, and distal face shows strong concave exinal thickenings that disappears at corners.

Dimension: Maximum diameter (2 specimens) 38 (40) 42 µm.

Gleicheniidites rasilis Bolkhovitina, 1968

(pl. 5, fig. 18)

Rekarks: Both *Gleicheniidites rasilis* and *Gleicheniidites feronensis* have irregularly triangular ambs with concave and undulate sides. But *G. rasilis* differs in having rounded corners and very thick (5 µm) exine at corners that increases up to 18 µm thick at interradial sides.

Dimension: Maximum diameter (1 specimen) maximum 85 µm.

Genus: ***Murospora*** Somers, 1952

Type species: *Murospora kosankeii* Somers, 1952, p. 21, fig. 13a.

Remarks: *Murospora* spores are frequently misidentified in the local Cretaceous records of Egypt as *Matonisporites*; the latter spores are not as large as *Murospora*. The larger diameter of *Murospora* specimens in the present material (58-87 µm) and their patinate structure distinguishes them from *Matonisporites* (Mahmoud et al., 2007).

Murospora cf. ***kosankei*** Somers, 1952

(pl. 5, fig. 17)

Description: Trilete spore, amb triangular with concave sides and rounded apices. Nexinal body triangular, concave with 5-7 µm thick wall enveloped by a very thick patina. Laesura with prominent non-elevated lips extending to full radius of nexinal body.

Remarks: The form of the present material shows great similarity with *Murospora kosankei* except the specimen has a greater diameter (type species 23-

31 µm; Pocock's (1961a) comparative material of type species: 40 µm), and by the exinal thickenings (13 µm wide) which flank the laesural lips.

Dimension: Maximum whole grain diameter (1 specimen) 70 µm, nexinal body diameter 63 (64) 65 µm.

Murospora florida (Balme) Pocock, 1961

(pl. 3, fig. 19; pl. 5, figs. 12, 22)

1957: *Cingulatisporites florida* Balme, p. 26, pl. 5, figs. 60, 61.

1961: *Murospora florida* (Balme) Pocock, p. 123, pl. 1, figs. 6, 7.

Remarks: *Murospora florida* differs from *Murospora* cf. *kosankei* and *Murospora* cf. *mesozoica* in having a sub-triangular to sub-rounded amb with sides that are straight to strongly concave sides of highly variable thicknesses, and rounded to protruding apices.

Dimension: Maximum whole grain diameter (5 speimens) 52 (89) 100 µm, nexinal body diameter 50 (63) 73 µm.

Murospora cf. ***mesozoica*** Pocock, 1961

(pl. 5, fig. 20)

Description: Trilete spore, amb triangular with convex to slightly concave sides and rounded apices. Nexinal body triangular convex to slightly concave with a 2.5-3 µm thick wall enveloped by a very thick (4-8 µm) patina. Laesura straight with prominent non-elevated lips, extending to full radius of nexinal body.

Remarks: The form of the present material shows great similarity with *Murospora mesozoica* except the specimens have a greater diameter (type species: 35 µm) and some forms develop occasional exinal thickenings flanking the laesural lips.

Dimension: Maximum whole grain diameter (1 specimen) 65 (77) 92 µm, nexinal body diameter 57 (64.5) 74 µm.

Murospora sp. 1

(pl. 3, fig. 17; pl. 5, fig. 19)

Description: Trilete spore, amb sub-triangular to semi-circular with concave sides and broadly rounded apices. Nexinal body rounded triangular with 5-10 µm thick wall enveloped by thin patina. Laesura extend to full radius of nexinal body with prominent non-elevated lips, occasionally exinal thickenings flanking the raised lips may develop.

Remarks: This form differs from *Murospora florida* in having a more rounded amb, a spore wall of uniform thickness, and a thin patina. *Deltoidospora equiexinus* (as *Matonisporites equiexinus* Couper) Muir, 1964 differs from *Murospora* sp.1 in having a smaller diameter (40-68 µm) and a thinner wall (2.5-3.5 µm).

Dimension: Maximum diameter (7 specimens) 95 (94) 105 µm.

4.3.2 Gymnosperm pollen

A. Circumpolles pollen

Genus: ***Classopollis*** Pflug 1953 emend. Pocock & Jansonius, 1961

Type species: *Classopollis classoides* Pflug, p. 91, pl. 16, figs. 29-31.

Classopollis classoides Pflug, 1953

(pl. 1, fig. 18)

Description: Spherical to circular in equatorial section. Monoporate with a circular distal pore. Exine ornamented by striate band or girdle surrounding the equator, intexine thin, laevigate, occasionally showing a small trilete mark at the proximal pole, rays of trilete mark about 3 μm long.

Remarks: The use of the generic names *Circulina* Malyavkina, 1949, *Corollina* Malyavkina, 1949 and *Classopollis* Pflug, 1953 in the literature has led to a great confusion amongst palynologists. Klaus (1960) and Cornet & Traverse (1975) regarded *Classopollis* as a junior synonym of *Corollina*. Traverse (2004) proposed conservation of the name *Classopollis* against *Circulina* and *Corollina* because the original description of *Classopollis* Pflug, 1953 was provided with good illustrations. In Skog's (2005) report, the proposal to conserve *Classopollis* against *Circulina* and *Corollina* was accepted. Accordingly, in the present study all forms will be treated under the generic name *Classopollis.*

Dimension: Maximum diameter (5 specimens) 31 (32) 35 μm.

Classopollis brasiliensis Herngreen, 1975

(pl. 10, fig. 15)

1973: *Classopollis jardinei* Herngreen, p. 544, pl. 2, figs. 2, 6.

1975: *Classopollis brasiliensis* Herngreen, 1975.

Remarks: *Classopollis brasiliensis* differs from *Classopollis classoides* in having a larger diameter and laking a proximal trilete mark or distal pore.

Dimension: Maximum length (1 specimen) 45 μm, breadth 26 μm.

Genus: ***Dicheiropollis*** Trevisan, 1972

Type species: *Dicheiropollis etruscus* Trevisan, p. 568, pls. 1-15.

Dicheiropollis etruscus Trevisan, 1972

(pl. 1, figs. 14-16)

Description: A peculiar structure consisting of a pair of pollen grains connected together with two bundles of delicate strings. Individual grains have a hemispherical shape; proximal face invaginated and bordered near the equator with a C-shaped exinal thickening and inner striations. Exine is 1.5-2 μm thick, that thickens to 3-4 μm at the C-shaped equatorial thickening, with inner layer showing packed pillar-like elements ending freely inward, fusing together at the equatorial thickening to form striae running parallel to the equator. Release of individual grains is frequent. No pore, rimula, or triangular mark detected.

Remarks: Trevisan (1972) studied the wall structure of the *Classopollis* and *Dicheiropollis* using the transmission electron microscope and discovered a great similarity in the wall structure between the two

genera: a refractive inner layer and an outer complex layer with pillar-like elements and striae. Accordingly, she suggested that *Dicheiropollis* was botanically close to plants which produced *Classopollis* pollen grains, and it possibly belonged to the conifer family Cheirolepidaceae.

Dimension: Individual grain maximum equatorial diameter (3 specimens) 36 (38) 40 µm.

B. Polyplicate pollen and allies

Genus: ***Ephedripites*** Bolkhovitina, 1953 ex Potonié, 1958

Type species: *Ephedripites mediolobatus* Bolkhovitina, 1953 ex Potonié, 1958, p. 60, pl. 9, fig. 15.

Diagnosis: Outline elliptical, narrow ends not always ogival; more than five longitudinal ribs, in part more than ten; no zig-zag line discernible. The exine may show a tear between the ribs (Potonié, 1958).

Remarks: Singh (1964, 1971) considered the genus *Ephedripites* invalid according to Article 34 (1) of the International Code of Botanical Nomenclature (1959) of Lanjouw et al., (1961) because Bolkhovitina (1961) stated that the type species *Ephedripites mediolobatus* should be transferred to the genus *Schizaea*. However, Jansonius & Hills (1976, card 944) stated that transferring the type species *E. mediolobatus* to another genus does not invalidate the generic name *Ephedripites*. Accordingly, the generic name *Ephedripites* will be used in the present study.

Ephedripites irregularis Herngreen, 1973

(pl. 10, fig. 14)

Description: Polyplicate pollen of irregular ellipsoidal shape and with smooth 5-7 μm thick, leaf-like ridges running parallel to the long axis.

Remarks: *Ephedripites irregularis* shows great similarity to *Alaticolpites limai* Regali et al., 1974, however, *Ephedripites irregularis* is characterised by its smaller size (*Alaticolpites limai*: 70-72 x 48-68 μm) and irregular from the ellipsoidal shape and radial symmetry of *Alaticolpites limai*.

Dimension: Maximum length (1 specimen) 40 μm, breadth 34 μm; ridge length 20 (21) 24 μm, width 7 (10) 13 μm.

C. Elaterate pollen

Remarks: Dino et al., (1999) pointed out that the great similarity in exine ultrastructure and wall stratification between the Cretaceous ephedroid pollen *Equisetosporites* from Brazil and the elaterate pollen (*Sofrepites, Elaterosporites* and *Elateroplicites*) revealed in their study, and the similarity in morphology and ultrastructure between Cretaceous *Ephedripites* of Italy and pollen of Gnetales (*Ephedra* and *Welwitschia*) revealed by Trevisan (1980), suggests that the elaterate and polyplicate pollen are botanically related and of gnetalean origin.

Genus: ***Elaterocolpites*** Jardiné & Magloire, 1965

Type Species: *Elaterocolpites castelainii* Jardiné & Magloire, 1965, p. 206, pl. 4, figs. 6, 7.

Elaterocolpites castelainii Jardiné & Magloire, 1965

(pl. 10, figs. 5-8)

Description: Pollen grains of ellipsoidal to sub-spherical shape carrying 10 simple cylindrical appendices which broaden towards their free end. Grain wall thin, simple and smooth to scabrate.

Remarks: In Jardiné's (1967) emended diagnosis he distinguished two forms of *Elaterocolpites castelainii*: Form 'A' that represents immature grains having a narrow ring structure surrounding the whole grain, and Form 'B' that represents mature grains with well-developed appendages. Dino et al., (1999) through their study of Brazilian Albian-Cenomanian material identified another form, Form 'C' which is bigger in size and has two solid globular expansions at the end of the long axis of the grain. In the present material all recorded specimens of *Elaterocolpites castelainii* belong to Form 'B'.

Dimensions: Maximum main body length (7 specimens) 31 (35.5) 40 µm; appendage length 18 (19.5) 23 µm, width 5 (5.5) 7 µm.

Genus: ***Elateroplicites*** Herngreen, 1973

Type species: *Elateroplicites africaensis* Herngreen, 1973, p. 550, pl. 5, figs. 5-7.

Elateroplicites africaensis Herngreen, 1973

(pl. 10, figs. 1-4)

1967: Incertae sedis Form A, Jardiné, p. 255, pl. 3, figs. K-M.

1973: *Elateroplicites africaensis* Herngreen, 1973, p. 550, pl. 5, figs. 5-7.

Description: Ellipsoidal polyplicate grains with 3-4 twisted ridges 2.5 (4) 13 μm wide and 1.5-2.5 μm thick separated by irregular narrow furrows. Grains carry 2-4 appendages which form the continuation of the ridges.

Remarks: Dino et al. (1999) studied *Elateroplicites africaensis* with light, scanning and transmitted electron microscopy from the Brazilian and Ecuadorian material and provided the following important obervations: (1) Appendages always turn towards one surface of the grain, suggesting that the opposite surface may represents the internal (proximal) face. (2) The ribs surrounding the longitudinal axis converge and may be fused at the end of the axis in a manner similar to ribs of polyplicate forms (i.e. *Ephedripites* and *Equisetosporites*). (3) Grains lack definite apertures, however, the two expansions (up to 12 μm) in the foot layer beneath the ribs on opposite sides may have served as the germinal apparatus.

Dimension: Maximum main body length (4 specimens) 30 (36) 44 μm, breadth 19 (21.5) 24 μm; appendage length 24 (24.5) 27 μm, width 2.5 (3.5) 4 μm.

Genus: ***Elaterosporites*** Jardiné, 1967

Type species: *Elaterosporites verrucatus* (Jardiné & Magloire) Jardiné, 1967, p. 244, pl. 2, figs. E-G; pl. 3, fig. G.

Elaterosporites verrucatus (Jardiné & Magloire) Jardiné, 1967

(pl. 9, figs. 1, 3)

1965: *Galeacornea verrucata* Jardiné & Magloire, p. 204, pl. 3, figs. 28-31.

1967: *Elaterosporites verrucatus* (Jardiné & Magloire) Jardiné, p. 244, pl. 2, figs. E-G; pl. 3, fig. G.

Description: Grains with ellipsoidal plano-convex to sub-hemispherical body with three U-shaped horns implanted on the convex distal face. Proximal face flat or depressed, bounded by 3-8 µm wide annular ring structure parallel to the equator ending with protruding ends parallel to the long axis. These three U-shaped appendages with their middle part running parallel to the longest axis; one is placed over the distal pole, the other two are placed laterally. The appendages are solid, circular in cross section and of uniform diameter. Exine is granulate to verrucate.

Remarks: Jansonius (1990) in Jansonius & Hills (1990, card 4657) argued that the specimens of *Elaterosporites verrucatus* photographed by Jardiné (1967) in his pl. 3, fig. G shows grains in a tetrad, arranged with their flat surface facing out, and thus the flat surface should be distal face and the convex horn-bearing surface should be the proximal face.

Dimension: Maximum main body length (2 specimens) 40 (53.5) 67 µm, breadth 30 (32) 34 µm; appendage length 33 (36.5) 40 µm, width 3.5 (4.5) 5.5 µm.

Elaterosporites acuminatus (Stover) Jardiné, 1967

(pl. 9, figs. 2, 8)

1963: *Galeacornea acuminata* Stover, p. 89, pl. 2, figs. 8-10; text-fig. 6.

1967: *Elaterosporites acuminatus* (Stover) Jardiné, p. 246, pl. 3, figs. D, E.

Description: Grians with ellipsoidal plano-convex to sub-hemispherical body with three U-shaped horns implanted on the convex distal face. Proximal face flat or depressed, bounded by 8-12 µm wide annular ring structure parallel to the equator, commonly appears acuminate in lateral view. The three U-shaped appendages have their middle part running parallel

to the longest axis, one is placed over the distal pole, the other two are placed laterally. The appendages are solid, circular in cross section, of uniform diameter, and with a sharply tapering end. Exine is densely and uniformly packed with spines 4-6 µm high and 2.5-3 µm wide.

Dimension: Maximum main body length (2 specimens) 40 (51) 62 µm, breadth 40 (47.5) 55 µm; appendage length 32 (36) 40 µm.

Elaterosporites klaszii (Jardiné & Magloire) Jardiné, 1967

(pl. 9, figs. 5-7, 9-16)

1965: *Galeacornea klaszi* Jardiné & Magloire, p. 205, pl. 4, figs. 2, 3.

1967: *Elaterosporites klaszi* (Jardiné & Magloire) Jardiné, p. 246, pl. 3, figs. H-N.

Description: Grains with ellipsoidal plano-convex to sub-hemispherical body with three U-shaped horns implanted on the convex distal face. Proximal face flat or depressed, bounded by 4-8 µm wide annular ring structure parallel to the equator. The three U-shaped appendages have their middle part running parallel to the longest axis, one is placed over the distal pole, the other two are placed laterally. The appendages are solid, circular in cross section and of uniform diameter. Exine is smooth.

Remarks: *Elaterosporites klaszii* differs from species of *Galeacornea* in lacking a definite aperture, in contrast to *Galeacornea* which has a well-defined one. Jardiné (1967) distinguished *Elaterosporites* from *Galeacornea* by its bilateral symmetry, number and shape of appendages (in *Galeacornea* there is a solid Y-shaped appendage).

Dimensions: Maximum main body length (7 specimens) 43 (52) 62 µm, breadth 22 (32) 34 µm; appendages length 20 (23.5) 27 µm, width 3 (4) 5 µm.

Elaterosporites protensus (Stover) Jardiné, 1967

(pl. 9, fig. 4)

1963: *Galeacornea protensa* Stover, p. 88, pl. 2, figs. 11, 15; text-fig. 5.

1967: *Elaterosporites protensus* (Stover) Jardiné, p. 244, pl. 3, figs. A-C.

Remarks: Stover (1963) distinguished *Elaterosporites protensus* from *Elaterosporites acuminatus* by its larger size (*Elaterosporites acuminatus*: 52 x 28 µm), greater ring width, and appendages ending with round tips rather than with sharply tipped ends as in the latter species. Dino et al., (1999) suggested that the immature unexpanded pollen grains photographed by Stover (1963) in pl. 2, fig. 15 are aligned with their sculptured horn-bearing surface towards the tetrad centre, and accordingly the convex surface should be the proximal face contrasting Stover's (1963) suggestion that the unexpanded grains are aligned with their flat proximal surface towards the tetrad centre.

Dimension: Maximum main body length (1 specimen) 69 µm, breadth 38 µm; appendage length and width undetermined due to grain orientation.

Genus: ***Galeacornea*** Stover, 1963

Type species: *Galeacornea clavis* Stover, 1963, p. 86, pl. 1, figs. 1-15; text-figs. 2, 3.

Galeacornea causea Stover, 1963

(pl. 10, fig. 10)

Description: Ellipsoidal grain with a sheet-like crescent-shaped flap crossing the distal surface diagonally. Body surrounded completely by a zona of

more or less elliptical outline with its major axis oblique to the body's axis. Wall of the flap and zona is smooth.

Remarks: In Stover's (1963) original description of the type species, he identified a narrow slit-like aperture in the proximal face. In the present material the aperture could not be identified due to grain orientation.

Dimension: Maximum length (1 specimen) 55 μm, breadth 31 μm.

Genus: ***Sofrepites*** Jardiné, 1967

Type species: *Sofrepites legouxiae* Jardiné, 1967, p. 255, pl. 3, figs. H, J; text-fig. 5.

Sofrepites legouxiae Jardiné, 1967

(pl. 9, figs. 17-21)

Description: Grain with ellipsoidal to sub-spherical shape with 2-3 simple short appendages located at the ends of the longitudinal axis, or at the apices of the triangular outline. Exine is smooth and shows frequent wall rupture and folding parallel to the longitudinal axis.

Remarks: The scanning electron microscope study made by Dino et al., (1999) on *Sofrepites legouxiae* from Brazilian material revealed that the species is a monocolpate pollen (p. 223, pl. 13, fig. 6; pl. 14, fig. 5), in contrast to Jardiné's (1967, p. 255) original description of the type species " .., often shows a torn area with thinned exine but no furrow or well defined germination structure; .. ".

Dimension: Maximum length (5 specimens) 38 (40) 42 μm, breadth 19 (21.5) 25 μm; appendage length 8 (11) 12 μm, width 5 (6.5) 7 μm.

4.3.3 Angiosperm pollen

A. Monosulcate and monoporate pollen

Genus: ***Retimonocolpites*** Pierce, 1961

Type species: *Retimonocolpites dividuus* Pierce, 1961, p. 47, pl. 3, fig. 87.

Retimonocolpites matruhensis Penny, 1986 - ***Retimonocolpites ghazalii*** Ibrahim, 2002a complex

(pl. 6, figs. 4, 8)

Remarks: The species *Retimonocolpites ghazalii* Ibrahim, 2002a shows great similarity under the light microscope to the species *Retimonocolpites matruhensis* Penny, 1986, where they share more or less the same features, such as, the grain outline and the aperture characteristics. Important diagnostic charateristics such as that of the reticulum cannot be determined under the light microscope because the two species have very minute reticula (0.7-1.4 μm wide lumina in *R. ghazalii* and 0.46-1.7 μm wide lumina in *R. matruhensis*). The species *R. matruhensis* is only differentiated from *R. ghazalii* by its smaller size; however, Schrank & Mahmoud (2002) extended its size range from 31.3-45.8 μm to 43-67 μm. As a result *R. matruhensis* falls within the size range 58-88 μm of *R. ghazalii*, consequently the use of the grain size under light microscope is not applicable to differenetiate the two species. Nevertheless, the scarcity of reticulate monocolpate pollen grains in the present material prohibited any attempt to study and differentiate these two taxa by using the scanning electron microscope. Therefore, specimens will be treated here according to their maximum diameter range as follows: ≤ 43-57 μm as *R. matruhensis*, 58-67 μm as R.

matruhensis-ghazalii complex, and ≥ 68-88 μm as *Retimonocolpites ghazalii*.

Angiosperm pollen	Dimensions	Shape	Other diagnostic features
Retimonocolpites ghazalii Ibrahim, 2002	L: 58 (65) 88 μm W: 32 (40) 44 μm	Elliptical with pointed ends to elongate oval	Lumina: 0.7-1.4 μm, polygonal of different size. Muri: 0.4-0.7 μm, with thick segments. Aperture: sulcus, simple slit running from pole to pole, narrow at ends and occasionally gaping at middle. L/W: 1.6
Retimonocolpites matruhensis Penny, 1986	L: 31.3 (37.2) 45.8 μm W: 20.0 (23.0) 25.2 μm [43 (51) 67 μm Schrank & Mahmoud, 2002]	Elliptical, blunt-ended to tapering sharply at poles	Lumina: 0.46 (1.2) 1.7 μm, rounded to polygonal, with occasional microlumina. Muri: 0.3 (0.5) 0.7 μm, with transverse ridges. Aperture: colpus, extending whole grain length, closed or slightly open at poles or gaping. L/W: 1.5 (1.6) 1.8

Table 4.1 Comparison of important taxonomic characteristics of *R. matruhensis* and *R. ghazalii*.

Description: Monocolpate elliptical to elongate oval pollen grains with pointed ends. Exine reticulate, composed of minute (0.5-1.7 μm) lumina separated by 0.3-0.7 μm thick muri. Colpus running whole grain length, narrow at the ends and occasionally gaping at the middle. Grains may show infrequent folding.

Dimensions: Maximium length (8 specimens) 58 (63) 67 μm, breadth 37 (42) 49 μm.

Retimonocolpites ghazalii Ibrahim, 2002a

(pl. 6, figs. 1, 2)

Dimension: Maximium length (7 specimens) 68 (76.5) 88 μm, breadth 25 (32) 36 μm.

Retimonocolpites matruhensis Penny, 1986

(pl. 6, figs. 3, 5)

Dimension: Maximium length (8 specimens) 43 (48) 57 μm, breadth 29 (31) 33 μm.

Retimonocolpites pennyi Schrank & Mahmoud, 2002

(pl. 6, figs. 9, 12)

Remarks: *Retimonocolpites pennyi* diffres from *Retimonocolpites textus* in having a larger overall size and larger lumina (Schrank & Mahmoud, 2002).

Dimensions: Maximum diameter (6 specimens) 33 (34) 36 μm.

Retimonocolpites variplicatus Schrank & Mahmoud, 1998

(pl. 6, fig. 7; pl. 12, figs. 13, 14)

1998: *Retimonocolpites variplicatus* Schrank & Mahmoud, p. 187, figs. 7u; 8a-e, j-k, m.

Description: Monocolpate elliptical to highly variable pollen grains. Exine thin, reticulate, composed of 1-3 μm wide lumina separated by 0.5-1 μm thick muri. Infrequent minute foveae less than 0.5 μm wide may occur at mural intersections. Exine thin (1 μm) thus the grains are often highly folded. Colpus extends over nearly the full length of the elongated grains, and ranges in form from closed and slit-like to wide, open, elliptical or irregular.

Remarks: Schrank & Mahmoud (1998) distinguished *R. variplicatus* from the type species *R. dividuus* and from other *Retimonocolpites* species by its large size 62 (82) 100 μm, strongly folded exine, and highly variable outline.

Dimensions: Maximum length (5 specimens) 61 (68) 79 μm, breadth 54 (55) 56 μm.

Retimonocolpites textus (Norris) Singh, 1983

(pl. 12, figs. 5, 6, 9-12)

Remarks: *Retimonocolpites textus* is distinguished from *Retimonocolpites reticulatus* by its larger overall size and larger lumina (Ward, 1986).

Dimensions: Maximum diameter (6 specimens) 22 (23) 24 μm.

Retimonocolpites sp. 1 Schrank & Mahmoud, 2002

(pl. 7, fig. 4)

Remarks: Monocolpate oval to sub-circular blunt-ended pollen grain. Exine 1 μm thick, consisting of a fine reticulum made of about 0.5 μm wide lumina of uniform size over the whole grain. Colpus extends from pole to pole with inward folding of exine. Schrank & Mahmoud (2002) identified a similar specimen of maximum diameter 42 μm under the LM/SEM from the upper Barremian rocks of the Dakhla Oasis of Egypt, which shares the same charactersitics of the present specimen under the light microscope.

Dimensions: Maximum length (1 specimen) 42 μm, breadth 30 μm.

Retimonocolpites sp. 1

(pl. 12, figs. 1, 2)

Description: Monocolpate spherical to elliptical pollen grain. Sexine columellate, and coarsely recticulate consisting of 4-7 μm wide polygonal lumina separated by about 1 μm thick muri covered by faint microspines or transverse ridges, which under the light microscope appear as minute dark points, with the lower surface of the muri bearing 3-4 μm tall pila-like columellae. The inner nexinal layer is spherical to elliptical, thin (1 μm), smooth and of a maximum diameter of 32 μm.

Remarks: This specimen interestingly shows a close match to *Retimonocolpites excelsus* Ward, 1986, however, the ornamented muri of the present sepcimen distinguishes it from the latter.

Dimension: Maximum diameter (1 specimen) 41 μm.

Genus: ***Stellatopollis*** Doyle in Doyle et al., 1976

Type species: *Stellatopollis barghoornii* Doyle in Doyle et al., 1976, p. 462, pl. 7, figs. 1-8; pl. 8, figs. 1-5; pl. 9, figs. 1-4.

Stellatopollis barghoornii Doyle in Doyle et al., 1976

(pl. 6, figs. 15, 16)

Description: Monosulcate elliptical pollen grains. Exine semitectate, reticulate, composed of 3-5 μm wide rounded lumina separated by broad muri (0.6-1.3 μm) bearing 4-8 (usually 6) supratectal projections of sub-triangular to occasionally elliptical or rarely irregular shape.

Remarks: *Stellatopollis barghoornii* is distinguished from *Stellatopollis densiornatus* only by muri that are densely packed with the supratectal elements (Ward, 1986), and from Stellatopollis bituberensis by its larger size, and by having supratectal projections of only triangular shape rather than triangular shape occasionally separated by elliptical to rectangular projections as in *Stellatopollis bituberensis*.

Dimension: Maximium length (7 specimens) 56 (68) 79 μm, breadth 42 (51) 56 μm.

Stellatopollis bituberensis Penny, 1986

(pl. 6, figs. 14, 19)

Remarks: Specimens of *Stellatopollis bituberensis* recorded in the present material show a larger maximum diameter than that described by Penny (1986: 27.1 (33.7) 43.2 μm). Schrank & Mahmoud (2002) also recorded 9 specimens of *Stellatopollis bituberensis* from the Dakhla Oasis, southern Egypt, from rocks of late Barremian age, which have larger maximum diameter of 31 (48) 68 μm. This could suggest extending the maximum size of *Stellatopollis bituberensis* to at least 64 μm.

Dimension: Maximum length (9 specimens) 45 (54) 64 μm, breadth 38 (44) 50 μm.

Stellatopollis dejaxii Ibrahim, 2002a

(pl. 7, figs. 6, 7)

Remarks: Ibrahim (2002a) differentiated *Stellatopollis dejaxii* from other species of *Stellatopollis* by its circular to sub-circular outline that densely packed with supratectal projections of globular, elliptical to rarely triangular

shape, and from *R. densiornatus* by its circular rather than oval outline, and larger projections.

Dimension: Maximum length (4 specimens) 40 (52) 60 μm, breadth 37 (39) 42 μm.

Stellatopollis doylei Ibrahim, 2002a

(pl. 7, fig. 2)

Remarks: *Stellatopollis doylei* is diffrentiated from *Stellatopollis barghoornii* by its smaller size and smaller supratectal projections (Ibrahim, 2002a).

Dimension: Maximum length (3 specimens) 38 (39.5) 43 μm, breadth 28 (29.5) 32 μm.

Stellatopollis hughesii Penny, 1986

(pl. 6, fig. 18; pl. 7, fig. 1)

Remarks: *Stellatopollis hughesii* is distinguished from other *Stellatopollis* species by its sub-circular outline, and polygonal to sub-rounded lumina separated by narrow muri bearing few triangular projections separated by numerous elliptical to rectangular projections.

Dimension: Maximum diameter (5 specimens) 30 (37) 48 μm.

Stellatopollis limai Ibrahim, 2002a

(pl. 7, fig. 3)

Remarks: Ibrahim (2002a) distinguished *Stellatopollis* limai from other *Stellatopollis* species by its narrow muri, large lumina, and widely separated projections.

Dimension: Maximum diameter (2 specimens) 35 (38) 41 μm, breadth 20 (23) 26 μm.

B. Zonosulcate pollen

Genus: ***Dichastopollenites*** May, 1975

Type species: ***Dichastopollenites reticulatus*** May, 1975, p. 532-533, pl. 1, figs. 1-9; pl. 2, figs. 1-6.

Dichastopollenites ghazalatensis Ibrahim, 1996

(pl. 6, figs. 11, 13, 17)

Description: Zonoculcate spherical pollen grains, usually spliting into two more or less equal hemispheres along the aperture. Sexine columellate, reticulate, with 2-4 μm polygonal lumina becoming smaller and uneven in size towards the equatorial aperture, separated by smooth 0.6-1.3 μm muri thick with their lower surface bearing 1-1.4 μm long columellae. The nexine layer is spherical, smooth and closely attached to the sexine. Aperture is an equatorial ring furrow running around the circumference of the grain.

Remarks: In the present material this species is frequently found split into individual hemispheres, and show a larger grain diameter than that recorded by Ibrahim (Ibrahim, 1996: 22 (28) 34 μm).

Dimension: Maximum diameter (6 specimens) 28 (36) 48 μm.

C. Zonisulculate and inaperturate reticulate pollen

Genus: ***Afropollis*** Doyle et al., 1982

Type species: *Afropollis jardinus* (Brenner) Doyle et al., 1982, p. 45, pl. 1, figs. 1-6; pl. 2, figs. 1-8.

Afropollis jardinus (Brenner) Doyle et al., 1982

(pl. 8, figs. 10-20)

1968: *Reticulatasporites jardinus* Brenner, p. 381, pl. 10, figs. 5, 6.

1982: *Afropollis jardinus* (Brenner) Doyle et al., p. 45, pl. 1, figs. 1-6; pl. 2, figs. 1-8.

Description: Inaperturate spheroidal pollen grains, heteropolar and with radial symmetry. Sexine non-columellate, reticulate to rugulo-reticulate separated over most of the grain surface from an inner dark and conspicuous to nearly invisible nexinal layer. Nexinal body spherical, thin, smooth, and of a diameter less than half that of the whole grain. Reticulum composed of 2-5 μm wide polygonal to irregular lumina separated by 0.5 μm thick muri. Muri usually sinuous with their upper surface segmented into simple or laterally coalescent transverse ridges giving muri with a dentate outline. Lumina at the point of nexine attachment to sexine become smaller in diameter (< 1 μm) and form a small patch of fossulate sculpture.

Remarks: Specimens of the present study show variation in their nexinal body diameter and of a bimodal: fine or coarse reticulum.

Dimensions: Maximum diameter (12 specimens) 33 (41) 42 μm.

Afropollis aff. ***jardinus*** Doyle et al., 1982

(pl. 8, figs. 5-9)

Remarks: These specimens differ from *Afropollis jardinus* in having thinner muri, bigger lumina (2-7 μm), and larger nexinal bodies with a diameter larger than half that of the whole grain.

Dimensions: Maximum diameter (7 specimens) 37 (45.5) 53 μm.

Afropollis kahramanensis Ibrahim & Schrank 1995

(pl. 10, fig. 18)

1986: Pollen PO-304 Lawal & Moullade, p. 76, pl. 2, figs. 26-28.

1992: *Afropollis* n. sp. Ibrahim, p. 62, pl. 7, figs. 10-12; pl. 12, figs. 1-9.

Remarks: *Afropollis kahramanensis* differs from the heteropolar species AFROPOL-COLUMN, AFROPOL-LUMPS, *A*. aff. *jardinus*, and *A*. *jardinus* in lacking the small patch of fossulate sculpture, from AFROPOL-LUMPS, *A*. aff. *jardinus*, and *A. jardinus* in having columellate sexine, from the zonasulculate species *A*. *opercualtus*, *A*. *zonatus*, and *A*. aff. *zonatus* in lacking the circular ring-furrow aperture, and from the monosulcoid species *A*. *schrankii* in lacking the sulcoid aperture. Circular forms of *A*. *kahramanensis* may be similar to AFROPOL-MURIGROOVE by having columellate sexines, but the latter differs in having frequent lacunae at the intersection of the large lumina. *A*. *kahramanensis* may also be similar to *Afropollis* sp. B Doyle et al., 1982 in having elliptical grain outline and columellate sexine, but the latter has a larger lumina diameter (4-5 μm) rather than smaller (1-3 μm) lumina of *A*. *kahramanensis*.

Dimension: Maximum length (3 specimens) 42 (45) 47, breadth 32 (34) 36 μm.

Afropollis operculatus Doyle et al., 1982

(pl. 7, figs. 5, 11-18)

1977: *Reticulatasporites jardinus* Brenner 1968, Doyle et al., pl. 2, figs. 1-4.

1982: *Afropollis operculatus* Doyle et al., p. 47, pl. 5, figs. 8, 9; pl. 7, figs. 1-9; pl. 8, figs. 1-4.

Description: Zonasulculate sub-oblate pollen grains, heteropolar, of radial symmetry and with a circular ring-furrow (zonasulculus) 1/2 to 2/3 the diameter of the grain, surrounding one pole and forming an operculum. Sexine columellate, coarsely reticulate, separated over most of the grain surface from an inner dark and conspicuous to nearly invisible nexinal layer. Reticulum composed of 2-6 μm wide polygonal lumina separated by 0.4-0.8 μm thick sinuous muri with their upper surface usually transversely segmented or with longitudinal ridging, and with their lower smooth surfaces bearing 1-2 rows of short (ca. 0.2 μm) stubby sparse to abundant columellae. Lumina at the polar operculate area become smaller in diameter (< 1 μm) and form a small patch of fossulate sculpture at the point of nexine attachment to the sexine and is surrounded by a ring-furrow structure (zonasulculus). Nexinal body spherical, thin, smooth, and of a diameter intermediate between that of the zonasulculus and that of the whole grain.

Remarks: Ibrahim (2002a) studied Aptian material from the northern Western Desert of Egypt and identified two *Afropollis operculatus* subspecies: *Afropollis operculatus* subsp. *operculatus* characterised by its larger

lumina diameter at the (operculate) distal pole as well as at the proximal pole, and *Afropollis operculatus* subsp. *microreticulatus* characterised by a smaller lumina diameter at the (operculate) distal pole than lumina at the proximal pole. In the present material both *Afropollis operculatus* subspecies are recorded.

Dimension: Maximum diameter (17 specimens) 40 (48) 62 μm.

Afropollis zonatus Doyle et al., 1982

(pl. 7, figs. 20-22)

1981: *Reticulatasporites jardinus* Brenner 1968 (Type 2), Hochuli, pl. 1, figs. 7, 8.

1982: *Afropollis zonatus* Doyle et al., p. 48, pl. 8, figs. 5-8; pl. 9, figs. 1-8; pl. 10, figs. 1-8.

Description: Zonasulculate sub-oblate pollen grains, isopolar, of radial symmetry and with a ring furrow (zonasulculus) oriented perpendicular to the rotational (polar) axis dividing the grain into two equal or nearly equal hemispheres. Sexine non-columellate, coarsely reticulate to rugulo-reticulate, separated over most of the surface of both hemispheres from an inner dark and conspicuous to nearly invisible nexinal layer, sexine reticulum become finer and attached to nexine near the aperture margins. Reticulum composed of 3-7 μm wide polygonal to highly irregular lumina separated by 0.4-0.8 μm thick muri. Muri usually sinuous with their upper surface and sides segmented into sharp transversely to obliquely oriented ridges, giving the muri a dentate outline in lateral view; lower mural surfaces smooth or irregularly sculptured but lacking definite columellae. Lumina at the equatorial

(zonasulculate) area become smaller in diameter (1-2 μm) and grade into a ring-furrow structure (zonasulculus). Nexinal body sub-oblate, thin, smooth, and of a diameter intermediate between that of the zonasulculus and that of the whole grain.

Dimension: Maximum diameter (5 specimens) 30 (38) 44 μm.

Afropollis aff. ***zonatus*** Doyle et al., 1982

(pl. 7, fig. 19)

Remarks: These specimens differ from *Afropollis zonatus* in having sparse stubby columellae, and two unequal hemispheres making the specimens heteropolar.

Dimensions: Maximum diameter (3 specimens) 35 (41) 50 μm.

Afropollis sp. B Doyle et al., 1982

(pl. 8, figs. 1-4)

Remarks: These specimens are characterised by having columellae, a coarse reticulum of 4-5 μm wide lumina, large nexinal body whose diameter is larger than 2/3 that of whole grain diameter, and a large grain size.

Dimensions: Maximum diameter (5 specimens) 54 (61) 66 μm.

Retiacolpites columellatus Schrank in Schrank & Mahmoud, 2002

(pl. 12, figs. 3, 4)

Description: Inaperturate circular to ellipsoidal pollen grains. Sexine thin (about 1.5 μm), reticulate, with 1.8-2 μm polygonal to sub-rounded lumina, separated by about 0.8-1 μm wide muri; inner nexinal layer closely attached to the sexine. Some grains show a small round, dark area of about 25 % grain diameter within the reticulum.

Rekarks: All recorded specimens show the small round dark body. The area where this body projects from the reticulum shows what looks like a rupture in the reticulum, which could serve as an aperture, however, this cannot be confirmed under the light microscope.

Dimensions: Maximum diameter (4 specimens) 37 (38.5) 42 μm.

4.3.4 Pollen tetrads

Genus: ***Droseridites*** Cookson, 1947 ex Potonié, 1960

Type species: *Droseridites spinosus* (Cookson) Potonié, 1960, p. 137-139.

Droseridites baculites Ibrahim, 1996

(pl. 11, fig. 20)

Description: Pollen tetrads made of sub-spherical to oval inaperurate individual grains with their exine covered with about 1.5-2 μm tall baculate-spinose sculpture.

Dimension: Maximum tetrad diameter (1 specimen) 26 μm.

Droseridites senonicus Jardiné & Magloire, 1965

(pl. 11, figs. 18, 19)

Description: Pollen tetrads made of sub-spherical to oval inaperurate individual grain with their exine sculptured with about 0.5-0.7 µm tall spines.

Remarks: The present specimens show greater tetrad diameters than that of the original specimens (12-19 µm) descriped by Jardiné & Magloire (1965).

Dimension: Maximum tetrad diameter (3 specimens) 19 (21) 22 µm.

4.3.5 Freshwater algae

Genus: ***Chomotriletes*** Naumova, 1939

Type species: *Chomotriletes vedugensis* Naumova, 1953, p. 53, pl. 7, fig. 21.

Chomotriletes minor (Kedves) Pocock, 1970

(pl. 5, fig. 5, pl. 12, fig. 18)

1961: *Schizaeoisporites minor* Kedves, p. 129, pl. 6, figs. 11-16.

1970: *Chomotriletes minor* (Kedves) Pocock, p. 61, pl. 11, fig. 14.

Description: Alete, amb sub-circular, wall thin, ornamented with ridges separated by furrows arranged in concentric circles parallel to the equatorial margin.

Remaks: Similar or identical forms have also been placed in the genera *Circulisporites*, *Concentricystes* and *Pseudoschizaea,* the latter two which are considered to be junior synonyms of *Chomotriletes* (Jansonius & Hills 1978, card 3322).

Dimension: Maximum diameter (3 specimens) 34 (42.5) 52 µm.

4.3.6 Dinoflagellate cysts

Division: **Dinoflagellata** (Bütschli) Fensome et al., 1993b

Subdivision: **Dinokaryota** Fensome et al., 1993b

Class: **Dinophyceae** Pascher, 1914

Subclass: **Peridiniphycidae** Fensome et al., 1993b

Order: **Gonyaulacales** Taylor, 1980

Suborder: **Ceratiineae** Fensome et al., 1993b

Family: **Ceratiaceae** Willey & Hickson, 1909

Genus: ***Aptea*** Eisenack, 1958

Type species: *Aptea polymorpha* Eisenack, 1958, p. 394, pl. 22, figs. 5-12; pl. 24, fig. 5

Aptea polymorpha Eisenack, 1958

(pl. 15, fig. 17)

1958a: *Aptea polymorpha* Eisenack, p. 394, pl. 22, figs. 5-12; pl. 24, fig. 5.

1986: *Pseudoceratium polymorphum* (Eisenack) Bint, p. 145.

1992: *Aptea polymorpha* Eisenack, Quattrocchio & Sarjeant, p. 2-234.

Remarks: *Aptea polymorpha* is distinguished from *Pseudoceratium* cysts by its lenticular to rounded triangular ambitus with short apical, antiapical, and extensively reduced postcingular horns, and by its large size.

Dimensions: Maximum length (4 specimens) 98 (108) 120, breadth 50 (73) 80 µm.

Genus: ***Muderongia*** Cookson & Eisenack, 1958

Type species: *Muderongia mcwhaei* Cookson & Eisenack, 1958, p. 41, pl. 6, figs. 1-5.

Muderongia aequicorna Århus in Århus et al., 1990

emend. Monteil, 1991b

(pl. 13, figs. 1, 2)

Remarks: Århus's (1990) assignment of species *aequicorna* to the genus *Muderongia*, and the latter broad emendation of *Muderongia aequicorna* made by Monteil (1991b), which encompassed features of the genus *Muderongia* (e.g. smooth, cavate) and the genus *Phoberocysta* (e.g. ornamented, proximate to proximochorate) makes this assignment argumental. Becaues the few species that posesses processes (e.g. *Phoberocysta neocomica* and *Phoberocysta tabulata*), where considered by Monteil (1991b) as junior synonyms of other similar *Muderongia* species were retained under the generic name *Phoberocysta* (Fensome & Williams, 2004). However, the nomenclature *Muderongia aequicorna* as in Fensome & Williams (2004) will be followed here for taxonomical stabilization.

Dimensions: Maximum length with horns (2 specimens) 120 (121) 122 µm, length of central body 71 (78) 85.5 µm, breadth 54 (58) 62 µm.

Muderongia pariata Duxbury, 1983 emend. Monteil, 1991b

(pl. 13, fig. 4)

Remarks: *Muderongia pariata* differs from *Muderongia aequicorna* in having four prominent, distally perforated horns: one apical, two subequal lateral, and one tapering and distally closed antapical.

Dimensions: Maximum length without operculum (3 specimens) 60 (66.5) 72 µm, length of central body 53 (57.5) 62 µm, breadth 40 (51) 60 µm.

Muderongia tomaszowensis Alberti, 1961 emend. Riding et al., 2001

(pl. 13, fig. 5)

Remarks: *Muderongia tomaszowensis* differs from *Muderongia pariata* in having five horns: one apical, two subequal, lateral, and two antapical, with the right antapical horn significantly reduced to a protuberance, and also differs from *M. pariata* in lacking the fine perforations at the distal half of the horns.

Dimensions: Maximum length without operculum (3 specimens) 51 (65) 78, length of central body 40 (53.5) 65 µm, breadth 36 (48) 55 µm.

Phoberocysta neocomica (Gocht) Millioud, 1969 emend. Helby, 1987

(pl. 13, fig. 10)

Remarks: Monteil (1991b) considered *Muderongia* and *Phoberocysta* are synonyms based on their great morphological similarity, where he proposed that *Muderongia* evolved into *Phoberocysta* by retraction of the periphragm and production of processes. Accordinglly, Monteil (1991b) considered

Phoberocysta neocomica the senior synonym of *Muderongia tomaszowensis*. However, Riding et al. (2001) retained *Muderongia tomaszowensis*, which is followed here.

Dimensions: Maximum length with horns (1 specimen) 114.5 µm, length of central body 62 µm, breadth 70 µm.

Genus: ***Odontochitina*** Deflandre, 1937 emend. El-Mehdawi, 1998

Type species: *Odontochitina operculata* (Wetzel) Deflandre & Cookson, 1955, p. 291-292.

Odontochitina operculata (Wetzel) Deflandre & Cookson, 1955

(pl. 14, fig. 5)

1933: *Ceratium* (*Euceratium*) *operculatum* Wetzel, p. 170, pl. 2, figs. 21, 22; text-fig. 3.

1955: *Odontochitina operculata* (Wetzel) Deflandre & Cookson, p. 291-292.

Description: Cyst cornocavate ceratioid, with three long, straight, ponited horns: one apical, one antapical, and one right lateral. Endocyst sub-spherical in shape and with a little developed rounded bulge at the base of the lateral horn and more oval outline at the base of the antapical horn. Archeopyle apical, Type (4A).

Dimensions: Maximum length without operculum (2 specimens) µm, length of central body (3 specimens) 48 (52.5) 53 µm, breadth 38 (39.5) 45 µm, length of operculum (1 specimen) 83 µm.

Odontochitina ancala Bint, 1986

(pl. 15, fig. 13)

Remarks: Bint (1986) differentiated *Odontochitina ancala* from *Odontochitina operculata* by having an elbow and cingular notch in the right lateral horn.

Dimensions: Maximum length without operculum (2 specimens) 73 (76.5) 80 µm, length of central body (2 specimens) 37 (41) 45 µm, breadth 47 (50) 53 µm.

Odontochitina costata Alberti, 1961 emend. Clarke & Verdier, 1967

(pl. 17, fig. 16)

Remarks: *Odontochitina costata* diffes from *O. operculata* and *O. ancala* in having horns that are sculptured with striae and irregulary located perforations, where perforations may confined to the distal part of the horns or randomly distributed over the entire length of the horns.

Dimensions: Maximum length without operculum (1 specimen) 151 µm, length of central body (1 specimen) 47 µm, breadth 56 µm.

Odontochitina porifera Cookson, 1956

(pl. 17, fig. 19)

Remarks: *Odontochitina porifera* differs from *Odontochitina costata* in having the apical horn completely perforated by small four-sided or oval openings arranged in several longitudinal rows, and the antapical and the right lateral horns are medially perforated by small regularly arranged holes.

Dimensions: Maximum length without operculum (2 specimens) 107 (110) 112.5 µm, length of central body (2 specimens) 54.5 (56) 57 µm, breadth 52 (53.5) 55 µm.

Genus: ***Pseudoceratium*** Gocht, 1957

Type species: *Pseudoceratium pelliferum* Gocht, 1957, p. 166-168, pl. 18, figs. 1, 2; text-figs. 1-3.

Pseudoceratium pelliferum Gocht, 1957

(pl. 13, fig. 12)

Remarks: *Pseudoceratium pelliferum* is distinguished from other *Pseudoceratium* by having three well-developed, long tapering horns.

Dimension: Maximum length without operculum (2 specimens) 50 (60) 70 µm, breadth 55 (60) 65 µm, length of operculum (1 specimen) 60 µm.

Pseudoceratium almohadense (Below) Lentin & Williams, 1989

(pl. 15, fig. 16)

1984: *Aptea almohadensis* Below, p. 635, pl. 1, figs. 5a-b, 6, 7.

1989: *Pseudoceratium almohadense* (Below) Lentin & Williams, p. 306.

Remarks: *Pseudoceratium almohadense* is distinguished from other *Pseudoceratium* species by having sub-spherical body with rounded to narrow bulge horns.

Dimension: Maximum length without operculum (1 specimen) 62 µm, breadth 65 µm.

Pseudoceratium anaphrissum (Sarjeant) Bint, 1986

emend. Harding, 1990

(pl. 14, figs. 4, 16)

1966: *Doidyx anaphrissa* Sarjeant, p. 206, pl. 22, fig. 8; pl. 23, fig. 6; text-fig. 55.

1986: *Pseudoceratium anaphrissum* (Sarjeant) Bint, p. 145.

Remarks: *Pseudoceratium anaphrissum* is differentiated from other *Pseudoceratium* species by having oval, biconical, sub-rounded to sub-pentagonal cyst outline, and short blunt apical and antiapical horns. Two antiapical horns when exist are expressed as well developed lobes, and two lateral postcingular lobes may also develop. Cyst surface densely ornamented by simple short, capitate to briefly bifurcate processes without mid-ventral and mid-dorsal processes reduction.

Dimension: Maximium length with operculum (1 specimen) 80 µm, length without operculum (6 specimens) 70 (73) 75 µm, breadth 72 (78) 85 µm.

Pseudoceratium expolitum Brideaux, 1971

Remarks: *Pseudoceratium expolitum* is differentiated from other *Pseudoceratium* species by a complete lack of processes and has smootth, scabrate to granulate surface.

Dimension: Maximum length with operculum (4 specimens) 74 (83) 94 µm, breadth 50 (65) 77 µm.

Pseudoceratium retusum Brideaux, 1977

(pl. 14, figs. 1-3, 9, 12, 14)

Remarks: *Pseudoceratium retusum* is similar to other *Pseudoceratium* species in having a sub-spherical to asymmetrically triangular body and cyst surface ornamented by processes, but it differs in usually having these processes linked basally to form an anastomosing network in a reticulate pattern, with occasional mid-ventral and mid-dorsal sculpture reduction.

Dimension: Maximum length with operculum (7 specimens) 80 (103) 120 µm, length without operculum (5 specimens) 65 (75.5) 84 µm, breadth 60 (80) 94 µm.

Pseudoceratium securigerum (Davey & Verdier) Bint, 1986

(pl. 15, figs. 1, 2)

1974: *Aptea securigera* Davey & Verdier, p. 642-643, pl. 91, figs. 2, 3; text-fig. 5 (vii).

1986: *Pseudoceratium securigerum* (Davey & Verdier) Bint, p. 145.

Remarks: *Pseudoceratium securigerum* is similar to *P. retusum*, *P. anaphrissum*, and *P. expolitum* in having rounded triangular body, but *P. securigerum* differs in having a strongly convex left side and slightly convex to straight right epicystal and hypocystal sides that meet at approximately right angles in the cingular region. Cyst surface usually has strong mid-ventral and mid-dorsal reduction of processes.

Dimension: Maximum length with operculum (5 specimens) 75 (92) 102 µm, length without operculum (7 specimens) 62 (63) 68 µm, breadth 49 (68.5) 80 µm.

Order: **Peridiniales** Haeckel, 1894b

Suborder: **Peridiniineae** (Autonym)

Family: **Peridiniaceae** Ehrenberg, 1831

Subfamily: **Palaeoperidinioideae** (Vozzhennikova) Bujak & Davies, 1983

Genus: ***Palaeoperidinium*** Deflandre, 1934 ex Sarjeant, 1967b

Type species: *Palaeoperidinium pyrophorum* (Ehrenberg ex Wetzel) Sarjeant, 1967b, p. 246.

Palaeoperidinium cretaceum (Pocock) Lentin & Williams, 1976

emend. Harding, 1990a

(pl. 15, figs. 4, 9)

1962: *Astrocysta cretacea* Pocock, p. 80, pl. 14, figs. 219-221 ex Davey, 1970, p. 359.

1976: *Palaeoperidinium cretaceum* (Pocock) Lentin & Williams, p. 110.

Remarks: *Palaeoperidinium* is distinguished from *Subtilisphaera* by having a rhomboidal to pentagonal ambitus, observable paratabulation, and a usually indeterminate endocyst (Lentin & Williams, 1976).

Dimensions: Maximum length (4 specimens) 60 (73) 83 µm, breadth 52 (61) 68 µm.

Genus: ***Subtilisphaera*** Jain & Millepied, 1973

emend. Lentin & Williams, 1976

Type species: *Subtilisphaera senegalensis* Jain & Millepied, 1973, p. 27-28, pl. 3, figs. 31-33.

Subtilisphaera senegalensis Jain & Millepied, 1973

(pl. 14, figs. 8, 15)

1973: *Subtilisphaera senegalensis* Jain & Millepied, p. 27-28, pl. 3, figs. 31-33.

Description: Bicavate peridinioid cyst with an ovoidal to sub-circular ambitus with a short pointed apical horn, and one eccentrically located left (or two unequal symmetrically located) antapical horns. Endocyst ovoidal to sub-spherical, adpressed to pericyst in dorsal and ventral regions, surrounded by small apical and antapical pericoels. Periphragm laevigate, scabrate or finely granulate.

Remarks: A few recorded *Subtilisphaera senegalensis* specimens show partial paratabulation patterns.

Dimension: Maximum length (7 specimens) 48 (54) 63, breadth 38 (44.5) 52 µm.

Subtilisphaera perlucida (Alberti) Jain & Millepied, 1973

(pl. 14, figs. 7, 11)

1959b: *Deflandrea perlucida* Alberti, p. 102, pl. 9, figs. 16, 17.

1973: *Subtilisphaera perlucida* (Alberti) Jain & Millepied, p. 27.

Description: Cavate peridinioid cyst with an ovoidal to sub-circular or pentagonal ambitus, with one apical and only one eccentrically located antapical horn. Endocyst ovoidal to ellipsoidal, usually surrounded by complete pericoel, and may be adpressed to the pericyst in dorsal and ventral regions. Periphragm laevigate or finely scabrate.

Remarks: The present specimens of *Subtilisphaera perlucida* show intraspecific variations in morphology, where they range from forms with small apical

pericoels and broadly-rounded periphragms ending with a relatively short apical horns to forms with large apical and small antiapical pericoels, with ovoidal periphragms ending with large apical and small antapical horns. Similar morphological variations within *Subtilisphaera perlucida* specimens were detected by Duxbury (1983) from the Aptian-lower Albian of the Isle of Wight, Southern England.

Dimension: Maximum length (10 specimens) 55 (65.5) 72, breadth 43 (47.5) 52 µm.

Subtilisphaera scabrata Jain & Millepied, 1973

(pl. 15, figs. 3, 7)

Description: Cavate peridinioid cyst with a biconical to pentagonal ambitus and well-developed single apical and antapical horns. The third antapical horn was often absent or sometimes showed as a slight projection. Endocyst ovoidal to sub-circular and surrounded by a complete pericoel, typically large at apical and antapical regions. Periphragm ornamented by granuloscabrate sculpture.

Dimension: Maximum length (5 specimens) 65 (71) 84, breadth 40 (50.5) 64 µm.

Subtilisphaera terrula (Davey) Lentin & Williams, 1976

emend. Harding, 1986a

(pl. 14, figs. 6, 10)

1974: *Deflandrea terrula* Davey, p. 65, pl. 8, figs. 4, 5.

1976: *Subtilisphaera terrula* (Davey) Lentin & Williams, p. 119.

Description: Cavate peridinioid cyst with an ovoidal to sub-circular ambitus, a rounded apex which ends with a short broad apical horn, and an ovoidal antapex bearing one eccentrically located left antapical horn. Endocyst ovoidal to sub-spherical, adpressed to pericyst in dorsal and ventral regions. Periphragm scabrate and bearing penetabular granulae.

Remarks: The present specimens shows a distinct and traceable paratabulation pattern similar to specimens studied and illustrated by Harding (1996a), where he provided a complete paratabulation formula.

Dimension: Maximum length (2 specimens) 60 (61) 62, breadth 45 (47) 49 µm.

Subfamily: **Deflandreoideae** Bujak & Davies, 1983

Genus: ***Senegalinium*** Jain & Millepied, 1973

Type species: *Senegalinium bicavatum* Jain & Millepied, 1973, p. 23, pl. 1, figs. 1-4; text-fig. 1b.

Senegalinium aenigmaticum (Boltenhagen) Lentin & Williams, 1981

(pl. 17, figs. 11, 18)

1977: *Deflandrea aenigmatica* Boltenhagen, p. 86-88, pl. 14, figs. 5a-b, 6-10.

1981: *Senegalinium aenigmaticum* (Boltenhagen) Lentin & Williams, p. 250.

Description: Bicavate peridinioid cyst of ovoidal to sub-circular ambitus with three conical horns: one short, pointed apical, and two inequal symmetrically located antapical horns. Endocyst ovoidal to sub-spherical, adpressed to pericyst in dorsal and ventral regions, with small apical and antapical pericoels. Periphragm covered by very minute, 3-4 µm long hair-like spines arising from microverrucae. Archeopyle is intercalary, and is not always observable.

Remarks: *Senegalinium* is distinguished from *Subtilispahaera* by having a well marked intercalary archaeopyle, where in *Subtilispahaera* the archeopyle is usually indeterminate (Jain & Millepied, 1973).

Dimension: Maximum (8 specimens) 65 (75) 94 , breadth 36 (52) 69 µm.

PALYNOSTATIGRAPHY AND PALYNOZONATION

5.1 Previous work on Egyptian Cretaceous palynology

Most of the palynological research conducted on Egyptian Cretaceous successions has been based on deep borehole samples taken from exploratory wells. These boreholes were drilled as a result of intensive exploration activities for hydrocarbons in the northern part of Egypt, especially the northern part of the Western Desert. Examples of work on borehole samples are: Abdelmalik et al. (1981), Penny (1986, 1988a, 1992), Omran et al. (1990), Schrank & Ibrahim (1995) and Mahmoud & Deaf (2007). Hence washed ditch cutting samples were and still are the most widely accessible and routinely used material for Egyptian Cretaceous palynological research. However, core samples have sometimes been available for palynostratigraphers to use, for example in the papers of Abdelmalik et al. (1981), El-Beialy (1994a, 1994b, 1994c) and Ibrahim (1996, 2002a). In the southern part of the Western Desert, ditch cutting and core samples from shallow hydrological boreholes drilled during governmental reclamation projects has been the main source for palynological investigations. Examples of work based on such material are those of Schrank (1982, 1983), Schrank & Mahmoud (1998, 2000, 2002) and Mahmoud (2003). In southern Egypt, mining activities centred on the Upper Cretaceous phosphate deposits of the Duwi Formation have also enabled some palynological research to be carried out (e.g. Schrank, 1984a-b). The reason productive samples are generally restricted to borehole samples results from present day environmental conditions. Egypt is located in the subtropical arid zone and all the Cretaceous and younger outcrops are have been subjected to extensive deep weathering, and as a result they have been found to be palynologically barren (e.g. Schrank, 1983). Personal observations of samples taken from black and green

shale horizons from the middle Cretaceous of Gabal Dist in the Bahariya Oasis in the Western Desert proved the barren nature of outcrop samples save for some phytoclast fragments.

The lower Cretaceous rocks of the northern basinal area of Egypt were mainly deposited in very shallow marine (brackish to coastal) to inner neritic open marine conditions (Kerdany & Cherif, 1990; Said, 1990), which were unfavourable for proliferation of planktonic forams and nannofossils. Consequently, no independent age control is available for these successions. The upper Cretaceous interval is generally composed of pre-Campanian middle to upper shelf deposits, and of deeper upper to middle slope deposits for the Campanian-Maastrichtian interval, which is mainly represented by thick carbonate successions (Kerdany & Cherif, 1990; Said, 1990). The planktonic foraminifera-calibrated palynological work of Abdel-Kireem et al. (1996) on upper Cretaceous (Cenomanian-Maastrichtian) subsurface samples from the Kahraman-1 and Abu Gharadiq-1 boreholes in the northern Western Desert is one of the few attempts to provide micropalaeontologically calibrated palynological work (Fig. 5.1). Most of the independently calibrated palynological work has been done by oil exploration companies and has not been published.

As most of the Egyptian palynological work has been carried out on ditch cutting samples where no independent age control was available, palynostratigraphers have identified different palynomorph assemblages, which have then been correlated with similar assemblages from other palaeogeographically related areas in order to date the Egyptian Cretaceous successions. As a result, several informal palynological zonal schemes (Fig. 5.2) and age assignments for different rock units have been proposed for the Cretaceous rocks of Egypt. The informal zones proposed by Schrank & Ibrahim (1995)

represent the most complete palynological zonal scheme for the Egyptian upper lower and upper Cretaceous sedimentary sequence (Fig. 5.2).

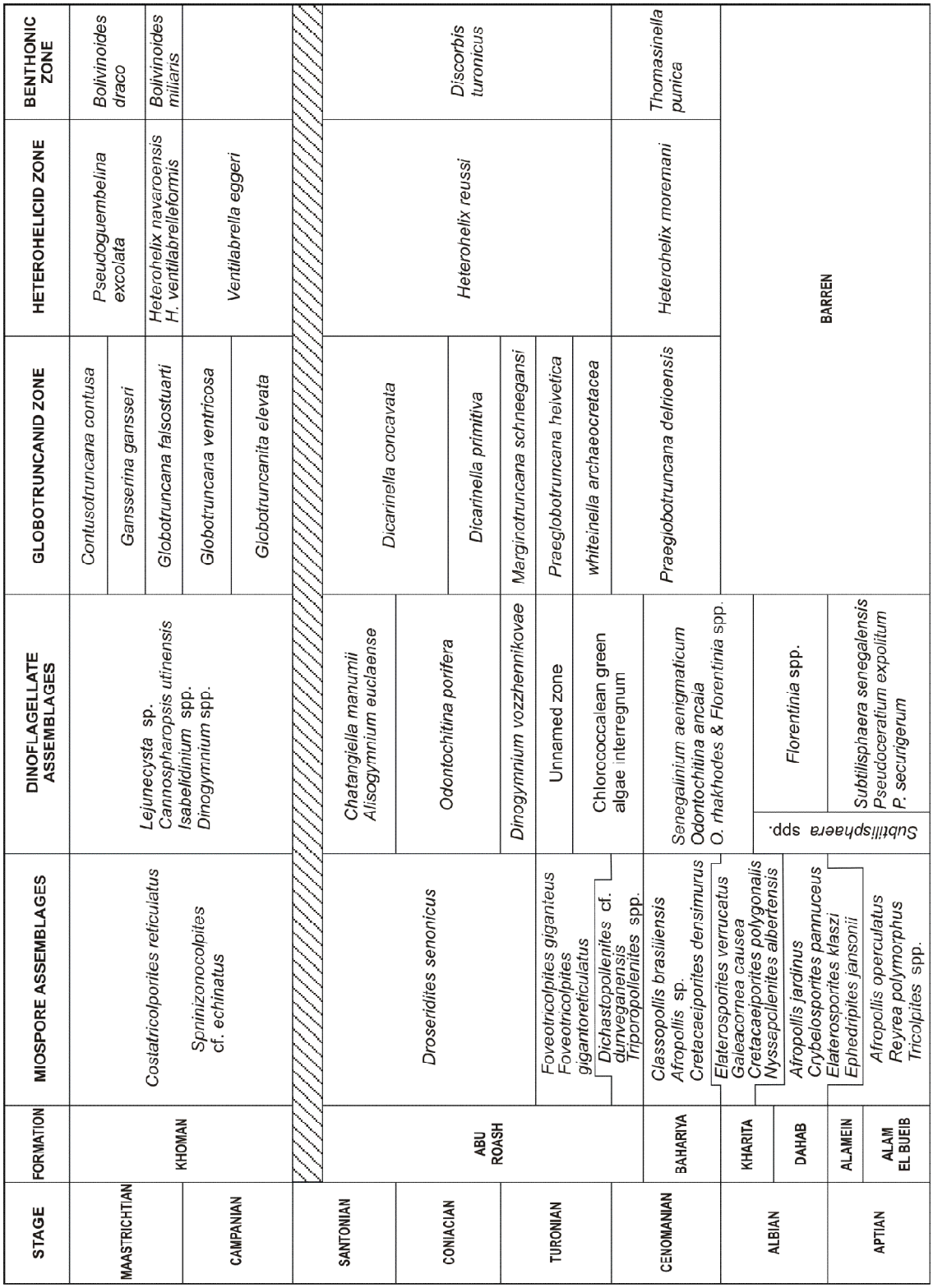

Figure 5.1 Cretaceous palynological assemblages and foraminiferal biozones in the north Western Desert of Egypt (Abdel-Kireem et al., 1996).

Age / Authors	Saad, 1978 W. D.	Sultan, 1986 W.D.	Sultan & Aly, 1986 W.D.	El-Beialy et al., 1990 Nile Delta	Omran et al., 1990 W.D.	El-Shamma, 1991 W.D.
Campanian-Maastrichtian						CE 5 Upper unnamed
Santonian						CE 4 *Afropollis jardinus*
Coniacian						CE 3 *E. Klaszii*
Late Turonian						CE 2 Lower unnamed
Early Turon.						CE 1 *Cretac.scabratus*
Late Cenom.						
Cenomanian			III *Elateropl.africaensis* *Soritites legouxae*	VI *Foveotricolpites* sp. *Triporopollenites* sp. *Tricolpites gigantoreticulatus*		
Late Albian Early Cenom.			II *Elatero. castelainii* *Galeacornea causa* *Matoni.phlepopteroides*	V *Elaterosporites klaszii* *Ephedripites irregularis* *Afropollis jardinus*	PS 2 *Elaterosporites* spp. *Tricolpites* spp. *Ephedripites multicostatus* *Afropollis* spp.	
Albian	III *Elaterosporites* *Tricolpites*		I *E. klazii / A. jardinus* *Concavi. verrucatus* *Concavi. punctatus* *Reyrea polymorphus*	IV *Ephedripites ovalis* *Murospora florida* *Cicatricosisporites* sp.		
Aptian	II *Murospora* *Cicatricosisporites* *Reticulatasporites jardinus*	III *Murospora* sp. *Ephedripites irregulatus* *Afropollis jardinus* *Ephedripites* sp.		III *Inaperturopollenites* *atlanticus* *Ephedripites* sp.	PS 1 *Callialasporites* *trilobatus* *Cicatricosisporites* *sinuosus*	
Barremian	I *Callialasporites* *trilobatus* *Klukisporites*	II *Dicheiropolis etruscus* *Inaperturo. limbatus* *Ephed. multicostatus* *Ephedripites ovalis*		II *Impardecispora* *apiverrucata* *Lygodiosporites* *perverrucatus*		
Hauteriv.		I *Concavissimisporites* *punctatus* *Inaperturopollenites* *giganteus* *Dicheiropolis etruscus* *Cingulatosporites* sp.				
Valang.						
Berriasian						

Figure 5.2 (part) Correlation of most of the important palynozones for the Cretaceous of the northern Egyptian deserts. (W.D. = Western Desert).

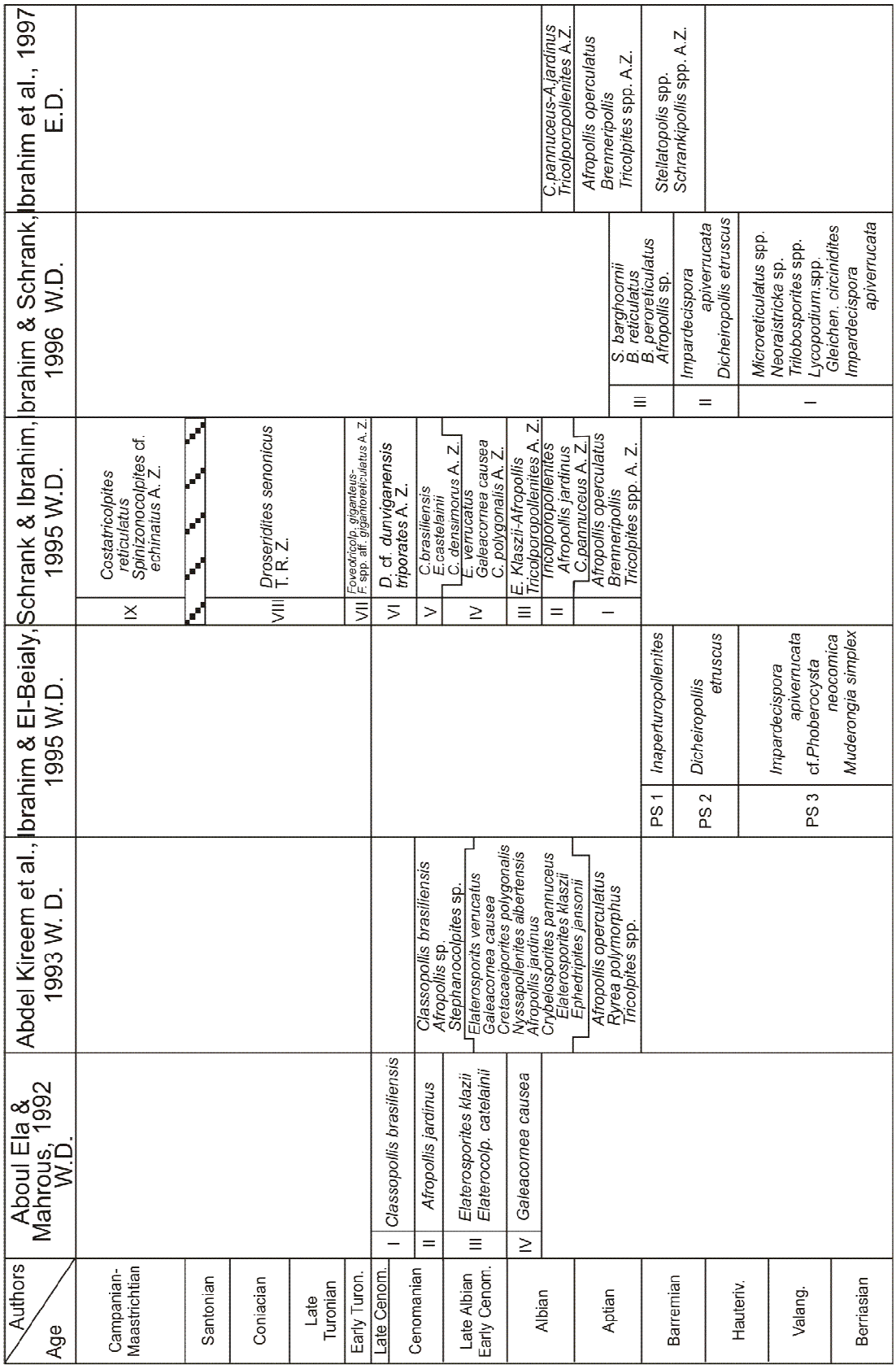

Figure 5.2 (continued).

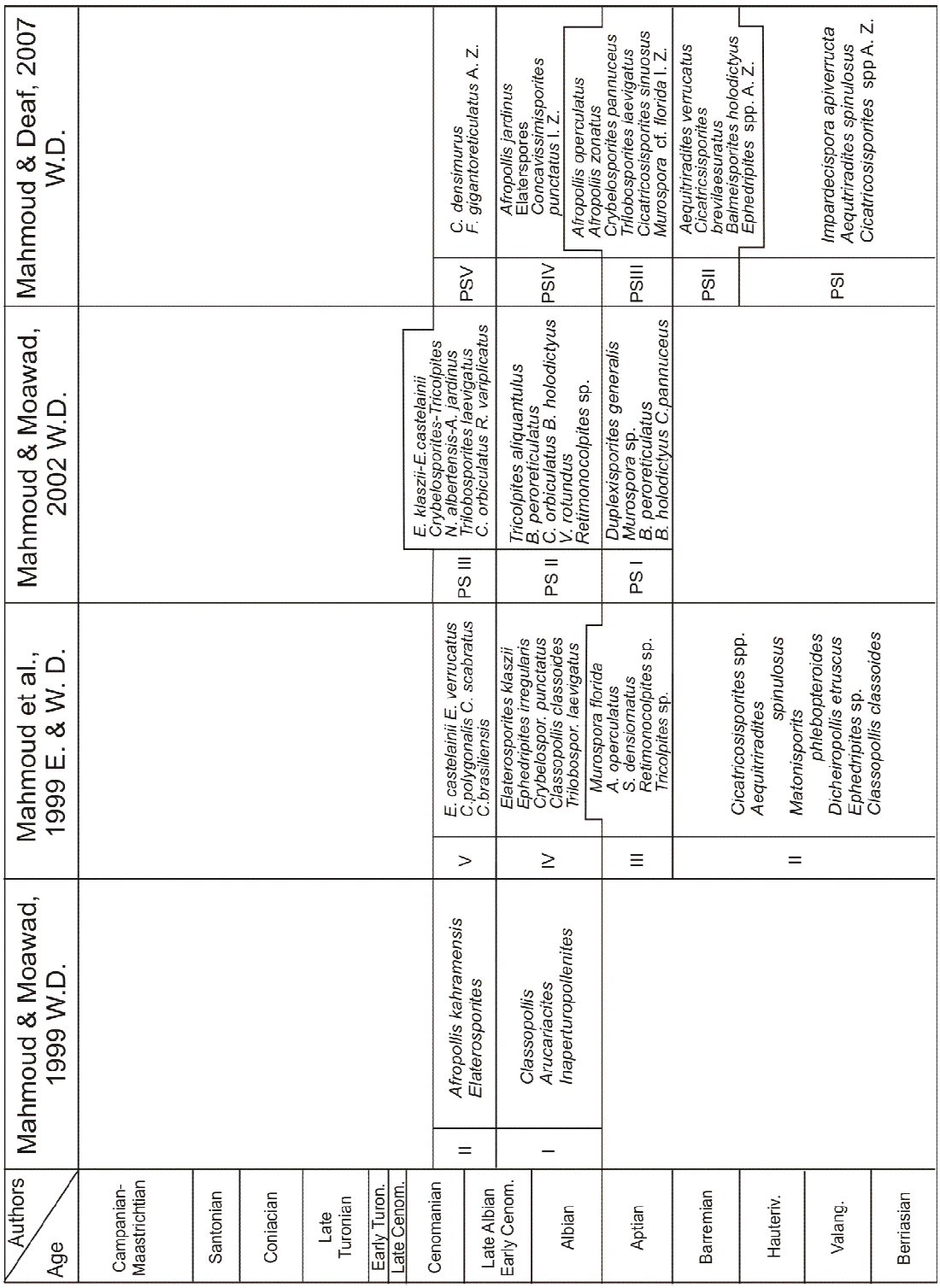

Figure 5.2 (continued).

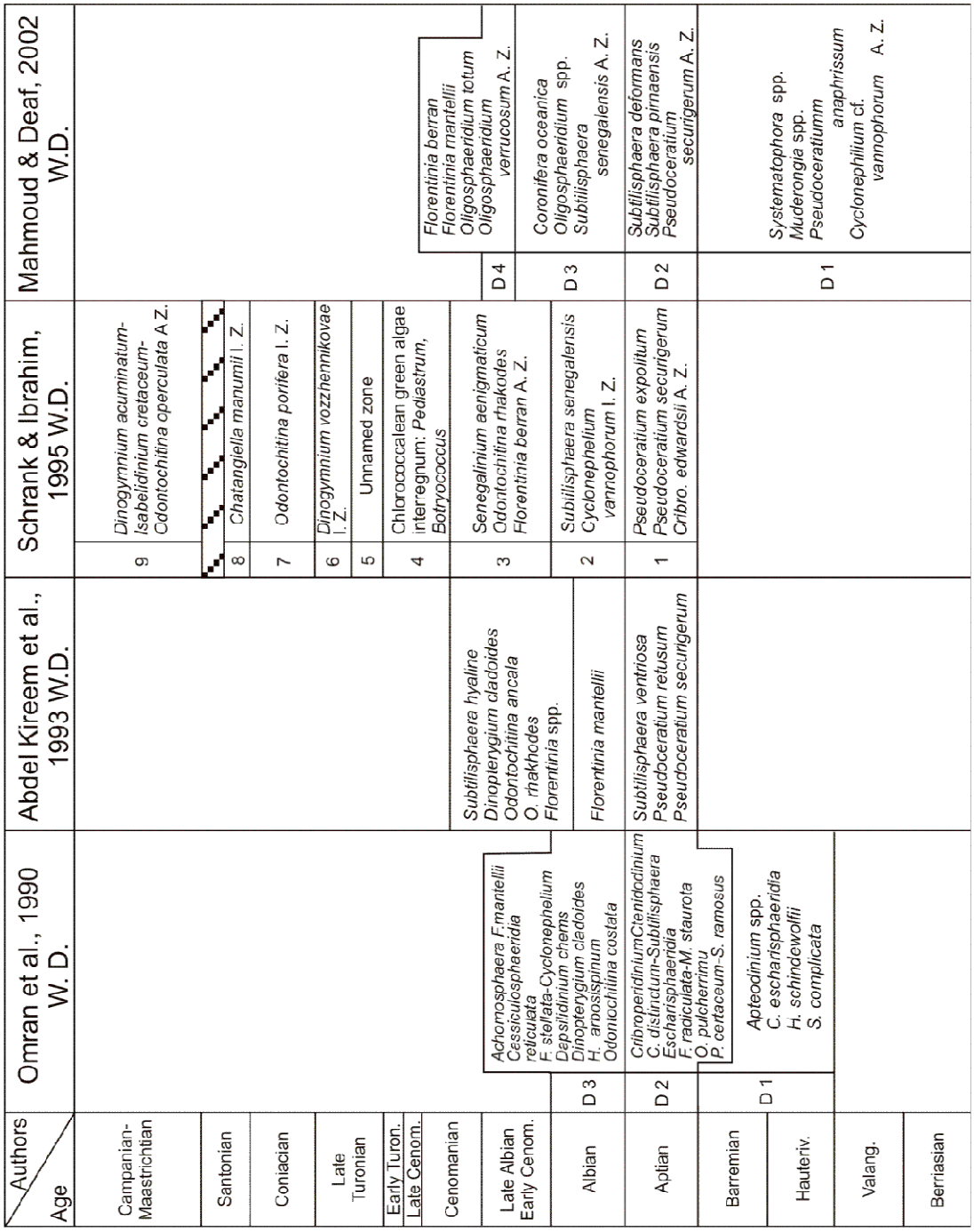

Figure 5.2 (continued).

The Cretaceous biostratigraphic work of Schrank & Mahmoud (1998) in the Dakhla Basin in Central Egypt contributed to the understanding of this basin, where successions below the well-known Duwi Phosphate Formation had received little geological study, usually being referred to as the Nubian Sandstone Formation. Later work by Schrank & Mahmoud (2000) on the Cenomanian of the Dakhla Basin resulted in the identification of new spore and angiosperm pollen species, and revealed the geological importance of this area, whereas the northern Western Desert was the research focus for palynostratigraphers studying early angiosperm pollen (e.g. Penny, 1988a, 1988b, 1989, 1991). The palynological work of Schrank & Mahmoud (2002) in the Barremian of the Dakhla Basin also yielded new early angiosperm pollen. All of the new species described in the latter work are recognised in the present study of the Cretaceous succession of the Western Desert, providing better correlation between the Barremian of Central Egypt and that of the north Western Desert. It is thus possible to put the lower Cretaceous of Central Egypt into the framework of the regional Egyptian Cretaceous, previously best known from the Western Desert.

Perhaps the most important development for Egyptian palynology has been the development of the scanning electron microscope (SEM) which has been used to erect several dozen new angiosperm species (Schrank, 1982, 1983; Penny, 1986, 1988a, 1988b, 1989, 1991; Schrank & Ibrahim, 1995; Ibrahim, 1996; Ibrahim & Abdel-Kireem, 1997; Kedves, 1998; Schrank & Mahmoud, 1998; Kedves, 1999; Schrank & Mahmoud, 2000, 2002; Ibrahim, 2002a). The use of the SEM to study early angiosperm pollen from Lower Cretaceous successions has revealed the diverse nature of these angiosperm assemblages (Penny, 1992; Ibrahim, 2002a). The resultant high resolution SEM-driven taxonomy has provided much information about the evolutionary trends of certain early angiosperm pollen taxa, for example

the *Afropollis* complex (Fig. 5.3), and hence increased their biostratigraphic importance.

In the past most palynostratigraphers (e.g. Omran et al., 1990) assigned *Afropollis* specimens to *Afropollis* spp. based on routine light microscopic investigations. Later SEM studies carried out by Schrank & Ibrahim (1995) and Ibrahim (1996, 2002a) resulted in identification of new *Afropollis* species and provided better SEM microphotographs of previously described *Afropollis* species.

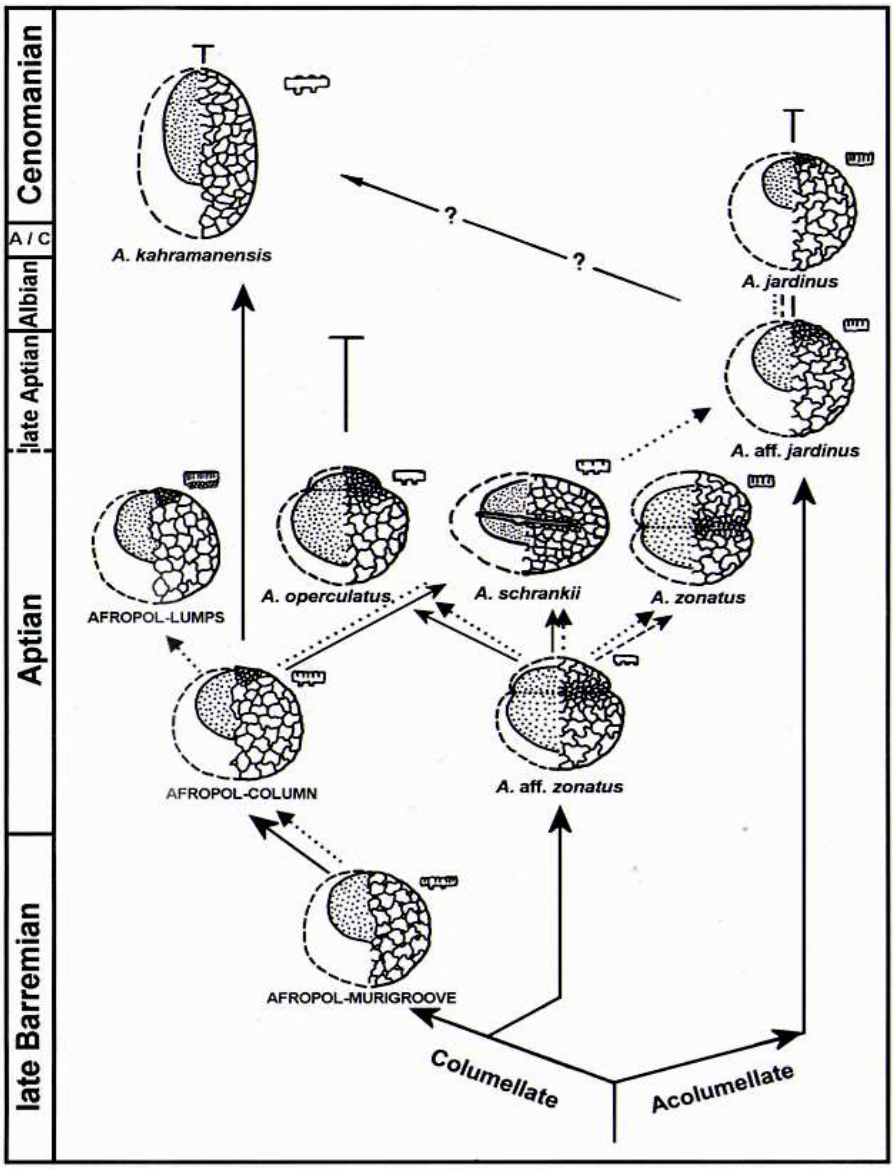

Figure 5.3 Phylogenetic relationships between different *Afropollis* species of Doyle et al. (1982). Dotted line: possible evolutionary trends according to Penny (1989). Modified by Schrank & Ibrahim (1995) and Ibrahim (2002a).

The SEM (e.g. Schrank, 1983; Penny, 1986, 1988a, 1989) has also contributed toward a better understanding of the palaeolatitudinal migration of early angiosperm pollen producing plants (Doyle et al., 1977; Doyle, 1992; Penny, 1992). Doyle (1992) compared his lower Potomac (USA) Zone I palynological assemblage of possible Aptian age to late Barremian and Aptian "Southern Laurasian" *Cerebropollenites* assemblages of England and supposed late Barremian and Aptian assemblages of Gabon from the *Dicheiropollis etruscus*/*Afropollis* Province. A gap in the early Aptian assemblage of Gabon has been filled by the better represented Egyptian early Aptian assemblage described by Schrank (1983) from the Mawhoub West 2 borehole in the southern part of the Western Desert, and by Penny (1986, 1988a, 1988b, 1989) from the Mersa Matruh-1 borehole in the northern Western Desert. The Egyptian palynoflora has permitted a better correlation between the *Cerebropollenites* and the *Dicheiropollis etruscus*/*Afropollis* provinces, and provided more evidence that Northern Gondwana was the main centre of early angiosperm radiation.

5.2 Age assessments

A thorough review of the literature of Egyptian palynological work has showed that some of the proposed age assignments have been misinterpreted because they refer to species ranges which have no independent age control, or to sedimentary sequences of doubtful ages. For example, the work of Mahmoud & Moawad (2002) on subsurface upper Jurassic-lower upper Cretaceous deposits from the West Tiba-1 borehole in the northern Western Desert provides important information on the upper Jurassic. However, in the lower Cretaceous, their assignment of *Afropollis jardinus* to the Aptian is unjustified, because *Afropollis jardinus* unequivocally marks the base of the Albian (e.g. Doyle et al., 1982) in the Albian-Cenomanian Elaterate Province. It is necessary to compile biostratigraphic data on palynomorph index species by selecting only those with independently

calibrated age ranges from the published literature (Fig. 5.4). The age assignments for the successions of the Abu Tunis 1x and the BB80-1 boreholes studied here are thus based on diagnostic palynomorph taxa as well as on correlation with better-dated contemporaneous regional and interregional palynofloral assemblages. Correlation to intercontinental palynofloral assemblages was made in the context of the phytogeographic provinces which developed across Africa (including Egypt) and northern South America. These provinces include those such as the pre-Albian *Dicheiropollis etruscus*/*Afropollis* Phytogeographic Province of Herngreen et al. (1996) for spores and pollen grains, and the Tethyan Realm for the dinoflagellate cysts.

It is important to note that the micropalaeontologically calibrated palynological work of Thusu et al. (1988) on Libyan lower Cretaceous sediments, which has a partial correlation to the formal lower Cretaceous dinoflagellate zonation of the European Tethys (Leereveld, (1997a) should be approached with some caution. Leereveld (1997a) pointed out that the lower part of Zone V of Thusu et al. (1988) of proposed Berriasian age contains a typical Valanginian species, *Calpionellites darderi* (Allemann & Remane, 1979), which better correlates that zone to the Valanginian. The middle part of Zone V which Thusu et al. (1988) assumed to be of Valanginian age, is actually consistent with an Hauterivian age based on the presence of the dinoflagellate index species *Muderongia staurota* (Leereveld, 1997a). This revised age assessment made by (Leereveld, 1997a) for the Zone V of Thusu et al. (1988) will be followed here.

It is important to note that most of the independently calibrated dinoflagellate cyst events in the Albian of the European Tethys (Davey & Verdier, 1973; Habib & Drugg, 1983; Erba et al., 1999; Torricelli, 2006) cannot be recognised in the

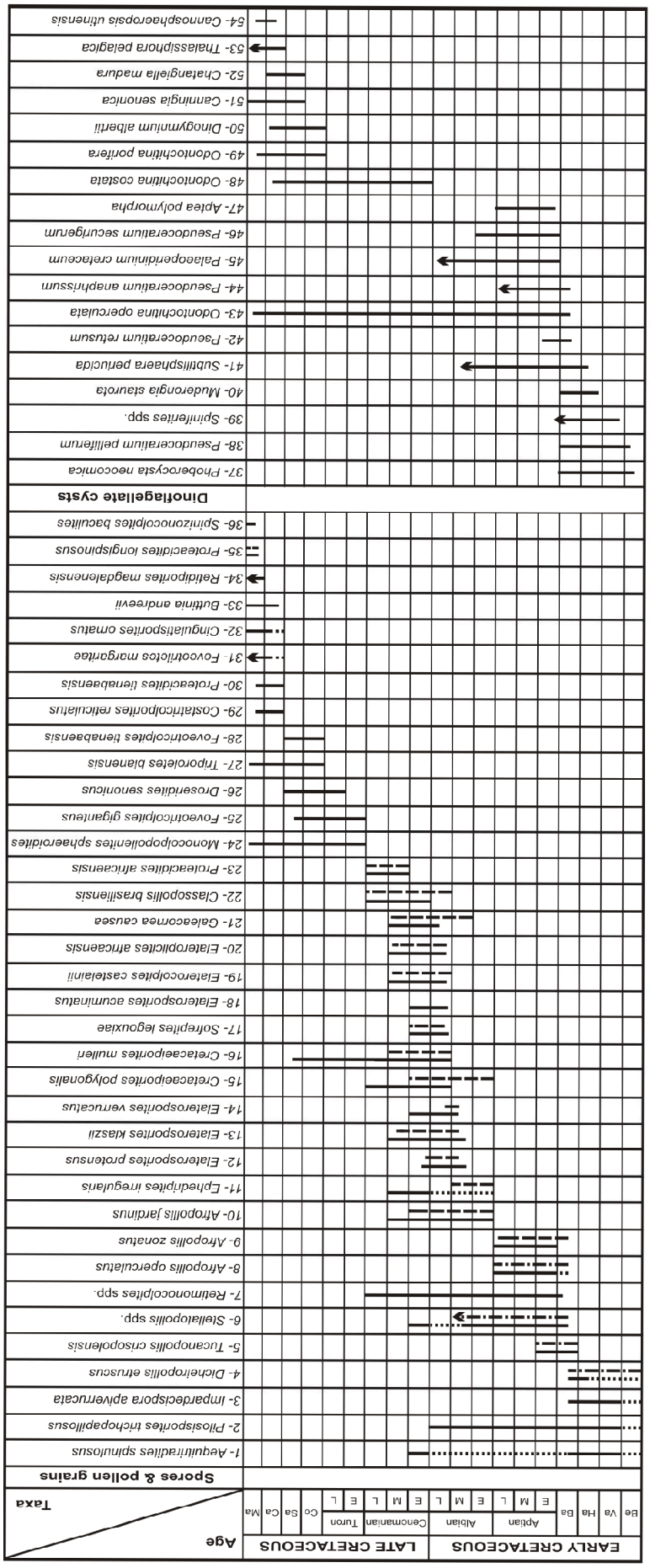

Fig. 5.4 Compilation of the biostratigraphic range of most of the important Cretaceous marker species in different phytogeographic provinces of North and West Africa and North South America and the Tethyan Realm.

African range (Tethyan ranges for dinoflagellate cysts are included): Independently dated ——, Not independently dated ……
Northern South American range: Independently dated — — —, Not independently dated —·—·—

Sources for African ranges: Doyle et al., 1982 (8, 9, 10); Gubeli et al., 1984 (8); Hochuli, 1981 (4, 9, 13, 20, 21); Hochuli & Kelts, 1980 (8, 10); Jan Du Chêne et al., 1978 (31, 34); Jardiné, 1967 (13, 14, 15, 17, 18, 19, 20, 21, 23); Jardiné & Magloire, 1965 (10, 12, 13, 14, 15, 16, 17, 19, 22, 23, 24, 25, 26, 28, 30, 35); Lawal & Moullade, 1986 (15, 16, 22, 23, 24, 25, 26, 27, 31, 32, 33, 34, 36); Schrank & Ibrahim, 1995 (11, 13, 15, 19, 20, 22, 25, 26, 29); Schrank & Mahmoud, 1998 (1, 3); Tee-Yassi et al., 1999 (27, 31, 32, 33); Thusu & Van Der Eem, 1985 (1, 2, 3, 4, 5, 6, 7, 22); Thusu et al., 1988 (1, 2, 3, 4, 5, 6, 7). **Sources for NS American ranges**: Brenner, 1968 (13, 15, 21); Herngreen, 1973 (11, 12, 13, 14, 15, 16, 17, 19, 20, 21, 22, 23); Herngreen, 1975 (10); Herngreen & Dueñaz Jimenez, 1990 (12, 13, 14, 17, 19, 20, 21); Müller, 1966 (10, 13, 14, 21); Regali & Viana, 1989 (4, 6, 7, 8, 9, 11, 15); Regali et al., 1974 (4, 7, 10, 12, 14, 35). **Sources for Tethyan ranges**: Clark & Verdier, 1967 (48, 50, 51); Davey & Verdier, 1973 (45); Davey & Verdier, 1974 (45, 46, 47); Duxbury, 1983 (46); Erba, 1999 (37); Foucher et al., 1994 (44, 46, 47); Habib & Drugg, 1983 (37, 38); Hoedemaeker & Leereveld, 1995 (38, 39, 44); Jan Du Chêne et al., 1978 (53); Leereveld, 1997a (38, 39); Leereveld, 1997b (40, 41, 42, 43); Lister & Batten, 1988 (46, 47); Roncaglia & Corradini, 1997 (43, 54); Schrank & Ibrahim, 1995 (43, 48, 49, 50, 51, 52, 53, 54); Srivastava, 1994 (42); Thusu et al., 1988 (37, 38, 39, 40, 44); Torricelli, 2000 (37, 38, 40, 41, 43, 45, 47); Torricelli, 2001 (37, 40, 45, 46, 47); Torricelli, 2006 (41, 45); Torricelli & Amore, 2003 (43, 50, 51, 52, 54); Wilpshaar, 1995 (38, 40, 42, 43).

southern Tethyan region (e.g. Libya and Egypt). This may be due to environmental exclusions.

Despite the fact that North and West Africa and northern South America are confined to the same phytogeographic province, some differences in palynofloral assemblages and in the range of some taxa have been noted (Doyle et al., 1982; Salard-Cheboldaeff, 1990; Herngreen et al., 1996). This may be dependent on the palaeolatitudinal position of each region, and possibly on proximity to the centre of angiosperm radiation. In northern Morocco in the Agadir-Essaouira Basin and in the southwestern Tarfaya Basin, the Albian-Cenomanian palynoflora exhibits Albian-Cenomanian Elaterate Province characteristics, but contain some forms which are characteristic for the *Cerebropollenites* Province of Herngreen et al. (1996), for example some temperate palynomorphs represented by bisaccate pollen grains (e.g. *Alisporites*, *Podocarpidites*, *Vitreisporites, Cerebropollenites,* (Bettar & Méon, 2001, 2006). Moreover, there are differences in the ranges of some of the pre-Aptian palynomorph between Senegal and the Ivory Coast and the Congo and Gabon (e.g. the index gymnosperm pollen *Dicheiropollis etruscus*). A close similarity in the pre-Aptian palynoflora and sedimentary sequence between that of Gabon and Congo and northeast Brazil have also been documented (Viana, 1968; Jardiné et al., 1974; Doyle et al., 1977; Salard-Cheboldaeff, 1990). From a palaeogeographic point of view, northern Egypt was located at around 8° N (Fig. 5.5) during the Hauterivian (Lawver et al., 2004, www.ig.utexas.edu/research/projects/plates/), whereas Libya, Nigeria, Senegal and the Ivory Coast were nearly confined to the same palaeolatitude, where they possessed palynofloras of more similar stratigraphic ranges than that of the palaeosubtropical regions mentioned above. As it shown from the above discussion, the pre-Aptian stratigraphic units of the palaeotropical and palaeosubtropical regions could be diachronous.

Schrank & Ibrahim (1995) argued for an early late Cretaceous diachroneity of the stratigraphic units in NE Africa and West Africa, based on the foraminiferally controlled extension of *Droseridites senonicus* down into the late Turonian of Egypt. However, this late Turonian lower limit of *D. senonicus* has been also recorded in the foraminiferally dated late Turonian of NE Nigeria (Lawal & Moullade, 1986). Added to that, most of the foraminiferally dated elaterate index forms of West Africa have also been found in Egyptian foraminifera-controlled sediments (Schrank & Ibrahim, 1995) of ages similar to those of West Africa, and thus does not support the proposed diachroneity. In contrast, a greater similarity in the palynofloral stratigraphic ranges could be proposed in the light of African plate movement during the Cretaceous. This tectonic plate was moving anticlockwise towards Laurasia, as a result of the opening of the southern Atlantic Ocean, bringing the early Cretaceous palaeotropical region into a relatively subtropical position by the late Cretaceous (Fig. 5.6), where stratigraphic units of NE Africa and West Africa show palynofloral assemblages of more similar stratigraphic age ranges.

Therefore, the micropalaeontologically dated palynological work carried out in Libya (Thusu & van der Eem, 1985; Thusu et al., 1988), Nigeria (Lawal & Moullade, 1986), and Senegal and the Ivory Coast (Jardiné & Magloire, 1965; Jardiné, 1967) will be employed here for dating the pre-Aptian sequences studied, with the West African palynofloral stratigraphic age ranges employed for the latest early and late Cretaceous sample interval.

Spore and pollen grains are considered a powerful tool for biostratigraphic purposes, because their vertical distribution is continuous and they exhibit reliable lineage trends (e.g. *Afropollis* complex). Dinoflagellate cyst taxa on the other hand have been found to be facies controlled in the lower Cretaceous sediments, and while they are extremely diluted by microforaminiferal test linings in upper

Cretaceous carbonate sediments, these dinoflagellate taxa are the only biostratigraphic tools that can be used to date the carbonate succession.

In general, the vertical distribution of dinoflagellate cysts is subject to greater facies control in marginal facies in comparison to that of the miospores. For this reason, the spore and pollen grain ranges have been used for palynostratigraphic purposes, with dinoflagellate cysts giving additional supporting evidence. The first appearance datum (FAD) of the index spores and pollen have been used in the delineation of most of the biostratigraphic units, with their last appearance datum (LAD) used when no (FAD) is available, and also to provide supporting evidence to the determinations. The vertical quantitative (grain/gram) distribution (Fig. 5.7) of certain taxa with well-known ranges (e.g. *Afropollis zonatus*) has been used to provide evidence of limited caving. This has been proven to be minor in the studied boreholes. The numbers in parentheses after the names of the taxa refer to the position of these species in the quantitative range chart.

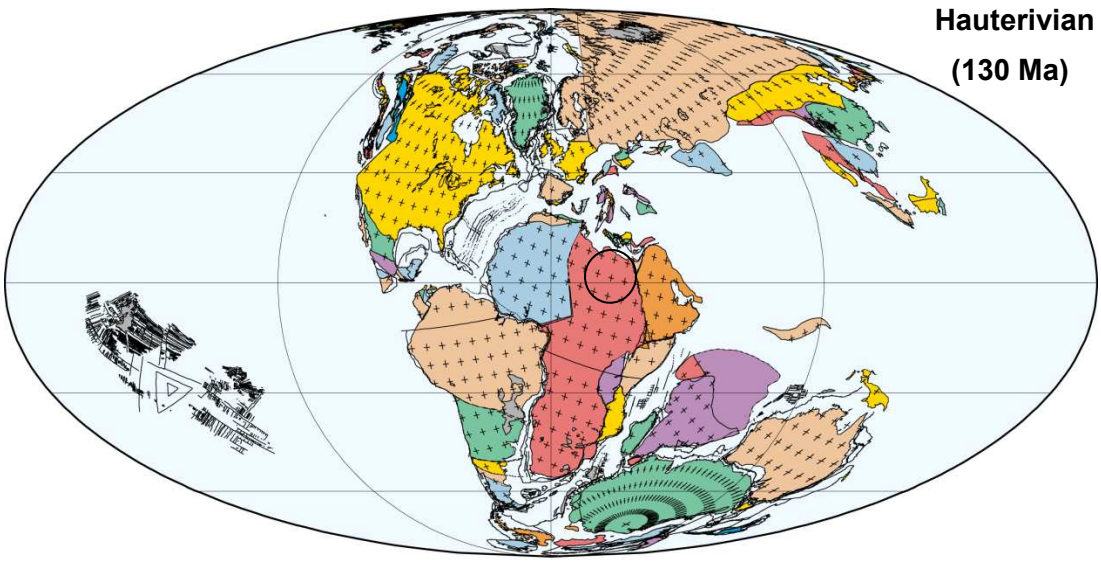

Figure 5.5 World palaeogeographic map showing the position of north Egypt during the Hauterivian time (after Lawver et al., 2004).

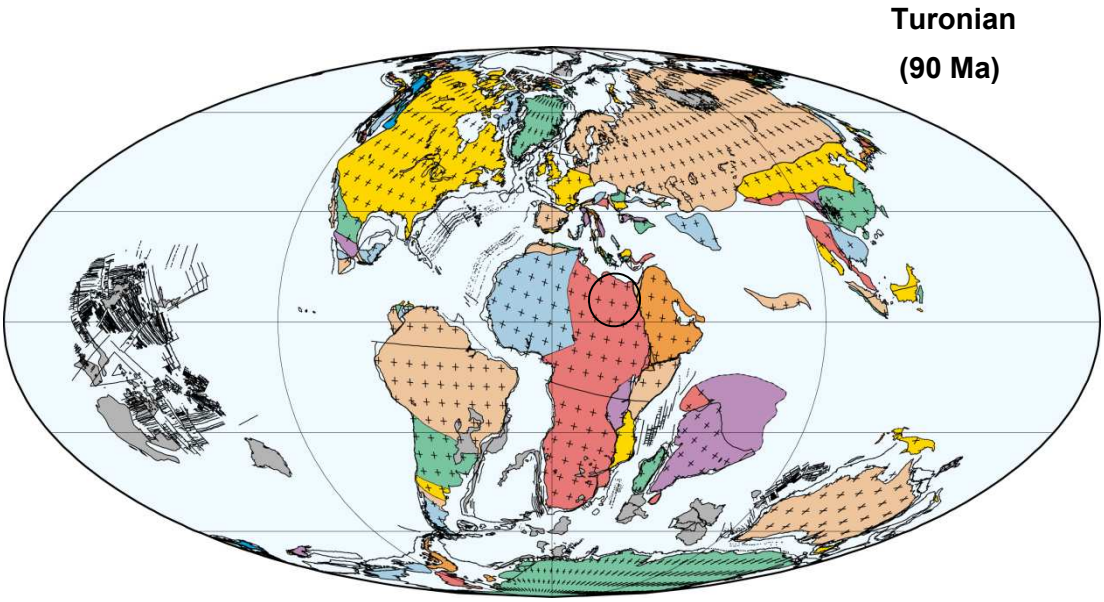

Figure 5.6 World palaeogeographic map showing the position of north Egypt during the Turonian time (after Lawver et al., 2004).

5.2.1 Age assignments for the Abu Tunis 1x borehole

Late Jurassic (Sample 1)

This sample (at 10150 ft, 3094 m) is characterized by the long ranging spore taxa *Deltoidospora* spp., *Concavisporites* spp., *Triplanosporites* sp., *Dictyophyllidites* spp., and *Crybelosporites brenneri*, and the gymnosperm pollen grains *Araucariacites australis*, *Balmeiopsis limbatus*, *Inaperturopollenites* spp., *Exesipollenites* spp. (= *Spheripollenites* and *Taxacites sahariensis*) and *Classopollis* spp. (Fig. 5.7), which range from the late Jurassic to the early Cretaceous in Egypt and NE Libya (Schrank, 1984a-a; Thusu & van der Eem, 1985; Thusu et al., 1988). The lack of an adequate number of samples below 10150 ft did not enable a more precise Jurassic age for this sample. However, there is a complete absence from Sample 1 of *Impardecispora apiverrucata*, *Aequitriradites spinulosus*, and *Pilosisporites trichopapilosus*, which are considered as early Berriasian-Valanginian marker forms (Thusu et al., 1988; Schrank & Mahmoud, 1998) and *Dicheiropollis etruscus,* which is characteristic of the late Hauterivian-early Barremian (Hochuli, 1981; Thusu et al., 1988). The abrupt appearance of all of these forms in the overlying Sample 2 is therefore compatible with a Jurassic age for Sample 1. From a lithostratigraphic point of view, the position of this sample below an unconformity conforms with the major unconformity which separates the Jurassic from the overlying Cretaceous succession in most of the northern Western Desert rocks (Morgan, 1990). The upper Jurassic (Kimmeridgian)-lower Cretaceous (Berriasian-Barremian) rocks were exposed and subjected to erosion in most of the north western basinal areas, except in the extreme north, where continuous sedimentation took place in the Matruh and Sidi Barrani basins (Kerdany & Cherif, 1990). A late Jurassic age is also in accordance with the age of the Masajid Formation, where the

drilling company (WEPCO, 1968) originally designated this part of the borehole as representing the Masajid, and also allocated a Jurassic age.

Palynozone 1: late Hauterivian-early Barremian (Samples 2-9)

Samples: This zone includes samples from 2 to 9, which are recovered from a depth of 10100 to 9750 ft (3078-2972 m).

Definition: Total range of *Dicheiropollis etruscus* (89).

Associated taxa: *Deltoidospora* spp. (1), *Cicatricosisporites* spp. (7), *Concavissimisporites punctatus* (10), *Concavisporites* spp. (19), *Dictyophyllidites harrisii* (28), *Cibotiumspora jurienensis* (37), *Deltoidospora australis* (38), *Trilobosporites hannonicus* (52), *Impardecispora uralensis* (60), *Balmeiopsis limbatus* (63), *Classopollis classoides* (64), *Araucariacites australis* (69), *Inaperturopollenites undulatus* (77), *Taxacites sahariensis* (84), *Circulodinium distinctum* (173), *Cribroperidenium* sp. (183), *Muderongia tomaszowensis* (203), *Muderongia* spp. (206), *Phoberocysta* spp. (215).

Discussion concerning age assessment: These samples are similar to Sample 1 in their microfloral content, where smooth-walled pteridophytic spores and gymnosperm pollen grains dominate the microfossil assemblage, and there are very rare occurrences of some dinoflagellate cysts. However, these samples witness the first appearance of the gymnosperm index pollen *Dicheiropollis etruscus,* along with the marker spores: *Impardecispora apiverrucata*, *Aequitriradites spinulosus*, and *Pilosisporites trichopapillosus* (Fig. 5.7). Thusu & van der Eem (1985) and Thusu et al. (1988) recorded *Impardecispora apiverrucata* from calpionellid-dated Valanginian rocks in NE Libya, where they correlated its range to that of the palynologically dated Saharan Subzone 5c of NE Algeria and Southern Tunisia (Reyre, 1973) of Neocomian age. *Aequitriradites spinulosus* ranges from the calpionellid-dated

Valanginian rocks of Libya to the foraminifera-dated Early Cenomanian rocks of Egypt (Thusu & van der Eem, 1985; Thusu et al., 1988; Schrank & Ibrahim, 1995). Schrank & Mahmoud (1998) regarded *Impardecispora apiverrucata* and *Aequitriradites spinulosus* as marker Berriasian-Valanginian species in Egypt, based on well dated European, Libyan and other sequences. The spore *Pilosisporites trichopapilosus*, which was recorded from well-dated Valanginian-Hauterivian sequences of NE Libya (Thusu & van der Eem, 1985; Thusu et al., 1988), occurs in most of these samples.

In the palaeotropical region, *Dicheiropollis etruscus* was recorded in NE Libya from foraminifera and dinoflagellate dated rocks of late Hauterivian-early Barremian age (Thusu & van der Eem, 1985; Thusu et al., 1988) and similarly from the palynologically dated late Hauterivian-early Barremian rocks of Senegal and the Ivory Coast (Salard-Cheboldaeff, 1990). In the palaeosubtropical region (± 15-20° N and S), the latest occurrence of *D. etruscus* has been recorded in Morocco from dinoflagellate-dated marine sediments of early Barremian age (Hochuli, 1981) and its earliest occurrence from the base of turbidite sediments of early Berriasian age (Gübeli et al., 1984). In Sudan, Gabon and other palaeosubtropical African countries, *D. etruscus* has been recorded from palynologically dated continental and shallow marine sediments of Neocomian-Barremian age (Jardiné et al., 1974; Doyle et al., 1977; Penny, 1986; Kaska, 1989; Salard-Cheboldaeff, 1990; Awad, 1994). Similarly, in North South America, *D. etruscus* has been recorded in NE Brazil from palynologically dated fluvio-lacustrine rocks of Berriasian-early Barremian age (Regali et al., 1974; Regali & Viana, 1989).

The phytoplankton assemblage of the Palynozone 1 is represented by rare occurrences of some facies controlled ceratoid dinoflagellate species of pre-Hauterivian-Barremian and post-Barremian age ranges: *Phoberocysta neocomica* of late Berriasian-Barremian stratigraphic range in the Tethyan Realm (Habib &

Drugg, 1983; Thusu et al., 1988; Erba et al., 1999; Torricelli, 2000, 2001), *Muderongia pariata*, which has an early Hauterivian-early Albian range in Italy (Torricelli, 2000, 2001), and *Pseudoceratium pelliferum,* which has a Tethyan late Berriasian-Barremian range (Habib & Drugg, 1983; Thusu et al., 1988; Hoedemaeker & Leereveld, 1995; Wilpshaar, 1995; Leereveld, 1997a; Torricelli, 2000). *Muderongia aequicorna* is present in the lower part of the interval, and is known from the late Hauterivian in the Southern Alps of Italy (Torricelli, 2000), where it was accurately dated by a variety of means (Erba et al., 1999). This latter species represents the only marine evidence for a late Hauterivian age proposed for the lower part of the Palynozone 1.

From the presence of marker species with their first appearance in the Valanginian and Berriasian alone, an initial suggestion of a Berriasian lower age limit for these samples might be made. However, the associated presence of the characteristic endemic Northern Gondwana *Dicheiropollis etruscus,* which has a foraminifera-dated late Hauterivian-early Barremian age range in the palaeosubtropical African region, provides strong evidence that Samples 2-9 are of an age younger than the Berriasian-early Hauterivian. The uppermost occurrence of *D. etruscus* in Sample 9, just below the first appearance of the *Stellatopollis* spp., coincides with the same event documented in the *Dicheiropollis*/*Afropollis* Phytogeoprovince (Doyle et al., 1977; Gübeli et al., 1984; Thusu et al., 1988; Regali & Viana, 1989; Fig. 5.4), and supports an age not younger than the early Barremian. As a result, a late Hauterivian-early Barremian age is adopted for this interval (Fig. 5.8).

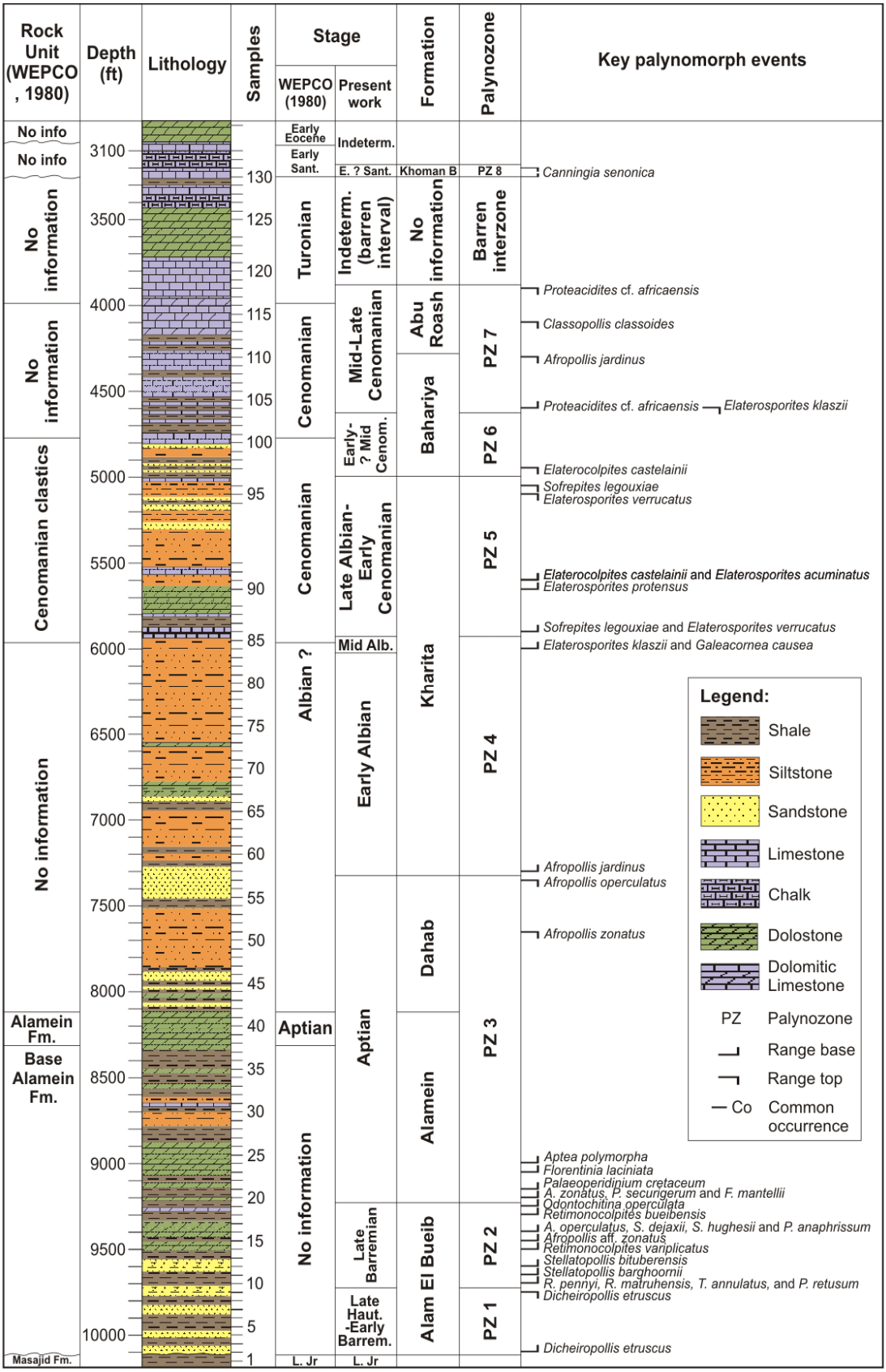

Figure 5.8 The Abu Tunis 1x borehole with lithological column, sample positions, original age dating, key biostratigraphic events and ages deduced in the current work.

Correlation:

- Zone PC-18 (*Dicheiropollis etruscus*) of early Barremian age of Regali et al (1974), Sergipe/Alagoas Basin, northeast Brazil.

- Zones CII-CIV (Neocomian-Barremian) of Doyle et al., (1977), in the pre-salt deposits of northeast Gabon.

- Zone C (late Hauterivian-early Barremian) of Gübeli et al. (1984), northern Morocco.

- Upper part of Zone V and the lower part of Zone VI (late Hauterivian-early Barremian) of Thusu et al. (1988), northeast Libya.

- Assemblage of Section 1 of "Neocomian" and early Barremian age of Penny (1991), in the Mersa Matruh-1 well, northern Western Desert, Egypt.

- Zone PS2 (late Neocomian-early Barremian) of Ibrahim & El-Beialy (1995), in the Malha-1 well, northern Sinai, Egypt.

- Zone II (late Hauterivian-early Barremian) of Ibrahim & Schrank (1996), in the Kahraman-1 well, northern Western Desert, Egypt.

Palynozone 2: late Barremian (Samples 10-19)

Samples: This zone is represented by samples 10 to 19 and covers a depth from 9700 to 9250 ft (2957-2819 m).

Definition: From the FAD of *Retimonocolpites matruhensis* (131), *Retimonocolpites matruhensis-ghazalii* complex (132), *Tucanopollis annulatus* (133), *Retimonocolpites pennyi* (136), *Pseudoceratium retusum* (199) and below the FAD of *Stellatopollis bituberensis* (137) to just below the FAD of *Afropollis zonatus* (128), *Florentinia mantellii* (172) and *Pseudoceratium securigerum* (185).

Associated taxa: *Balmeisporites longirimosus* (20), *Microfoveolatosporites skottsbergii* (21), *Murospora* cf. *mesozoica* (31), *Leptolepidites major* (43), *Gleicheniidites rasilis* (44), *Leptolepidites psarosus* (45), *Crybelosporites striatus* (46), *Aequitriradites verrucosus* (47), *Echinatisporis varispinosus* (54), *Ephedripites* spp. (65), *Reyrea polymorpha* (81), *Retimonocolpites variplicatus* (97), *Afropollis* sp. B Doyle et al., 1982 (130), *Cribroperidinium edwardsii* (190), *Subtilisphaera scabrata* (192), *Circulodinium* cf. *attadalicum* (210), *Cyclonephelium* cf. *vannophorum* (211), *Cyclonephelium vannophorum* (212).

Discussion concerning age assessment: Whilst this interval shows a similarity in its microfloral content with the underlying samples, it is also characterised by the incoming of true (columellate) angiosperm pollen grains: for example, *Retimonocolpites* spp. and *Stellatopollis* spp.. The oldest records of these pollen are widely accepted to mark the late Barremian (Penny, 1991; Doyle, 1992; Penny, 1992; Schrank, 1992; Schrank & Mahmoud, 1998; Doyle, 1999) in the *Dicheiropollis*/*Afropollis* Phytogeoprovince. In the foraminifera and dinoflagellate-dated Libyan late Barremian, *Stellatopollis* spp. and *Tucanopollis crisopolensis* were recorded from the base, and *Retimonocolpites* spp. were recorded from the latest part of the late Barremian (Thusu & van der Eem, 1985; Thusu et al., 1988). In the well marine-dated sediments of Morocco, *Retimonocolpites* spp. and *Stellatopollis* spp. have been recorded from the late Barremian (Gübeli et al., 1984). Hughes et al. (1979) recorded *Stellatopollis hughesii* and *Retimonocolpites* sp. from the independently dated late Barremian rocks of southern England. Hughes (1994) also recorded *Stellatopollis* (as biorecords CfA Superret-croton and Superret-triang), *Retimonocolpites* spp. (as CfA Retisulc-dentat) with supramural spines similar to *Retimonocolpites pennyi*, and *Tucanopollis crisopolensis* (as CfA Barremian-ring) from Barremian ('Phase 3') and Barremian-Aptian ('Phase 4') rocks of southern England. The heteropolar, zonasulculate pollen grain *Afropollis operculatus* is

widely accepted as an Aptian marker species in the pre-Albian *Dicheiropollis etruscus*/*Afropollis* Phytogeographic Province. *Afropollis operculatus* has been recorded (as *Reticulatasporites jardinus* Type 1) from a planktonic foraminifera- and calcareous nannoplankton-dated early Aptian section at DSDP, Site 418B in the Western North Atlantic (Hochuli & Kelts, 1980), from the well dated early Aptian of Gabon and Senegal (Doyle et al., 1982; Doyle, 1992), and from the supposed early Aptian of Egypt (e.g. Schrank, 1983; Schrank & Ibrahim, 1995). However, a pre-Aptian range of this species was recorded in Morocco by Gübeli et al. (1984) from well-dated marine rocks of late Barremian age, and in the supposed late Barremian of Gabon, Egypt and NE Brazil (Regali & Viana, 1989; Schrank & Mahmoud, 1998; Doyle, 1999; Schrank & Mahmoud, 2002).

The zone itself is characterised by a number of angiosperm pollen grains. In Egypt, the ages of the angiosperm grains mentioned below are cited as probably late Barremian, but it should be born in mind that the dating of the Egyptian successions has mainly been accomplished by correlation with similar angiosperm assemblages from the better-dated English Barremian sequences (e.g. Hughes et al., 1979) and the palynologically dated pre-salt sequence (Zones CV-CVIII) of Gabon of probable Barremian-Aptian age (Doyle et al., 1977).

Retimonocolpites matruhensis was erected by Penny (1986) from the believed late Barremian of the Mersa Matruh-1 well, from the northern Western Desert, a species later recorded by Schrank & Mahmoud (2000) from the Six Hills Formation, Central Egypt, also of probable late Barremian age. *Retimonocolpites pennyi*, erected by Schrank & Mahmoud (2002) from the Six Hills Formation, had previously been described by Penny (1991) under the Hughesian biorecord Reticol-speckle from the late Barremian of the Mersa Matruh-1 well, and (as *Clavatipollenites rotundus*) by Dejax (1987) from the supposed late Barremian of the Congo. The base of this interval is also characterised by the presence of other

potential marker pollen grains first described from the supposed late Barremian of Egypt, such as *Stellatopollis bituberensis* Penny (1986) from the Mersa Matruh-1 well, and *Tucanopollis annulatus* and *Retiacolpites* sp.1 Schrank & Mahmoud (2002) from the Six Hills Formation. The pollen grain *Retimonocolpites bueibensis*, which was described by Ibrahim (Ibrahim, 2002a) from the ?upper Barremian rocks of the Ghazalat-1 well, northern Western Desert, Egypt also occurs in the interval. *Stellatopollis barghoornii* was described by Doyle in Doyle et al. (1975) from the supposed Barremian-Albian? rocks of the Potomac Group, North America and from the probable Barremian of the Congo by Doyle et al. (1977). In Egypt this species has been found to range from the probable late Barremian to the Aptian (Ibrahim & Schrank, 1996; Ibrahim et al., 2002). This species occurs in most of the samples from this interval. *Stellatopollis hughesii* Penny (1986) from the late Barremian of the Mersa Matruh-1 well, had previously been reported from rocks of a similar age from southern England by Hughes et al. (1979), and was later discovered by Ibrahim (2002a) from the supposed late Barremian of the Ghazalat-1 well. *S. hughesii* has a distribution in the upper part of this sample interval in the Abu Tunis core. Also distributed in the upper part of this sample interval are *Stellatopollis dejaxii* and *Retimonocolpites ghazalii*, described by Ibrahim (2002a) from the supposed late Barremian to mid Aptian of the Ghazalat-1 well, and *Afropollis* aff. *zonatus*. The latter taxon, was recognised in Gabon from the pre-salt early Aptian rocks (Doyle et al., 1982; Doyle, 1992) below the ammonite-dated carbonate sequence (Reyment & Tait, 1972) of late Aptian-Albian age, and from the palynologically dated early Aptian (Schrank, 1983; Schrank & Ibrahim, 1995) and the late Barremian-early Aptian (Penny, 1986) of Egypt. The two possible late Barremian pollen grains *Retiacolpites columellatus* and *Retimonocolpites* sp.1 of Schrank & Mahmoud (2002) are confined to the last sample of this sample interval.

However, there are rare occurrences of *Arecipites microfoveolatus* in the middle part of this sample interval, a taxon which was described by Ibrahim (2002a) from believed Aptian age sediments from the Ghazalat-1 well. In addition, there are scarce occurrences of *Dichastopollenites ghazalatensis* of Aptian-Cenomanian age (Ibrahim, 1996, 2002a) in the upper part of the interval, but until an independent extension of the range of these two taxa into the late Barremian is confirmed, their distribution in the present interval will be considered as due to possible caving.

In terms of dinoflagellate cysts, the lower boundary of this sample interval is also marked by the FAD of the late Barremian Tethyan species *Pseudoceratium retusum* (Srivastava, 1984; Wilpshaar, 1995; Leereveld, 1997b). The phytoplankton assemblages also record first appearances of some Hauterivian-Barremian dinoflagellate species, including *Subtilisphaera senegalensis* and *Circulodinium brevispinosum*, which have Tethyan late Hauterivian-Albian ranges (Thusu et al., 1988; Leereveld, 1997b; Torricelli, 2000, 2001). In the middle part of the interval, two Tethyan latest Hauterivian/early Barremian-Albian dinoflagellate species appear: *Subtilisphaera terrula* (Habib & Drugg, 1983; Torricelli, 2001) and *Subtilisphaera perlucida* (Habib & Drugg, 1983; Thusu et al., 1988; Leereveld, 1997b; Torricelli, 2000, 2001). *Subtilisphaera scabrata*, which was used by Leereveld (1997b) to delineate the lower boundary of his Tethyan Zone (Ssc) of Early Barremian age, also occurs in the middle part of the interval.

The upper part of the interval is characterised by the appearance of *Pseudoceratium anaphrissum*, regarded as a late Barremian-Aptian marker species in the Tethyan Realm (Thusu et al., 1988; Foucher et al., 1994; Hoedemaeker & Leereveld, 1995; Fig. 5.4). The inception of *Odontochitina operculata* was used in the Tethyan Realm to determine the base of the late Barremian (Wilpshaar, 1995; Leereveld, 1997b; Torricelli, 2000, 2001), and appears in the uppermost part of this

sample interval, as does *Odontochitina ancala*, which was recorded from the late Barremian of Italy (Torricelli, 2000) and ranges into the early Albian.

Also present is *Florentinia cooksoniae*, which was originally described by Singh (1971) from the Albian lower Shaftsbury Formation, Canada, and is also known from the supposed Albian-Cenomanian rocks of Egypt and NE Libya (Uwins & Batten, 1988; Omran et al., 1990). The downward extension of the range of *F. cooksoniae* into Palynozone 2 could be a true stratigraphic extension, as this species was recovered by Duxbury (1980) from the Barremian Speeton Clay of East Yorkshire, England.

The appearance in this sample interval of dinoflagellate cyst taxa characteristic of the latest Hauterivian/early Barremian-Aptian, together with several late Barremian-early Aptian angiosperm pollen grains might suggest a late Barremian-early Aptian age. However, in the overlying sample (20) the presence of the Aptian angiosperm pollen marker *Afropollis zonatus* and the characteristic early Aptian dinoflagellates *Pseudoceratium securigerum* and *Palaeoperidinium cretaceum* indicates that this interval should be dated as late Barremian.

Correlation:

- Zones CVI-CVII (late Barremian) of Doyle et al. (1977), in the pre-salt deposits of northeast Gabon.
- Zone D (late Barremian) of Gübeli et al. (1984), northern Morocco.
- Zone VI (late Barremian) of Thusu et al. (1988), northeast Libya.
- *Stellatopollis bituberensis* Zone (late Barremian) of Regali & Viana (1989), northeast Brazil.

- Assemblage of Section 2 (late Barremian) of Penny (1991), in the Mersa Matruh-1 well, northern Western Desert, Egypt.
- Zone PS1 (late Barremian) of Ibrahim & El-Beialy (1995), in the Malha-1 well, northern Sinai, Egypt.
- The lower part of Zone IV (late Barremian-early Aptian) of Ibrahim & Schrank (1996), in the Kahraman-1 well, northern Western Desert, Egypt.
- The upper part of the *Stellatopollis* spp.-*Schrankipollis* spp. Assemblage Zone (Barremian) of Ibrahim et al. (1997), from the Abu Hammad-1, Q-71-1X and the Kabrit-1 wells, northern Eastern Desert, Egypt.
- Assemblage "A1" (core #15) of late Barremian age of Ibrahim (2002a), in the Ghazalat-1 well, northern Western Desert, Egypt.

Palynozone 3: Aptian (Samples 20-57)

Samples: This zone includes samples from 20 to 57, which were taken from depths between 9200 to 7350 ft (2804-2240 m).

Definition: From the FAD of *Afropollis zonatus* (128), *Pseudoceratium securigerum* (185) and *Florentinia mantelii* (172) and just below the FAD of *Palaeoperidinium cretaceum* (187) to just below the FAD of *Afropollis jardinus* (92).

Associated taxa: *Crybelosporites pannuceus* (2), *Cicatricosisporites orbiculatus* (4), *Balmeisporites* cf. *holodictyus* (9), *Triporoletes reticulatus* (12), *Cicatricosisporites sinuosus* (13), *Murospora florida* (17), *Microfoveolatosporites skottsbergii* (22), *Matonisporites* spp. (24), *Kyrtomisporis* spp. (27), *Aequitriradites norrissii* (40), *Gemmatrilites* sp. (41), *Januasporites* sp. (42), *Tricolpites* sp. (93), *Tricolpites vulgaris* (104), *Downiesphaeridium* spp. (165), *Florentinia* spp. (167),

Coronifera albertii (174), *Coronifera tubulosa* (177), *Oligosphaeridium complex* (179), *Oligosphaeridium poculum* (180), *Pseudoceratium almohadense* (208).

Discussion concerning age assessment: The samples of this interval are different in their floral content to the underlying intervals, as phytoplankton increases in abundance and diversity, from a maximum of 155 (~ 33) cysts/gram, comprising some 16 species in the underlying interval, to a maximum 1171 (~ 100) cysts/gram, and with a diversity of some 25 species in this sample interval. However, pteridophyte spores, gymnosperms, and those angiosperm pollen found in the underlying Barremian interval still dominate the microfloral assemblage. The base of this interval is characterized by the incoming of the zonasulculate isopolar pollen *Afropollis zonatus*, which is regarded as an early Aptian marker species in the *Dicheiropollis etruscus*/*Afropollis* Phytogeographic Province (Fig. 5.4). *A. zonatus* was first described from the palynologically dated sediments of early Aptian age of Gabon (Doyle et al., 1982; Doyle, 1992). This species was later recorded (as *Reticulatasporites jardinus* Type 2) from foraminifera-dated rocks of early Aptian age in southern Switzerland (Hochuli, 1981) and from dinoflagellate-dated sediments of early Aptian age in northern Morocco (Gübeli et al., 1984).

Whereas the presence of *Afropollis* spp., *Tricolpites* spp. and *Brenneripollis* spp. is widely accepted to mark the onset of the early Aptian in West Africa and Egypt (Doyle et al., 1977; Schrank, 1983; Penny, 1986; Schrank, 1991; Doyle, 1992; Schrank & Ibrahim, 1995), the absence of *Brenneripollis* in this sample interval might be taken to suggest a late Barremian age for the interval. However, Doyle (1992) pointed out the dangers of using the absence of *Brenneripollis* to infer a late Barremian age. This is more likely to be due to palaoecological conditions or unfavourable lithologies, especially given that the upper part of this sample interval mainly consists of coarse clastic sediments. *Afropollis* aff. *jardinus*, which was reported from palynologically-dated rocks of late Aptian-early Albian age in West

Africa and Egypt (Doyle et al., 1982; Penny, 1989; Schrank & Ibrahim, 1995; Ibrahim, 1996) also occurs in this interval.

However, overall this interval contains relatively few Aptian marker angiosperm pollen grains, and it is the dinoflagellate species which are of greater biostratigraphic importance. The base of this interval is also delineated by the FAD of *Pseudoceratium securigerum,* diagnostic for the early Aptian in the Tethyan Realm (Fig. 5.4), as it has been recorded from the base of the ammonite-dated Aptian type section in SE France (Davey & Verdier, 1974), from the foraminifera-dated Aptian of Algeria (Foucher et al., 1994), and from the dinoflagellate-dated marine sediments of southern Italy (Torricelli, 2001). In southern England, *P. securigerum* was also recovered by Duxbury (1983) and Lister & Batten (1988) from partly ammonite-calibrated Boreal marine sediments of early Aptian age. In NW Egypt and NE Libya this same species was recovered from rocks of believed early Aptian age (Uwins & Batten, 1988; Omran et al., 1990; El-Beialy, 1994b; Schrank & Ibrahim, 1995).

Another early Aptian marker form with its FAD just above the base of this sample interval is *Palaeoperidinium cretaceum,* which has been recovered from ammonite, planktonic foraminifera, and calcareous nannoplankton calibrated rocks of early Aptian age in the Tethyan Realm of SE France and Italy (Davey & Verdier, 1974; Torricelli, 2000, 2001, 2006), from dinoflagellate-dated rocks of the DSDP Site 543A in the Western Central Atlantic (Habib & Drugg, 1983), and from the supposed early Aptian of Egypt and NE Libya (Batten & Uwins, 1985; Schrank & Ibrahim, 1995). The later appearance of *Aptea polymorpha* in Sample 24 above the lower part of this sample interval is consistent with its FAD in the late early Aptian in the Tethyan Realm (Fig. 5.4) and elsewhere (Davey & Verdier, 1974; Lister & Batten, 1988; Foucher et al., 1994; Torricelli, 2000, 2001).

Other characteristic Aptian dinoflagellate species which appear in this interval are: *Florentinia laciniata* (recorded from ammonite-dated rocks of Aptian-early Cenomanian age in SE France: (Davey & Verdier, 1973); and from well-dated Aptian rocks of Italy: (Torricelli, 2001), and *Florentinia mantelii* (also of Aptian aspect, being recorded from the ammonite-dated Late Aptian of SE France: (Davey & Verdier, 1974); and the dinoflagellate-dated Late Aptian of Italy: Torricelli, 2000, 2001).

Based on the presence of the Aptian dinoflagellate and angiosperm marker forms mentioned above, and with the FAD of the diagnostic early Albian angiosperm *Afropollis jardinus* in the overlying Sample 58, an Aptian age is suggested for this interval.

Correlation:

- Zones CVII-CIX (Aptian) of Doyle et al. (1977), in the pre-salt deposits of northeast Gabon.
- Zone II (Aptian) of Saad (1978), in the Umbarka 1X well, northern Western Desert, Egypt.
- Assemblage II (early-late mid Aptian) of Uwins & Batten (1988), northeast Libya.
- *Exesipollenites tumulus* Zone (Aptian) of Regali & Viana (1989), northeast Brazil.
- Zone E and lower part of Zone F (Aptian) of Gübeli et al. (1984), northern Morocco.
- Zone II (Aptian) of Sultan (1986), in the Shibin El Kom well, Nile Delta, Egypt.
- Zone IV (Aptian) of El-Beialy et al. (1990), in the Sindy-1 well, Nile Delta, Egypt.
- *Afropollis operculatus-Brenneripollis-Tricolpites* spp. Assemblage Zone (Aptian) of Schrank & Ibrahim (1995), in the Kahraman-1 well, northern Western Desert, Egypt.

- Zone III (Aptian) of Mahmoud et al. (1999), in the Ramis-1X and Shaltut-1X wells, northern Western Desert and the Misri-1 well, northern Sinai, Egypt.
- PSI Zone (Aptian) of Mahmoud & Moawad (2002), in the Sanhur-1X borehole, northern Western Desert, Egypt.
- assemblages “A2” and “A3” (cores #14 and #15) of early-mid Aptian age of Ibrahim (2002a), in the Ghazalat-1 well, northern Western Desert, Egypt equate to the lower part of this zone.
- Zone PSIII (Aptian) of Mahmoud & Deaf (2007), in the Siqeifa 1-X borehole, northern Western Desert, Egypt.

Palynozone 4: early-mid Albian (Samples 58-85)

Samples: This zone includes samples from 58 to 85 which span a depth from 7300 to 5950 ft (2225-1814 m).

Definition: From the FAD of *Afropollis jardinus* (92) to just below the FAD of *Sofrepites legouxiae* (71) and *Elaterosporites verrucatus* (72).

Associated taxa: *Verrucosisproites obscurilaesuratus* (8), *Ephedripites irregularis* (78), *Tricolporopollenites* sp. (99), *Rousea delicipollis* (100), *Triporites* sp. (102), *Retimonocolpites textus* (105), *Stellatopollis densiornatus* (118), *Afropollis* aff. *jardinus* (122), *Tetracolpites* sp. (123), *Senegalinium aenigmaticum* (158), *Trichodinium castanea* (160), *Coronifera oceanica* (170), *Oligosphaeridium albertense* (178), *Oligosphaeridium complex* (179), *Oligosphaeridium poculum* (180), *Pseudoceratium anaphrissum* (184), *Pseudoceratium securigerum* (185).

Discussion concerning age assessment: The microflora of this interval is characterised by the first appearance of tricolporate (e.g. *Tricolporopollenites*) and triporate (e.g. *Triporites*) angiosperm pollen, while tricolpate pollen (e.g. *Tricolpites*) present in the underlying interval continue to appear. Pteridophyte spores and

gymnosperm pollen grains continue to dominate the microfloral assemblage, and less angiosperm pollen taxa which appeared in the late Barremian is found in the interval. The phytoplankton assemblage shows a slight increase in abundance in the underlying interval (from a maximium 1170 and average 105 cysts/gram) to a maximium 1750 and average 130 cysts/gram here, but with decreasing diversity (from 25 species in the underlying interval to 12 species).

The lower boundary of the early Albian is defined by the FAD of *Afropollis jardinus* just above the LAD of the two marker Aptian forms *Afropollis operculatus* and *Afropollis zonatus*. The extinction of the latter two species was used by Doyle et al. (1982) and Schrank & Ibrahim (1995) to document the Aptian/Albian boundary in West Africa and Egypt. *A. jardinus* is widely accepted as entering the stratigraphic record in the early Albian in the Albian-Cenomanian Elaterate Phytogeographic Province (Fig. 5.4). In West Africa, it has been recorded from foraminifera-dated rocks of early Albian age: in Senegal (as S. Cl. 156 *Incertae sedis*) by Jardiné & Magloire (1965), and in Gabon-Congo-Senegal by Doyle et al. (1982). In north South America this same taxon, has been recorded from foraminifera-dated early Albian age; in Brazil (Herngreen, 1973; Regali et al., 1974; Herngreen, 1975; Regali & Viana, 1989), Peru (Brenner, 1968), and in Colombia from sediments dated by ammonite as being of late Albian-early Cenomanian age (Herngreen & Jimenez, 1990), and finally from Western North Atlantic DSDP Site 418A, *A. jardinus* was also recorded (as *Reticulatasporites jardinus* Type 3) from foraminifera-dated rocks of late Albian-early Cenomanian age (Hochuli & Kelts, 1980).

The lower boundary of the mid Albian interval can be distinguished in these samples by the FAD of *Elaterosporites klaszii*, which is widely accepted to document the base of the mid Albian in the Albian-Cenomanian Elaterate Phytogeographic Province (Fig. 5.4). This taxon has been recorded in West Africa: in Senegal and

the Ivory Coast from foraminifera-dated rocks of mid Albian-mid Cenomanian age (Jardiné & Magloire, 1965; Jardiné, 1967). Foraminiferally dated sediments from Brazil and Columbia have also indicated this taxon to be of mid Albian-mid Cenomanian age (Müller, 1966; Herngreen, 1973; Herngreen & Jimenez, 1990), and it has also been recorded in the Albian-Cenomanian of Peru (Brenner, 1968). Finally, in northern Italy, *E. klaszii* has also been documented as a late Albian form in foraminifera-dated upper Albian rocks by Hochuli (1981).

Although the index gymnosperm pollen *Galeacornea causea* was recorded from foraminifera-dated early Cenomanian age in Senegal (e.g. Jardiné, 1967), its range extends into the late Albian from palynologically dated studies in Gabon and NE Nigeria (Doukaga, 1980; Lawal & Moullade, 1986). *G. causea* was also recovered from rocks of mid Albian-mid Cenomanian age in Brazil and Colombia with foraminifera and ammonite age controls (Müller, 1966; Herngreen, 1973; 1974b; Herngreen & Jimenez, 1990). Thus samples 84 and 85 are more likely to be of mid Albian age.

Gnetaceaepollenitess cf. *clathratus* occurs in the topmost samples of this depth interval, and was identified in Senegal by Stover (1963) from sediments of supposed Cenomanian-Turonian age, later being recorded from the proposed late Albian-mid Cenomanian of NE Nigeria (Lawal & Moullade, 1986).

The problematic occurrence of the gymnospermous tetrad *Droseridites senonicus* in samples 77 and 82 may be due to possible caving, as it has only been recorded from rocks of post-mid Albian age: for example in foraminiferally controlled Coniacian-Santonian sequences in NE Nigeria and the Angola Basin (Morgan, 1978; Lawal & Moullade, 1986), and in Egypt from foraminifera-dated rocks of late Turonian-early Santonian age (Schrank & Ibrahim, 1995).

Based on the data above an early to mid Albian age is suggested from this sample interval.

Correlation:

- Sequence XI (early-mid Albian) of Jardiné & Magloire (1965), Senegal Basin.
- Zone I (early-mid Albian) of Herngreen (1973), in the 1-QS-1-MA well, Maranhao Basin, Brazil.
- Zone I (early-mid Albian) of Sultan & Aly (1986), in the WD-9-15-1 well, northern Western Desert, Egypt.
- Lower part of the Zone V (Albian) of El-Beialy et al. (1990), in the Sindy-1 well, Nile Delta, Egypt.
- Zones II and III (early-mid Albian) of Schrank & Ibrahim (1995), in the Kahraman-1 well, northern Western Desert, Egypt.
- Lower part of Zone IV (Albian) of Mahmoud et al. (1999), in the Ramis-1X and Shaltut-1X wells, northern Western Desert, and in the Misri-1 well, Northern Sinai, Egypt.
- Lower part of the Zone PSII (Albian) of Mahmoud & Moawad (2002), in the Sanhur-1X well, northern Western Desert, Egypt.

Palynozone 5: late Albian-early Cenomanian (samples 86-96)

Samples: This zone includes samples from 86 to 96, which cover a depth from 5900 to 5050 ft (1798-1539 m).

Definition: Total range of *Sofrepites legouxiae* (71).

Associated taxa: *Classopollis classoides* (64), *Ephedripites* spp. (65), *Araucariacites australis* (69), *Afropollis jardinus* (92), *Tetraporopollenites* sp. (95), *Rousea delicipollis* (100), *Tricolpites vulgaris* (104), *Retimonocolpites textus* (105), *Rousea brenneri* (106), *Tricolpites parvus* (107), *Triporopollenites* spp. (109), *Tricolpites micromunus* (110), *Dichastopollenites ghazalatensis* (111), *Tricolpites* cf. *crassimurus* (112), *Tricolpites sagax* (114), *Retimonocolpites ghazalii* (115), *Stephanocolpites* sp. (116), *Stellatopollis barghoornii* (117), *Stellatopollis densiornatus* (118), *Striatopollis* cf. *trochuensis* (119) *Trichodinium castanea* (160), *Xiphophoridium alatum* (168), *Cribroperidinium edwardsii* (181).

Discussion concerning age assessment: The microfloral assemblage of this interval is characterised by elaterate pollen grains, and a noticeable increase in abundance of both tricolpate angiosperm pollen and the genus *Afropollis,* from a maximum 1500 (average ~ 400) grains/gram in the underlying interval to a maximum of 5375 (average ~ 3400) grains/gram. This increase is accompanied by a decrease in spore diversity, which are mainly represented by *Deltoidospora* and *Cicatricosisporites* spp.. The abundance of phytoplankton continues to decrease (244 maximum/average 100 cysts/gram) throughout the interval but with the same low diversity (~14 species) as in the underlying interval.

Sofrepites legouxiae is an index taxon in this interval which was found to range from the upper Albian to lower Cenomanian in foraminiferally dated rocks of Senegal by Jardiné & Magloire (1965), Jardiné (1967), and in Brazil by Herngreen (1973) and Herngreen & Jimenez (1990). Another taxon present in this study interval is *Elaterosporites verrucatus,* recorded in Senegal and the Ivory Coast from rocks dated foraminiferally to be of mid Albian-early Cenomanian age (Jardiné & Magloire, 1965; Jardiné, 1967: Figure 5.4). However, in foraminifera- and ammonite- dated rocks from Brazil, this same taxon was recorded from the latest mid to earliest late Albian (Herngreen, 1973; Regali et al., 1974; Herngreen &

Jimenez, 1990) and a single occurrence has been reported from the middle part of the ammonite-dated upper Albian rocks of Columbia (Herngreen & Jimenez, 1990). *Cretacaeiporites densimurus* appears in the lower part of this sample interval, and was first described by Schrank & Ibrahim (1995) from foraminifera-dated rocks of early-mid Cenomanian age, and was later recorded by Ibrahim (2002b) from the late Albian-early Cenomanian of Egypt. Single specimens of other species of this genus have been found in the upper part of this sample interval: *C. polygonalis*, which has a late Albian-late Cenomanian range in Senegal (Jardiné & Magloire, 1965), and *C. mulleri*, which ranges from the late Albian up to the Santonian in Senegal and NE Nigeria (Jardiné & Magloire, 1965; Lawal & Moullade, 1986), and is recorded as of late Albian-mid Cenomanian age in Brazil (Herngreen, 1973).

Appearing throughout the upper part of this interval, the range of *Elaterocolpites castelainii* was used to document the base of the late Albian and top of the mid Cenomanian Elaterate Phytogeographic Province in Senegal (Fig. 5.4; (Jardiné & Magloire, 1965; Jardiné, 1967) and Brazil (Herngreen, 1973; Herngreen & Jimenez, 1990). This taxon was also recorded by Hochuli (1981) from the foraminifera-dated late Albian of southern Switzerland. Other elaterate pollen grains present in these samples that are characteristic of the late Albian-early Cenomanian are *Elaterosporites acuminatus* and *E. protensus* (Fig. 5.4). *E. acuminatus*, was reported from the late Albian-early Cenomanian of Senegal (Jardiné, 1967), and occurs in the lower part of this interval. *E. protensus* is found in the same samples and was recorded from foraminifera-dated rocks of mid Albian to latest Albian/earliest Cenomanian age in Senegal and the Ivory Coast (Jardiné & Magloire, 1965; Jardiné, 1967) and Brazil (Herngreen, 1973; Herngreen & Jimenez, 1990).

Afropollis kharamanensis was recorded by Schrank & Ibrahim (1995) and Ibrahim (2002b) from the foraminifera-dated early-mid Cenomanian of Egypt. However, the former authors mentioned that the taxon described as Pollen PO-304

by Lawal & Moullade (1986) from the supposed late Albian-mid Cenomanian of NE Nigeria was identical to their new species. Therefore, the presence of *Afropollis kharamanensis* in this interval does not contradict the proposed late Albian-Cenomanian age. *Foveotricolpites gigantoreticulatus* was recorded from foraminifera-dated rocks of Turonian-Santonian age in Senegal and NE Nigeria (Jardiné & Magloire, 1965; Lawal & Moullade, 1986). However, Schrank & Ibrahim (1995) and Schrank & Mahmoud (1998) documented an older occurrence of this species in the palynologically dated Albian-Cenomanian of Egypt. Thus, the presence of *F. gigantoreticulatus* in the middle part of this interval may not conflict with the proposed late Albian-early Cenomanian age of the interval. The rare presence of *Triporites* spp. in this interval is in accordance with the late Albian-early Cenomanian, as rare *Triporites* spp. were recorded from the early Cenomanian of Senegal (Jardiné & Magloire, 1965).

The questionable occurrence of *Droseridites baculites* in this interval, which was described by Ibrahim (1996) from the well-constrained lower Turonian of Egypt, may be attributed to possible caving.

As for the dinocysts, *Florentinia berran* appears in the lower part of the interval, a taxon that was recorded from the Albian-early Cenomanian of the southern Tethyan Realm in Morocco and NE Libya (Below, 1982b, 1984; Uwins & Batten, 1988). *F. laciniata* and *F. mantellii* first appear in this interval and are known from ammonite-dated Aptian-early Cenomanian sequences in the Tethyan Realm: they continue upward into the overlying intervals.

Based on the presence of the few late Albian-early Cenomanian elaterate and few marker angiosperm forms mentioned above, a late Albian-early Cenomanian age is postulated for the interval.

Correlation:

- Sequences X-VIII (late Albian-early Cenomanian) of Jardiné & Magloire (1965), Senegal Basin.

- Zone II (late Albian-early Cenomanian) of Herngreen (1973), in the 1-QS-1-MA well, Maranhao Basin, Brazil.

- Subzone Ia (late Albian-early Cenomanian) of Lawal & Moullade (1986), upper Benue Basin, northeast Nigeria.

- Zone I (late Albian-early Cenomanian) of Sultan & Aly (1986), in the WD-9-15-1 well, northern Western Desert, Egypt.

- Zone III (late Albian-early Cenomanian) of Aboul Ela & Mahrous (1992), in the East Tiba-1 well, northern Western Desert, Egypt.

- Zone 5 (late Albian-early Cenomanian) of Schrank (1992), Egypt and north Sudan.

- Intervals 3 and 4 (late Albian-early Cenomanian), in the Manndra 1 well and intervals c and d (late Albian-early Cenomanian), in the Oued Melah 1 well of Foucher et al., (1994), Algeria.

- Zone IV (late Albian-early Cenomanian?) of Schrank & Ibrahim (1995), in the Kahraman-1 well, northern Western Desert, Egypt.

- Assemblage “A” (late Albian-early Cenomanian) of Ibrahim (2002b), in the Abu Gharadig-5 well, northern Western Desert, Egypt.

Palynozone 6: early-? mid Cenomanian (samples 97-103)

Samples: This zone is represented by samples from 97 to 103 and spans a depth from 4950 to 4650 ft (1509-1417 m).

Definition: From the LAD of *Sofrepites legouxiae* (71) to the FAD of *Proteacidites* cf. *africaensis* (91).

Associated taxa: *Deltoidospora* spp. (1), *Crybelosporites pannuceus* (2), *Cicatricosisporites orbiculatus* (4), *Balmeiopsis limbatus* (63), *Classopollis classoides* (64), *Ephedripites* spp. (65), *Elaterosporites klaszii* (66), *Araucariacites australis* (69), *Elaterocolpites castelainii* (70), Afropollis jardinus (92), *Rousea delicipollis* (100), *Cretacaeiporites mullerii* (101), *Triporites* spp. (102), *Florentinia mantellii* (172), *Florentinia laciniata* (176).

Discussion concerning age assesment: The microfloral assemblage of this interval lacks any diagnostic sporomorphs. Miospores are represented by pteridophyte and schizaeacean spores, xerophytic gymnosperm, and two elaterate pollen species, and three angiosperm pollen species. The index angiosperm pollen *Proteacidites* cf. *africaensis*, which is widely accepted to document the base of the mid Cenomanian in the Albian-Cenomanian Elaterate Province (e.g. Jardiné & Magloire, 1965; Lawal & Moullade, 1986) first appears in the overlying interval (in Sample 104), and thus delineates the lower boundary of the mid Cenomanian. Consequently, the present interval could be of a possible early Cenomanian age.

The phytoplankton assemblage shows a slight increase in abundance over the interval below (maximum 370/average 120 cysts/gram) but with a consistent diversity (~10 species), and they provide some important implications for dating the interval. *Florentinia berran*, which was found from sediments as young as the early-mid Cenomanian in Egypt (Schrank & Ibrahim, 1995; Ibrahim, 2002b), becomes extinct in the lower part of the overlying interval, thus favouring an early-mid Cenomanian age for this sample interval.

Correlation:

- Zone V (early-mid Cenomanian) of Schrank & Ibrahim (1995), in the Kahraman-1 and Abu Gharadiq-18 wells, northern Western Desert, Egypt.
- Zone 3 (early-mid Cenomanian) of Ibrahim (1996), in the Ghazalat-1 well, northern Western Desert, Egypt.
- Assemblage "B" (early-mid Cenomanian) of Ibrahim (2002b), in the Abu Gharadiq-5 well, northern Western Desert, Egypt.

Palynozone 7: mid-late Cenomanian (samples 104-119)

Samples: This zone includes samples from 104 to 119 and covers a depth from 4600 to 3850 ft (1402-1173 m).

Definition: Total range of *Proteacidites* cf. *africaensis* (91).

Associated taxa: *Deltoidospora* spp. (1), *Crybelosporites pannuceus* (2), *Alisporites* cf. *grandis* (62), *Balmeiopsis limbatus* (63), *Ephedripites* spp. (65), *Elaterosporites klaszii* (66), *Retimonocolpites variplicatus* (97), *Tricolporopollenites* sp. (99), *Senegalinium aenigmaticum* (160), *Trichodinium castanea* (165), *Surculosphaeridium* cf. *longifurcatum* (166), *Xiphophoridium alatum* (177), *Florentinia* spp. (176), *Florentinia mantellii* (181).

Discussion concerning age assessment: The palynofloral assemblage of this interval shows similar characteristics to the underlying interval, but with a continuing decrease in the abundance of spores (maximum 48/average 24 grains/gram) and diversity (only two species), the complete disappearance of gymnosperm pollen grains at the end of the interval, and the occurrence of only three angiosperm pollen grains. The phytoplankton increase in their abundance (maximum 3160/average 140 cysts/gram), but have a very low diversity (~8 species).

The inception of *Proteacidites* cf. *africaensis* at the base of this interval is taken here to mark the lower boundary of the mid Cenomanian interval, as it was recorded in West Africa, in Senegal and Nigeria (e.g. Jardiné & Magloire, 1965; Jardiné, 1967; Lawal & Moullade, 1986) and Brazil (Herngreen, 1973), from foraminifera-dated rocks of mid-late Cenomanian age.

The occurrence of *Afropollis jardinus* in these samples requires explanation as the extinction of this species is diachronous across palaeotropical African regions, occurring either in the early or mid Cenomanian, something attributed by Doyle et al. (1982) to palaeoclimatic influences. In the Gabon reference section for *Afropollis* species, Doyle et al. (1982) found that the abundance of *A. jardinus* declined in the foraminifera-dated late Albian-early Cenomanian Subzones C-XIIb and C-XIIc, and disappeared before the appearance of *Proteacidites africaensis* (as *Triorites africaensis*) in foraminifera-dated mid-late Cenomanian age sediments (Jardiné & Magloire, 1965; Jardiné, 1967). However, in the other reference section for *Afropollis,* in Senegal, Doyle et al. (1982) noted that *A. jardinus* became rare in the late Albian-Early Cenomanian - later than in the Gabon section - and disappeared in the mid Cenomanian, contemporary with the appearance of *Proteacidites africaensis*. Jardiné & Magloire (1965) recorded an upward extension of *A. jardinus* (as *Incertae sedis* S. CI. 156) into the mid Cenomanian in their foraminifera-dated Sequence VIIa and VIIb, prior to the first appearance of *Proteacidites africaensis*. Doyle et al. (1982) interpreted this persistence of *A. jardinus* through the mid Cenomanian as due to more favourable (wetter) conditions, suggesting *Afropollis* thrived in coastal areas and flourished during marine transgression cycles. The same scenario could also apply to Egypt, which lay at a similar palaeolatitude and where *A. jardinus* may have persisted into the mid Cenomanian due to marine sedimentation and wet climatic conditions similar to those of Senegal (Abdel-Kireem et al., 1996; Ibrahim, 2002b).

In the foraminifera-dated Zone V (early-mid Cenomanian) of Schrank & Ibrahim (1995) and in the foraminifera-dated Assemblage Zone “B” of early-mid Cenomanian age of Ibrahim (2002b), *A. jardinus* has its LAD at the topmost interval. Therefore, the LAD of *A. jardinus* in Sample 110 is used to delineate the upper boundary of the mid Cenomanian.

Afropollis kharamanensis, which was recorded in the foraminifera-dated lower-middle Cenomanian rocks of Egypt (Schrank & Ibrahim, 1995; Ibrahim, 2002b), has its LAD at the same level as the LAD of *A. jardinus*. *Elaterosporites klaszii* has its last appearance in the lower part of this interval, and is known to terminate in the mid Cenomanian in the Elaterate Province of Oman (Jardiné & Magloire, 1965; Müller, 1966; Jardiné, 1967; Herngreen, 1973; Herngreen & Jimenez, 1990; Fig. 5.4). The presence of *Cretacaeiporites densimurus* is also consistent as it has its uppermost occurrence at the top of the mid Cenomanian in Egypt (Schrank & Ibrahim, 1995; Ibrahim, 2002b).

The late Cenomanian age of the upper part of this zone is inferred from the upward continuation of *Proteacidites* cf. *africaensis* and from the very rare occurrence (and later complete disappearance) of the gymnosperm pollen *Classopollis* spp.. In Senegal, Jardiné & Magloire (1965) recorded high abundances of *Classopollis* spp. (up to 80 %) from the Barremian to the mid Cenomanian, which then declined rapidly and became extinct by the end of the late Cenomanian. Similarly, Schrank & Ibrahim (1995) and Ibrahim (2002b) recorded rare latest occurrences of *Classopollis* in the middle Cenomanian rocks of Egypt.

Florentinia berran of early-mid Cenomanian range in Egypt (Schrank & Ibrahim, 1995) is last recorded in the lower part of this interval, and thus supports a mid Cenomanian age for the lower part of the zone.

A mid-late Cenomanian age is assigned for this interval based on the presence of the index palynomorph taxa mentioned above.

Correlation:

- Sequence VII (mid-late Cenomanian) of Jardiné & Magloire (1965), Senegal Basin.
- Zone III (late Cenomanian) of Herngreen (1973), in the 1-QS-1-MA well, Maranhao Basin, Brazil.
- Zone II (mid-late Cenomanian) of Lawal & Moullade (1986), upper Benue Basin, northeast Nigeria.
- Zone VI (mid?-late Cenomanian) of Schrank & Ibrahim (1995), in the Kahraman-1 and Abu Gharadiq-18 wells, northern Western Desert, Egypt.
- Zone 4 (mid?-late Cenomanian) of Ibrahim (1996), in the Ghazalat-1 well, northern Western Desert, Egypt.

Palynozone 8: early ?Santonian (samples 130-131)

Samples: This zone includes samples from 130 to 131 and covers a depth from 3250 to 3200 ft (991-975 m) . (The two overlying samples, 132 and 133, are barren. Sample 134 is separated from 132 and 133 by an unconformity surface and exhibits very poor dinoflagellate recovery. Therefore, samples 132 to 134 are unsuitable for the definition of palynozones and were excluded from the present discussion).

Definition: Total range of *Canningia senonica* (152).

Associated taxa: *Alisporites* cf. *grandis* (62), *Spiniferites* spp. (150), *Exochosphaeridium bifidum* (153), *Dinogymnium* spp. (155), *Senegalinium aenigmaticum* (158), *Trichodinium castanea (160), Surculosphaeridium* cf. *longifurcatum* (161), *Downiesphaeridium* sp. (165).

Discussion concerning age assessment: Palynological assemblages from this zone are lacking in terrestrial palynomorphs except for the gymnosperm *Alisporites* cf. *grandis*, and are completely composed of phytoplankton: these forms are the only tools to date the sequence. *Canningia senonica* appears in both sample 130 and 131, a species characteristic of the Santonian-Maastrichtian. *C. senonica* has been recorded from the ammonite-dated late Santonian of the Isle of Wight, southern England (Clarke & Verdier, 1967), from the foraminifera-dated early Santonian-late Maastrichtian of Egypt (Schrank & Ibrahim, 1995), and from the nannoplankton-dated late Campanian of Italy (Torricelli & Amore, 2003).

This interval contains a few long-ranging species of pre-Coniacian to Maastrichtian range, such as *Dinogymnium denticulatum*, recorded from the ammonite-dated Late Santonian of the Isle of Wight (Clarke & Verdier, 1967), from the foraminifera-dated Coniacian-Maastrichtian of Egypt (Schrank & Ibrahim, 1995), and from the foraminifera-dated Coniacian-Santonian of Algeria (Foucher et al., 1994). *Chlamydophorella discreta* appears first in this interval, a species which has its last appearance in the late Santonian of the Isle of Wight (Clarke & Verdier, 1967), and ranges in Egypt from the early Cenomanian to the Turonian (Schrank & Ibrahim, 1995). *Isabelidinium acuminatum* was recorded (as *Deflandrea acuminata*) from the ammonite-dated late Santonian of the Isle of Wight (Clarke & Verdier, 1967), and from the foraminifera-dated Coniacian-Santonian of Algeria (Foucher et al., 1994). *Eucladinium gambangense*, which was identified by Cookson & Eisenack (Cookson & Eisenack, 1970a) from the Senonian rocks of Australia, occurs at the base of this interval.

There are no index angiosperm pollen taxa that one might expect for the Turonian, such as *Foveotricolpites giganteus* or *F. gigantoreticulatus* which are characteristic of early Turonian-Santonian ranges in West Africa (Jardiné & Magloire, 1965; Lawal & Moullade, 1986; Schrank & Ibrahim, 1995). Nor is

Droseridites senonicus present, which is diagnostic of the late Turonian-early Santonian (e.g. Lawal & Moullade, 1986; Salard-Cheboldaeff, 1990; Schrank & Ibrahim, 1995; Ibrahim, 1996).

Thus, based on the presence of the early Santonian index form *Canningia senonica* and the complete absence of index Turonian sporomorphs mentioned above, an early Santonian age is proposed for this interval.

Correlation:

- Zone 8 (early Santonian) of Schrank & Ibrahim (1995), in the Kahraman-1 well, northern Western Desert, Egypt.

5.2.2 The BB80-1 borehole

Palynozone 1: mid Albian (sample 1)

This biozone is only represented by sample 1 at a depth of 5400 ft (1646 m), whereas samples from 2 to 7 (depth 5390-5260 ft, 1643-1603 m) are barren of palynomorphs. The palynological assemblage of sample 1 is characterised by the presence of the index angiosperm pollen *Afropollis jardinus* which has an early Albian-mid Cenomanian range (Jardiné & Magloire, 1965; Doyle et al., 1982), and the gymnosperm pollen *Elaterosporites klaszii*, which is diagnostic for the mid Albian-mid Cenomanian (e.g. Jardiné & Magloire, 1965; Jardiné, 1967; Figure 5.9). Miospores are also represented by *Cicatricosisporites orbiculatus*, *Crybelosporites pannuceus*, *Murospora* spp., *Trilobosporites laevigatus* and the long ranging spores *Deltoidospora* spp. and *Triplanosporites* sp.. Although *Crybelosporites pannuceus* has an Albian-Cenomanian range in north South America (Brenner, 1968; Herngreen, 1973; Regali et al., 1974; Herngreen & Jimenez, 1990), and is regarded by Schrank & Ibrahim (1995) and Ibrahim (1996) to mark the early Albian-Cenomanian in Egypt. It has also been recorded from foraminifera-dated Aptian rocks of Algeria (Foucher et al., 1994), from well dinoflagellate-dated Aptian rocks of Morocco (Gübeli et al., 1984), from palynologically dated Aptian rocks of West Ghana (Atta-Peters & Salami, 2006) and from the Barremian-Aptian of other intertropical West African countries (Salard-Cheboldaeff, 1990). Gymnosperms are only represented by *Ephedripites* spp. and *Elaterosporites klaszii*. Phytoplankton shows a very low diversity (4 species) and abundance (average ~4 grains/gram).

A mid Albian age is suggested for this sample (Fig. 5.10) based on the presence of *Elaterosporites klaszii* and the complete absence of other late Albian-Cenomanian elaterate pollen, such as *Elaterocolpites castelainii* and *Elateroplicites africaensis*, which appear in the overlying Interval (Fig. 5.9). The assemblage of this

sample is similar to that of the Zone III (mid Albian) of Schrank & Ibrahim (1995) in the Kahraman-1 well, and to that of Zone 2 (mid Albian) of Ibrahim (1996) in the Ghazalat-1 well, northern Western Desert, Egypt.

Palynozone 2: late Albian-early Cenomanian (samples 8-24)

Samples: This zone is represented by samples from 8 to 24 and spans a depth from 5220 to 4840 ft (1591-1475 m), with samples 14, 19, and 20 being palynologically barren.

Definition: From the FAD of *Elaterocolpites castelainii* (11), *Elateroplicites africaensis* (12) and *Afropollis kharamanensis* (20) to the end of the succession.

Associated taxa: *Cicatricosisporites orbiculatus* (1), *Crybelosporites pannuceus* (2), *Deltoidospora* spp. (3), *Ephedripites* spp. (10), *Classopollis classoides* (13), *Classopollis brasiliensis* (14), *Tricolpites* sp. (16), *Stellatopollis* spp. (17), *Retimonocolpites variplicatus* (18), *Cretacaeiporites densimurus* (19), *Tricolporopollenites* sp. (21), *Rousea* sp. (23), *Florentinia berran* (31), *Dinopterygium tuberculatum* (33), *Florentinia mantellii* (34), *Senegalinium aenigmaticum* (39), *Florentinia clavigera* (40), *Xiphophoridium alatum* (42), *Florentinia laciniata* (44), *Florentinia radiculata* (48).

Discussion concerning age assessment: The microfloral assemblage of this interval is characterised by an increase in the abundance of spores by comparison with the underlying samples, the appearance of monocolpate, tricolpate, tricolporate, and polyporate pollen grains, and an increase in the abundance and diversity of phytoplankton species. This interval witnesses the presence of two elaterate forms characteristic of the late Albian-mid Cenomanian (*Elaterocolpites castelainii* and *Elateroplicites africaensis*) and the marker species *Afropollis kharamanensis* (Fig. 5.9). *Elateroplicites africaensis* was recorded from foraminiferally dated rocks of

early Cenomanian age (as *Incertae sedis* form A) in Senegal by Jardiné (1967), in southern Switzerland by Hochuli (1981) from the foraminifera-dated late Albian, and in Brazil by Herngreen (1973) from foraminifera-dated upper Albian-middle Cenomanian rocks.

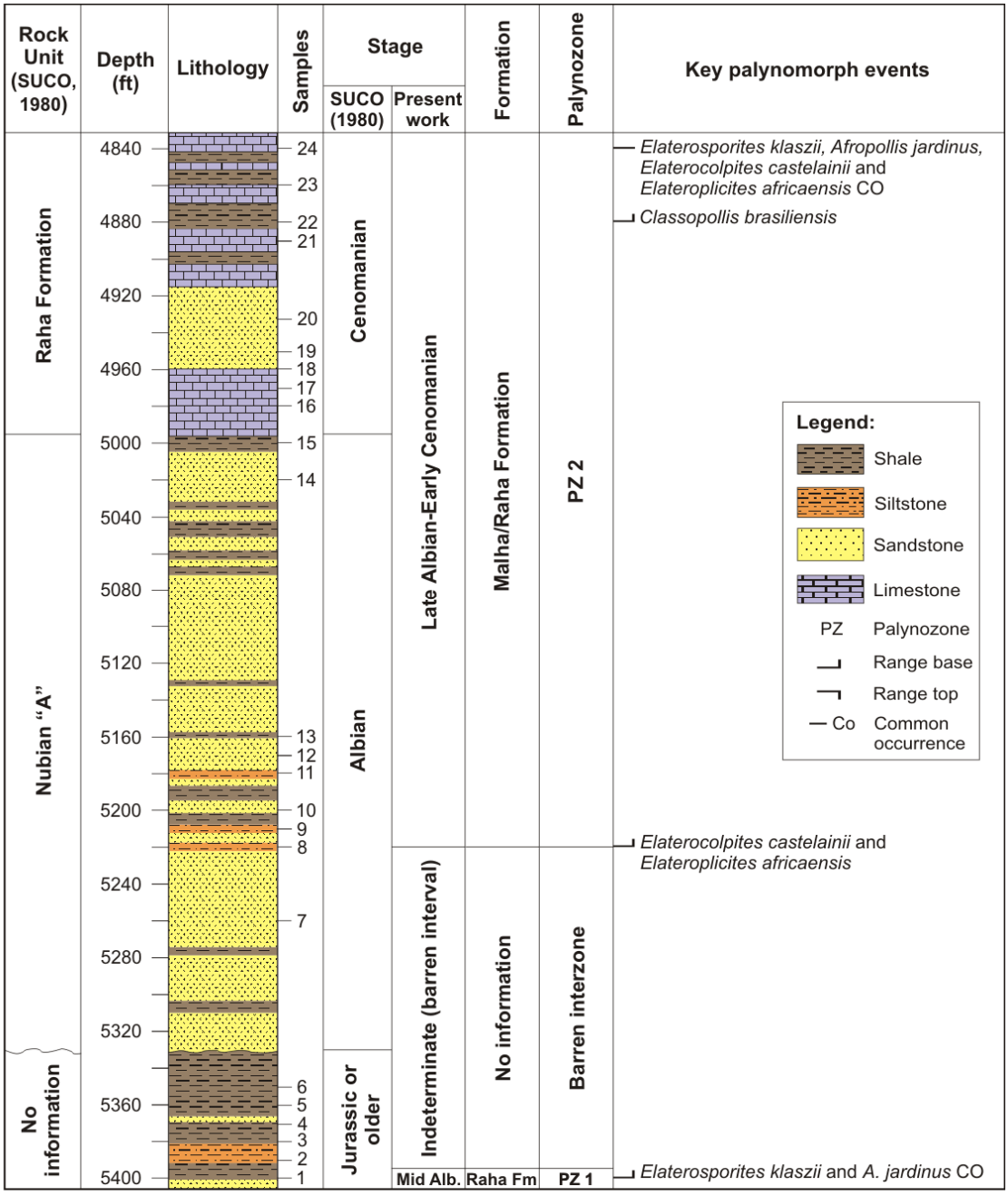

Figure 5.10 The BB80-1 borehole with lithological column, sample positions, initial dating by drilling company, key biostratigraphic events and newly inferred ages.

Afropollis kharamanensis was described from the foraminifera-dated early-mid Cenomanian of Egypt (Schrank & Ibrahim, 1995; Ibrahim, 2002b), in Nigeria by Lawal & Moullade (1986) in the palynologically dated Subzone Ia (late Albian-early Cenomanian) and Subzone Ib (mid Cenomanian). *Classopollis brasiliensis* also appears in this zone, which was also recorded in Egypt in the same foraminifera-dated Zone V of Schrank & Ibrahim (1995) and in Assemblage "B" of Ibrahim (2002b), both of early-mid Cenomanian age. In NE Nigeria, *C. brasiliensis* was recorded by Lawal & Moullade (1986) in their Subzone Ib of mid Cenomanian age, but from the foraminiferally dated late Albian to late Cenomanian in Brazil by (Herngreen, 1973). *Cretacaeiporites densimurus* appears in the upper part of this sample interval, and was described by Schrank & Ibrahim (1995) from foraminifera-dated rocks of early-mid Cenomanian age, although it may range down in to the late Albian of Egypt (Ibrahim, 2002b). A single occurrence of *Triporites* sp. is documented in the lower part of this interval, and a parallel may be drawn with the recorded rare occurrence of *Triporites* spp. in the early Cenomanian of Senegal (Jardiné & Magloire, 1965).

Phytoplankton taxa in this interval do not provide an accurate correlation with micropalaeontologically calibrated Albian-Cenomanian dinoflagellate events in the European Tethyan Realm; they are considered to be palaoeoenvironmentally controlled and of no biostratigraphic significance to this study.

A late Albian-mid Cenomanian age may be proposed for this interval based on the stratigraphic range of the two late Albian-mid Cenomanian elaterate pollen taxa, and the other index pollen forms mentioned above that disappear in the mid Cenomanian. However, the sharp rise in the abundance of *Afropollis* spp. in the upper part of the interval strongly supports an age not younger than the early Cenomanian, as this genus was reported by Doyle et al. (1982) to have a second

abundance maximum in the late Albian-early Cenomanian of Senegal and the Ivory Coast.

Correlation:

- Sequences X-VIII (late Albian-early Cenomanian) of Jardiné & Magloire (1965), Senegal Basin.
- Zone II (late Albian-early Cenomanian) of Herngreen (1973), in the 1-QS-1-MA well, Maranhao Basin, Brazil.
- Subzone Ia (late Albian-early Cenomanian) of Lawal & Moullade (1986), upper Benue Basin, northeast Nigeria.
- Zone I (late Albian-early Cenomanian) of Sultan & Aly (1986), in the WD-9-15-1 well, northern Western Desert, Egypt.
- Zone III (late Albian-early Cenomanian) of Aboul Ela & Mahrous (1992), in the East Tiba-1 well, northern Western Desert, Egypt.
- Zone 5 (late Albian-early Cenomanian) of Schrank (1992), Egypt and north Sudan.
- Intervals 3 and 4 (late Albian-early Cenomanian), in the Manndra 1 well and intervals c and d (late Albian-early Cenomanian), in the Oued Melah 1 well of Foucher et al. (1994), Algeria.
- Zone IV (late Albian-early Cenomanian?) of Schrank & Ibrahim (1995), in the Kahraman-1 well, northern Western Desert, Egypt.
- Assemblage “A” (late Albian-early Cenomanian) of Ibrahim (2002b), in the Abu Gharadig-5 well, northern Western Desert, Egypt.

5.3 Cretaceous African-Northern South American Phytogeographic Provinces in the context of this present study

Although no differences have been reported in palynofloral compositions or the biostratigraphic ranges of some spores and pollen grains in West African (Congo-Gabon) and northern South American (Brazilian) palynofloras, correlation of early Cretaceous sequences (Fig. 5.10) from North and West Africa (e.g. Egypt, Libya, Senegal, and Congo-Gabon) with those of northern South America (e.g. Brazil) do show differences (Jardiné, 1974; Doyle et al., 1982, Salarda-Cheboldaeff, 1990). This section will mainly focus on a comparison focussed on the West African (Senegal, the Ivory Coast and Nigeria) and North African (NW Egypt, NE Libya and northern Morocco) regions due to the close palynofloral and palaeogeographic relationships between these two areas.

The Berriasian-Barremian time interval interval in West Africa lacks any independent age control and is composed almost entirely of terrestrial to very shallow marine sediments in the late Barremian (Doyle, 1982), where even marine palynological dating cannot be applied. However, interregional correlation of North African and West African material (Fig. 5.10) shows that the well-dated Valanginian-Barremian interval of North Africa (Thusu, 1988, Libya; Gübeli, 1984, Morocco) could provide information which is capable of filling this palynostratigraphic Berriasian-Barremian gap in West Africa, and even serve as a reference section for this interval in both North and West Africa.

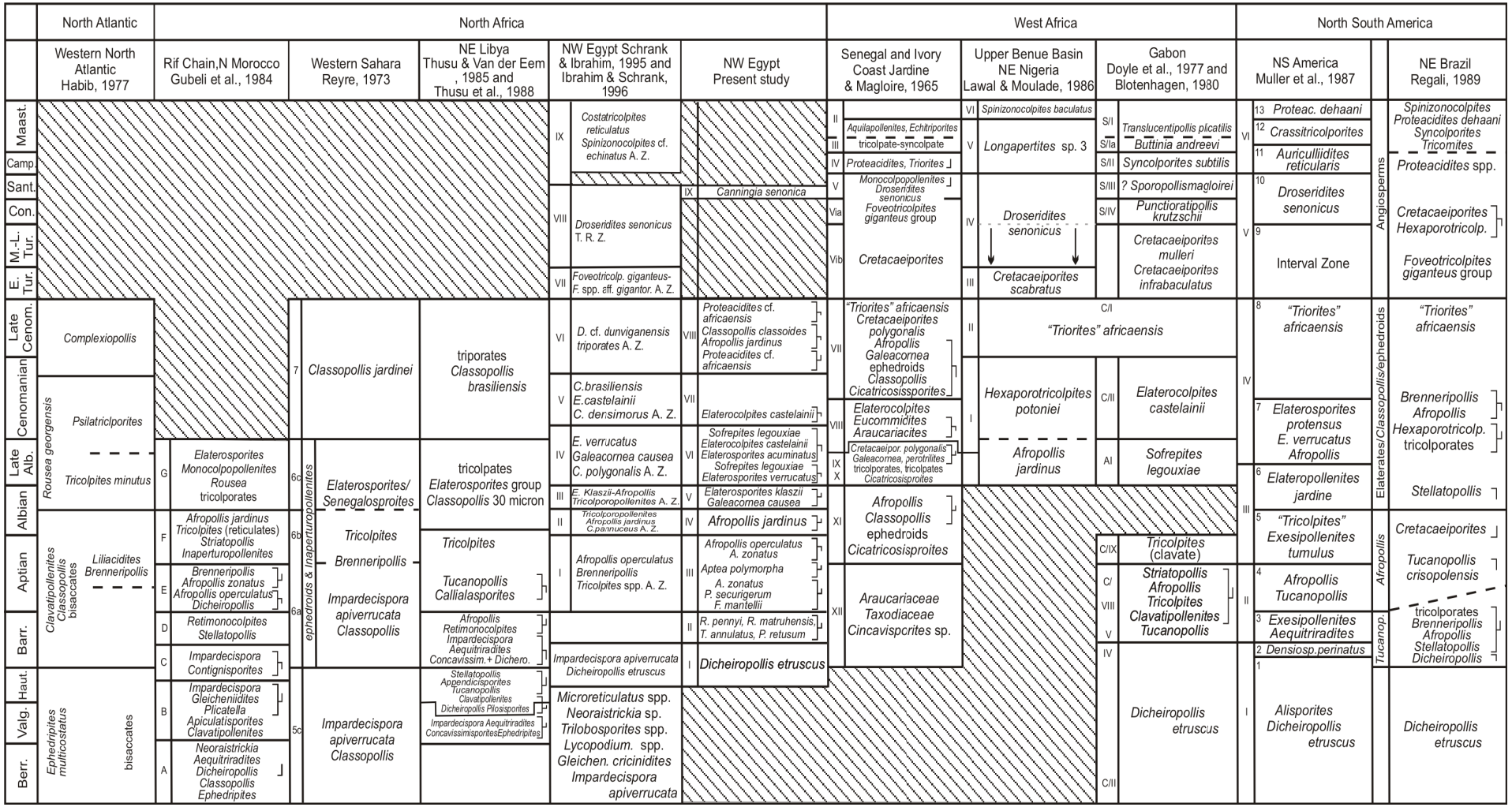

Figure 5.11 Cretaceous palynological biozonation correlation in North and West Africa and Northern South America (modified after Schrank, 1992) and the palynological zonation proposed in the present study.

5.3.1 The pre-Albian *Dicheiropollis*/*Afropollis* Phytogeographic Province

A. Discrepancies in the reported range of *Dicheiropollis etruscus*

Trevisan (1971) believed that *Dicheiropollis etruscus* had a cheirolepidiacean coniferous affinity, and, as with *Classopollis,* may have been both thermophilous and adapted to arid conditions. High abundances of *Classopollis* are associated with evaporites, salts, and redbed deposits, and also with cheirolepidiacean xeromorphic wood and leaf megafossils, which further support hot dry conditions for this genus (e.g. Doyle, 1999; Watson, 1988). *Classopollis* was most abundant during Barremian-Aptian time in the hot, dry subtropical latitudes (15-30° N and S of the palaeoequator), while it is found in lower abundances in the hot, but slightly wetter tropical region (Doyle, 1999). Doyle et al. (1982), Schrank (1990), and Brenner (1996) all suggested relatively wetter palaeoclimates for the African tropics (e.g. Egypt and Sudan), based on the presence of high abundances of fern spores (indicating humidity), and lower frequencies of *Classopollis* and the cooler-temperature coniferous genus *Araucariacites* than seen in the subtropics.

In the subtropical region, several authors (e.g. Doyle at al., 1977) have reported an earlier (Berriasian) appearance of *Dicheiropollis etruscus* in the palynologically dated continental clastic and salt deposits of West Africa (Gabon), in comparison to its delayed late Hauterivian appearance in the tropical NE African region (e.g. Thusu & Van der Eem, 1985; Uwins & Batten, 1988, Libya; Fig. 5.10). This situation could be interpreted in the light of one the two following explanations:

1. That the NE and West African sequences are diachronous: but this suggestion cannot be proven until independent age controls are provided for this species in West Africa or northern South America.

2. The taxon's distribution is palaeoecologically controlled in each area. Prior to the breakup of Western Gondwana, Egypt, Libya, Senegal and the Ivory

Coast lay approximately at the palaeoequator, in comparison to Morocco and Gabon, which lay around subtropical latitudes 10-15° N and S respectively. *D. etruscus* thus first appeared in hot, dry subtropical African regions, but as Western Gondwana broke up and the African plate moved north east, Egypt, Libya, and Sudan were brought into a palaeosubtropical position where more arid conditions allowed *D. etruscus* to migrate into these areas.

An older inception of *D. etruscus* has also been recorded by Gübeli et al. (1984) from the Berriasian of northern Morocco. However, caving may have contaminated the samples and could explain this downward range extension of *D. etruscus*, especially as *Dicheiropollis etruscus* is confirmed to have a late Hauterivian-early Barremian range in North East Africa in foraminifera- and dinoflagellate-dated sediments (Libya: Uwins & Batten, 1988). This latter range is therefore accepted here as applicable to Egypt and thus used to allocate a late Hauterivian-early Barremian age for Palynozone 1 of the Abu Tunis 1x borehole.

B. Acme events of Aptian *Afropollis* and local palaeoclimate effect

During the Aptian, Senegal, the Ivory Coast and Egypt were located at more or less the same palaeolatitude and possess similar angiosperm-dominated assemblages. In addition, the development of marine lower Cretaceous (uppermost Barremian-Aptian) sediments in Senegal and Egypt also serves to correlate this Cretaceous time interval across these three geographic areas.

Doyle et al. (1982) recorded a first acme of *Afropollis* in the foraminifera-dated (Castelain, 1965) Aptian of Senegal, where the persistent occurrence of *A. operculatus* and *A. zonatus* were reported to range from the early to late Aptian (Doyle et al., 1982). This bears a striking similarity to the first acme of *Afropollis* in the supposed Aptian of Egypt (Schrank & Ibrahim, 1995), and the occurrence of *A. operculatus* and *A.* aff. *jardinus* in the supposed late Aptian (just below the FAD of

A. jardinus) in the present study (Fig. 5.7). This further supports the view that the Aptian sequences of Senegal and Egypt are indeed synchronous. Doyle et al. (1982) attributed the upward persistence of *A. operculatus* and *A. zonatus* into the late Aptian to palaeoclimatic conditions. It has already been pointed out that the latter authors suggested that *Afropollis*-producing plants were better adapted to wetter, probably coastal humid environments. Doyle et al. (1982) attributed the upward decline in *Afropollis* from the pre-salt early Aptian Zone C-VII of Gabon into the late Aptian salt sequence Zones C-VIII-C-IX to increased aridity.

The wet costal conditions proposed for the *Afropollis* parent plants were later supported by Schrank (2001), where he reported exceptional relative abundances of *Afropollis* (35-78% of total palynomorphs) and elaterate pollen (11-15%) from Albian-Cenomanian continental sediments of northern Sudan, which also contained low salinity dinoflagellate cysts. Schrank (2001) compared these extraordinary abundances of *Afropollis* and elaterates with a similar event recorded by El-Shamma (1991) from marine Albian-Cenomanian sediments of northern Egypt, and suggested that parent plants of both *Afropollis* and elaterate pollen may have flourished in humid coastal habitats. Schrank (2001) believed that temporary humid conditions would have been brought to the intracontinental basins of Sudan by a short-lived transgression.

These observations permit the use of high abundances of *Afropollis* as a proxy indicator for warm, humid coastal conditions.

5.3.2 Albian-Cenomanian Elaterate Phytogeographic Province

The appearance and proliferation of elaterate gymnosperm pollen is the most important and well-documented event in the Albian-Cenomanian Elaterate Phytogeographic Province (e.g. Herngreen et al., 1996). The foraminifera-dated

Albian-Cenomanian gymnosperm and angiosperm events of West Africa (Doyle et al., 1982; Jardiné & Magloire, 1965; Lawal & Moulade, 1986), are represented by the early Albian appearance of *Afropollis jardinus* and the later appearance of the genus *Elaterosporites* along with other elaterate taxa in the mid Albian. This is followed by the appearance of *Elaterocolpites* and *Elateroplicites* in the late Albian, and the extinction of all these forms at the end of the mid Cenomanian. These events have been recorded all across North Africa: in Egypt (Aboul Ela & Mahrous, 1992; Schrank & IIbrahim, 1995; Sultan, 1986), in Libya (Thusu & Van der Eem, 1985), and in Morocco (Gübeli et al., 1984). This makes the Albian-Cenomanian interval easily and widely recognisable within the province. There are a few reports of small differences in the biostratigraphic ranges and palaeogeographic distributions of some of the spores and pollen grains present in this province between North and West Africa (Herngreen et al., 1996; Salard-Cheboldaeff, 1990), but generally the interregional correlation of biostratigraphic ranges and/or successive events of selected index gymnosperm (e.g. *Droseridites senonicus* and elaterates) and angiosperm (e.g. *Afropollis* and *Cretacaeiporites*) pollen between the foraminifera-dated Cenomanian-Coniacian sedimentary sequence of North and West Africa (Senegal and Ivory Coast: Jardiné & Magloire, 1965; Egypt: Schrank & Ibrahim, 1995) show a close match (Fig. 5.10), and support a synchronicity of these Cretaceous sequences.

In this study almost all described species of the elaterate group are recorded, which has enabled excellent correlation of studied section to contemporaneous sections in the Albian-Cenomanian Elaterate Phytogeographic Province (Fig. 5.10). In palynozones 4-7 of Abu Tunis 1x, and palynozones 1 and 2 of BB80-1, important Albian-Cenomanian biostratigraphic marker taxa have enabled very good regional (e.g. Egypt), interregional (e.g. Senegal and NE Nigeria), and

intercontinental (e.g. Brazil & Colombia) correlation, and provided good age constraints.

5.3.3 The Senonian Palmae Province

Regional palynological correlation of the post-Cenomanian sequences of North Africa is sparse (Fig. 5.10). In Egypt, this lack of post-Cenomanian palynostratigraphic work could be attributed to missing biostratigraphic and /or barren rock units, which is may be due to regional late Cretaceous tectonics (e.g. Meshref, 1990). Only the work of Schrank & Ibrahim (1995) on the Egyptian Cretaceous sheds some light on this time interval. In contrast, in West Africa this time interval is fairly well represented by the foraminifera-dated studies of Jardiné & Magloire (1965), Lawal & Moulade (1986), and Boltenhagen (1980).

In the present study an hiatus in the Abu Tunis 1x is documented by a disconformity where Turonian deposits are absent: this may be related to the Turonian uplift that affected most of the Western Desert basins of Egypt (Kerdany & Cherif, 1990). By the advent of the early Santonian a transgressional cycle is interpreted here to have covered the Faghur Sub-basin, based on marine palynomorphs recorded in the Abu Tunis 1x borehole sediments. Another disconformable surface separates the early Santonian from the overlying sediments, where a significant time gap (representing the late Santonian, Campanian and Maastrichtian) is recorded. This post-Santonian disconformity may be related to the late Santonian-Palaeocene folding and thrusting, which affected the whole of the northern basinal areas of Egypt (e.g. Said, 1990).

PLATE 1

Late Jurassic-Early Cretaceous spores and pollen grains

1. *Dictyophyllidits harrisii* Couper, 1958, slide AT-1A, 10150 ft, 12/127.7, (28).

2. *Dictyophyllidits* sp., slide AT-3A, 10050 ft, 11.9/120.5, (36).

3. *Concavisporites* sp., slide AT-6A, 9900 ft, 10.4/132.3, (19).

4. *Auritulinasporites scanicus* Nilsson, 1958, silde AT-7A, 9850 ft, 12/112, (53).

5. *Deltoidospora toralis* (Leschik) Lund, 1977, slide AT-1A, 10150 ft, 15.4/133.6, (16).

6. *Deltoidospora* sp., slide AT-4A, 10000 ft, 8.1/125.2, (1).

7. *Deltoidospora hallii* Miner, 1935, slide AT-5A, 9950 ft, 10.8/126.2, (5).

8. *Triplanosporites* sp., slide AT-3A, 10050 ft, 17/141.3, (3).

9. *Deltoidospora australis* (Couper) Pocock, 1970, slide AT-12A, 9600 ft, 20.7/132.8, (38).

10. *Exesipollenites* sp., slide AT-3B, 10050 ft, 12.1/131.8, (83).

11. *Balmeiopsis limbatus* (Balme) Archangelsky, 1979, slide AT-1A, 10150 ft, 14.5/117.7, (63).

12. *Arucariacites australis* Cookson ex Couper, 1953, slide AT-1A, 10150 ft, 6.3/116.7, (69).

13. *Inaperturopollenites undulatus* Weyland & Greifeld, 1953, slide AT-4A, 10000 ft, 13.7/121.9, (77).

18. *Classopollis classoides* Pflug, 1953, slide AT-6A, 9900 ft, 9.2/130.1, (13).

19. *Classopollis* sp. slide AT-10A, 9700 ft, 13.7/143.6, (68).

22. *Taxacites sahariensis* Reyre, 1973, slide AT-10A, 9700 ft, 11.4/123.4, (84).

23. *Crybelosporites brenneri* Playford, **19**71, slide AT-3B, 10050 ft, 10.8/131.7, (32).

Berriasian-Valanginian spore and pollen grains

17, 21. *Pilosisporites trichopapillosus* (Thiergrat) Delcourt & Sprumont, 1955, slide AT-4A, 10000 ft, 14.3/146, slide AT-5A, 9950 ft, 14.1/134.9, (56).

20. *Impardecispora apiverrucata* (Couper) Venkatachala et al., 1969, slide AT-2A, 10100 ft, 13.9/114.6, (61).

Late Hauterivian-Early Barremian spore and pollen grains

14, 15, 16. *Dicheiropollis etruscus* Trevisan, 1972, slide AT-2B, 10100 ft, 16.9/119.7, slide AT-3A, 10050 ft, 14.2/142.8, slide AT-3A, 10.1/130.5, (89).

PLATE 1

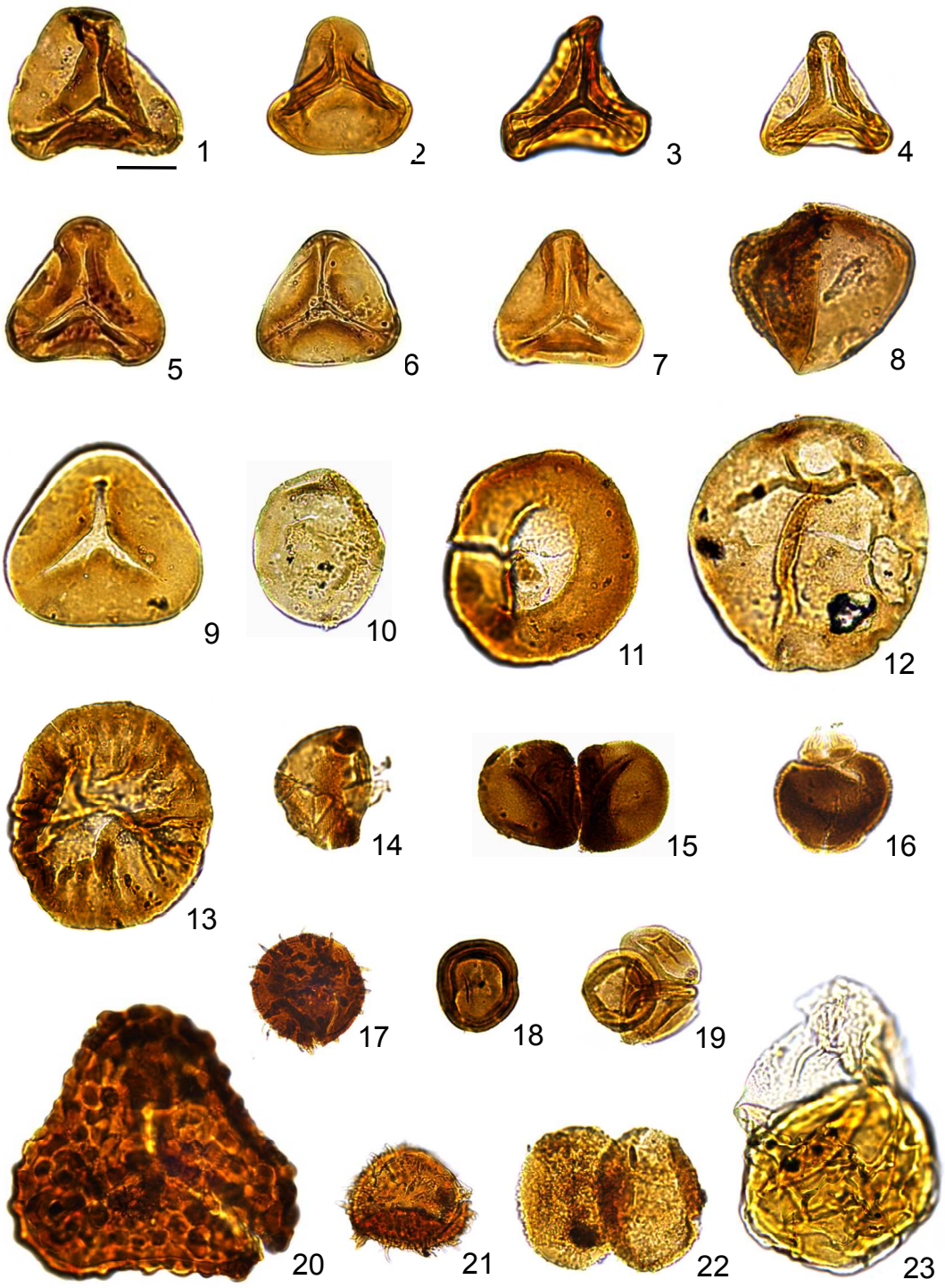

PLATE 2

Early Cretaceous spore and pollen grains

1. *Deltoidospora australis* (Couper) Pocock, 1970, slide AT-3A, 10050 ft, 12.9/135, (38).

2, 4, 12. *Deltoidospora psilostomata* Rouse, 1959, slide AT-8A, 9800 ft, 10.2/109.2, slide AT-3A, 10050 ft, 9.4/125.9, slide AT-8A, 9800 ft, 15/120.3, (33).

3. *Deltoidospora concavus* Bolkhovotina, 1956, slide AT-3A, 10050 ft, 18.5/121.6, (49).

5. *Deltoidospora hallii* Miner, 1935, slide AT-3A, 10050 ft, 11.6/135.6, (5).

6. *Cibotiumspora jurienensis* (Balme) Filatoff, 1975, slide AT-5A, 9950 ft, 11.2/143.1, (37).

7. *Biretisporites potoniaei* Delcourt & Sprumont, 1955, slide AT-6A, 9900 ft, 8.9/129.6, (30).

8. *Auritulinasporites intrastriatus* Nilsson, 1958, slide AT-7A, 9850 ft, 8.8/125.1, (55).

9. *Deltoidospora toralis* (Leschik) Lund, 1977, slide AT-8A, 9800 ft, 16.4/134.1, (16).

10. *Classopollis* sp. (21), slide AT-10A, 9700 ft, 10.1/122, (68).

11. *Cibotiidites* cf. *tuberculiformis* (Cookson) Srivastava, 1977, slide AT-5A, 9950 ft, 9.9/130.8, (57).

13. *Ischyosporites areolatus* (Singh) Fensome, 1987, slide AT-4A, 10000 ft, 6.5/140.1, (59).

14. *Cicatricosisporites* sp., slide AT-4A, 10000 ft, 16.4/116, (7).

15. *Echinatisporis varispinosus* (Pocock) Srivastava, 1977, slide AT-10A, 9700 ft, 12.5/113.9, (54).

16. *Cycadopites fragilis* Singh, 1964, slide AT-17A, 9350 ft, 16.8/127.3, (86).

17. *Cycadopites* sp., slide AT-18A, 9300 ft, 12.8/139.3, (67).

18. *Cycadopites* sp., slide AT-17A, 9350 ft, 11.6/145.7, (67).

19, 20. *Trilobosporites hannonicus* (Delcourt & Sprumont) Potonié, 1956, slide AT-4B, 10000 ft, 15.4/124.7, slide AT-7A, 9850 ft, 15.2/111.4, (52).

21. *Impardecispora uralensis* (Bolkhovitina) Venkatachala et al., 1969, slide AT-3A, 10050 ft, 10/129.7, (60).

22. *Concavissimisporites variverrucatus* Singh, 1964, slide AT-7B, 9850 ft, 12.5/136.6, (58).

23. *Concavissimisporites punctatus* (Delcourt & Sprumont) Brenner, 1963, slide AT-5A, 9950 ft, 7.2/117.5, (10).

24. *Concavissimisporites* sp., slide AT-5A, 9950 ft, 8.4/122.1, (11).

PLATE 2

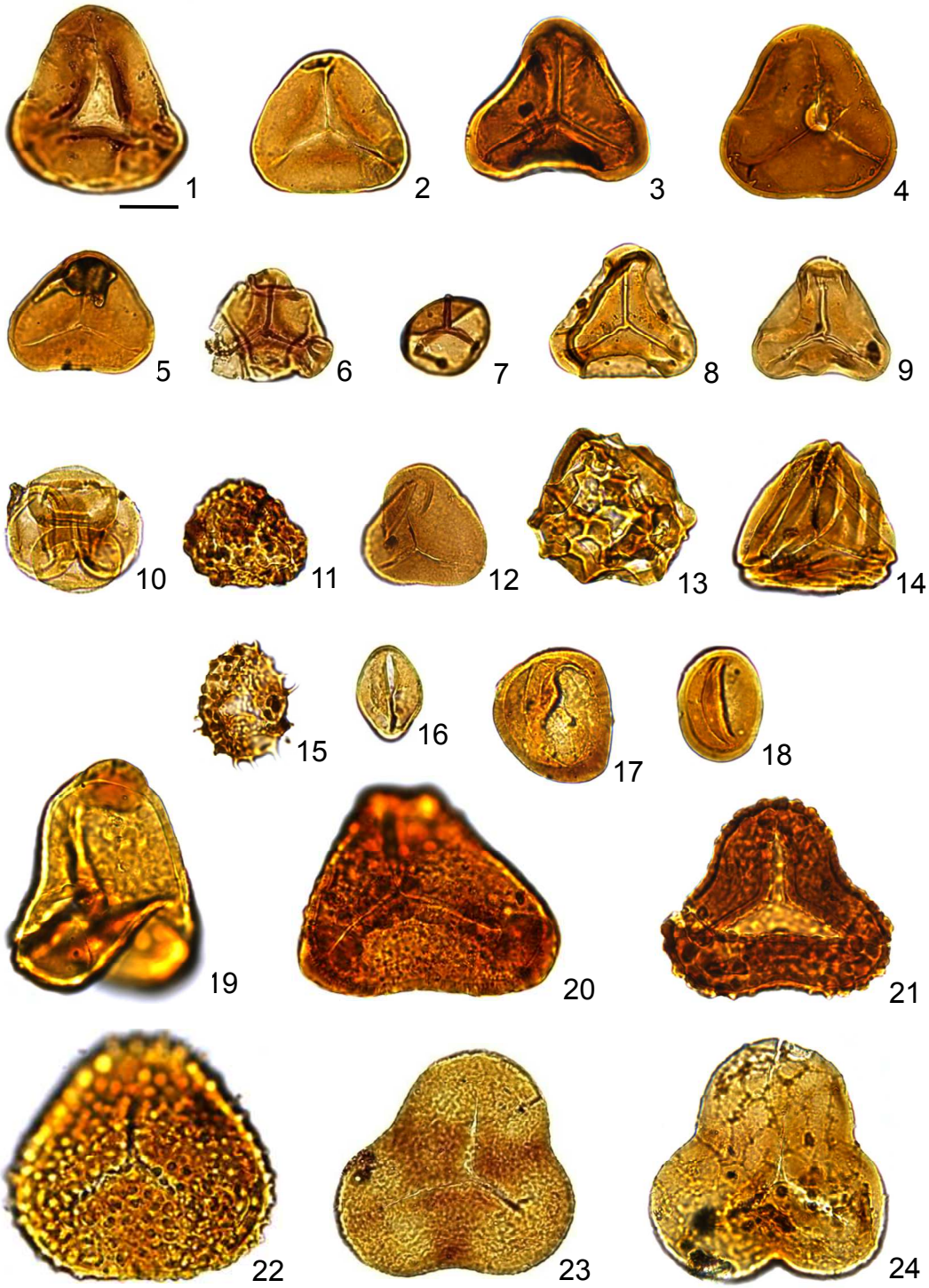

PLATE 3

Early Cretaceous spore and pollen grains

1. *Gleicheniidites feronensis* (Delcourt & Sprumont) Delcourt & Sprumont, 1959, slide AT-3A, 10050 ft, 15.7/117.7, (39).

2. *Gleicheniidites senonicus* Ross, 1949, slide AT-2B, 10100 ft, 2.7/124, (15).

3. *Auritulinasporites intrastriatus* Nilsson, 1958, slide AT-7A, 9850 ft, 8.8/125.1, (55).

4. *Deltoidospora australis* (Couper) Pocock, 1970, slide AT-12A, 9600 ft, 20.7/132.8, (38).

5, 7. *Callialasporites trilobatus* (Balme) Sukh Dev, 1961, slide AT-2A, 10100 ft, 13.1/137.1, slide AT-12A, 9600 ft, 14.7/117.8, (82).

6. *Callialasporites turbatus* Schulz, 1967, slide AT-4A, 10000 ft, 10.8/134.4, (85).

8. *Cicatricosisporites* sp., slide AT-14A, 9500 ft, 20.7/128.6, (7).

9. *Cicatricosisporites sinuosus* Hunt, 1985, slide AT-16A, 9400 ft, 6.7/122.8, (13).

10. *Classopollis* sp., slide AT-7A, 9850 ft, 6/117.3, (68).

11. *Concavissimisporites punctatus* (Delcourt & Sprumont) Brenner, 1963, slide AT-11A, 20.9/126.9, (10).

12. *Deltoidospora* sp., slide AT-16A, 9600 ft, 10.4/115.2, (1).

13. *Cicatricosisporites* sp., slide AT-11A, 9650 ft, 17.6/113, (7).

14. *Appendicisporites erdtmanii* Pocock, 1964, slide AT-16A, 9400 ft, 11.3/148.8, (50).

17. *Murospora* sp.1, slide AT-16A, 9400 ft, 11.7/145.5, (18).

18. *Kyrtomisporis* sp., slide AT-16A, 9400 ft, 5.4/144.9, (27).

19. *Murospora florida* (Balme) Pocock, 1961, slide AT-16A, 9400 ft, 12.7/135.3, (17).

Fresh water algae

15, 16. *Ovoidites parvus* (Cookson & Dettmann) Nakoman, 1966, slide AT-16A, 9400 ft, 18/137.1, slide AT-16A, 13.2/122.2, (145).

PLATE 3

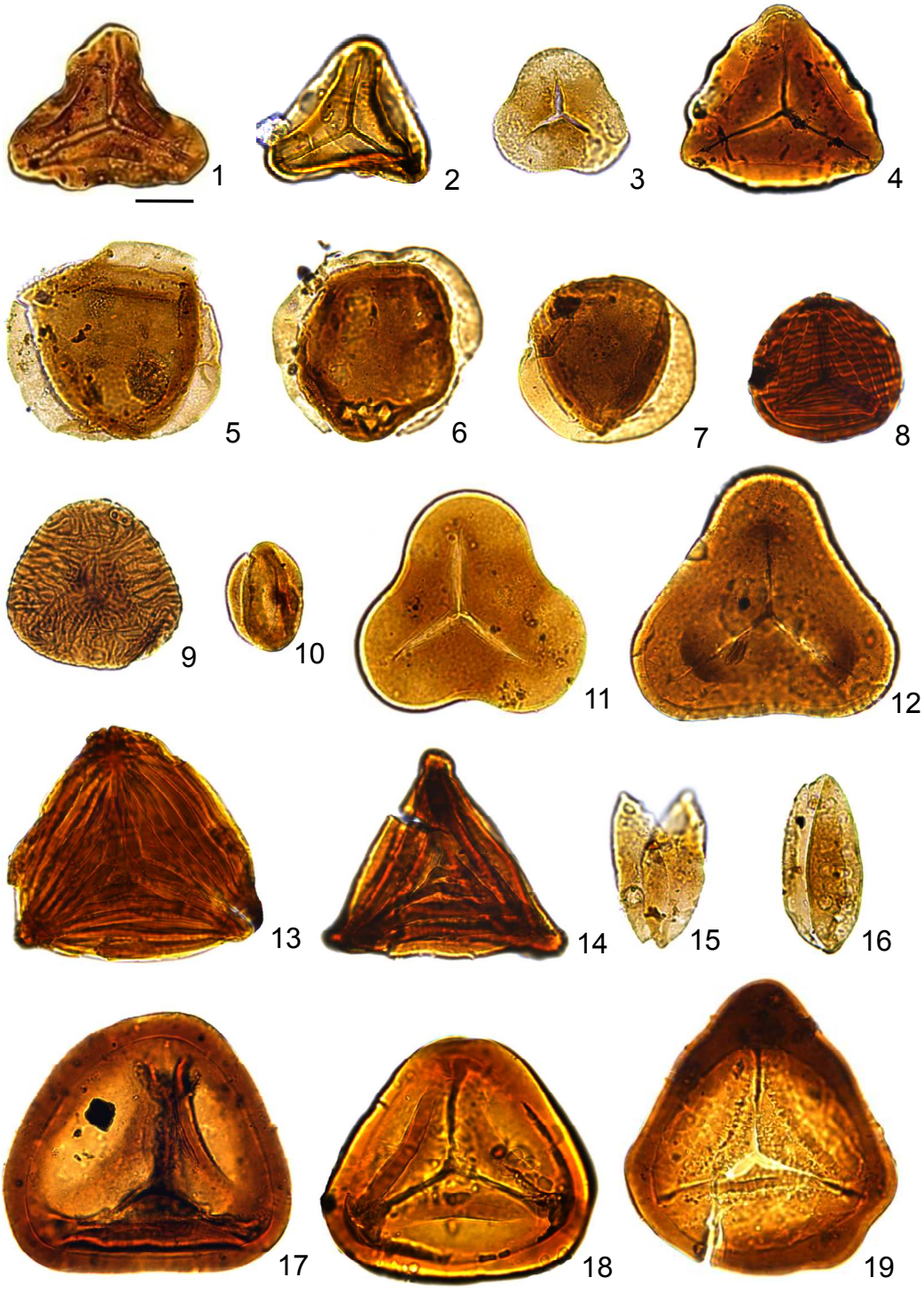

PLATE 4

Early Cretaceous spore and pollen grains

1. *Aequitriradites norrissii* Backhouse, 1988, slide AT-21A, 9150 ft, 11/135.9, (40).

2, 3. *Deltoidospora toralis* (Leschik) Lund, 1977, slide AT-18A, 9300 ft, 7.4/130.1, slide AT-17A, 9350 ft, 6.6/114.8, (16).

4. *Deltoidospora crassexina* (Nilsson) Lund, 1977, slide AT-21A, 9150 ft, 12.1/1287, (23).

5. *Aequitriradites verrucosus* (Cookson & Dettmann) Cookson & Dettmann, 1961, slide AT-18A, 9300 ft, 10.4/136.1, (47).

6, 7. *Biretisporites potoniaei* Delcourt & Sprumont, 1955, slide AT-19A, 9250 ft, 5.5/116, slide AT-23A, 9050 ft, 7.7/140.9, (30).

8. *Deltoidospora* sp., slide AT-17A, 9350 ft, 14/143.2, (1).

9. *Kyrtomisporis* sp., slide AT-20A, 9200 ft, 13.3/140.1, (27).

10. *Microfoveolatosporites skottsbergii* (Selling) Srivastava, 1971, slide AT-19A, 9250 ft, 15.5/141, (22).

11. *Ephedripites* sp., slide AT-10A, 9700 ft, 18.8/117.8, (65).

12. *Ephedripites* sp., slide BB-24A, 4840 ft, 17/131.9, (10).

13. *Ephedripites* sp., slide BB-24A, 4840 ft, 14.3/141.5, (10).

14. *Ephedripites* sp., slide AT-10A, 9700 ft, 9.2/133.9, (65).

15. *Ephedripites* sp., slide BB-23B, 4860 ft, 8/127, (10).

16. *Ephedripites* sp., slide BB-24A, 4840 ft, 15.1/139.6, (10).

17. *Ephedripites* sp., slide AT-11A, 9650 ft, 19/129.9, (65).

18. *Ephedripites* sp., slide BB-23B, 4860 ft, 7/127.3, (10).

19. *Ephedripites* sp., slide BB-24B, 4840 ft, 13.4/123, (10).

20. *Ephedripites* sp., slide AT-28A, 8800 ft, 4.3/124.1, (65).

21. *Ephedripites* sp., slide BB-22A, 4880 ft, 5.4/129.6, (10).

22. *Ephedripites* sp., slide AT-25A, 8950 ft, 5.3/125.6, (65).

23. *Ephedripites* sp., slide AT-28A, 8800 ft, 22.2/124.9, (65).

24. *Ephedripites* sp., slide AT-19B, 9250 ft, 9.6/145.2, (65).

25. *Ephedripites* sp., slide AT-21A, 9150 ft, 9.8/132, (65).

26. *Ephedripites* sp., slide AT-10A, 9700 ft, 4/130.6, (65).

27. *Ephedripites* sp., slide AT-23B, 9050 ft, 6.4/136.8, (65).

28. *Ephedripites* sp., slide AT-26B, 8900 ft, 5.5/111.7, (65).

29. *Ephedripites* sp., slide AT-23A, 9050 ft, 19.1/126, (65).

30. *Ephedripites* sp., slide AT-21A, 9150 ft, 9.8/134.8, (65).

31. *Ephedripites* sp., slide BB-24A, 4840 ft, 16/118.9, (10).

PLATE 4

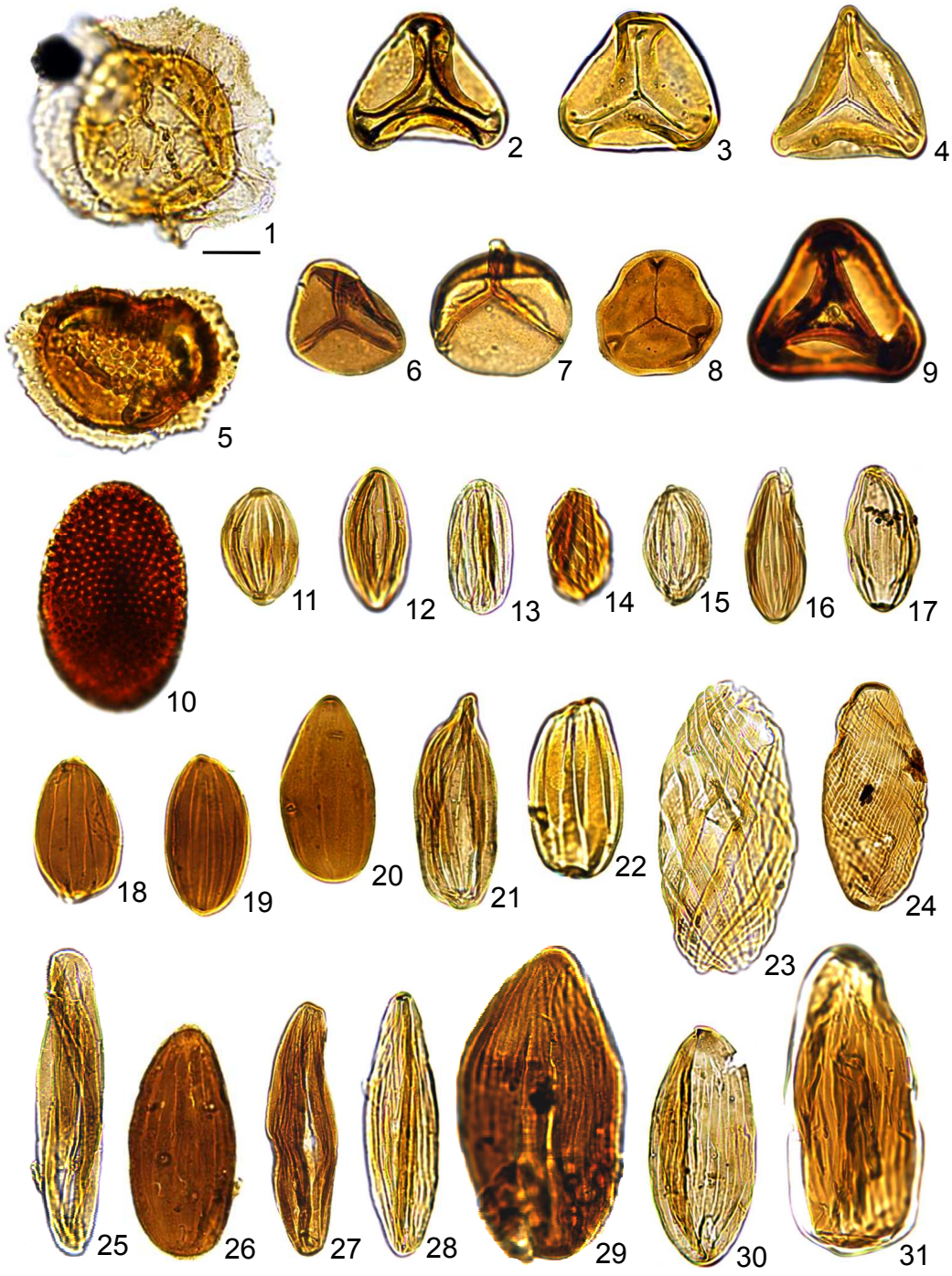
1
2
3
4
5
6
7
8
9
10
11
12
13
14
15
16
17
18
19
20
21
22
23
24
25
26
27
28
29
30
31

PLATE 5

Early Cretaceous spore and pollen grains

1. *Balmeisporites longirimosus* Kondinskaya, 1966, slide AT-24A, 9000 ft, 19.4/138.4, (20).

2. *Crybelosporites brenneri* Playford, **19**71, slide AT-18A, 9300 ft, 13.1/124.2, (32).

3. *Matonisporites* sp., slide AT-18A, 9300 ft, 17.9/116.3, (24).

4. *Leptolepidites psarosus* Norris, 1969, slide AT-19A, 9250 ft, 11.7/116.6, (45).

6. *Crybelosporites striatus* (Cookson & Dettmann) Dettmann, 1963, slide AT-18A, 9300 ft, 3.9/128.2, (46).

7. *Gemmatrilites* sp., slide AT-20B, 9200 ft, 10.6/132.6, (41).

8. *Triporoletes reticulatus* (Pocock) Playford, 1971, slide AT-42A, 8100 ft, 13.2/132.9, (12).

9. *Gleicheniidites senonicus* Ross, 1949, slide AT-32A, 8600 ft, 6.5/142.7, (15).

10. *Murospora* sp., slide AT-18, 9300 ft, 19.1/117.6, (48).

11. *Verrucosisproites obscurilaesuratus* Pocock, 1962, slide AT-63A, 7050 ft, 13.8/131.6, (8).

12, 22. *Murospora florida*, slide AT-18, 9300 ft, 13.1/140.2, slide AT-49B, 7750 ft, 16/123.3, (17).

13. *Cicatricosisporites* sp., slide AT-18, 9300 ft, 6/139, (7).

14. *Cicatricosisporites* sp., slide AT-24A, 9000 ft, 7/127.8, (7).

15. *Cicatricosisporites* sp., slide AT-28A, 8800 ft, 4.7/128.2, (7).

16. *Cicatricosisporites* sp., slide AT-30A, 8700 ft, 7.6/148.4, (7).

17. *Murospora* cf. *kosankei* Somers, 1952, slide AT-52, 7600 ft, 7.1/116.4, (21).

18. *Gleicheniidites rasilis* Bolkhovitina, 1968, slide AT-19B, 9250 ft, 14.3/112, (44).

19. *Matonisporites* sp., slide AT-49B, 7750 ft, 15.4/124.5, (24).

20. *Murospora* sp.1, slide AT-23A, 9050 ft, 16.8/121.9, (18).

21. *Kyrtomisporis* sp., slide AT-24A, 9000 ft, 16.6/130.7, (27).

Fresh water algae

5. *Chomotriletes minor* (Kedves) Pocock, 1970, slide AT-18A, 9300 ft, 21/134.3, (148).

PLATE 5

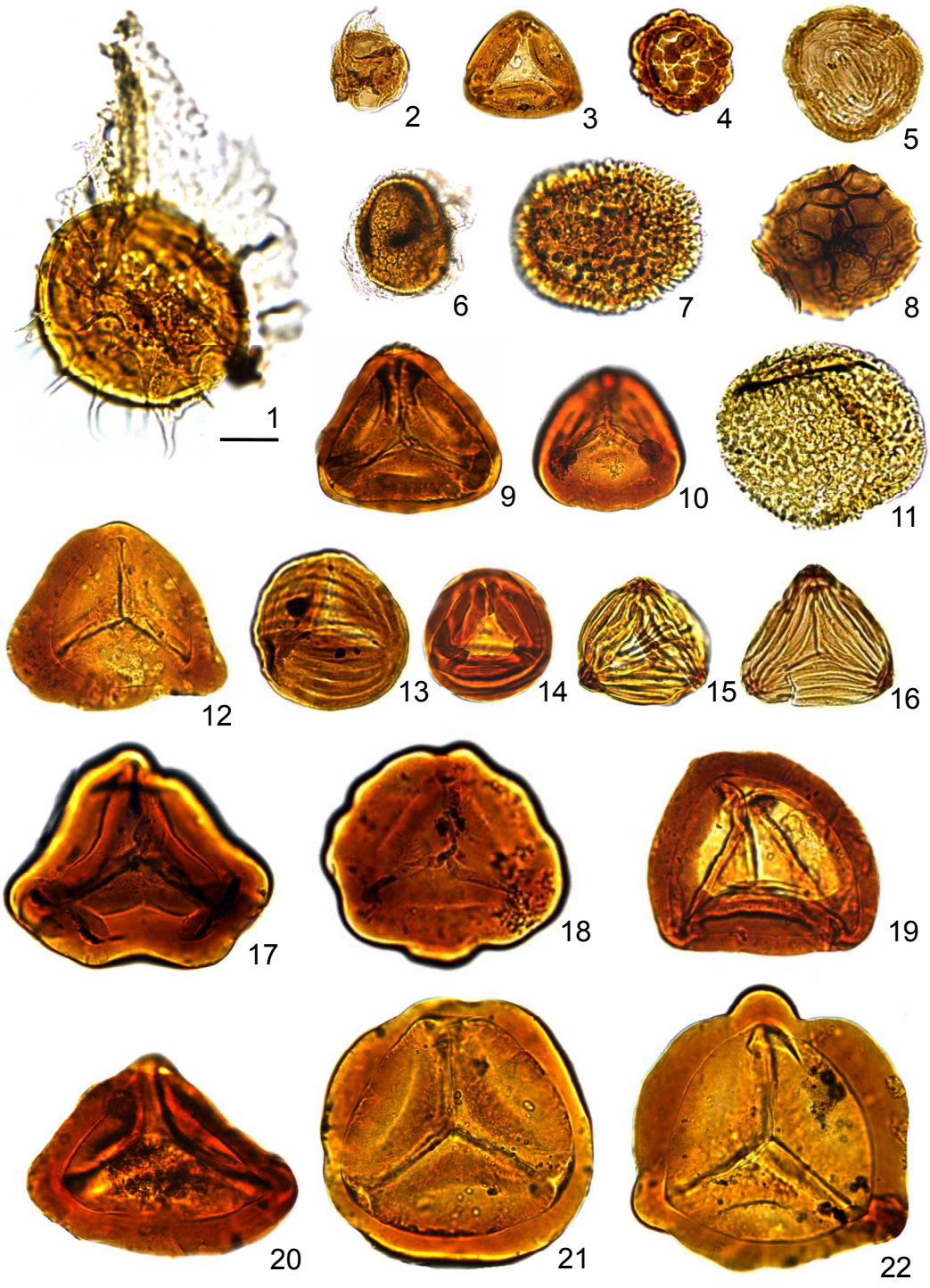

PLATE 6

Late Barremian angiosperm pollen grains

1, 2. *Retimonocolpites ghazalii* Ibrahim, 2002, slide AT-16A, 9400 ft, 6.6/140.6, slide AT-24A, 9000 ft, 16.2/128, (115).

3, 4. *Retimonocolpites matruhensis-Retimonocolpites ghazalii* complex, slide AT-23B, 9050 ft, 20.3/127.9, slide AT-10A, 9700 ft, 11.5/121.6, (132).

5, 8. *Retimonocolpites matruhensis* Penny, 1986, slide AT-16A, 9400 ft, 11/125.8, slide AT-24A, 9000 ft, 10/118, (131).

6, 10. *Retimonocolpites bueibensis* Ibrahim, 2002, slide AT-6A, 9350 ft, 16.5/137.7, slide AT-18A, 9300 ft, 5.6/147.7, (135).

7. *Retimonocolpites variplicatus* Schrank & Mahmoud, 1998, slide AT-14A, 9500 ft, 10.8/122.1, (97).

9, 12. *Retimonocolpites pennyi* Schrank & Mahmoud, 2002, slide AT-19A, 9250 ft, 4.3/137.5, slide AT-16A, 9400 ft, 11.7/122.5, (136).

11, 13, 17. *Dichastopollenites ghazalatensis* Ibrahim, 1996, slide AT-21B, 9150 ft, 21.2/115.5, slide AT-18B, 9300 ft, 7.7/136.5, slide AT-20B, 9200 ft, 14.3/118, (111).

14, 19. *Stellatopollis bituberensis* Penny, 1986, slide AT-19B, 9250 ft, 20.5/137, (137).

15, 16. *Stellatopollis barghoornii* Doyle in Doyle et al., 1976, slide AT-52B, 7600 ft, 9.3/130.2, slide AT-25B, 8950 ft, 3.3/129.5, (117).

18. *Stellatopollis hughesii* Penny, 1986, slide AT-33B, 8550 ft, 4.4/136.8, (129).

PLATE 6

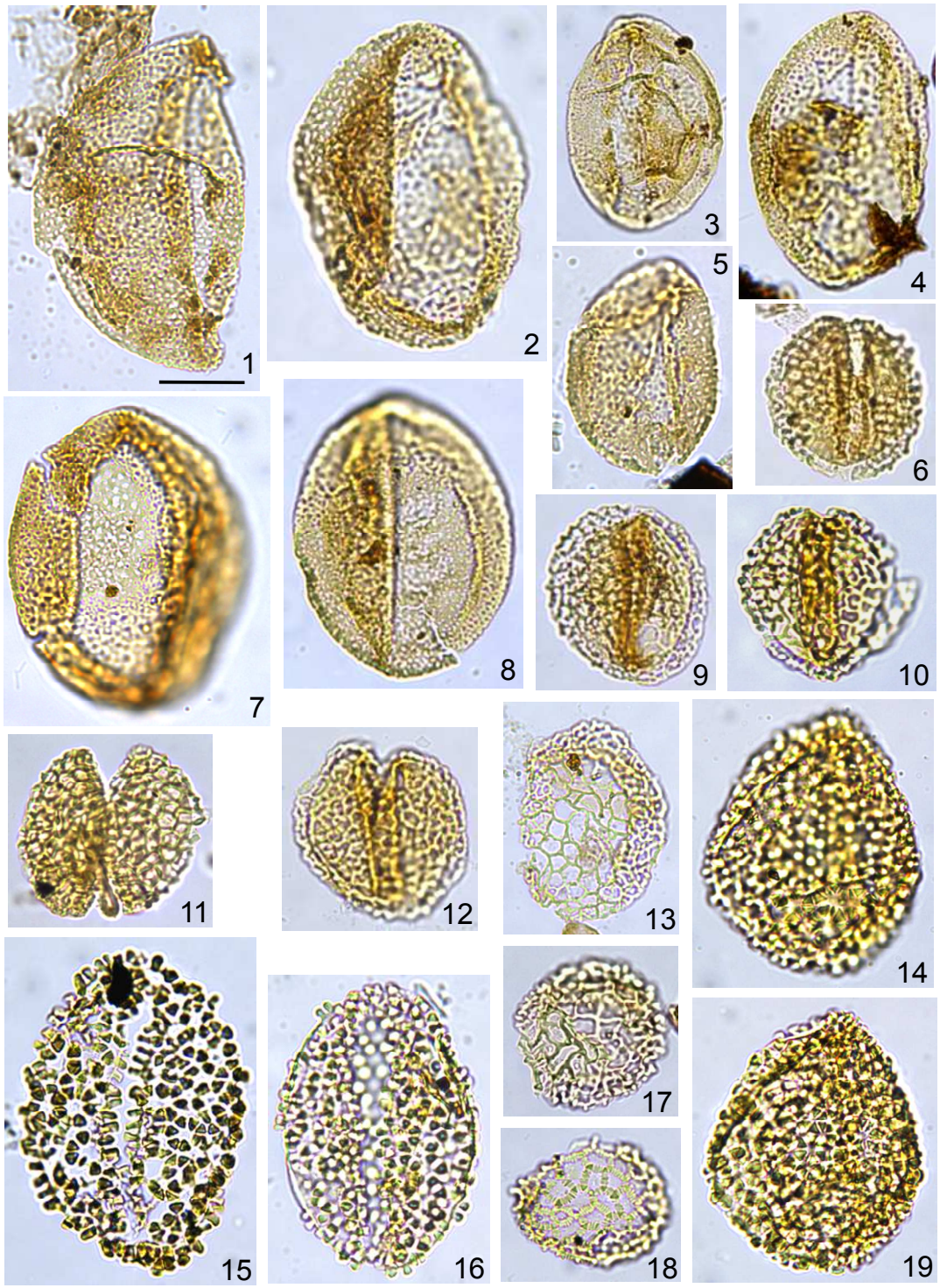

PLATE 7

Late Barremian angiosperm pollen grains

1, 3. *Stellatopollis hughesii* Penny, 1986, slide AT-16A, 9400 ft, 10.6/135, slide AT-16B, 11.6/137.7, (129).

2. *Stellatopollis barghoornii* Doyle in Doyle et al., 1976, slide AT-34A, 8500 ft, 10.8/118.1, (117).

4. *Retimonocolpites* sp.1 Schrank & Mahmoud, 2002, slide AT-14A, 9500 ft, 9/130, (139).

5, 11-18. *Afropollis operculatus* Doyle et al., 1982, 5, slide AT-37A, 8350 ft, 3.1/112.7; 11, slide AT-26B, 8900 ft, 13.3/133.1; 12, slide AT-29B, 8750 ft, 9.2/128.3; 13, slide AT-38A, 8300 ft, 7.2/136; 14, slide AT-36A, 8400 ft, 9.6/137.3; 15, slide AT-41A, 8150 ft, 15.8/122; 16, slide AT-49B,7750 ft, 11.8/130.5; 17, slide AT-40A, 10.1/147.8; 18, slide AT-31A, 8650 ft, 10.4/136.6, (126).

6, 7. *Stellatopollis dejaxii* Ibrahim, 2002, slide AT-24A, 9000 ft, 19.1/113.9, slide AT-19A, 9250 ft, 18.3/113.1, (120).

8, 9. *Tucanopollis annulatus* Schrank in Schrank & Mahmoud, 2002, slide AT-23A, 9050 ft, 16.9/114.9, slide AT-17A, 9350 ft, 16.1/130.7, (133).

10. *Retiacolpites columellatus* Schrank in Schrank & Mahmoud, 2002, slide AT-21A, 9150 ft, 10.2/122.7, (134).

19. *Afropollis* aff. *zonatus* Doyle et al., 1982, slide AT-20B, 9200 ft, 9.3/138.7, (127).

Early Aptian angiosperm pollen grains

20-22. *Afropollis zonatus* Doyle et al., 1982, slide AT-20B, 9200 ft, 15.8/134.6, slide AT-33A, 8550 ft, 2.5/143.5, slide AT-23A, 9050 ft, 1.9/134.9, (128).

PLATE 7

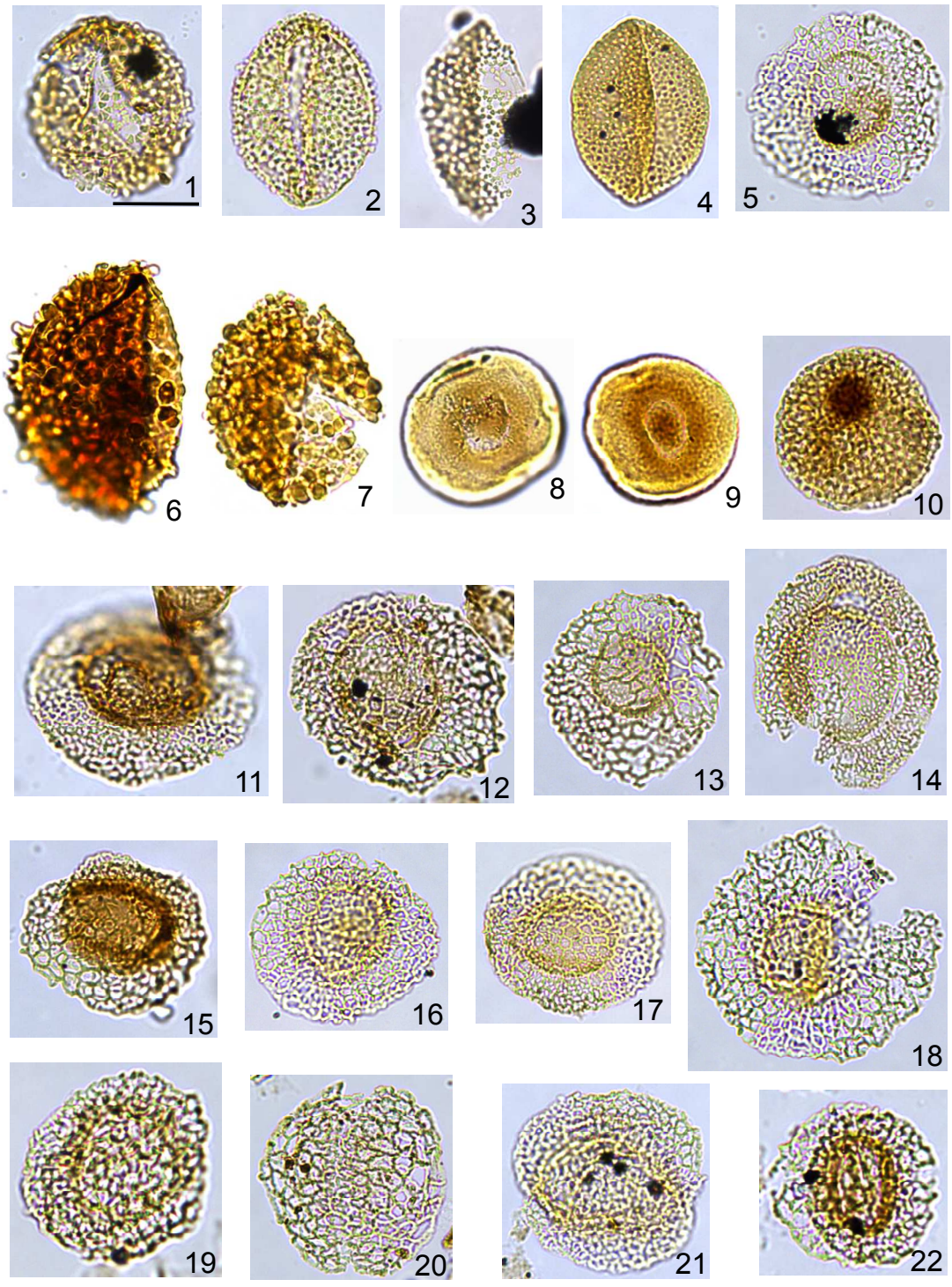

PLATE 8

Late Aptian angiosperm pollen grains

1-4. *Afropollis* sp. B Doyle et al., 1982, 1, slide AT-16B, 9400 ft, 11.7/122.9 ; 2, slide AT-17A, 9350 ft, 15.9/120.7 ; 3, slide AT-24B, 9000 ft, 14.6/131.2 ; 4, slide AT-29A, 8750 ft, 7.9/145, (130).

5-9. *Afropollis* aff. *jardinus* Doyle et al., 1982, 5, slide AT-39A, 8250 ft, 3.8/128.9; 6, slide AT-38A, 8300 ft, 12/124; 7, slide AT-38A, 13/144; 8, slide AT-33A, 8550 ft, 3.5/130.8; 9, slide AT-16B, 9400 ft, 7.5/143.4, (122).

Albian angiosperm pollen grains

10-20. *Afropollis jardinus* Doyle et al., 1982, 10, slide BB-8A, 5220 ft, 17/122.8; 11, slide AT-89A, 5750 ft, 9.1/113.4; 12, slide AT-89B, 9.8/122.4; 13, slide BB-8B, 5220 ft, 16.4/131.9; 14, slide AT-93, 5500 ft, 12.5/119; 15, slide BB-11B, 5180 ft, 6.4/138.2; 16, slide AT-110A, 4300 ft, 14.6/145.2; 17, slide BB-22A, 4880 ft, 13.2/117.5; 18, slide BB-22A, 12.3/115.5; 19, slide AT-110A, 4300 ft, 14.6/145.2; 20, slide BB-8A, 5220 ft, 5.6/126.4, (92, 15).

PLATE 8

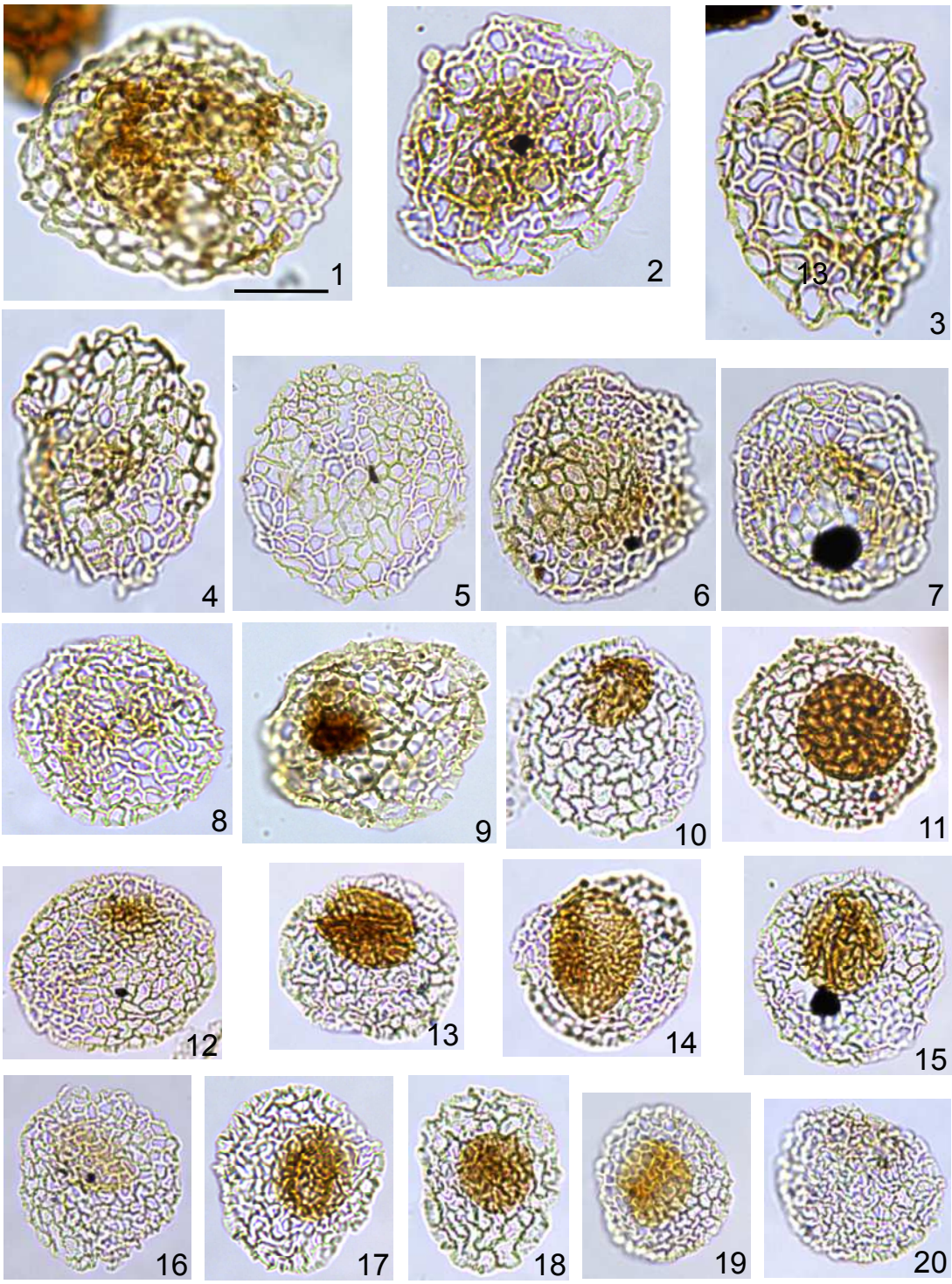

PLATE 9

Mid Albian elaterate gymnosperm pollen grains

1, 3. *Elaterosporites verrucatus* (Jardiné & Magloire) Jardiné, 1967, slide AT-88A, 5800 ft, 13.7/130.5, slide AT-93A, 5500 ft, 16.5/123.1, (72).

2, 8. *Elaterosporites acuminatus* (Stover) Jardiné, 1967, slide AT-93A, 5500 ft, 18.3/144.5, slide AT-91A, 5600 ft, 17.8/132.2, (73).

4. *Elaterosporites protensus* (Stover) Jardiné, 1967, slide AT-90A, 5650 ft, 6.2/116.2, (74).

5-7, 9-16. *Elaterosporites klaszii* (Jardiné & Magloire) Jardiné, 1967, 5, slide AT-97A, 4950 ft, 18.3/113.8; 6, slide BB-22A, 4880 ft, 5.7/126; 7, slide BB-9A, 5210 ft, 14.2/130.1; 9, slide BB-8B, 5220 ft, 8.3/120.3; 10, slide BB-8B, 8.3/120.3; 11, slide BB-22A, 4880 ft, 4.8/130.8; 12, slide BB-8A, 5220 ft, 9/134.2; 13, slide BB-21B, 4890 ft, 3.7/137; 14, slide BB-9A, 5210 ft, 11.5/143.1; 15, slide BB-9B, 17.5/119.7; 16, slide BB-9B, 17.5/119.7, (66, 9).

Late Albian elaterate gymnosperm pollen grains

17-21. *Sofrepites legouxiae* Jardiné, 1967, 17, slide AT-86B, 5900 ft, 9.8/130.2; 18, slide AT-93A, 5500 ft, 14.3/132.3; 19, slide AT-93A, 16.7/126.9; 20, slide AT-93A, 7.5/123.3; 21, slide AT-95A, 5100 ft, 17.5/117.1, (71).

PLATE 9

PLATE 10

Late Albian elaterate gymnosperm pollen grains

1-4. *Elateroplicites africaensis* Herngreen, 1973, slide BB-24A, 4840 ft, 9.6/121.2, slide BB-22A, 4880 ft, 13.7/116, slide BB-8A, 5220 ft, 9.6/112.5, slide BB-22A, 4880 ft, 8.1/119.2 (12).

5-8. *Elaterocolpites castelainii* Jardiné & Magloire, 1965, slide BB-22A, 4880 ft, 11.2/118.4, slide BB-9A, 5210 ft, 13.9/139.9, slide BB-10A, 5200 ft, 14.5/133.5, (11).

Late Albian-Mid Cenomanian pollen grains

9. *Gnetaceaepollenitess* cf. *clathratus* Stover, 1964, slide AT-83A, 6050 ft, 16.3/143.3, (75).

10. *Galeacornea causea* Stover, 1963, slide AT-84A, 6000 ft, 15.8/145.6, (76).

11, 12. *Foveotricolpites gigantoreticulatus* (Jardiné & Magloire) Schrank, 1987a-b, slide AT-92A, 5550 ft, 5.6/130.8, slide AT-92A, 13.5/113.5 (92).

13. *Cretacaeiporites densimurus* Schrank & Ibrahim, 1995, slide BB-16B, 4980 ft, 11.4/131.5, (19).

14. *Ephedripites irregularis* Herngreen, 1973, slide AT-77B, 6350 ft, 22.7/119.8, (78).

15. *Classopollis brasiliensis* Herngreen, 1975, slide BB-22A, 4880 ft, 11.6/123.4, (14).

16. *Cretacaeiporites polygonalis* (Jardiné & Magloire) Herngreen, 1973, AT-94A, 5150 ft, 15.5/131.7, (108).

17. *Cretacaeiporites mullerii* Herngreen, 1973, slide AT-103A, 4650 ft, 5.9/125.3, (101).

18. *Afropollis kahramanensis* Ibrahim & Schrank 1995, slide AT-88A, 5800, 12/137.3, (98).

PLATE 10

PLATE 11

Albian-Cenomanian spore and pollen grains

1. *Tetracolpites* sp., slide AT-77B, 6350 ft, 19.1/128.1, (123).

2. *Tricolpites sagax* Norris, 1967, slide AT-92A, 5550 ft, 18.6/128.9, (114).

3. *Striatopollis* cf. *trochuensis* (Srivastava) Ward, 1986, slide AT-86A, 5900 ft, 9.8/141.9, (119).

4. *Stephanocolpites* sp., slide AT-91A, 5600 ft, 10/122.8, (116).

5. *Rousea* sp., slide BB-24A, 4840 ft, 4.5/138, (23).

6. *Tricolpites* cf. *crassimurus* (Groot & Penny) Singh, 1971, slide AT-85A, 5950 ft, 16.4/120.6, (112).

7. *Rousea delicipollis* Srivastava, 1977, slide AT-71A, 6650 ft, 22/134, (100).

8. *Tricolpites micromunus* (Groot & Penny) Singh, 1971, slide AT-75A, 6450 ft, 9.7/142.6, (110).

9. *Tricolpites parvus* Stanley, 1965, slide AT-94A, 5150 ft, 13.9/135.8, (107).

10. *Rousea* cf. *miculipollis* Srivastava, 1975, slide-AT-97A, 4950 ft, 11.4/138, (103).

11. *Proteacidites* cf. *africaensis* (Jardiné & Magloire) Schrank & Ibrahim, 1995, slide AT-85A, 5950ft, 12.3/141.5, (91).

12. *Tricolporopollenites* sp., slide AT-93B, 5500 ft, 3.8/114.5, (99).

13. *Papillopollis vancampoae* Kedves & Pittau, 1979, slide AT-104A, 4600 ft, 4.1/110.7, (96).

14, 15. *Tetraporopollenites* sp., slide AT-86A, 5900 ft, 19/115.9, slide AT-94, 5150 ft, 9.1/128.2, (95).

16. *Triporopollenites* sp., slide AT-94A, 5150 ft, 8/144.3, (109).

17. *Crybelosporites pannuceus* (Brenner) Srivastava, 197**7**, slide AT-91A, 14.9/143.5, (2).

18, 19. *Droseridites senonicus* Jardiné & Magloire, 1965, slide AT-89A, 5750 ft, 15.3/122.2, slide AT-77B, 6350 ft, 10.8/126.9, (143).

20. *Droseridites baculites* Ibrahim, 1996, slide AT-92A, 5550 ft, 9.8/140, (142).

21. *Rousea brenneri* Singh, 1983, slide AT-93A, 5500 ft, 14.3/146, (106).

22. *Cretacaeiporites densimurus* Schrank & Ibrahim, 1995, slide AT-95B, 5100 ft, 20/122.3, (94).

PLATE 11

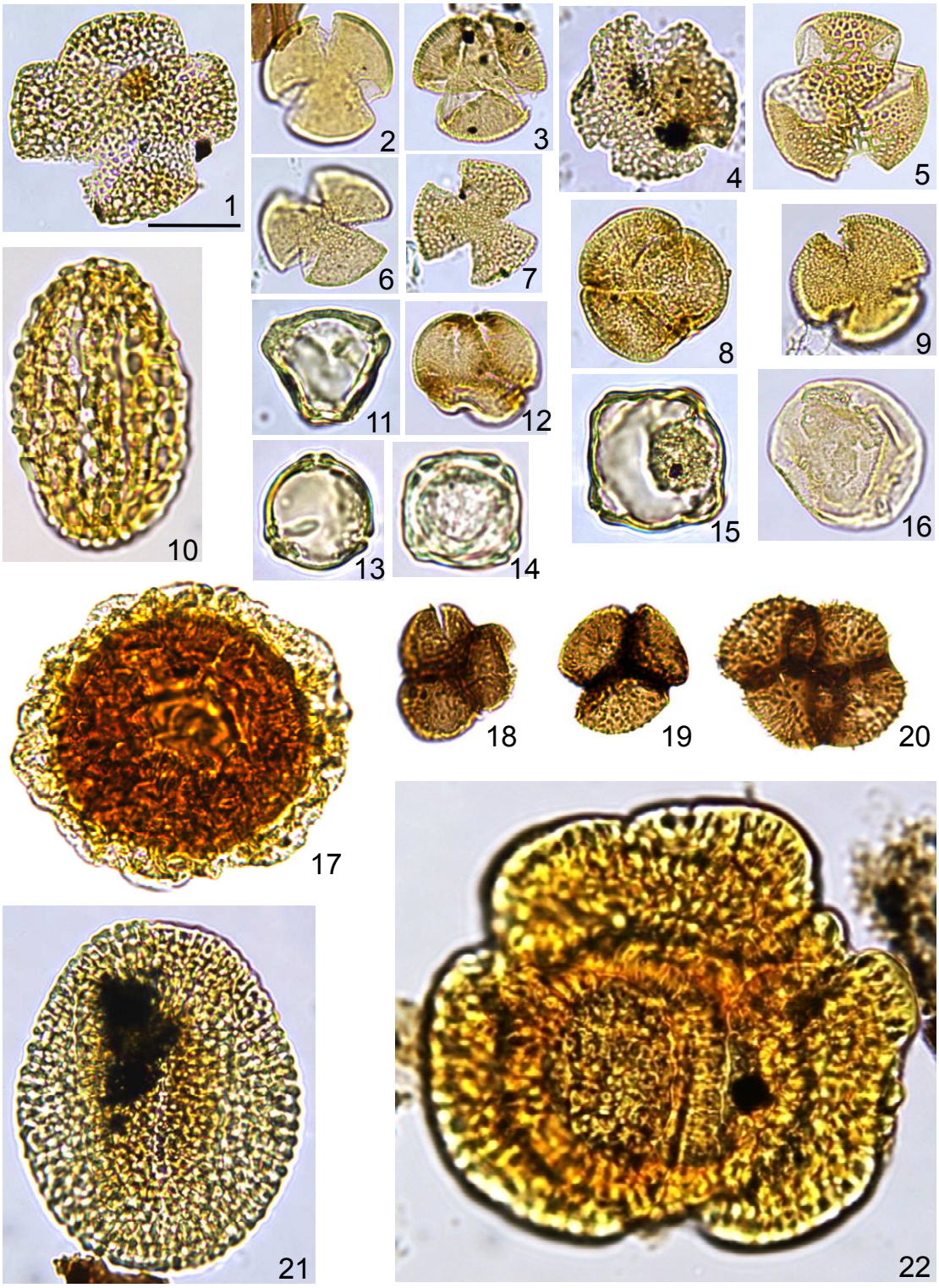

PLATE 12

Cretaceous spore and pollen grains

1, 2. *Retimonocolpites* sp. 1, slide AT-19B, 9250 ft, 6.9/131.2, (138).

3, 4. *Retiacolpites columellatus* Schrank in Schrank & Mahmoud, 2002, slide AT-19B, 9250 ft, 12.4/126, slide AT-21A, 9150 ft, 10.2/122.7, (134).

5, 6, 9-12. *Retimonocolpites textus* (Norris) Singh, 1983, 5 and 6, slide AT-94A, 5150 ft, 12.4/127.9; 9 and 10, slide AT-89A, 5750 ft, 16/139.3; 11, slide AT-94A, 5150 ft, 18.5/131.2; 12, slide AT-94A, 18.5/131.2, (105).

7. *Dichastopollenites ghazalatensis* Ibrahim, 1996, slide AT-88B, 5800 ft, 3.5/137.2, (111).

8. *Tricolpites vulgaris* (Pierce) Srivastava, 1969, slide AT-34A, 8500 ft, 10.3/120.5, (104).

13, 14. *Retimonocolpites variplicatus* Schrank & Mahmoud, 1998, slide BB-24B, 4840 ft, 13/133.9, slide AT-90A, 5650 ft, 10/129.7, (18, 97).

15. *Rousea* sp., slide BB-8B, 5220 ft, 5.1/121.1, (23).

Microforaminiferal test linigs

16. Biserial microforaminiferal test lining, slide BB-12A, 5170 ft, 12.6/123.9, (226).

19, 20. Planispiral microforaminiferal test linings, slide BB-13A, 5160 ft, 9.3/140.7, slide BB-8A, 5220 ft, 6.3/1337, (226).

Fresh water algae

17. Fungal fruiting body, slide AT-109B, 4350 ft, 12.5/134.2, (146).

18. *Chomotriletes minor* (Kedves) Pocock, 1970, slide AT-42A, 8100 ft, 7.1/145, (148).

21. *Botryococcus* sp., slide AT-99B, 4850 ft, 8.8/141.9, (147).

PLATE 12

PLATE 13

Early Cretaceous dinoflagellate cysts

1, 2. *Muderongia aequicorna* Århus in Århus et al., 1990, slide AT-4A, 10000 ft, 17.2/124, slide AT-4A, 13.2/131.9, (216).

3. *Circulodinium brevispinosum* (Pocock) Jansonius, 1986, slide AT-12A, 9600 ft, 20/140.2, (205).

4. *Muderongia pariata* Duxbury, 1983, slide AT-4A, 10000 ft, 13.6/115.3, (198).

5. *Muderongia tomaszowensis* Alberti, 1961, slide AT-6A, 9900 ft, 7.8/124.7, (203).

8, 12. *Pseudoceratium pelliferum* Gocht, 1957, slide AT-7A, 9850 ft, 20.5/128.3, slide AT-12A, 9600 ft, 20.6/135, (207).

9. *Circulodinim distinctum* (Deflandre & Cookson) Jansonius, 1986, slide AT-5A, 9950 ft, 9.1/127.2, (173).

10. *Phoberocysta neocomica* (Ghocht) Millioud, 1969, slide AT-4A, 10000 ft, 7.8/128.1, (217).

Acritarchs

6. *Veryhachium reductum* (Deunff) Downie & Sarjeant, 1965, slide AT-2A, 10100 ft, 15.6/124.6, (225).

7. *Veryhachium valiente* Cramer, 1964, slide AT-2A, 10100 ft, 9.9/128, (224).

11. *Baltisphaeridium* spp., slide AT-2A, 10100 ft, 8.8/130.4, (219).

PLATE 13

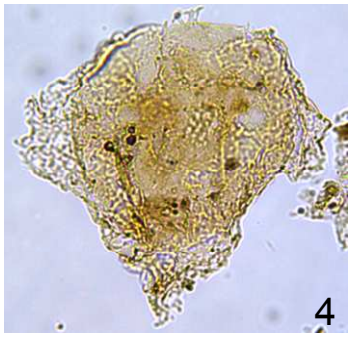

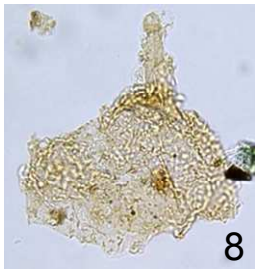

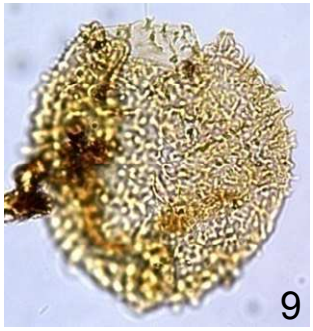

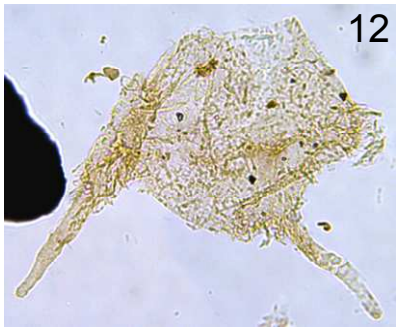

PLATE 14

Late Barremian dinoflagellate cysts

1-3, 9, 12, 14. *Pseudoceratium retusum* Brideaux, 1977, 1 ,slide AT-16A, 9400 ft, 13.7/123.3; 2, slide AT-24A, 9000 ft, 16.5/138.9; 3, slide AT-22A, 9100 ft, 19.7/139.2; 9, slide AT-21A, 9150 ft, 8.5/137.6; 12, slide AT-25A, 8950 ft, 14.9/147.8; 14, slide AT-22A, 9100 ft, 11.5/141.2, (190).

4, 16. *Pseudoceratium anaphrissum* (Sarjeant) Bint, 1986, slide AT-22A, 9100 ft, 6.3/136.1, slide AT-27A, 8850 ft, 6.3/136.1, (184).

5. *Odontochitina operculata* (Wetzel) Deflandre & Cookson, 1955, AT-19B, 9250 ft, 6.5/130.2, (151).

13. *Odontochitina ancala* Bint, 1986, slide AT-29A, 8750 ft, 3.4/129, (200).

Early Cretaceous dinoflagellate cysts

6, 10. *Subtilisphaera terrula* (Davey) Lentin & Williams, 1976, slide AT-31A, 8650 ft, 5.1/137, slide AT-6A, 9900 ft, 19.2/135.8, (194).

7, 11. *Subtilisphaera perlucida* (Alberti) Jain & Millepied, 1973, slide AT-28A, 8800 ft, 7.9/129, slide AT-22A, 9100 ft, 11.9/131.8, (188).

8, 15. *Subtilisphaera senegalensis* Jain & Millepied, 1973, slide AT-28A, 8800 ft, 16.1/120.6, slide AT-22B, 9100 ft, 4.4/135.6, (182).

PLATE 14

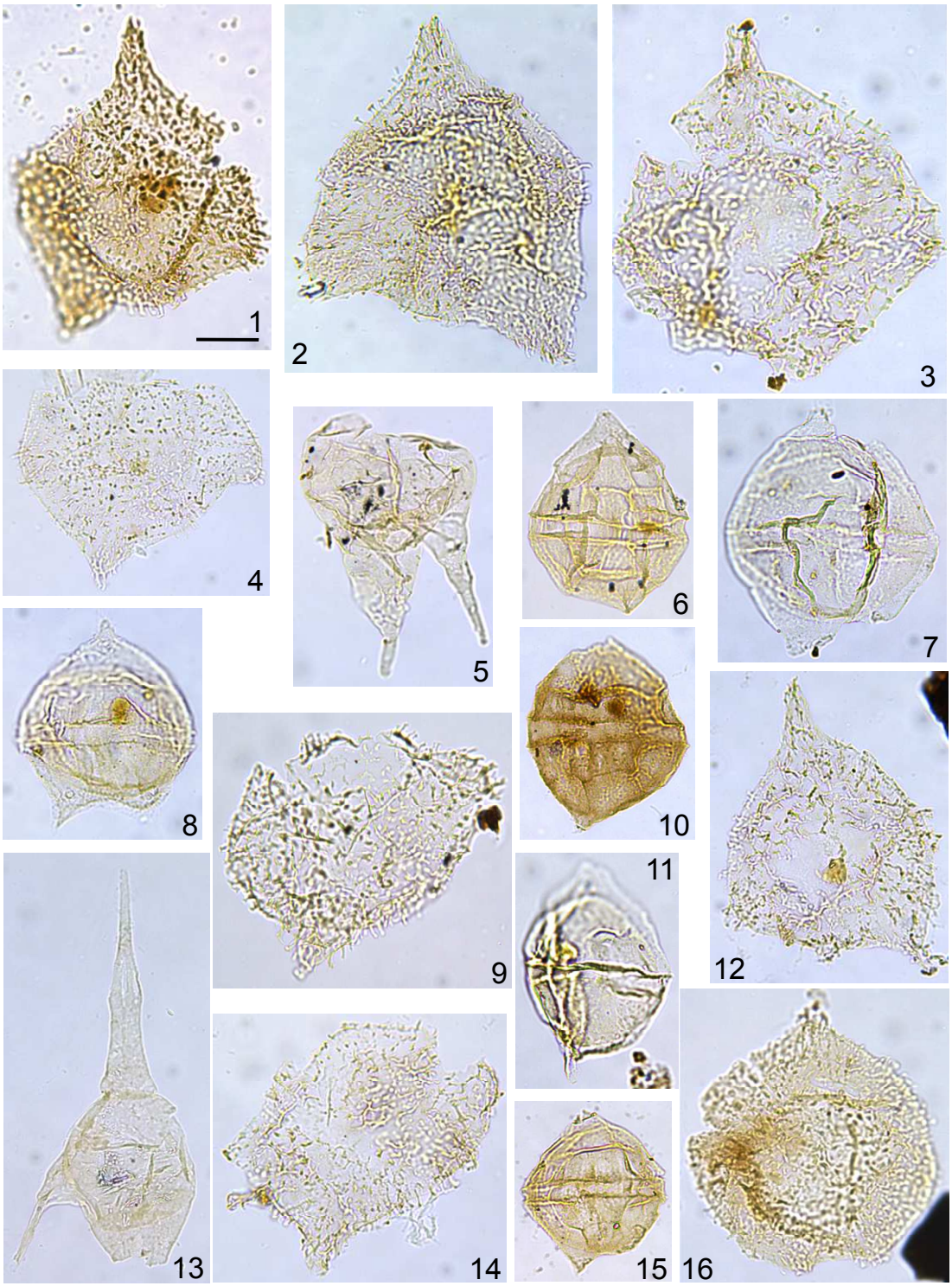

PLATE 15

Early Aptian dinoflagellate cysts

1, 2. *Pseudoceratium securigerum* (Davey & Verdier) Bint, 1986, slide AT-20A, 9200 ft, 6.8/139.4, slide AT-20B, 10.2/133.6, (185).

4, 9. *Palaeoperidinium cretaceum* (Pocock) Lentin & Williams, 1976, slide AT-36A, 8400 ft, 9/112.4, slide AT-21A, 9150 ft, 113.1/140.7, (187).

5, 6, 14. *Florentinia mantellii* (Davey & Williams) Davey & Verdier, 1973, slide AT-22A, 9100 ft, 10.2/150.1, slide AT-32A, 8600 ft, 4.4/136, slide AT-19A, 9250 ft, 8.4/122.9, (172).

13. *Florentinia laciniata* Davey & Verdier, 1973, slide AT-23A, 9050 ft, 13/136.6, (176).

17. *Aptea polymorpha* Eisenack, 1958a, slide AT-24A, 9000 ft, 12.8/129.6, (193).

Early Cretaceous dinoflagellate cysts

3, 7. *Subtilisphaera scabrata* Jain & Millepied, 1973, slide AT-20A, 9200 ft, 14.4/144.2 , slide AT-29A, 8750 ft, 6.2/145.7, (192).

8, 11. *Spinifereites* sp., slide AT-24A, 9000 ft, 10.4/127.2, slide AT-23A, 9050 ft, 8.1/142.2, (150).

10. *Cribroperidinium edwardsii* (Cookson & Eisenack) Davey, 1969, slide AT-27, 8850 ft, 17.5/141.2, (181).

12. *Florentinia cooksoniae* (Singh) Duxbury, 1980, slide AT-21A, 9150 ft, 15.4/129.9, (201).

15. *Cyclonephelium vannophorum* Davey, 1969, slide AT-12A, 9600 ft, 15.4/128.1, (212).

16. *Pseudoceratium almohadense* (Below) Lentin & Williams, 1989, slide AT-23A, 9050 ft, 3.5/142.1, (208).

PLATE 15

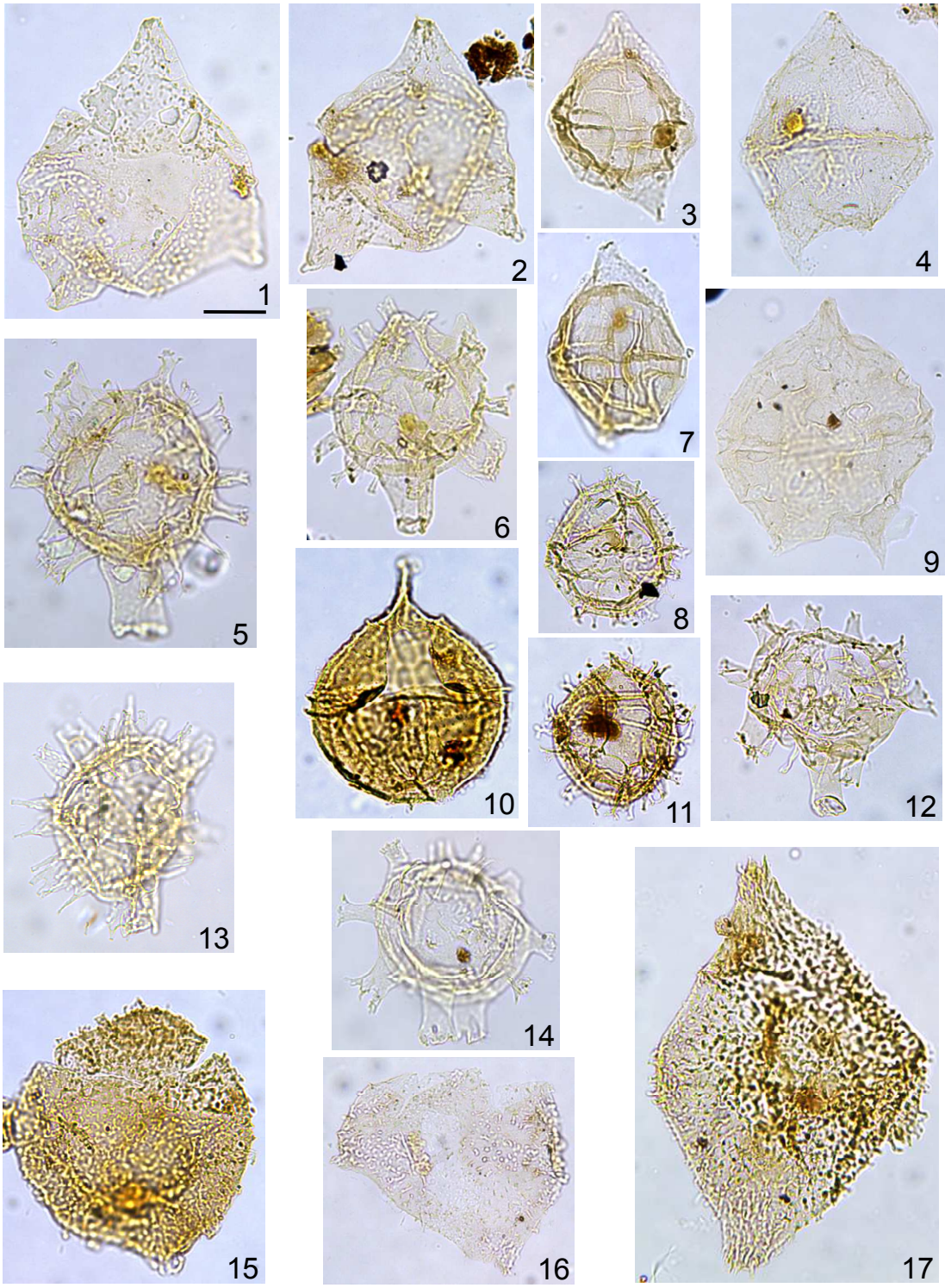

PLATE 16

Cretaceous dinoflagellate cysts

1. *Florentinia berran* Below, 1982, slide AT-45A, 7950 ft, 12.2/118.7, (171).

2, 8. *Oligosphaeridium albertense* (Pocock) Davey & Williams, 1969, slide AT-25A, 8950 ft, 6/134.6, slide AT-29A, 8750 ft, 10.1/146.7, (178).

3. *Oligosphaeridium poculum* Jain, 1977, slide AT-23B, 9050 ft, 13.1/122.6, (180).

4, 7. *Coronifera albertii* Millioud, 1969, slide AT-24A, 9000 ft, 7.6/134.9, slide AT-97A, 4950 ft, 5.2/118.4, (174).

5. *Downiesphaeridium* sp., slide AT-34A, 8500 ft, 6.5/114, (165).

11, 13. *Oligosphaeridium complex* (White) Davey & Williams, 1966, slide AT-25A, 8950 ft, 15.2/142.6, slide AT-22A, 9100 ft, 10.5/138.7, (179).

12. *Oligosphaeridium diluculum* Davey, 1982, slide AT-29B, 8750 ft, 9.7/123.9, (197).

Acritarchs

6. *Micrhystridium stellatum* Deflandre, 1945a, slide AT-37A, 8350 ft, 11.9/140.1, (223).

9. *Veryhachium metum* Davey, 1970, slide AT-42A, 8100 ft, 6.7/130.8, (222).

10. *Veryhachium collectum* Wall, 1965, slide AT-33A, 8550 ft, 3.2/139.1, (221).

PLATE 16

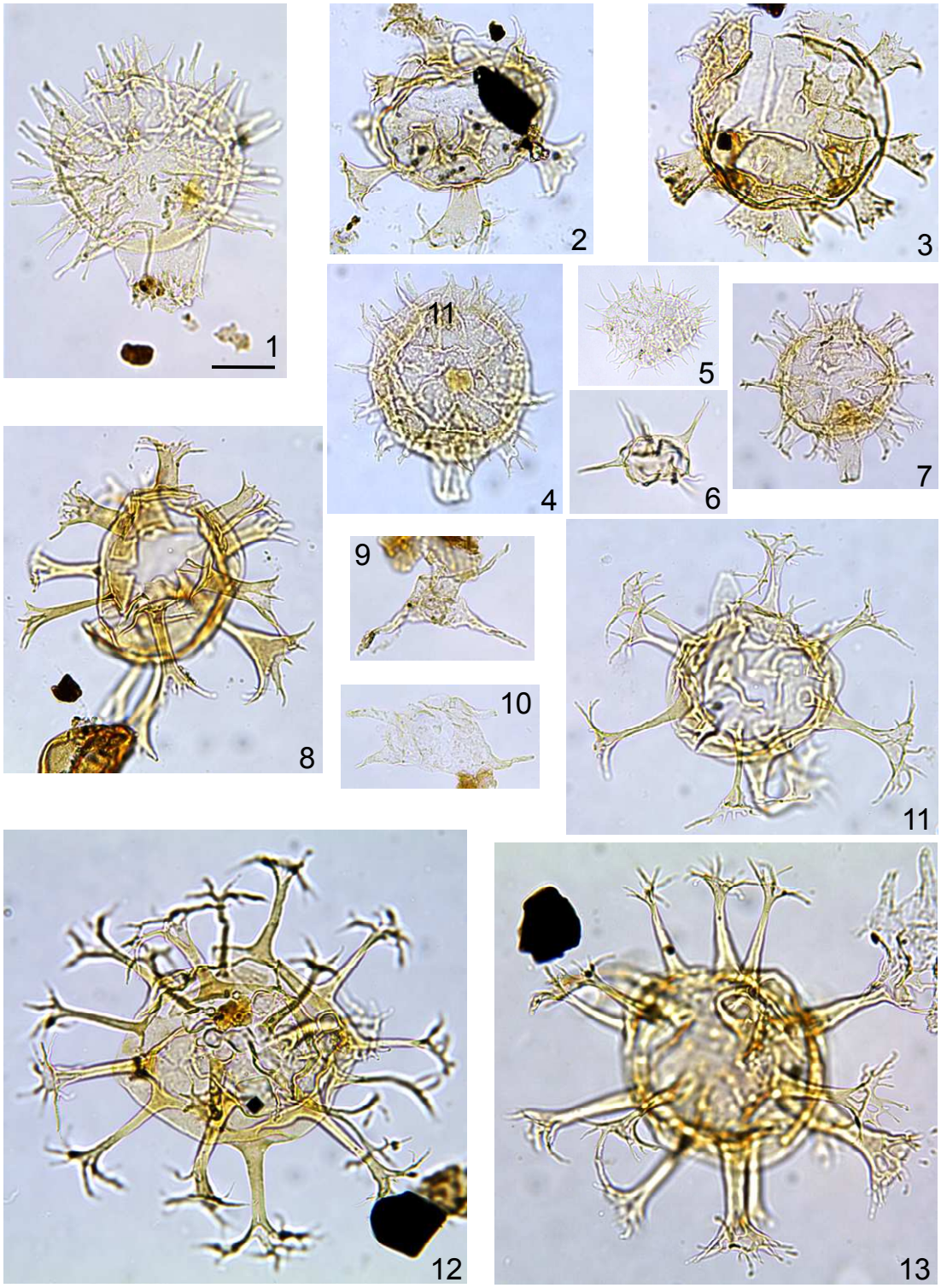

PLATE 17

Santonian dinoflagellate cyst

1. *Canningia senonica* Clarke & Verdier, 1967, slide AT-131B, 3200 ft, 15/122.3, (152).

Post-Turonian dinoflagellate cysts

2, 6, 15. *Dinogymnium denticulatum* (Alberti) Evitt et al., 1967, slide AT-130A, 3250 ft, 11.8/136.5, slide AT-130A, 10.7/141.5, slide AT-130B, 12.5/129.4, (162).

3, 7. *Eucladinium gambangense* (Cookson & Eisenack) Stover & Evitt, 1978, slide AT-130A, 3250 ft, 15.8/128.1, slide AT-130B, 11.7/142, (166).

4, 13. *Isabelidinium acuminatum* (Cookson & Eisenack) Stover & Evitt, 1978, slide AT-131A, 3200 ft, 6.6/1274, slide AT-131B, 14.2/143.8 (163).

9. *Dinogymnium* sp., slide AT-130B, 3250 ft, 8.4/144.3, (155).

10. *Dinogymnium* sp., slide AT-131B, 3200 ft, 5.7/126, (155).

12. *Chatangiella madura* Lentin & Williams, 1976, slide AT-134A, 2950 ft, 6.4/126.2, (154).

14. *Exochosphaeridium bifidum* (Clarke & Verdier) Clarke et al., 1968, slide AT-133A, 3100 ft, 22.4/111.2, (153).

17. *Cannosphaeropsis utinensis* Wetzel, 1933b, slide AT-117A, 3950 ft, 7.6/132.5, (169).

19. *Odontochitina porifera* Cookson, 1956, slide AT-133A, 3100 ft, 15.3/138.2, (157).

Cretaceous dinoflagellate cysts

5. *Trichodinium castanea* Deflandre, 1935, slide AT-116A, 4000 ft, 14.8/112.9, (160).

8. *Xiphophoridium alatum* (Cookson & Eisenack) Sarjeant, 1966b, slide AT-103B, 4650 ft, 20.4/142.7, (168).

11, 18. *Senegalinium aenigmaticum* (Boltenhagen) Lentin & Williams, 1981, slide AT-110A, 4300 ft, 18.3/113.4, slide AT-109A, 4350 ft, 8.2/130.6, (158).

16. *Odontochitina costata* Alberti, 1961, slide AT-134A, 2950 ft, 5.5/138.2, (156).

PLATE 17

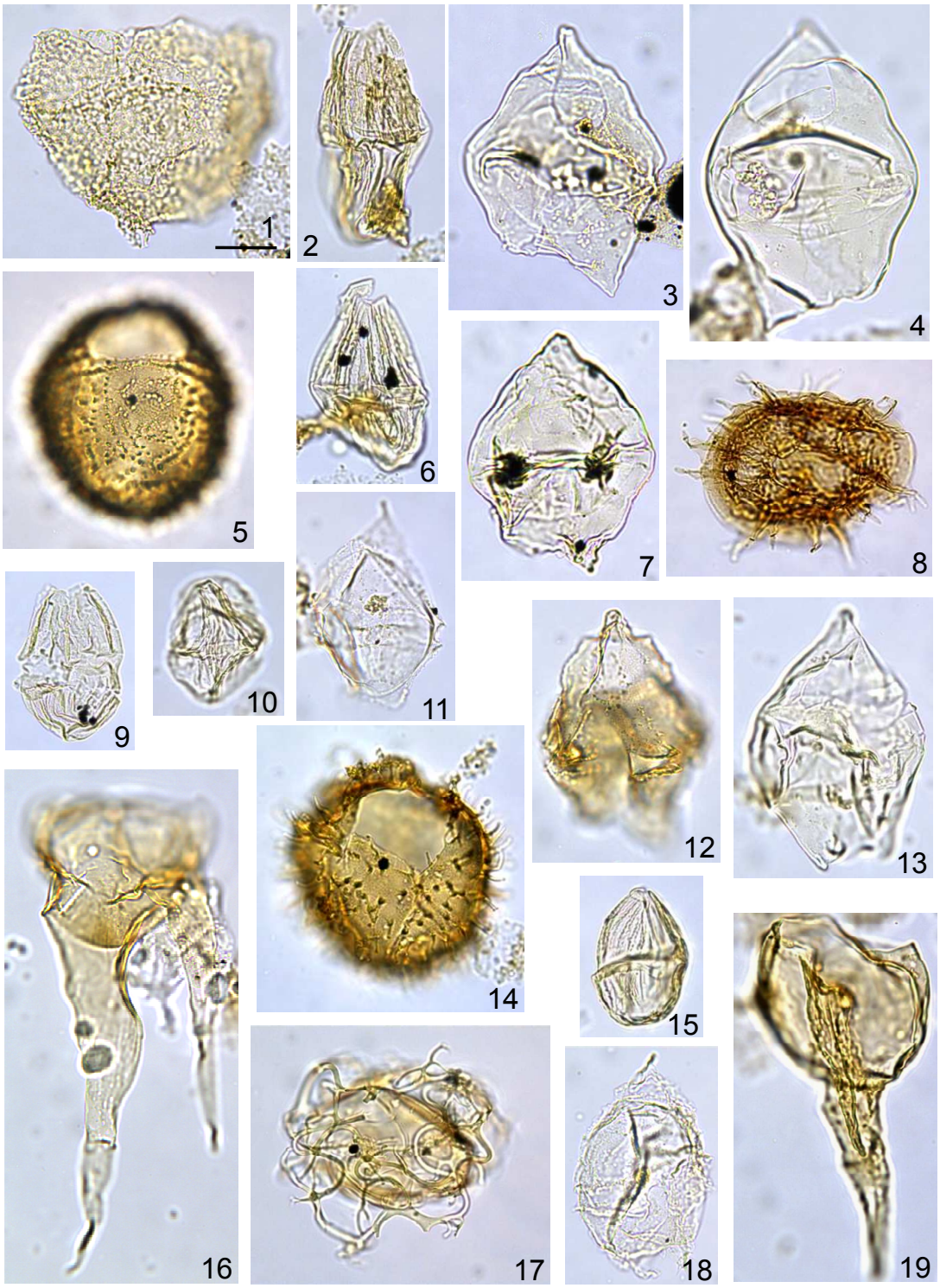

PALYNOFACIES ANALYSIS AND PALAEOENVIRONMENTAL INTERPRETATIONS

6.1 Introduction

The word palynofacies as defined by Combaz (1964) refers to the total complement of acid-resistant particulate organic matter recovered from sediments by palynological processing techniques.

Sedimentary organic matter is defined as biogenic material that is preserved in sedimentary rocks. This organic matter is composed of both (solvent-)insoluble materials known as kerogen, and soluble bitumen and oil (Miles, 1994). Both the composition and distribution of organic matter are controlled by ecological conditions and sedimentological processes in the depositional environment, while microbial, physical and biogeochemical processes in sediments affect its abundance (Tyson, 1995).

Combaz (1964) and Caratini et al. (1983) referred to palynofacies analysis as the process that involves identification of organic matter constituents, calculating their relative and absolute abundances, and determining their size and degree of preservation. Early palynofacies studies were directed towards palaeobotanical and palaeoenvironmental studies. In this sense, a variety of definitions of palynofacies were proposed, for example that of Powell et al. (1990), where a palynofacies was described as a distinctive assemblage of HCl- and HF insoluble particulate organic matter (palynoclasts) whose composition reflects a particular sedimentary environment. However, developments in the field of palynology led to the use of palynofacies analysis in visual appraisals of source rocks, and thus added another dimension to the concept of palynofacies analysis. Thus, Tyson (1995, p. 4)

introduced the more acceptable and widely used definition of palynofacies as "*a body of sediment containing a distinctive assemblage of palynological organic matter thought to reflect a specific set of environmental conditions or to be associated with a characteristic range of hydrocarbon-generating potential*". Consequently, Tyson (1995, p. 4) redefined palynofacies analysis as "*the palynological study of depositional environments and hydrocarbon source rock potential based upon the total assemblage of particulate organic matter*".

Compositional changes in palynofacies are useful in palaeoenvironmental interpretations of sedimentary rocks as such changes are the product of the interaction of several parameters (e.g. terrestrial *versus* marine palynomorph influx, source and rate of sediment influx, water salinity, depth and oxygen concentrations, etc.) within a given depositional environment (Tyson, 1993).

The nature of ditch cutting samples means that there is always some degree of equivocation in the identification of borehole lithologies because of possible caving during the drilling process, or due to mixing with other lithologies during sample splitting, shipment and final storage, and thus they are not considered here as a prime tool of choice for palaeoenvironmental interpretations. However, by examining downhole logs from the studied boreholes and sorting cuttings to isolate specific lithologies from ditch cutting samples from specific depth intervals prior to palynological processing, it is possible to maximise the quality of information that ditch cutting samples can provide. The palaeoenvironmental interpretations presented here will mainly depend on quantitative palynofacies characteristics, where the effects of caving and/or lithological mixing can be further assessed by investigating the vertical distribution of the palynofacies constituents.

The palaeoenvironmental interpretations presented for each palynofacies type are based on quantitative analyses of selected palynomorph components,

which are known to have a palaeoenvironmental significance. These include terrestrially derived palynomorphs such as miospores (which comprise pteridophyte spores, saccate, circumpolles, gnetalean and elaterate gymnosperm pollen and angiosperm pollen), and aquatic phytoplankton (e.g. dinoflagellate cysts). In addition, there may be terrestrially derived phytoclasts, which can be represented by black wood (inertinite/charcoal), brown wood (e.g. tracheids), plant cuticle and membranous tissues. Other minor constituents may include microforaminiferal test linings (MTLs) and freshwater algae. Certain sporomorphs are indicators of specific ecological parameters and thus allow not only a robust identification of palaeoclimatic conditions but also permit reconstruction of the vegetation growing on the source areas.

Many palynologists have proposed various classifications of palynofacies constituents (e.g. Staplin, 1969; Correia, 1971; Burgess, 1974; Bujak et al., 1977; Combaz, 1980; Claret et al., 1981; Pocock, 1982; Pocock et al., 1988) in which the maceral terminologies employed in reflected light microscopy of coal and palynological terminologies used in transmitted light studies have been mixed. However, the scheme applied here follows the scheme of Tyson (1993, 1995), which provides a detailed palynological classification of thermally immature to marginally mature palynofacies constituents based on a pure palynological terminology for palaeoenvironmental studies using transmitted light microscopy. In Tyson's (1995) classification of palynofacies components, palynological organic matter constituents can belong to one of two major categories: structureless or structured palynological organic matter (Fig. 6.1).

Structureless organic matter is defined as organic matter that lacks a definite internal structure when observed using light microscopy, lacks a distinct and recognizable outline, and which does not infer its biological affinity (Tyson, 1995).

Structureless organic matter thus includes such materials as amorphous organic matter (AOM), resin, and humic gel.

AOM is an heterogeneous, yellow to grey coloured material that is made of amorphous materials with pseudoamorphous inclusions (Fig. 6.1), and is mainly produced by biodegradation of algal phytoplankton blooms, derived from zooplankton faecal pellets, or derived from biodegradation of cyanobacteria and thiobacteria (Tyson, 1995). AOM is considered to be the major contributing component to structureless organic matter in ancient marine and lacustrine sediments (Tyson, 1995). The concentration of AOM has been used to indicate oxygenation (reducing or oxidizing) conditions of bottom water in ancient sedimentary depositional environments. The high relative or absolute abundances of AOM – usually associated with sediments beneath upwelling water masses – was taken to indicate bottom water of low (dysoxic) oxygen concentrations (Davey & Rogers, 1975; Tissot & Pelet, 1981; Summerhayes, 1983). AOM has been found to decrease in shallow shelf sediments and increase in a basinward direction, in darker-coloured, organic-rich facies with dysoxic-anoxic conditions (e.g. Dow & Pearson, 1975; Bujak et al., 1977).

Resin is a highly resistant, structureless material of yellow, red or orange colour that is known in ancient sediments as amber, and is mainly produced by coniferous gymnosperms and to a small degree by dicotyledonous angiosperm trees (e.g. Tyson, 1995). Amber has commonly been found to be deposited in ancient sediments of deltas (proximal delta front and distributary channels) and river mouths (Larsson, 1978; Trofimov, 1979; Parry et al., 1981). However, due to the lower specific gravity of amber (Langenheim, 1965), it can float in seawater of normal salinity and thus has been found in estuarine and other coastal areas (Langenheim, 1965; Larsson, 1978)

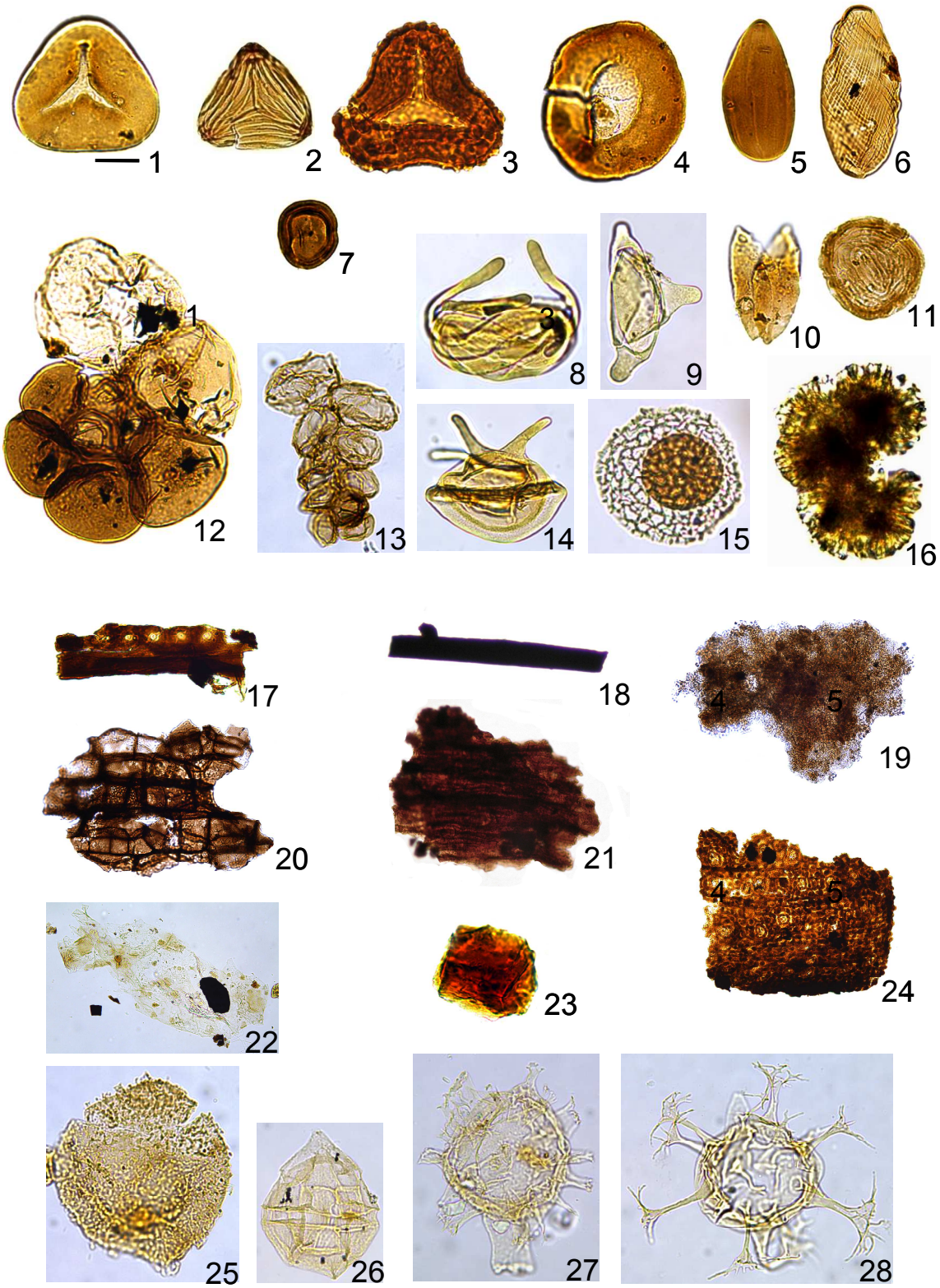

Figure 6.1 Different palynological structured and unstructured organic matter constituents recovered in the present study, scale bar represents 20 micron.

Palynofacies constituents of figure 6.1

Terrestrial palynomorphs

1- A pteridophyte spore grain of *Deltoidospora australis* (Couper) Pocock, 1970, slide AT-12A, 9600 ft.

2- A schizaeacean spore grain of *Cicatricosisporites* sp., slide AT-30A, 8700 ft.

3- A thick-walled, ornamented spore grain of *Impardecispora uralensis*, (Bolkhovitina) Venkatachala et al., 1969, slide AT-3A, 10050 ft.

4- A sphaeroidal gymnospermous pollen grain of *Balmeiopsis limbatus* (Balme) Archangelsky, 1979, slide AT-1A, 10150 ft.

5, 6- Xerophytic gymnospermous pollen grains of *Ephedripites* spp., slide AT-28A, 8800 ft; slide AT-19B, 9250 ft.

7- A thermophilous gymnospermous pollen grain of *Classopollis classoides* Pflug, 1953, slide AT-6A, 9900 ft.

8, 9, 14- Ephedroid gymnospermous elaterate pollen grains of *Elateroplicites africaensis* Herngreen, 1973, slide BB-8A, 5220 ft (8), *Sofrepites legouxiae* Jardiné, 1967, slide AT-95A, 5100 ft (9), *Elaterosporites klaszii* (Jardiné & Magloire) Jardiné, 1967, slide BB-22A, 4880 ft (14).

10, 11, 16- Freshwater algae, *Ovoidites parvus*, (Cookson & Dettmann) Nakoman, 1966, slide AT-16A, 9400 ft (10), *Chomotriletes minor* (Kedves) Pocock, 1970, slide AT-18A, 9300 ft (11), Botryococcus sp., slide AT-99B, 4850 ft (16).

12, 13- Planispiral, BB-13A, 5160 ft (12) and Biserial, slide BB-12A, 5170 ft (13) microforaminiferal test linings.

15- An angiospermous pollen grain of *Afropollis jardinus* Doyle et al., 1982, slide AT-89A, 5750 ft,

Structured and unstructured terrestrial plant debris

17- A structured phytoclast of probably gymnospermous plant, composed of one gymnosperm tracheid showing bordered pits arranged in one serial offset, slide AT-19B, 9250 ft.

18- An opaque lath-shaped phytoclast (black wood) with sharp angular outline, slide AT-7B, 9850 ft.

19- An amorphous organic matter particle (AOM), slide BB-107A, 4450 ft.

20- A cuticular phytoclast showing regular rectangular cell outlines of probably gymnospermous origin, slide AT-18A, 9300 ft.

21- A structured phytoclast showing fibrous parallel structure, slide 19B, 9250 ft.

22- A membranous tissue, slide AT-20A, 9200 ft.

24- A resin particle, slide AT-18A, 9300 ft.

25- A structured thick cuticular sheet of probably gymnospermous origin, slide AT-3A, 10050 ft.

Marine palynomorphs

23- A shallow marine (brackish) cavate peridinioid cyst of *Subtilisphaera terrula* (Davey) Lentin & Williams, 1976, slide AT-28A, 8800 ft.

26- A shallow marine (brackish) ceratoid proximate cyst of *Cyclonephelium vannophorum* Davey, 1969, slide AT-12A, 9600 ft.

27- A shallow marine (brackish) ceratoid proximate cyst of *Pseudoceratium securigerum* (Davey & Verdier) Bint, 1986, slide AT-20B.

28- An open marine gonyaulacoid chorate cyst of *Florentinia mantellii* (Davey & Williams) Davey & Verdier, 1973, slide AT-22A, 9100 ft.

29- An open marine gonyaulacoid chorate cyst of *Oligosphaeridium complex* (White) Davey & Williams, 1966, slide AT-25A, 8950 ft.

Humic gels are produced by biodegradation of the root and bark tissues of land plants, where these tissues were originally released from the plant roots and bark by destructive oxidation. Humic gels are considered as insignificant contributors to AOM in ancient marine sediments (Tyson, 1995).

Structured organic matter as defined by Tyson (1995) is made of discrete and recognizable individuals or colonial entities (i.e. palynomorphs) and plant or animal fragments (i.e. phytoclasts, zooclasts) that demonstrate their biological affinities. Palynomorphs can usually be assigned botanical or zoological affinities, whereas phytoclast particles with coherent, angular to irregular outlines that may show some internal structures can be attributed at least to a type of larger plant (i.e. phytoclasts) or animal (i.e. zooclasts) debris.

Phytoclasts are produced by land plants, and are represented by both opaque particles of generally equidimensional or elongate (lath-like) shapes (e.g. oxidised or carbonised wood tissues), and by partly translucent (at least at particle edges) particles of generally thin, tubular (e.g. fungal hyphae), elongate (e.g. wood tracheids), or sheet-like (e.g. cuticles) shapes with definitive biostructures. Translucent particles of irregular (e.g. degraded phytoclasts), massive angular (e.g. gelified phytoclasts), square (e.g. wood tissues), elongate (e.g. seaweed/seagrass or wood tracheid bands), or sheet-like (e.g. non-cellular, probably cuticles) shapes, with or without definitive biostructures, are also members of the phytoclast group.

Wood tracheids are one of the most common members of the biostructured translucent phytoclasts. Their high relative and absolute abundances in ancient marine sediments are known to indicate strong terrestrial influx, with deposition in nearshore proximal settings (e.g. fluvio-deltaic systems) that were close to the parent land plants (Müller, 1959; Pocklington & Leonard, 1979). Hydrodynamic equivalence of woody phytoclasts controls their distribution in sediments, as

woodyphytoclasts are made of relatively large and dense particles, their high concentrations have commonly been found to correlate to coarse silts and very fine sands (Habib, 1983; Firth, 1993; Tyson, 1993).

Black (opaque) wood concentrations in ancient sediments have also been found to be of great palaeoenvironmental significance, and they have been found to reflect deposition polarity (onshore-offshore location), distance of sediment transport, and oxygenation level of host sediments. High percentages of black wood fragments have been documented from ancient high energy, proximal, coarse-grained sediments of fluvial and delta-top systems (Fisher, 1980; Nagy et al., 1984; Smyth et al., 1992; Williams, 1992). This was taken to indicate deposition of originally translucent woody particles in oxidising environments, where *in situ* post-depositional oxidation was prevailing due to strong fluctuating water levels (e.g. Tyson, 1993, 1995). Hydrodynamic equivalence of black wood has been found to be controlled by particle size rather than its shape (Tyson, 1995), where large, lath-shaped particles have been found to increase in proximal, relatively high energy silt and sand lithologies (e.g. Van der Zwan, 1990; Baird, 1992). A general offshore decrease in the particle size of black wood has been recorded, for example by Habib (1982), Barnard & Cooper (1981), Caratini et al. (1983), and Gorin & Monteil (1990). Tyson (1995) attributed this phenomenon of offshore particle size decrease to fragmentation of large black wood particles during long-distance transport, which is also associated with a general offshore decline in black wood concentrations.

Cuticles are mainly derived from leaves of higher plants, where they constitute the outermost part of the epidermal layer of these plants (e.g. Tyson, 1995). High percentages of cuticles have commonly been documented from low energy, onshore fluvio-deltaic and lacustrine palaeoenvironments (e.g. Batten, 1973; Parry et al., 1981; Nagy et al., 1984; Smyth et al., 1992).

Membranous tissues are another type of structured plant debris that are derived from the collenchyma and parenchyma of the non-epidermal, non-lignified tissues. These tissues are of delicate structure and made of readily degradable cellulosic material (e.g. Tyson, 1995), and when oxic conditions prevail they tend to degrade three times faster than more durable lignified woods (e.g. Stout et al., 1981). Their high concentrations have been found commonly in non-marine and proximal deltaic facies and become rare in an offshore direction (e.g. Tyson, 1995). Therefore, their common proportions are taken to indicate high rates of sedimentation, where strong terrestrial organic matter influx is high enough to dilute sediments and remove these fragile membranous tissues form oxic sediments water interface.

Palynomorphs are represented by terrestrial palynomorphs (spores, pollen grains - collectively known as sporomorphs- , and fungal spores), marine phytoplankton (dinoflagellate cysts, acritarchs, and prasinophyte and chlorococcalean algae), and zooplankton (inner linings of microforaminifera, chitinozoa, and scolecodonts).

Spores are reproductive structures produced asexually or sexually by cryptogams (plants and fungi which do not reproduce by seed: Jackson, 1928). The hydrodynamic equivalence of spores has been found to be controlled by spore sizes, where high proportions of ornamented, thick-walled, more dense spores have been found to concentrate in proximal high energy nearshore settings and decrease away from the source land in comparison to smooth, thin-walled, less dense spores (e.g. Reyre, 1973; Lund & Pedersen, 1985; Mutterlose & Harding, 1987; Tyson, 1989; Dybkjaer, 1991). Relatively higher abundances of spores compared to saccate pollen grains in ancient environments have been considered as a good tool to indicate proximity to fluvio-deltaic systems. This is because spores are known to

be produced in lower abundances and tend show lower transport efficiency in comparison with saccate pollen grains (e.g. Reyre, 1973; Habib, 1979; Mutterlose & Harding, 1987; Prauss, 1989; Tyson, 1989). Pteridophyte spores are known to thrive in warm humid low lands (e.g. riversides and costal areas: Pelzer et al., 1992; Abbink et al., 2004) and therefore high abundances of pteridophyte spores (e.g. *Deltoidospora*, *Concavissimisporites*, and *Impardecispora*) have been suggested as a proxy for humid conditions (e.g. Abbink et al., 2004; Bornemann et al., 2005).

Pollen is another reproductive porpagule produced by vascular, non-flowering gymnospermous plants during their life cycles (Traverse, 2007). This type of pollen can take many forms: the sphaeroidal grains (e.g. *Araucariacites*), which are considered as some of the most buoyant members of the sporomorph group. The relative abundances of the circumpolles *Classopollis* has been documented to increase in a basinward direction (e.g. Hughes & Moody-Stuart, 1967; Habib, 1979), and thus suggested as an indicator of relative proximity to fluvio-deltaic systems (Tyson, 1984; 1993; 1995). The gymnospermous pollen *Classopollis* is known to been produced by thermophilous and drought-resistant Cheirolepidiacean conifers and thus provides a valuable proxy indicator for palaeoclimatic conditions. The gymnospermous gnetalean pollen *Ephedripites* is another xerophytic genus. A great similarity between the pollen produced by the modern xerophytic gnetalean plants *Ephedra* and *Welwitschia* and the fossil *Ephedripites* pollen has been recognised (Trevisan, 1980). The xeromorphic nature of contemporary gnetalean plants has been also supported by Crane's (1988, 1996) findings of the related macrofossils *Drewira* and *Eoanthus*.

Angiosperm pollen grains are also reproductive plant structures that are sexually produced by vascular, enclosed seed-generating, flowering plants during their life cycles (Armstrong & Brasier, 2005). Lower abundances of the angiosperm

pollen *Afropollis* of possible Winteraceaen affinity have been recorded from warm and dry intracontinental basins (e.g. Doyle et al., 1982). However, higher abundances of *Afropollis* have been interpreted by Doyle et al. (1982) and Schrank (2001) to indicate humid coastal conditions, habitats in which the *Afropollis*-producing plants flourished and to which they were better adapted.

In ancient environments sporomorph absolute abundances have been found to decrease exponentially in an offshore trend (e.g. Paproth & Streel, 1970; Reyre, 1973; Habib, 1982, 1983; Habib & Drugg, 1983). Size of miospores has been found to have an effect on their distribution in marine sediments, where high percentages of miospores of > 50 µm have been found to correlate with fine sands, whereas those with sizes < 30 µm correlate with medium silts (e.g. Hughes & Moody-Stuart, 1967; Batten, 1974). Tyson (1995) suggested that there is some correlation between high abundances of miospores commonly found in fluvio-deltaic systems with the sand and silt lithologies typically found in such systems.

Dinoflagellate cysts are usually organic-walled, fossilised bodies that are made of relatively resistant 'dinosporin' that are produced by unicellular algae during the non-motile resting (sexual) stage of their life cycle, and are documented in the geologic record from the late Triassic to the present day (Evitt, 1985). Most of the data on the absolute abundances of dinoflagellates comes from studies of recent sediments, where high dinoflagellate cyst concentrations have been found to show offshore increases to the continental slope, where with increased water depth they begin to decline (e.g. Balch et al., 1983; De Vernal & Giroux, 1991). The work of Davey (1970) on Cenomanian sediments of England, northern France, and North America also documented the same shelfal trend of an offshore increase in concentration of dinoflagellate cysts offshore. The ratio of dinocysts:sporomorphs (also known as the marine influx index, or the marine:continental ratio) has been

used to indicate transgressive-regressive trends in ancient sediments (Habib, 1979; Mutterlose & Harding, 1987; Lister & Batten, 1988; Prauss, 1989). The diversity (in terms of numbers of species) of dinoflagellate cysts is also of environmental significance, where dinoflagellate assemblages of high diversity and low dominance have been found to increase in more offshore shelfal settings of normal marine salinity (e.g. Goodman, 1979; Mutterlose & Harding, 1987; Lister & Batten, 1988; Habib et al., 1992). Low diversity, high dominance assemblages of dinocysts have conversely been taken to indicate restricted, brackish water conditions, as the dinocyst species diversity is much less in water of below normal salinity (Batten, 1983; Leckie & Singh, 1991). High dinoflagellate cyst diversity has been found to correlate with high stands of global sea level (Bujak & Williams, 1979; Goodman, 1987). Certain morphotypes of dinoflagellate cysts have been shown to have palaeoenvironmental importance. High abundances of cavate peridinioid (e.g. *Subtilisphaera*) and proximate ceratoid (e.g. *Pseudoceratium*, *Aptea*, and *Muderongia*) taxa are known to characterise marginal marine (brackish to coastal) conditions (Davey, 1970; Piasecki, 1984; Harding, 1986b; Lister & Batten, 1988), while high abundances of chorate gonyaulacoid (e.g. *Oligosphaeridium* and *Florentinia*) cysts indicate open marine (middle shelf) environments (Dale, 1983; Lister & Batten, 1988).

Acritarchs are hollow, organic-walled, eukaryotic unicells of unknown biological affinities, which range from the mid-Precambrian to pre-Quaternary (Armstrong & Brasier, 2005). High relative abundances of acritarchs have been found to correlate with shallow marginal marine settings of mainly brackish water environments in the Mesozoic (Davey, 1970; Downie et al., 1971; Burger, 1980; Schrank, 1984a-a; Prauss, 1989).

Prasinophyte algae are a group of non-cellulosic, green, flagellate algae, which have a geological range from the Ordovician to Recent (Armstrong & Brasier, 2005). The presence of fossilised structures (phycomata) of prasinophyte algae has been found to be associated with shelfal and oceanic settings with organic-rich sediments deposited in dysoxic-anoxic conditions (Tyson, 1984, 1989).

Chlorococcalean algae are freshwater green algae that live in colonial structures, and are represented by the two most common genera *Botryococcus* (Devonian to Recent) and *Pediastrum* (early Cretaceous to Recent). The presence of *Botryococcus* and/or *Pediastrum* in the sedimentary record is associated with the formation of high quality oil source rocks (Cane, 1976; Hutton, 1988). Fresh to brackish water conditions can be inferred from the presence of *Botryococcus,* as it has been recorded from ancient lacustrine, fluvial, lagoonal, and deltaic/nearshore marine sediments (Piasecki, 1986; Riding et al., 1991; Williams, 1992; Batten, 1998). *Pediastrum* has also been found with high abundances in low salinity lakes and also transported by fluvial systems into nearshore shelfal situations (Singh et al., 1981; Hutton, 1988). *Ovoidites* and *Chomotriletes* are other freshwater algae, when present in sediments are taken to indicate stressed environments of below normal salinity (Lister & Batten, 1988; Batten, 1999).

Microforaminiferal test linings are the inner chitinous linings produced by single-celled, benthic foraminifera to enclose their cytoplasmic soft tissue (De Vernal et al., 1992; Tyson, 1995). The relative abundances of microforaminiferal test linings can be used to indicate depositional settings under normal marine conditions (Schrank, 1984a-a; Lister & Batten, 1988; Stancliffe, 1989).

6.2 Methodology

6.2.1 Quantitative palynological analyses

The palaeoenvironmental interpretations in the following section have been based on an analysis of the absolute abundance data of different particulate organic matter (POM) constituents from the Abu Tunis 1x and BB80-1 boreholes in preference to relative abundance data. Relative abundance data is, by definition, hampered by data closure problems: when one variable increases the other variables decrease, making naturally independent variables artificially dependent on each other, and providing negative correlations between variables in a community analysis.

The absolute abundances (grains/g) of palynomorphs and phytoclasts have been categorized in terms of very rare (1-10 $x10^2$), rare (11-30 $x10^2$), present (31-60 $x10^2$), common (61-100 $x10^2$), frequent (101-150 $x10^2$), abundant (151-200 $x10^2$), very abundant (200-250 $x10^2$), and extremely abundant (>250 $x10^2$). Different counted palynofacies constituents are shown in Appendix 2. A second, independent count of the absolute abundances of the dinoflagellate cysts from the Abu Tunis 1x borehole was made in addition to palynofacies analysis, in order to counter the dilution effect of the extremely abundant terrestrial POM (i.e. sporomorphs and plant debris) in those samples, and to allow determination of the species diversity of the dinoflagellate cyst assemblages. In order to determine how many specimens of dinoflagellate cysts needed to be counted to provide a representative indication of species diversity, counts were made firstly of 50 and then of 100 specimens from a single sample. The count of 50 individuals was found to be both representative and practical, firstly as such numbers of individuals could be obtained from dinoflagellate-poor as well as from dinoflagellate-rich samples, and secondly was enough to register all species present in these relatively low diversity samples.

Samples that yielded <10 individual dinocyst specimens after scanning two microscope slides per sample were deemed effectively barren and thus not included in further interpretations.

The counts of the three main cyst morphotypes (proximate, cavate, chorate) of the dinoflagellate cyst assemblages were also recorded, and the dinoflagellate cyst species diversity was measured using the Simpson's diversity index (1-λ') as follows:

$$1\text{-}\lambda' = 1 - \{\sum_i N_i (N_i - 1)/N (N - 1)\} \quad (4)$$

Where;

1-λ' = Simpson's diversity index

N_i = number of individuals of species *i* in a sample

N = total number of individuals of all species in a sample

Simpson's diversity index (Simpson, 1949) has been used here because it takes into consideration both species richness and evenness, but moreover it is independent of the total count of the number of individuals, and thus it can be compared between samples from which different numbers of individuals have been counted. This is not the case with other measures of diversity, such as Shannon's diversity index, Margalef's index, and Brillouin's index (Clarke & Warwick, 2001).

The dinoflagellate cyst assemblages in the borehole BB80-1 were uniformly of very low concentrations, save for one sample, and were thus not suitable for independent dinoflagellate cyst counts. Absolute abundances of dinocysts from this borehole have thus been used from the main palynofacies (POM) count instead.

6.2.2 Cluster analysis

Absolute abundances of selected POM constituents (as described above) were used in an agglomerative cluster analysis to group samples having palynofacies of similar composition and abundance. The Bray-Curtis similarity coefficient (Bray & Curtis, 1957) was chosen over other forms of correlation (e.g. Pearson's product momentum *r*, Spearman's rank r_s) to assess similarity between the samples, because unlike other correlation coefficients, it takes into consideration changes in the abundances of the sample components (Etter, 1999). This is an important criterion in palaeoenvironemental interpretations. The Bray-Curtis similarity coefficient also has an advantage over other similarity coefficients as it yields zero similarity when two samples have completely different POM constituents, something which most similarity coefficients cannot do (Clark & Warwick, 2001).

It should be borne in mind that the clustering of the studied samples provides here an approximation of the original similarity between the different samples, and this is may be related to several factors. One of which is the stratigraphical position of the samples. This slightly biases the cluster analysis, as samples from very far stratigraphical positions would be clustered in different sets based on the occurrence of species of short stratigraphic range. The taphonomic processes could have also played a role in changing the original biological composition of the samples through the decay of some of the organic matter (Bennington & Bambach, 1996). Finally, sedimentary samples are the consequence of the time-average of accumulations during thousands of years. So, changes in the environmental conditions during that time would be also expected to alter the organic matter composition of sediments (Kidwell & Bosence, 1991).

A mild square root (√) transformation of the original absolute abundance data was made before clustering with *PRIMER v6* software of Clarke & Gorley (2006) in order to down-weight very abundant POM constituents and allow the less common POM groups to contribute more meaningfully to the similarity analysis. The clusters of each resultant palynofacies type was identified at about 72-75 % similarity levels (Fig. 6.2) according to Tyson's (1995) definition of palynofacies which is only based on the proportional distribution of the POM with no consideration to the sequence's lithologies. At higher levels of similarity (between 78-83 %), palynofacies sub-types were also identified within two of the palynofacies types. These sub-palynofacies were found to largely be controlled by lithological type.

6.2.3 Palynological ternary plots

A. Ternary palynomorph plot and depositional environments

Federova (1977) and Duringer & Doubinger (1985) have used plots of spores, pollen, and microplankton in a ternary diagram to indicate general depositional environments and associated regressive-transgressive trends. In recent work (e.g. Ibrahim, 2002b; Quattrocchio et al., 2006) carried out on Cretaceous sediments, the interpreted depositional environments and trends in marine deposition have been demonstrated by using the ternary palynomorph plot. Consequently, this ternary is considered here as a useful tool in help recognising and indicating the possible depositional environments and changes in trends of marine sedimentation (Fig. 6.3).

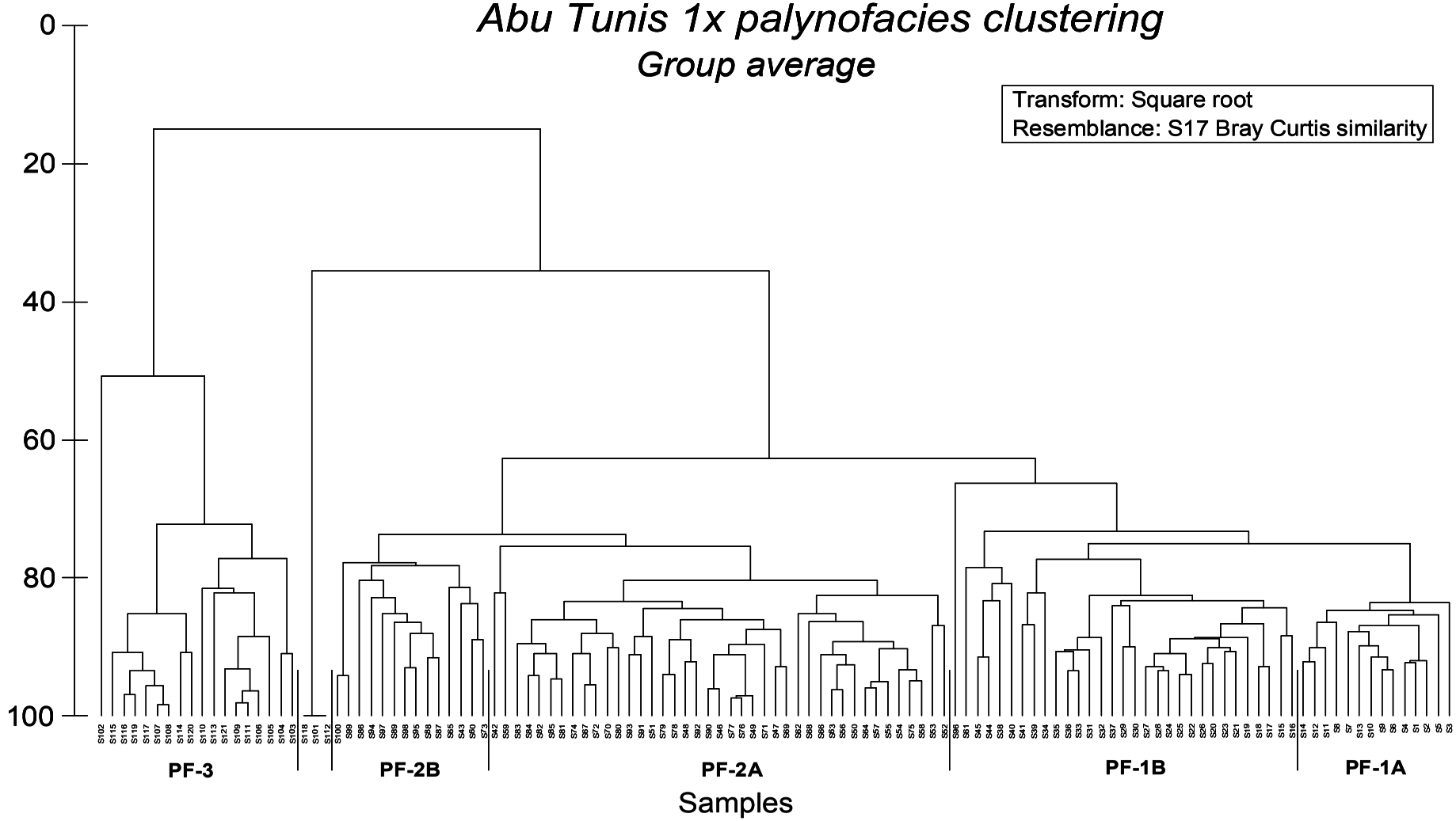

Figure 6.2 Dendrogram of the hierarchical cluster analysis (*PRIMER v6*) of the palynological samples of the Abu Tunis 1x and the resulted palynofacies types.

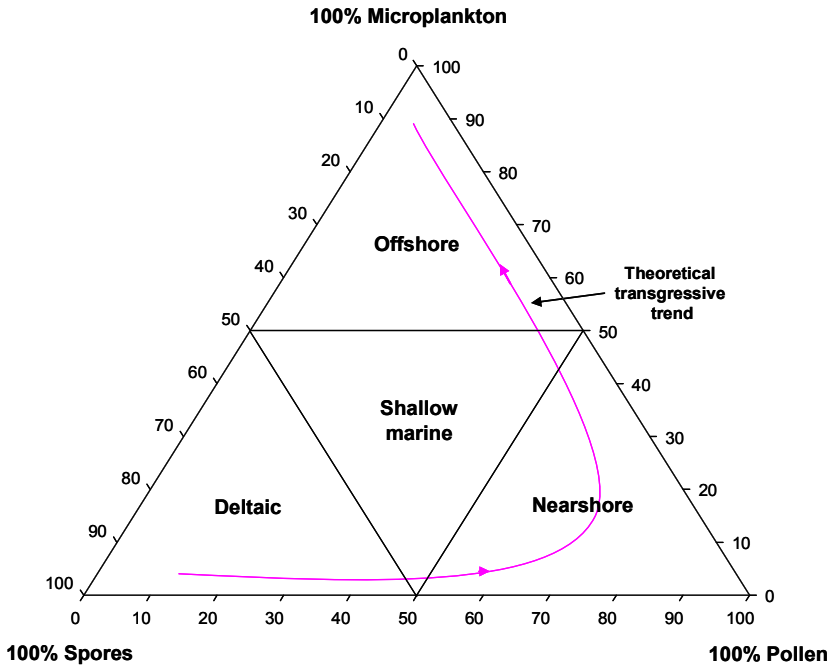

Figure 6.3 Ternary plot of spores, pollen and microplankton of Federava (1977) and Duringer & Doubinger (1985).

B. Ternary kerogen plots and oxygenation conditions

Tyson (1985, 1995) developed a ternary kerogen plot comprising the kerogen constituents AOM, phytoclasts and palynomorphs. Tyson (1995, p. 442) based his ternary plot on Late Jurassic sediments and other Mesozoic-Cenozoic rocks, and found that palynological kerogen of similar composition and palaeoenvironmental settings (from different geologic times) tends to occupy the same area in the ternary plot (Fig. 6.4). The resultant palynofacies plots indicating "relative proximity to terrestrial organic matter sources, kerogen transport paths, and the redox status of the depositional environments that control AOM preservation" (Tab. 6.1). This plot can also be used to determine oxic-anoxic conditions (Al-Ameri et al., 1999; Mustafa & Tyson, 2002; Al-Ameri et al., 2009), confirmed by comparing results with other physical parameters which assess the degree of preservation of AOM and hence, determine the oxygenation conditions of the depositional environment (e.g. Mustafa & Tyson, 2002; Al-Ameri et al., 2009).

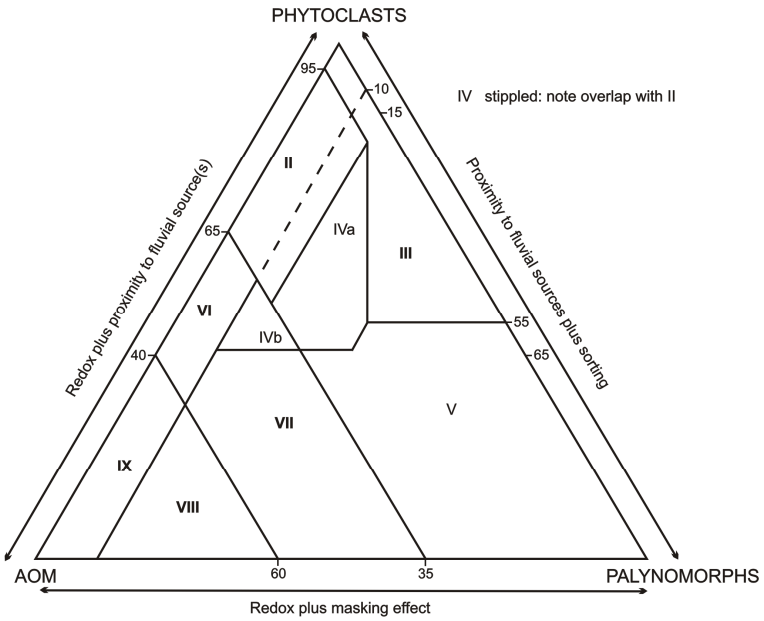

Figure 6.4 Ternary kerogen diagram of Tyson, 1995.

Palynofacies field and environment		Comments	Spores: Bisaccate	Microplankton	Kerogen type
I	Highly proximal dysoxic-anoxic basin	High phytoclast supply dilutes all other components	Usually high	Very low	III (gas prone)
II	Marginal dysoxic-anoxic basin	AOM diluted by high phytoclast input, but AOM preservation moderates to good. Amount of marine TOC dependent on basin redox state. Generally low AOM preservation.	High	Very low	III (gas prone)
III	Heterolithic oxic shelf ("proximal shelf")	Absolute phytoclast abundance dependent on actual proximity to fluvio-deltaic sources. Oxidation and reworking common.	High	Common to abundant dinocysts dominant	III or IV (gas prone)
IV	Shelf to basin transition	Passage from shelf to basin in time (i.e. increased subsidence/water depth) or space (e.g. basin slope). Absolute phytoclast abundance depends on proximity to source and degree of redeposition. Amount of marine TOC depends on basin redox state. Iva dysoxic-suboxic, IVb suboxic-anoxic.	Moderate to high	Very low-low	III or II (mainly gas prone)
V	Mud-dominated oxic (distal) shelf	Low to moderate AOM (usually degraded). Palynomorphs abundant. Light coloured biotrubated, calcareous mudstone are typical.	Usually low	Common to abundant dinocysts dominant	III > IV (gas prone)
VI	Proximal suboxic-anoxic shelf.	High AOM preservation due to reducing basin conditions. Absolute phytoclast content may be moderate to high due to turbiditic input and/or general proximity to source.	Variable low to moderate	Low to common dinocysts dominant	II (oil prone)
VII	Distal dysoxic-anoxic "shelf".	Moderate to good AOM preservation, low to moderate palynomorphs. Dark-coloured slightly biotrubated mudstones are typical.	Low	Moderate to common dinocysts dominant	II (oil prone)
VIII	Distal dysoxic-anoxic shelf.	AOM-dominante assemblage, excellent AOM preservation. Low to moderate palynomorphs (partly due to masking). Typical of organic-rich shales deposited under stratified shelf sea conditions	Low	Low to moderate dinocysts dominant, % prasinophytes increasing	II >> I (oil prone)
IX	Distal suboxic-anoxic basin.	AOM-dominant assemblages. Low abundances of palynomorphs partly due to masking. Frequently alginate-rich. Deep basin or stratified shelf sea deposits, especially sediments starved basins.	Low	Generally low, prasinophyte often dominant	II ≥ I (highly oil prone)

Table 6.1 Key to marine palynofacies fields defined in the ternary kerogen diagram of Tyson, 1995.

6.2.4 Wireline geophysical data

A. Resistivity data profile

The resistivity profile is a tool that can be used to help in identifying lithologies and in recording changes in sedimentary facies. Resistivity of sediments is a function of sediment porosity, when sediments porosity increases the sediments resistivity decrease logarithmically, and thus resistivity data registers changes in quartz proportions in a sand-shale mixture, as sandy sediments are more porous than shaly-sands and siltstones (Rider, 1986). Resistivity values change with changes in the porosity of lithologies: for example, porous sandstone containing salty formation water is of low resistivity, as salty water functions as an electrolyte which is a good conducting medium for electricity. Formations with porous lithologies and which contain hydrocarbons show high resistivity values. Despite the fact that shales are of very low porosity, they tend to show moderate resistivity. This is because some shales can conduct electricity *via* pore water, and also by shale-forming clay minerals, where these clay minerals generate ions on their surfaces, which are surrounded by formation water containing free ions.

B. Self-potential (SP) log

The self-potential is another tool that measures electric properties of sediments. Self-potential measures the differences of natural potential between an electrode in the borehole and a reference electrode at the surface, where no artificial current is applied (Rider, 1986). Self-potential can be used in several geological investigations, such as calculating formation-water resistivity, but is also used to indicate facies permeability, shale volumes, and changes in rock types (Rider, 1986). The self-potential does not deal with absolute value, as its profile moves between a predefined zero line. This zero line (also called shale base line) is defined

using a thick shale interval at which self-potential does not move. Maximum self-potential reading correlates with a permeable water-bearing formation with no shale, and thus detects changes in the sedimentary facies as it moves with changes in sand:shale volumes (Rider, 1986). Despite the fact that, there are some limitations that could hamper SP log interpretations (e.g. the measured bed is not thick enough to register or the presence of hydrocarbons), the SP log is regarded as a useful aid for determining rock types (Rider, 1986).

C. Gamma ray data

Gamma ray data in contrast registers the shale (clay) content of formations, where it measures the radioactivity of elements such as uranium, thorium, and potassium that are usually contained within minerals and organic matter, where porous clean sandstone and siltstone lithologies lack these radioactive elements. Therefore, higher gamma ray values mean higher shale volumes (Rider, 1986). Gamma ray logs are also good tools for detecting changes in sediment grain size and thus changes in lithological facies. Rider (1986) explained this as due to the fact that coarse-grained sands tend to have very low shale volumes, medium-grained sands tend to have some shale volume, whereas fine-grained sands tend to be more shale-rich.

As shown above, gamma ray data is considered a valuable tool in identifying lithological and thus sedimentary facies changes, and this technique will be used here for the BB80-1 borehole. Resistivity data is a good tool for identifying hydrocarbon shows in sediments, and in identifying borehole lithologies when hydrocarbons are absent. Resistivity and spontaneous potential were the only geophysical data available for studying the Abu Tunis 1x borehole, and as the Abu Tunis 1x is a dry borehole, it can be assumed that the resistivity data can be safely used to interpret the lithology of the borehole successions.

A framework for the following palaeoenvironmental interpretations has been made by integrating quantitative palynological data with the sedimentological characters identified herein from the geophysical data, and the original lithological descriptions provided by the operating company (based on geophysical logs and cuttings).

6.3 The Abu Tunis 1x borehole palaeoenvironments

6.3.1 Palynofacies PF-1A

Assemblage PF-1A (samples 1-14, spanning 10150-9500 ft) show strong terrestrial influence (Fig. 6.5), which is reflected here in frequent phytoclast (~ 15,000 particles/g) and present sporomorph (~ 5,000 grains/g) concentration, while marine palynomorphs are represented by rare dinoflagellate cyst (~ 1,250 cysts/g) and MTLs that are found only in Sample 1 in very low concentrations (~ 600 grains/g; Fig. 6.6).

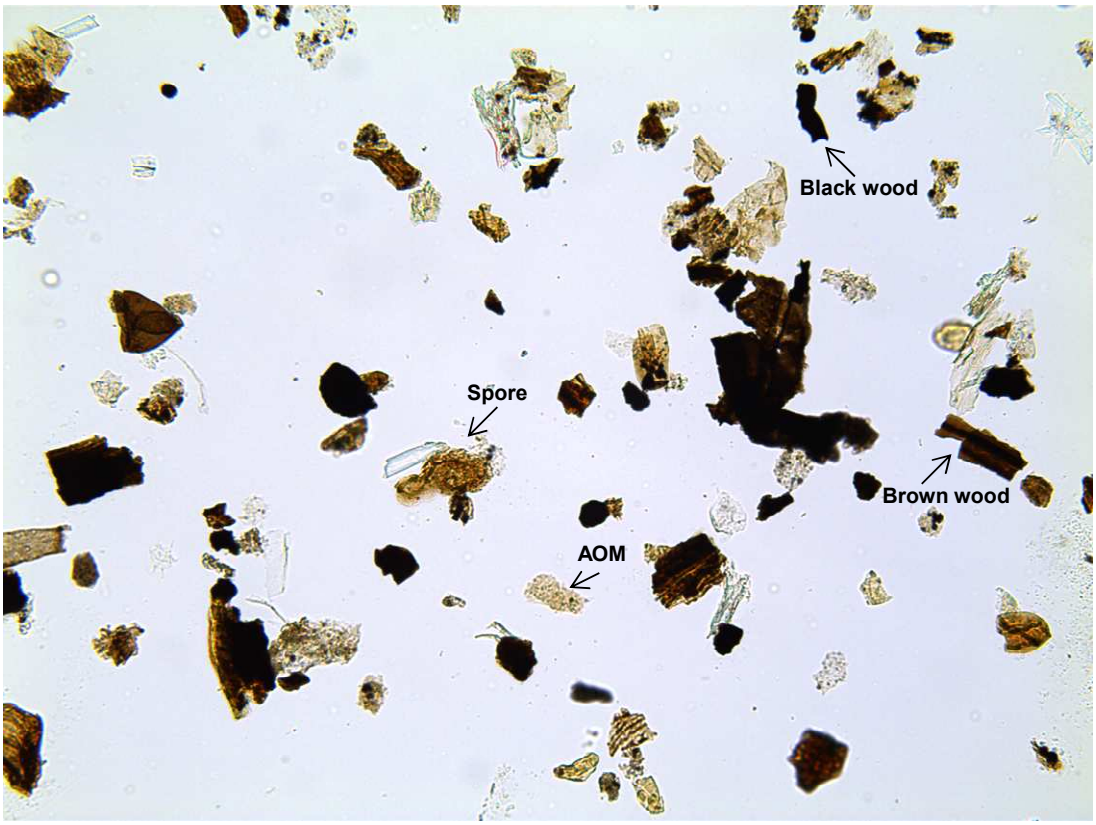

Figure 6.5 PF-1A dominated by terrestrially derived organic matter (sporomorphs and phytoclasts), sample 11b (9650 ft) at x250 magnification, the Abu Tunis 1x borehole, northern Western Desert, Egypt.

Figure 6.6 Absolute abundances (grains/g) of some selected palynomorphs and particulate organic matter of the Abu Tunis 1X borehole, northern Western Desert, Egypt.

Acritarchs are another marine phytoplankton that are found in Sample 2 in a very rare (25 grains/g) concentration.

The phytoclasts are dominated by extremely abundant tracheids (~ 39,200 particles/g) and abundant black wood (~ 18,000 particles/g) proportions. Cuticle fragments score here (~ 2,300 particles/g), with membranous tissues (~ 500 particles/g) of subordinate concentrations. The miospore assemblages are dominated by frequent pteridophyte spores (~ 11,300 grains/g), whilst low concentrations (~ 1,150 grains/g) of the xerophytic gymnosperm pollen *Classopollis* represent the second major component of the sporomorphs. Gymnosperm pollen are also represented here by very low concentrations (~ 200 grains/g) of araucariacean pollen (*Araucariacites* and *Balmeiopsis*) and *Exesipollenites*. Other terrestrial palynomorph components that are recorded in PF-1A but with very minor occurrences (avg < 50 grains/g) are the freshwater algae *Ovoidites* and *Chomotriletes*. Dinoflagellate cysts are of rare (~ 1,250 cysts/g) abundances but with high diversity (~ 0.78) and are represented by nearly equal proportions of cavate (~ 550 cysts/g) and proximate (~ 600 cysts/g) forms, and with very low (~ 80 cysts/g) chorate cyst concentrations (Fig. 6.8). Cavate cysts are mainly represented by *Subtilisphaera* and the low salinity genus *Muderongia*, while proximate cysts are mainly composed of *Cribroperidinium* and *Circulodinium*, with *Oligosphaeridium* genus mainly representing the chorate cysts community.

Lithology and changes in sedimentary facies of PF-1A

The changes in the self-potential profile are regarded here as a useful tool, which indicates changes in sand:shale volumes in samples of PF-1A. The resistivity data profile recorded against samples of the lower part of the Abu Tunis 1x borehole

and is equated here to PF-1A are masked by other controlling factors as discussed below and thus cannot be used here to interpret lithologies of PF-1A.

As it has been mentioned before, resistivity data can be useful in interpreting clastic lithologies given the fact that there are no hydrocarbon accumulations within the investigated sediments. The clastic sediments that are porous contain fresh formation waters, or made of tight sands could also result in bias in the lithology interpretations. Therefore, such an interpretation for PF-1A sedimentary sequence will be based here on self-potential data and the original description in the borehole log provided by the drilling company, in addition to the visual interpretation made on ditch cutting samples.

Self-potential readings indicate changes in the sedimentary facies of PF-1A, which are reflected in the development of several small scale sedimentary cycles that exhibiting coarsening upward sequences (Fig. 6.7). By integrating the available data (i.e. self-potential, original log description, and cuttings interpretations), the sedimentary sequence of PF-1A can be described as made of light grey to green shales with some black carbonaceous material and pyrite. These shale beds are intercalated with thin streaks of poorly sorted sandstones and a very few dolomite layers.

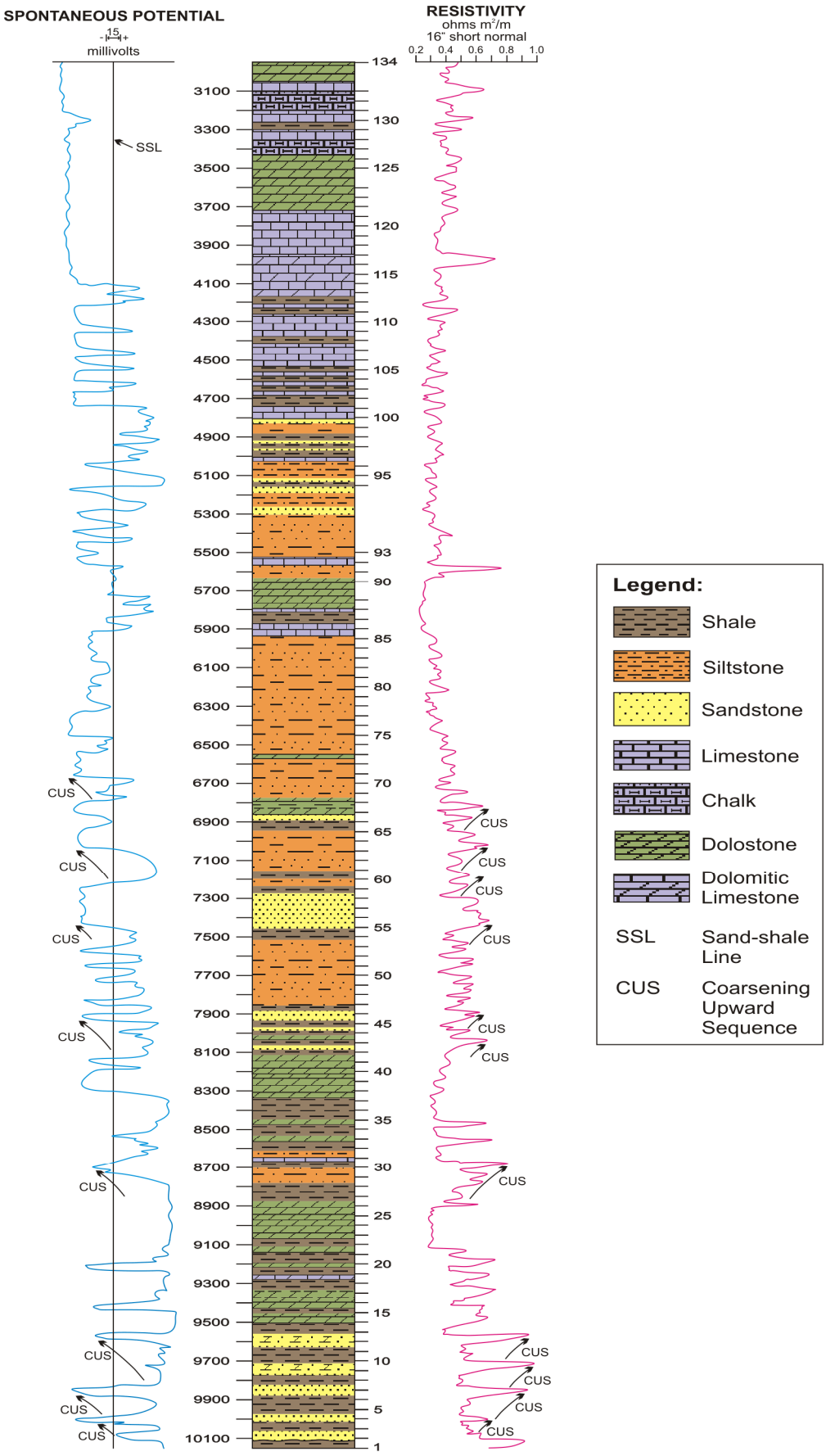

Figure 6.7 Lithological column, spontaneous potential, resistivity data (after WEPCO, 1968) and the interpreted sedimentary cycles of the Abu Tunis 1x borehole, northern Western Desert, Egypt.

Suggested depositional environment of PF-1A: deltaic (delta-top to delta-front)

The dinoflagellate cysts found within the sediments of PF-1A show low abundances and dominance but with high diversity. This could in part suggest deposition of sedimentary facies of PF-1A in waters of normal marine conditions, as high diversities of dinoflagellate cysts species were taken to indicate offshore marine settings of normal marine salinity (e.g. Goodman, 1979, Mutterlose & Harding, 1987; Lister & Batten, 1988; Habib et al., 1992). However, the dominance of cavate peridinioid and proximate ceratoid cysts, which are collectively characteristic of restricted (brackish-costal) marine conditions (e.g. Davey, 1970; Piasecki, 1984; Harding, 1986; Lister & Batten, 1988) over the chorate gonyaulacoid cysts characteristic of middle shelf open marine conditions (e.g. Lister & Batten, 1988), indicates stressed marine environments of below normal salinity. The presence of the genus *Muderongia* in sediments of PF-1A, which is well known to tolerate low salinity conditions (e.g. Piasecki, 1984; Harding, 1986; Lister & Batten, 1988) also supports these stressed marine conditions. These restricted conditions would in turn lead to the suggestion that the sedimentary facies of PF-1A was deposited in near shore, possibly transitional environments that were close enough to fluvio-deltaic systems, where mixing of continental fresh water with saline water of normal marine settings is a common process. The presence of acritarchs in Sample 2 in very rare (25 grains/g) concentrations, which are commonly taken to indicate brackish water conditions (Davey, 1970; Wall et al., 1977; Schrank, 1984a-a; Tyson, 1995) also supports these stressed marine conditions.

The distribution of terrestrial palynomorphs could also add some inference on the possible palaeoenvironmental settings of PF-1A. The dominance of pteridophyte spores over sphaeroidal gymnosperm pollen grains (*Araucariacites*, *Balmeiopsis*, and *Exesipollenites*) in the sporomorph assemblage of PF-1A

suggests that deposition of PF-1A sediments took place in settings that were close to fluvio-deltaic sources. This deduction is based here on the reproduction rates of the spores producing-plants, where these parent plants have been found to be less productive than the gymnosperm pollen-producing plants, in addition to the fact that, pteridophyte spores are known to be of relatively limited transport efficiency (e.g. Hughes & Moody-Stuart, 1967; Tschudy, 1969; Habib, 1982; Mutterlose & Harding, 1987, Prauss, 1989; Tyson, 1989).

The freshwater algae *Ovoidites* and *Chomotriletes* that present here in very low concentrations (avg < 50 grains/g), and have been taken to indicate stressed environments of below normal salinity (Lister & Batten, 1988; Batten, 1999) also supports proximal settings close to fluvio-deltaic systems.

These proximal nearshore settings would be consistent with such interpretations based on analysis of hydrodynamic equivalence of the highly dominant terrestrial plant debris that are concentrated here in the PF-1A sediments. High abundances of wood tracheids in sediments are one of the most important palynofacies parameters that are taken to indicate strong terrestrial influx into nearshore fluvio-deltaic systems, where these system are naturally close to or actually represent a source of land plants (e.g. Muller, 1959; Pocklington & Leonard, 1979). This interpretation was based on the hydrodynamic equivalences of these woody phytoclasts, where their distribution in sediments was found to be controlled by their particle size. As wood tracheids are generally made of relatively large and dense fragments, they tend to concentrate in their size-equivalent coarse silts and very fine sands that are commonly found in proximal environments (e.g. Habib, 1983; Firth, 1993; Tyson, 1993), and thus are taken to correlate with fluvio-deltaic facies, which typically contain high volumes of sand and silt lithologies.

Figure 6.8 The dinoflagellate cyst absolute abundances (grains/g), species diversity, and different cyst morphotypes, the Abu Tunis 1x borehole, northern Western Desert, Egypt.

As sediments of PF-1A are indeed made exclusively of fine sands (based on self-potential profile) and shale lithologies and are rich in wood tracheids, therefore, PF-1A is suggested to be generally deposited in fluvio-deltaic environments.

The high concentrations of black wood recorded herein are another important palynofacies indicator, which provide a better identification of the possible depositional environment that originated PF-1A. High percentages of black wood fragments have been recorded from coarse-grained proximal facies of fluvial and delta-top systems, where these facies have been interpreted to be deposited in high energy settings (e.g. Fisher, 1980; Nagy et al., 1984; Smyth et al., 1992; Williams, 1992). This interpretation was based on studying the hydrodynamic equivalence of black woods, which have been also found to be controlled by their particle sizes (Tyson, 1995), where large, lath-shaped particles have been found to increase in proximal, relatively high energy silt and sand lithologies (Van der Zwan, 1990; Baird, 1992). This phenomenon is typically found here, where black wood fragments are found to concentrate in the coarse sand lithologies of PF-1A, which clearly correlate to the strong peaks of self-potential profile recorded herein (Fig. 6.7). Therefore, PF-1A is suggested to be originated in fluvial or delta-top environments. Given the fact that sediments of PF-1A contain marine palynomorphs leads to exclusion of the (continental) fluvial environment and attests that PF-1A was deposited in at least the sub-aerial delta-top sub-environment. However, a delta-top setting is known to suffer from strong fluctuations in the water table (e.g. Boggs, 1987) and thus cannot account alone for occurrence and preservation of the considerable numbers of the dominant peridinioid cysts recorded here in PF-1A, where these peridinioid cysts are well known to be intolerant to destructive oxidation processes (e.g. Schrank, 1984a-b). This would imply that PF-1A must had a bimodal depositional history during which coarse deposits (sands) of the partly submerged delta-top and fine deposits

(fine sands, silts, and shale) of the continuously submerged delta-front settings, must have accumulated and made up the sedimentary facies of PF-1A. Another possible line of evidence for the alternating sub-aqueous delta-top and delta-front sub-environments origin of PF-1A, is shown here by the very low concentrations of the fragile, oxic-sensitive membranous tissues. The generally low concentrations of membranous tissues imply that PF-1A was mainly located in the sub-aqueous delta-top, where large amounts of these tissues could not survive strong oxidation conditions. Thus the coarse sand intervals of PF-1A are found here to be very poor in membranous tissue concentrations, with only low concentrations of tissues having been temporary removed from the oxic-dominated sub-aqueous delta-top by original deposition or possibly by re-deposition in the almost submerged fine facies of the delta-front sub-environment.

The presence of some black carbonaceous material and pyrite in the shale horizons of PF-1A implies preservation of organic matter in at least periodically low oxygen concentrations in pore-water, where reactive iron was converted into pyrite (Tyson, 1995). These occasional reducing conditions are also supported by plotting the PF-1A constituents in the kerogen diagram, where the plot suggests suboxic-anoxic conditions for PF-1A facies (Fig. 6.9).

From the discussions based on the palynological and sedimentological characteristics mentioned above, it is suggested that deposition of the samples yielding assemblages clustered as PF-1A took place in a deltaic environment (Fig. 6.12), specifically in sub-aqueous delta-front to delta-top sub-environments, with the delta-front sub-environment experienced some periodic anoxic pore-water conditions.

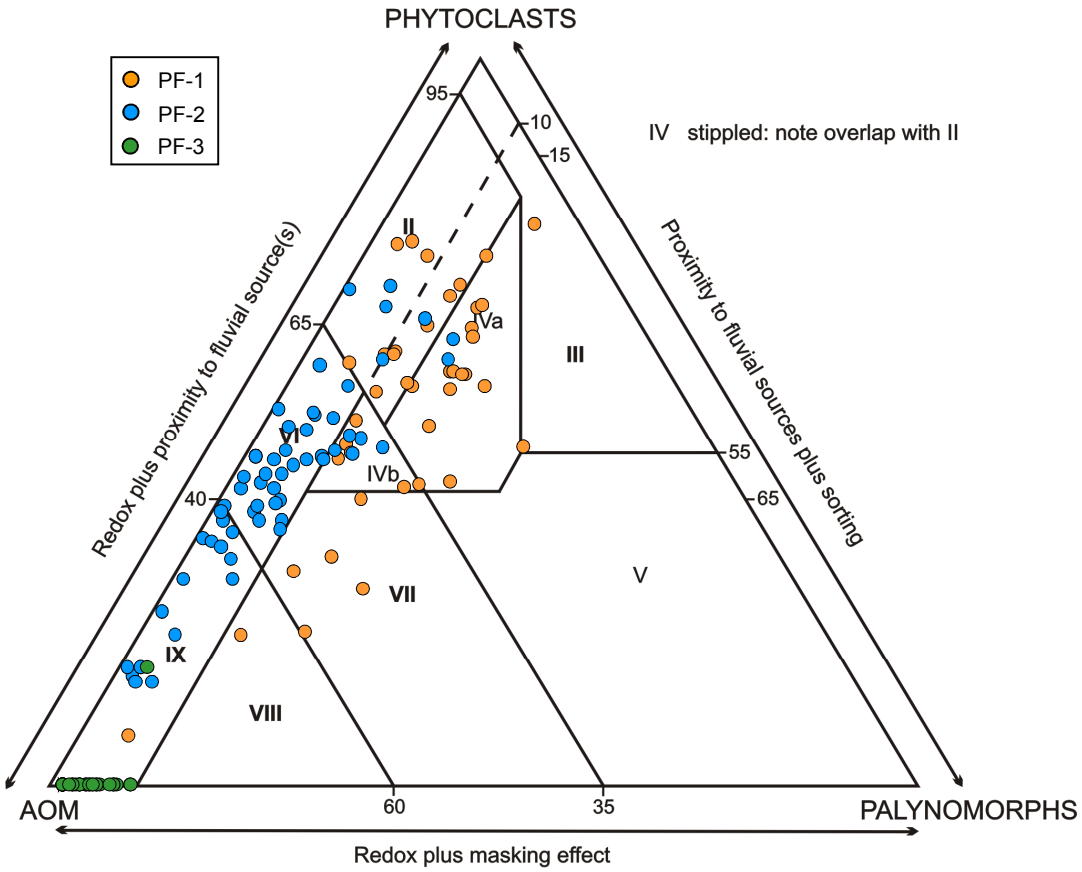

Figure 6.9 The Abu Tunis 1x palynofacies plot in the ternary kerogen plot of Tyson, 1995.

A general decrease in the absolute abundances of pteridophyte spores, brown and black wood in samples of PF-1A (Fig. 6.6) suggests a relative rise in sea level (e.g. Tyson, 1993; Batten, 1999). This could be specially supported by the distribution trend of the sporomorphs concentrations in PF-1A, where in ancient depositional environments sporomorphs absolute abundances have been found to decrease exponentially in an offshore trend (e.g. Paproth & Streel, 1970; Reyre, 1973; Habib, 1982, 1983; Habib & Drugg, 1987).

6.3.2 Palynofacies PF-1B

Those samples clustered in PF-1B (samples 15-42; 9450-8100 ft) demonstrate a strong decrease in concentrations of terrestrially derived organic matter (Fig. 6.10) with both sporomorphs and phytoclasts are of average (~ 6,550 grains/g) and (~ 790 particles/g) respectively, but an increase in dinoflagellate cyst concentration (~ 2,420 cysts/g), and with MTLs are still of very low concentration (194 grains/g).

The structured plant debris is still dominated by tracheids (~ 17,000 particles/g), and black wood (~ 4,800 particles/g) are still the second common component, while reductions in the concentration of cuticles (~ 2,500 particles/g) and increases in membranous tissues (~ 1,800 particles/g) appear for the first time in this palynofacies.

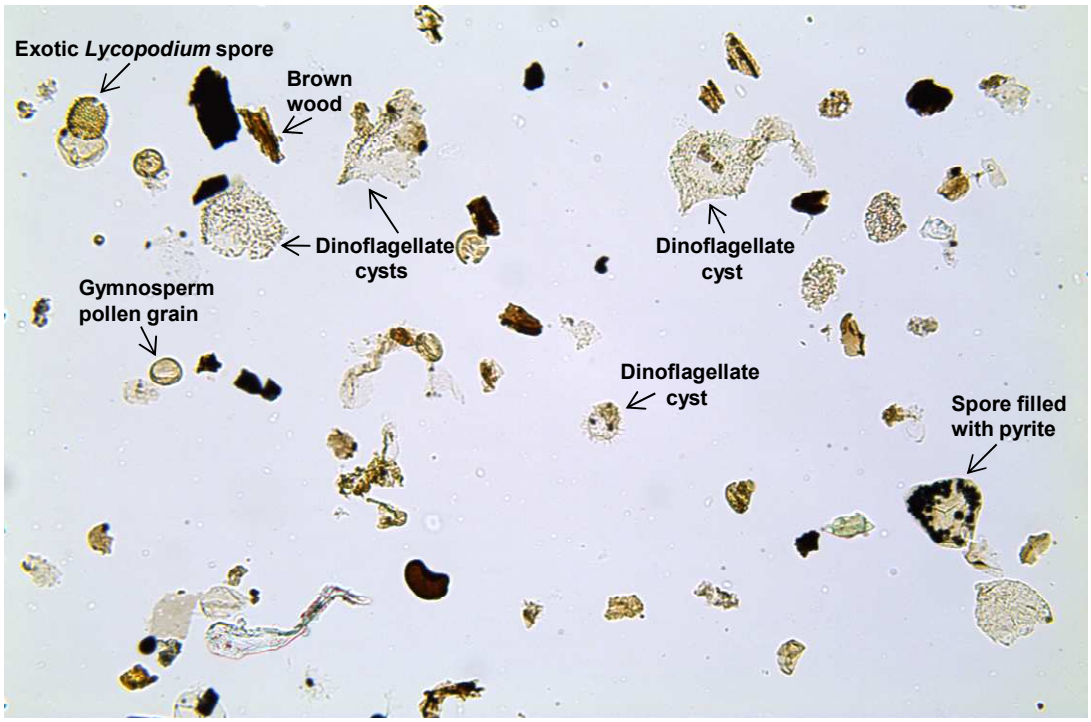

Figure 6.10 PF-1B with a reduced abundance of terrestrially derived organic matter and increased dinoflagellate cyst concentrations, sample 32a (8600 ft) at x250 magnification, the Abu Tunis 1x borehole, northern Western Desert, Egypt.

Sporomorphs are found here in low concentration (~ 790 grains/g), with miospores represented by rare pteridophyte grains (~ 2,355 grains/g; including rare schizaeacean taxa), rare *Classopollis* (~ 1,300 grains/g), and very rare saccate (mainly *Araucariacites* and *Balmeiopsis*) and monoporoid (*Exesipollenites*) gymnosperm pollen grains (~ 400 grains/g). The dinoflagellate cysts are of slightly higher abundances than those of the PF-IA, but are still rare (~ 2,420 cysts/g) and of high diversity (~ 0.77). The dinoflagellate cysts assemblage is dominated by proximate cysts (~ 1,200 cysts/g), with subordinate cavate (~ 700 cysts/g) and chorate (~ 300 cysts/g) concentrations. The proximate cysts are represented by *Pseudoceratium* and *Circulodinium*, while the cavate cysts are mainly represented by *Subtilisphaera*, with the few specimens of *Oligosphaeridium* and *Florentinia* representing the chorate cysts.

Lithology and changes in sedimentary facies of PF-1B

Geophysical data once again are not useful here for interpreting the lithology of PF-1B, as sedimentary sequence of this palynofacies is almost evenly made of carbonate lithology. This is because electric geophysical logs (i.e. self-potential and resistivity) deal in the first place with the electric properties of clastic sediments. Therefore, by depending upon the original description provided in the borehole log and the visual interpretation of the ditch cutting samples, the rock section equated to the PF-1B can be described as follows:

The succession is represented by an alternation of clastic units (similar to that of PF-1A) and light yellow to brown dolostone. The lower clastic unit is overlain by 200 feet (61 m) of dolostone, which in turn is overlain by a second upper clastic unit which contains shale beds with traces of carbonaceous material, but which appears to demonstrate no sedimentary cyclicity. These shale beds are intercalated with thin

dolostone beds, and are in their turn overlain by a second sequence (also 200 feet/61m thick) of pale brown dolostone. The upper dolomite unit is identified as the Alamein (Dolomite) Formation, which has a wide regional extent over the northern part of Egypt (Said, 1990; Kerdany & Cherif, 1990).

The lithology of the Alamein dolomite raised much controversy about its origin, where for example a petrographic study made by Metwalli & Abd El-Hady (1975) proposed that the dolomite of the Alamein Formation is of primary origin, which developed by chemical precipitation from hypersaline shallow marine environment under low energy conditions. In contrast, other studies such as that of Abou-Khadrah and Khaled (1978) suggested that the Alamein Formation consists of secondary dolomites that originated from accumulation of lime mud and fine-grained calcium carbonate in a low energy, relatively deep neritic environment. Given the fact that dolomite lithology raised the same controversy about its origin amongst the petrographer community worldwide, which shows that origin of dolomite lithology is still poorly understood (e.g. Boggs, 1987). Therefore, such an interpretation of its palaeoenvironmental indication in the current palynofacies analysis will be unjustified. However, the palynological and geological "palynogeological" characters of its disseminated organic matter could provide useful information about its possible depositional environment.

Suggested depositional environment: inner shallow marine

The dinoflagellate cysts assemblage of this palynofacies shows substantial increases in their abundance in comparison to that of PF-1A (Fig. 6.6), but with a similar species diversity. This increase in the dinoflagellate cysts abundance would indicates the development of normal and deeper marine conditions than that recorded to prevail in the underlying PF-1A. Such an interpretation is deduced here

from the trend of the dinoflagellate cyst abundance with depth, where high concentrations of dinoflagellate cysts have been found to exhibit offshore increases with increased water depth (e.g. Balch et al., 1983; De Vernal & Giroux, 1991). Added to that, the species diversity of dinoflagellate cysts encountered in PF-1B is high, like that of PF-1A, but shows here less variability than that recognised in PF-1A (Fig. 6.8). This means that the marine conditions under which the sediments of PF-1B were deposited were probably more stable, which in turn implies a proliferation of normal marine conditions in comparison to the stressed conditions recorded in the underlying PF-1A. Several authors (Wall et al., 1977; Tyler et al., 1982) noticed that dinoflagellate cysts in modern (Quaternary) sediments show increases in diversity in offshore environments, while they decrease and show more variability in their diversity in onshore environments, with the greatest variability in diversity attained in unstable proximal settings such as estuarine. Another line of evidence that could also support these normal marine conditions is the high species diversity of dinoflagellate cysts and low dominance that is also accompanied with increases in the open marine dinoflagellate species (e.g. *Oligosphaeridium* and *Florentinia*) recorded herein. The assemblages of dinoflagellate cysts that show high diversity and low dominance have been found to increase in basinward shelfal settings of normal marine salinity (e.g. Goodman, 1979, Mutterlose & Harding, 1987; Lister & Batten, 1988; Habib et al., 1992). The increases in specimens of *Oligosphaeridium* and *Florentinia* in PF-1B that are well know to be representative for the open marine (middle shelf) conditions (Wall et al., 1977; May, 1980; Dale, 1983; Lister & Batten, 1988; Smelror & Leereveld, 1989) may represent periodically slightly more offshore/deeper water conditions or the influence of onshore currents re-depositing more offshore taxa. Furthermore, the increase in the dinoflagellate cyst abundances along with sharp declines in the overall concentrations of the terrestrially derived organic matter also suggests a relative rise in sea level (Tyson,

1993, 1995; Batten, 1999), which would also be consistent with these deeper marine conditions, and may correspond to the late Barremian-Aptian transgressive cycle (Fig. 6.11).

The distribution of the different phytoclast components of PF-1B can only add a general inference about the depositional setting under discussion. The rare concentrations of cuticles and membranous tissues along with the strong decrease in brown and black wood concentrations imply deposition of the PF-1B sediments in a more offshore setting than that of PF-1A, as high proportions of the brown and black wood are known to concentrate in proximal onshore settings that are close to fluvio-deltaic environments.

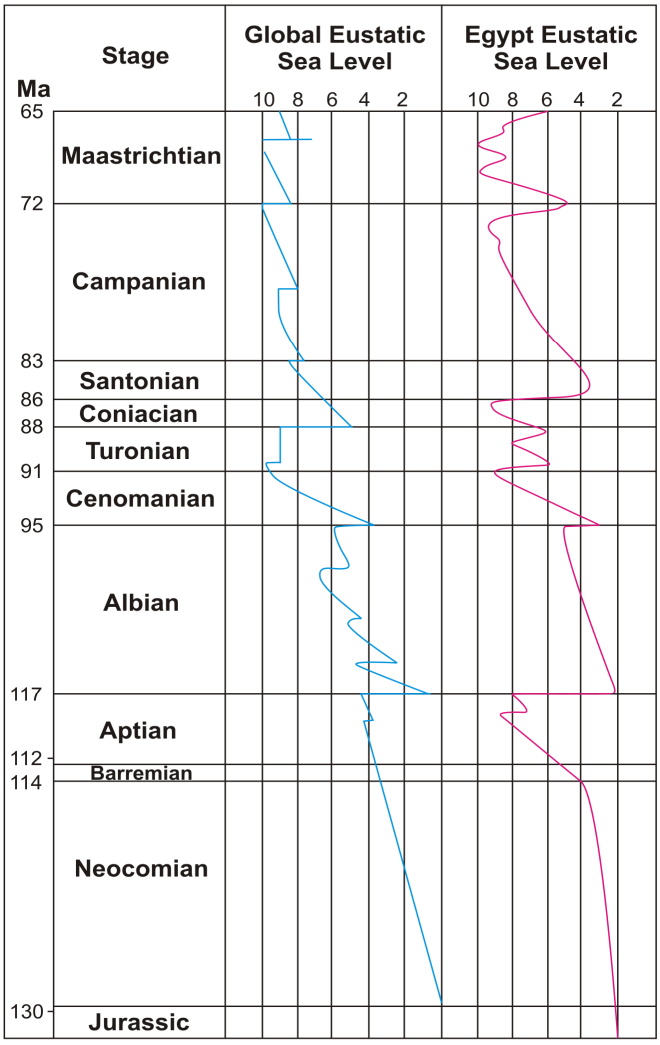

Figure 6.11 Global and Egyptian Cretaceous eustatic sea level cycles (after Vail, et al., 1977).

The latter interpretation was based on the hydrodynamic equivalence of these brown and black wood fragments as it has been inferred in the previous discussion of underlying PF-1A, where their proportions have been found to correlate with proximal, coarse-grained, high energy environments. Rare concentrations of black wood do not contradict this more offshore condition, as black wood is known to commonly blown by winds from fluvial and delta-top sediments and is also transported from the delta-front and re-deposited into more offshore sediments by waves and tide action (Tyson, 1993, 1995).

The strong decline in the sporomorphs concentrations recorded here in PF-1B would also lead to a such deduction that would tie in with the general suggestion of a more offshore marine setting, as sporomorphs absolute abundances recorded from sediments of ancient environments have been found to decrease exponentially in an offshore trend (e.g. Paproth & Streel, 1970; Reyre, 1973; Habib, 1982, 1983; Habib & Drugg, 1987).

Such an interpretation deducted from the distribution pattern of sphaeroidal sporomorphs would also be compatible with the suggestion of more offshore settings as made above. The slight increase in concentrations of *Classopollis* and other sphaeroidal pollen grains such as *Araucariacites* and *Balmeiopsis* over those found in PF-1A infer more offshore marine settings, as the hydrodynamic equivalence (buoyancy) of these sphaeroidal pollen grains allows them to increase in an offshore trend (Hughes & Moody-Stuart, 1967; Habib, 1979, Tyson, 1995).

Membranous tissues have been found to be common in terrestrial and proximal deltaic sediments and decline in an offshore direction. However, they can show some concentrations in depocentre settings of dysoxic-anoxic conditions provided that fungal activity is absent or at least very low, and thus considerable amounts of these delicate tissues were taken to indicate at least occasional

reducing conditions (e.g. Tyson, 1995). As these tissues are exclusively concentrated here in the shale horizons of the PF-1B, it would be suggested then that rare proportions of these fragile, oxic-intolerant tissues were deposited in low energy distal nearshore marine settings during occasional low stands in water tables.

Combining all the information mentioned above one can suggest that sediments of PF-1B were deposited in normal open marine conditions. However, the considerably high concentrations of the cavate and proximate cysts that collectively outnumber the chorate cysts in the dinoflagellate cyst community of PF-1B would rather indicate proximal offshore, most likely inner shallow marine conditions (Fig. 6.12). Furthermore, occasional reducing (anoxic) conditions are suggested to prevail during the deposition of the studied sediments of PF-1B. This is also shown from plotting palynological constituents of PF-1B in the kerogen diagram, which also indicates proximal shelf settings of suboxic-anoxic conditions (Fig. 6.9).

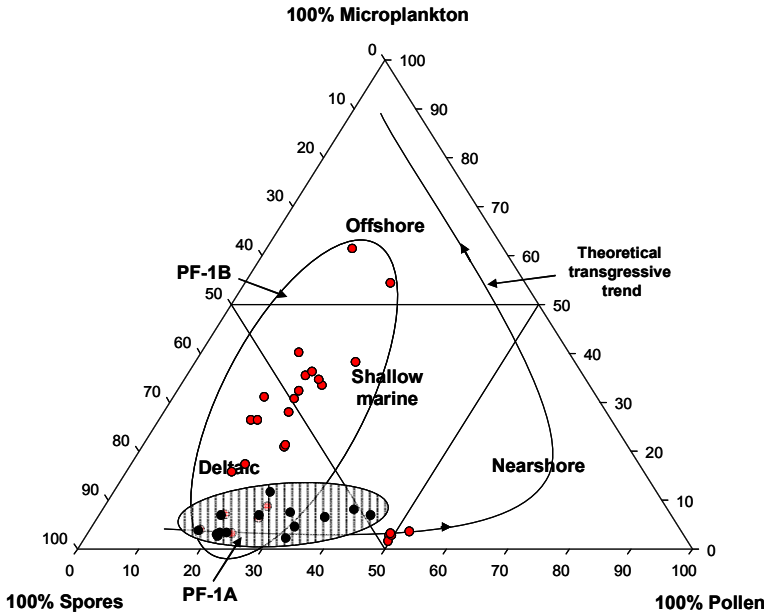

Figure 6.12 Ternary plot of spores, pollen and microplankton, illustrating the recognized palynofacies types; PF-1A and PF-1B of the Abu Tunis 1x borehole and their probable depositional environment (Federova, 1977; and Duringer & Doubinger, 1985).

6.3.3 Palynofacies PF-2A

The organic remains contained within samples 43-85 (8050-5950 ft) cluster as PF-2A, characterised by a very strong terrestrial influence (Fig. 6.13), reflected in the extremely abundant phytoclasts (~ 88,000 particles/g) and concentrations of sporomorphs which although still low, increase (~ 4,700 grains/g) over those in PF-1B below. Dinoflagellate concentrations decrease by comparison to the underlying PF-1B (~ 1,650 cysts/g) and there are only low MTLs concentrations (~ 1150 grains/g) detected in the palynofacies.

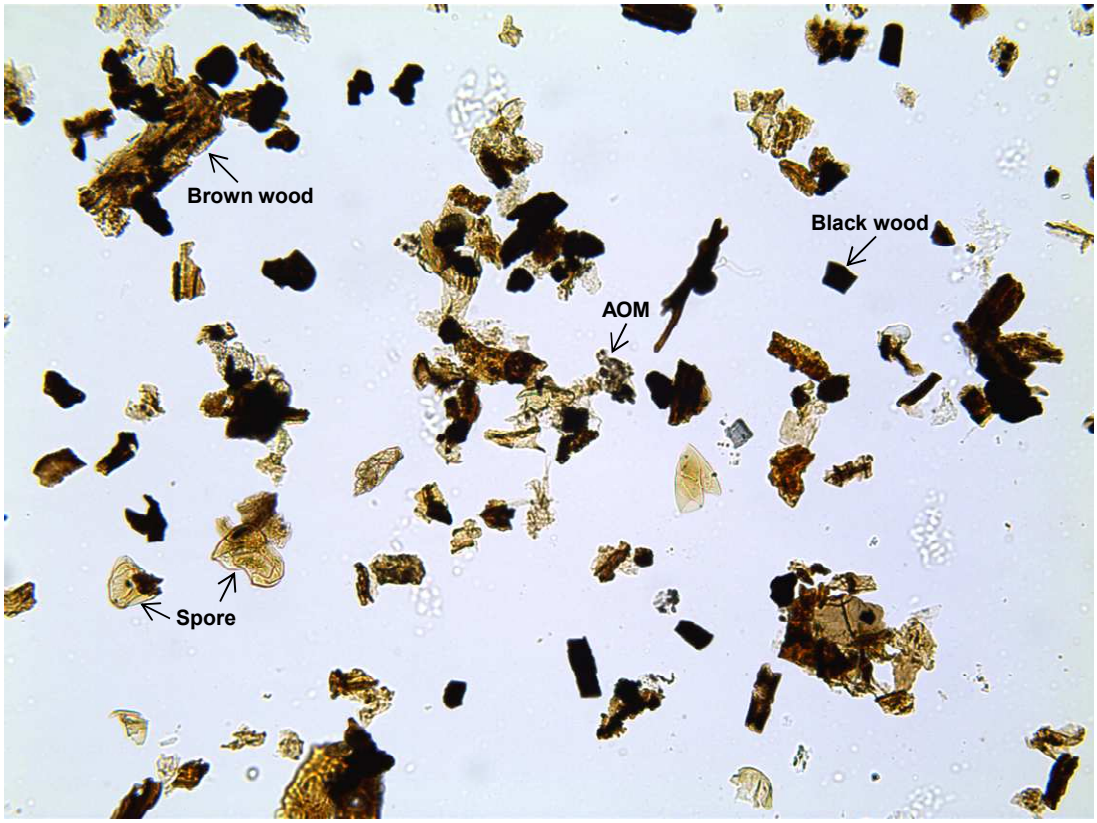

Figure 6.13 PF-2A showing terrestrial palynomorphs and phytoclasts dominance, sample 46a (7900 ft) at x250 magnification, the Abu Tunis 1x borehole, northern Western Desert, Egypt.

Extremely high abundances of tracheids (~ 185,150 particles/g) and common cuticle (~ 8,700 particles/g) dominate the phytoclast assemblages (Fig. 6.6). Membranous tissues are common (~ 6,000 particles/g) and black wood is present (~ 5,000 particles/g). Here the strong increase in the sporomorph abundances over PF-1B assemblages is exemplified by frequent pteridophyte spore concentrations (~ 13,200 grains/g). Concentrations of *Classopollis* (~ 1,900 grains/g) and other sphaeroidal and saccate gymnosperm pollen show a noticeable increase (~ 2,050 grains/g) in PF-2A. A very few freshwater algae, including representatives of *Ovoidites*, *Botryococcus*, and *Chomotriletes* occur along with rare acritarchs. Dinoflagellate cysts show a decrease in abundance (~ 1,650 cysts/g) and diversity (~ 0.67), and are again dominated by cavate (~ 850 cysts/g) and proximate (~ 500 cysts/g) forms, with chorates showing the lowest concentrations (~ 300 cysts/g). The cavate cysts are once more mainly represented by the genera *Subtilisphaera* and *Senegalinium* with subordinate *Palaeoperidinium* spp.. The proximate cyst assemblage is composed of *Pseudoceratium* and *Cribroperidinium* species, while *Oligosphaeridium* and *Florentinia* are the only genera in the chorate cyst community.

Lithology and changes in sedimentary facies of PF-2A

Downhole log responses for the sample depths yielding PF-2A indicate the development of several coarsening upward sequences, which is reflected in increases in the self-potential profile as it crosses the sand:shale line (SSL) and also from the decreases in resistivity readings (Fig. 6.7).

As is shown here the generally low resistively data readings imply high sand volumes intercalated with a few resistivity peaking shale horizons. The sand lithologies was also indicated in the original lithological description provided by the

drilling operating company, and found here to be consistent with the visual lithology interpretation based on the ditch cuttings samples. Therefore, by combining the original lithology descriptions with such interpretations made herein, this part of the sequence can be interpreted as comprising a very thick sandstone unit, which is composed of fine to medium grained sandstone beds with a silicic to carbonate matrix, which contains pyrite and traces of anhydrite. These beds are intercalated with thin light grey to green fissile shale horizons, which contain traces of carbonaceous material.

Suggested depositional environment: deltaic (delta channel)

By comparison with the underlying succession, in PF-2A the general decrease in dinoflagellate cyst abundance and a dominance of restricted marine species (e.g. *Subtilisphaera* and *Pseudoceratium*) suggests that sediments of PF-2A, whilst still demonstrating a marine signal, were deposited during a regressive phase (e.g. Tyson, 1993, 1995), and furthermore in more salinity-stressed brackish conditions than that of the two previous palynofacies. This latter interpretation is based on the reduced dinoflagellate cyst species diversity in PF-2A, which is known to be much lower in waters of less than normal salinity (e.g. Batten, 1983; Leckie & Singh, 1991).

Such an interpretation would tie in with the very high abundances of terrestrially derived organic matter, and the decline in dinoflagellate cyst abundance and diversity, both characteristics of marginal marine (brackish-coastal) conditions. The work of Degens & Mopper (1976) also suggests that very strong influxes of terrestrially derived phytoclasts can be indicative of sedimentation in estuarine and very nearshore areas during either regressive event. The highest concentrations of miospores have been reported from medium to coarse silts and fine-grained

sandstones (Hughes & Moody-Stuart, 1967; Batten, 1974), and Tyson (1995) indicates high concentrations are associated with fluvio-deltaic systems. The samples from which this palynofacies has been isolated are indeed comprised of a coarser clastic facies than the samples from lower part of the succession, and they would thus have been deposited under relatively higher energy conditions than PF-1A or PF-1B. These coarse clastic lithologies are again supported by the extremely high abundances of tracheids recorded here. As high concentrations of tracheids have been found (e.g. Habib, 1983; Firth, 1993, Tyson, 1993) to concentrate in fine sands and coarse silts facies, where these high concentrations of tracheids were taken by (e.g. Muller, 1959; Pocklington & Leonard, 1979) to indicate deposition in proximal transitional environments that were close to parent land plant, and specifically the fluvio-deltaic systems. Common concentrations of cuticles in PF-2A could be another line of evidence for the deltaic sub-environments proposed above, as high percentages have been commonly found in delta top, distributary channels, and prodelta settings (e.g. Batten, 1973; Parry et al., 1981; Nagy et al., 1984).

Furthermore, the presence of freshwater algae and acritarchs also suggest deposition in very near shore deltaic environments, where marine palynomorphs are often extremely diluted by terrestrially derived POM, especially under regressive regimes (e.g. Habib, 1982; Summerhayes, 1987; Tyson, 1995).

Occasional short-lived or local anoxic conditions are reflected in the presence of some pyrite and carbonaceous material. These reducing conditions are interpreted as suboxic to anoxic conditions by plotting PF-2A into the kerogen ternary diagram (Fig. 6.9). Membranous tissues have been found typically common in the non-marine and proximal deltaic facies and become rare in a basinward direction (e.g. Tyson, 1995), and as these tissues can not tolerate oxidation conditions and degrade three times faster than lignified wood (e.g. Stout et al.,

1981). Therefore, their common proportions are taken here - something that Tyson (1995) has suggested - to indicate high rate of sedimentation, where the fragile membranous tissues have been removed from the destructive oxic sediments water interface by rapid sediments accumulation, which thus keep membranous tissues away from oxic sediment water interface. This is also consistent with the high regime proposed here for PF-2A, which must have been associated with fine sands and silt deposition. The present concentrations of black wood do not contradict this reducing condition, as mentioned above, where black wood is commonly blown by winds from fluvial and delta-top sediments and is also transported from the delta front and re-deposited into prodelta sediments by waves and tide action (Tyson, 1993, 1995). These deltaic depositions under regressive periods are also indicated by plotting PF-2A constituents in the ternary palynomorph diagram (Fig. 6.12).

Combining all of these characteristics, and given the predominance of sand in this part of the succession, the sediments of PF-2A were probably deposited in a deltaic channel system which may have incised into or prograded out over the underlying prodelta sequence as a response to sea level fall.

6.3.4 Palynofacies PF-2B

The palynofacies constituents of samples 86-100 (5900-4800 ft) show a strong decrease in the terrestrially derived organic matter (phytoclasts and sporomorphs) in comparison to the underlying PF-2B (Fig. 6.14), although phytoclasts still dominate the POM assemblages with concentrations averaging 33,000 grains/g. Sporomorphs concentrations are now diminishing (~ 4,300 grains/g), but dinoflagellate cyst concentrations increase considerably in PF-2B (~ 2,420 cysts/g), while MTLs are still of low concentration (800 grains/g) they show lower concentration than that in PF-2A.

The phytoclasts are still dominated by the extremely abundant (~ 82,600 particles/g) tracheid and common (~ 9,550 particles/g) cuticle particles. Present (~ 5,600 particles/g) membranous tissues and a single frequent (10,450 particles/g) occurrence of black wood at the base of the palynofacies are also detected. The persistent decreases in the miospore concentrations that started to show in PF-2A end here in PF-2B with a significant decrease. However, pteridophyte spores are still the dominant (~ 8,600 grains/g) palynomorph constituent, with subordinate (~ 1,050 grains/g) schizaeacean spores, (~ 800 grains/g) saccate and (~ 700 grains/g) *Classopollis* pollen grain concentrations recorded in PF-2B. The dinoflagellate cysts exhibit here slight increases in abundance (~ 2,420 cysts/g) and dominance, but with decreases in dinoflagellate cysts diversity (~ 0.55).

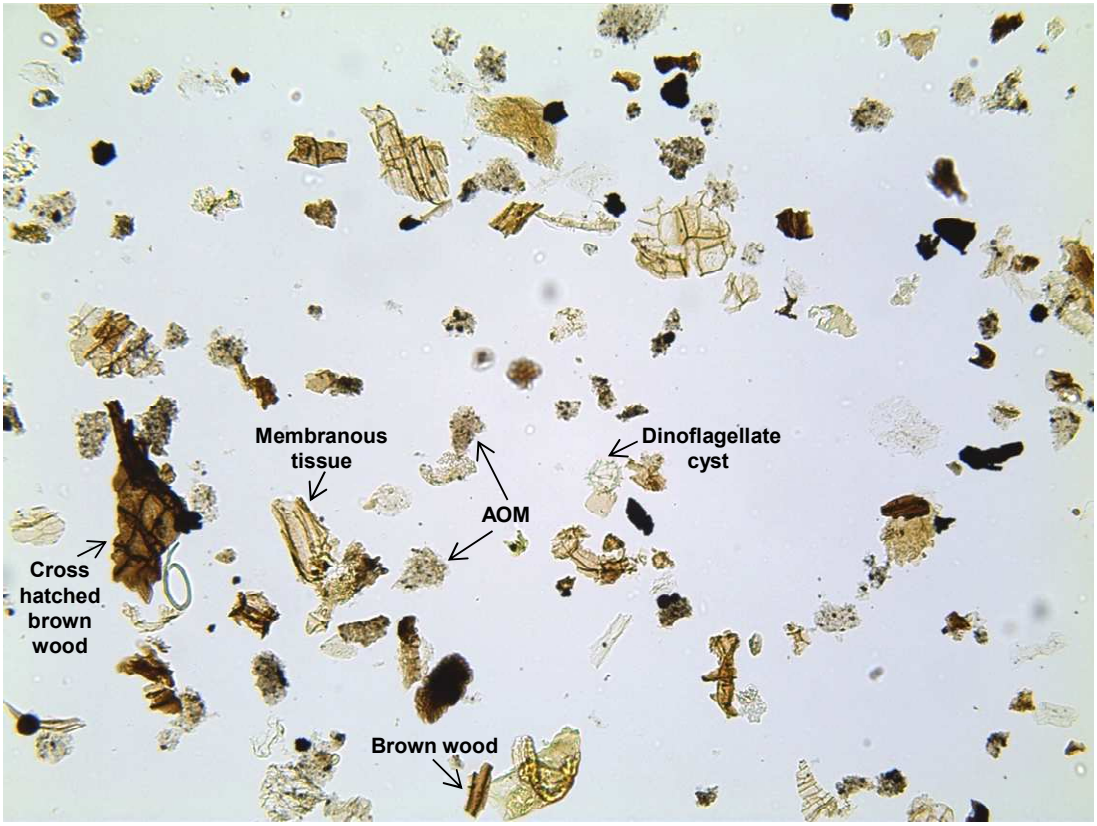

Figure 6.14 PF-2B showing another increase in dinoflagellate cyst abundances accompanied by a slight decline in terrestrial palynomorphs and phytoclasts in comparison to PF-2A, sample 96a (5050 ft) at x250 magnification, the Abu Tunis 1x borehole, northern Western Desert, Egypt.

The dinoflagellate cysts community is dominated by (1,350 cysts/g) the cavate cyst *Senegalinium*, while proximate (e.g. *Trichodinium*) and chorate (e.g. *Oligosphaeridium, Coronifera*, and *Florentinia*) cysts are of very minor occurrences (400 cysts/g) and (300 cysts/g) respectively.

Lithology and changes in sedimentary facies of PF-2B

Interpretations from the self-potential or resistivity data are not informative here for the lower part of this palynofacies sequence. However, the original description provided on the borehole log and visual interpretations based on cutting samples indicate a lower carbonate sequence, which is made of alternating shale and limestone beds, overlain by a pale brown dolostone unit. For the upper part of PF-2B sequence, the conventional integrated data (i.e. geophysical data, original log description, and cutting samples interpretation) are more informative. The upper part of the PF-2B that overlies the carbonate sequence is interpreted as a clastic unit, which is made of thick sandstone beds with dolomitic cement, alternating with thin light grey silty-shale streaks.

Suggested depositional environment: lagoonal

Here the dinoflagellate cysts show a different story from that of PF-2A, where slight increases in the dinoflagellate cyst abundance indicate the deposition of PF-2B in more offshore settings than that of PF-2A, which could also correlate with a relative sea level rise (Fig. 6.15). This trend of increases in the dinoflagellate cysts abundance with depth has been documented on dinoflagellate cyst work (Davey, 1970) carried out on Cretaceous sequences of England, northern France, and North America. Here again, the slight increase in the dinoflagellate cyst abundance along

with overall sharp declines in the concentration of the terrestrially derived organic matter (Fig. 6.6) suggests a relative rise in sea level (Tyson, 1993, 1995; Batten, 1999). This relative sea rise, which is detected here in the Abu Tunis 1x sediments and therefore in the Faghur Basin, could be related to the late Albian-early Cenomanian global sea level rise as indicated from both the global and Egyptian seal level curves (Vail et al., 1977). On the other hand, the dominance of the cavate dinoflagellate cyst *Senegalinium* over other dinoflagellate cyst morphotypes, which is also accompanied with a general decrease in the dinoflagellate cysts species diversity in comparison to that in the underlying PF-2A suggests more restricted marine conditions of below normal salinity (e.g. Batten, 1983; Lister & Batten, 1988; Leckie & Singh, 1991).

The upward increase in silt and shale volumes indicated by the self-potential profile for the upper part of PF-2B also suggests a more offshore setting of lower energy conditions than that detected in PF-2A. An interpretation, which is perhaps supported by the hydrodynamic properties of fine silts and shale. The fine silts and shale lithologies are known to be deposited from suspension load in low energy conditions in different offshore environments such as, lagoons, estuarine, and the deep-sea. However, other terrestrial and transitional settings such as, lakes and distal delta facies also contain these fine lithologies (e.g. Boggs, 1987). The fact that terrestrial organic matter are of diminishing concentration in FP-2B suggests exclusion of environments that are known to be very rich in terrestrially derived organic matter, such as lakes and delta. Deep-sea environments are also excluded here based on the high dominance and low diversity of dinoflagellate cysts recorded, which are characteristic of restricted marine conditions rather than normal open marine settings. This leads to the suggestion that PF-2B is more likely to be deposited in lagoonal or estuarine environments. Lister & Batten (1988) interpreted

the silts and laminated mudstones of the Weald Clay of South England as of lagoonal origin. Lister & Batten (1988) based their interpretation on low frequencies of terrestrial palynomorphs, dinoflagellate cysts that show low diversity and dominated by low salinity species, and small amounts of sphaeroidal (bisaccate) pollen grains, in addition to the presence of minor amounts of fresh water chlorococcalean algae. In fact, the same scenario applies here, where fine silts with occasional shale horizons of PF-2B contain dinoflagellate of high dominance and low diversity, associated with low abundances of terrestrial organic matter, and with minor occurrences of the fresh water algae *Ovoidites* and *Botryococcus*. The low occurrences of *Classopollis* and sphaeroidal saccate pollen grains are also recorded in PF-2B. Another piece of information that would support the argument for lagoonal settings is that chorate dinoflagellate cysts of PF-2B show the same average concentrations to those in the underlying PF-2A, where they would be expected to increase here in PF-2B with increasing depth of depositional environment. This in turn indicates that the depositional system of PF-2B was at least partly isolated for some time from normal marine conditions, which would brought more concentrations of dinoflagellate cysts that are representative of deeper marine conditions if it was permanently connected to open marine waters (Lister & Batten, 1988).

From the data and discussion noted above, a lagoonal setting, which was occasionally influenced by some marine incursions is suggested for PF-2B. The suboxic-anoxic conditions that persisted in the underlying PF-2A are also interpreted to prevail during or after the deposition of PF-2B, and this is based on both the continuous occurrences of the oxic intolerant membranous tissues and the kerogen plot (Fig. 6.9).

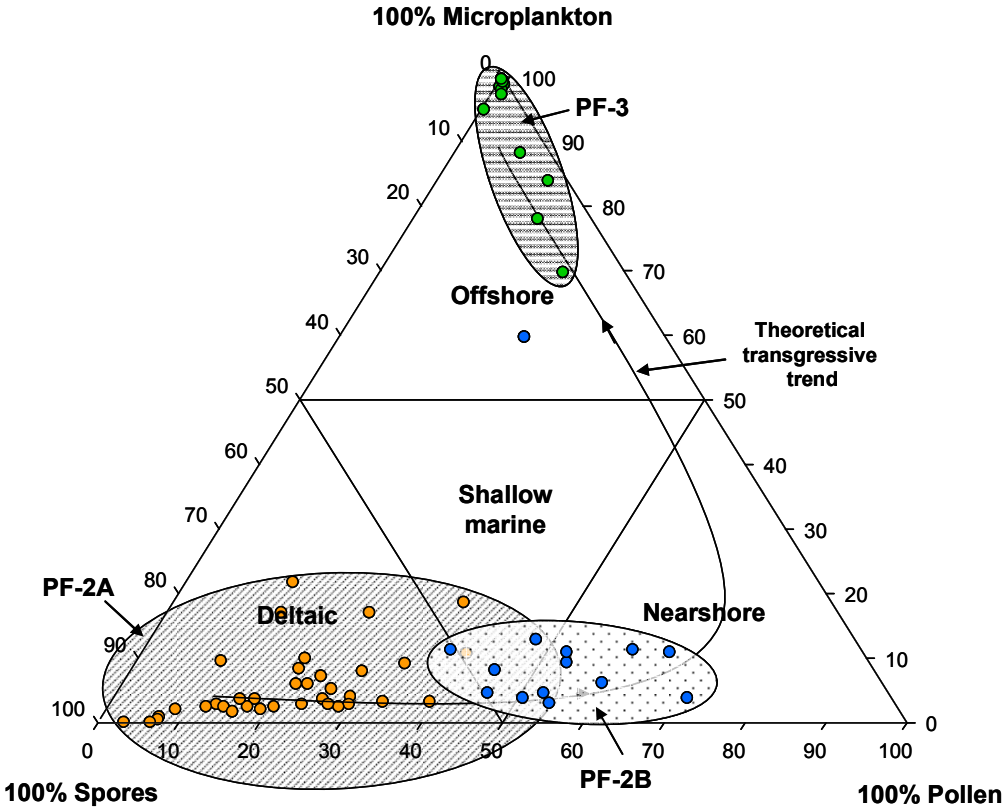

Figure 6.15 Ternary plot of spores, pollen and microplankton, illustrating the recognized palynofacies types; PF-2A, PF2-B, and PF-3 of the Abu Tunis 1x borehole and their probable depositional environments (Federova, 1977; Duringer & Doubinger, 1985).

6.3.5 Palynofacies PF-3

Samples 100-121 (4750-3750 ft) witnessed a strong marine influence, where PF-3 is almost entirely composed of marine palynomorphs with minor (~ 132 cuticles, 113 tracheids, 75 membranous tissues, and 28 pteridophyte spores grains/g) terrestrially derived organic matter concentrations (Fig. 6.6, 6.16). Marine palynomorphs are represented by low (~ 1,700 cysts/g) dinoflagellate cyst and very rare MTLs (865 grains/g) concentrations.

The diversity of the dinoflagellate cyst species in this palynofacies is even lower (~ 0.33) than that recorded in the all previous palynofacies types recorded in the Abu Tunis 1x borehole. The cavate cysts continue to dominate the

dinoflagellate assemblage (~ 1,360 cysts/g) and are represented by the genus *Senegalinium*, with subordinate concentrations of the chorate (~ 78 cysts/g) cysts *Spiniferites* and *Florentinia*, and the proximate (~ 78 cysts/g) cyst *Trichodinium*.

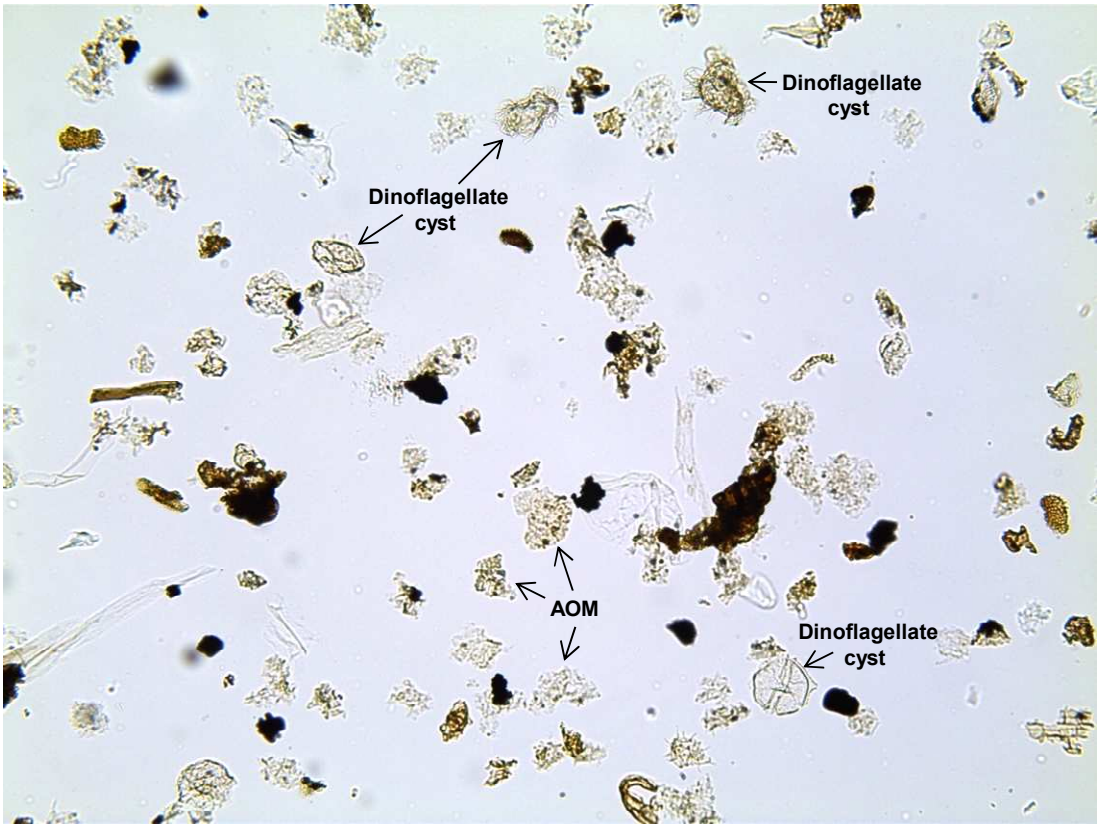

Figure 6.16 PF-3 showing dominance of the dinoflagellate cysts and an almost complete lack of terrestrial POM constituents, sample 110a (4300 ft) at x250 magnification, the Abu Tunis 1x borehole, northern Western Desert, Egypt.

Lithology and changes in sedimentary facies of PF-3

The self-potential profile is found here to be useful in indicating changes in sand:shale volumes, and the same applies for resistivity data. The sedimentary facies of the PF-3 as interpreted from the cutting ditch samples and as also indicated in the original borehole log description, is composed of a lower carbonate unit made of white to pale grey, microcrystalline limestone with a very few silt and shale intercalations. This limestone unit is overlain by a light brown dolomitic

limestone, overlain by another limestone unit, which is toped with a dolostone unit followed by chalk and another dolostone unit.

Suggested depositional environment: outer shallow marine

The presence of dinoflagellate cysts of low abundances and species diversity accompanied with very minor terrestrially derived organic matter suggests that the deposition of PF-3 took place in settings that were very far from the shoreline, at least in shallow shelf environments. This is can be explained in the context of offshore trend of the dinoflagellate cysts abundance and diversity. The work of Davey (1970), Habib (1983), and Tyson (1984) on fossil dinoflagellate cysts, which is found to be consistent with that of Balch et al. (1983) and De Vernal & Giroux (1991) on modern dinoflagellates indicated that dinoflagellate cysts tend to increase in an oceanward direction until they reach the continental slope, after which dinoflagellate start to show a reduction in species abundances and diversity. As the dinoflagellate cysts assemblage of PF-3 is dominated here by shallow marine peridinioid cavate cysts rather than the open marine (middle shelf) chorate gonyaulacoid cysts, this then leads to the suggestion that PF-3 is deposited in relatively outer shallow rather than open marine environments.

The very minor occurrences of terrestrially derived organic matter recorded here in PF-3 also indicate that sediments of PF-3 were removed far enough from the active fluvio-deltaic systems. Where, very weak terrestrial influxes must have reached the open marine settings only during periods of excessive rainfall and strong terrestrial input. This was also have been accompanied with active turbidity currents that would transport and re-deposit phytoclasts in the shelfal environments during temporary low sea stands (e.g. Habib, 1982; Summerhayes, 1987).

The carbonate lithologies of PF-3 could be further supporting evidence for this general shallow marine environment. Limestones are known to be deposited in outer shelf environments where little terrigenous clastic inputs are provided from surrounding lands. However, the limestone lithologies can be also deposited in such transitional marine settings that normally receive appreciable amounts of terrigenous clastic discharge such as that of lagoons and tidal flat environments (Boggs, 1987). However, these transitional settings cannot be a candidate environment for PF-3, as these environments are known to be rich terrestrial organic matter, some thing that the sediments of PF-3 clearly lack. In the meantime, outer shelf environments are not possible settings for PF-3, as dinoflagellate cysts here are dominated by the cavate cysts that are generally characteristic for shallow marine environments. Therefore, outer shallow marine settings would be consistent with settings that are far enough from effective terrestrial influx but also not so deep as dinoflagellate assemblage lack considerable amounts of open marine representative dinoflagellate cysts.

This shallow marine conditions could be also supported by the presence of a very few calcareous nannoplankton forms, which are recorded from the whole carbonate sequence. This outer shallow marine setting (Fig. 6.15) could be related to the local and global late Cenomanian rise in sea level (Fig. 6.11).

Basinal reducing (suboxic-anoxic) conditions are suggested to prevail during or after the deposition of PF-3 based on the kerogen plot information (Fig. 6.9).

6.4 The BB80-1 borehole palaeoenvironments

6.4.1 Palynofacies PF-1

The palynological organic matter constituents disseminated in the sediments of PF-1 are dominated by terrestrially derived organic matter (Fig. 6.17) and represented by extremely abundant (~ 27,300 particles/g) phytoclasts that are exclusively comprised here of wood tracheids, but with rare (~ 1,900 particles/g) concentrations of sporomorphs mainly composed of pteridophyte spores. However, present (~ 3,350 cysts/g) concentrations of the marine phytoplankton dinoflagellate cysts are also recorded in the palynofacies (Fig. 6.18).

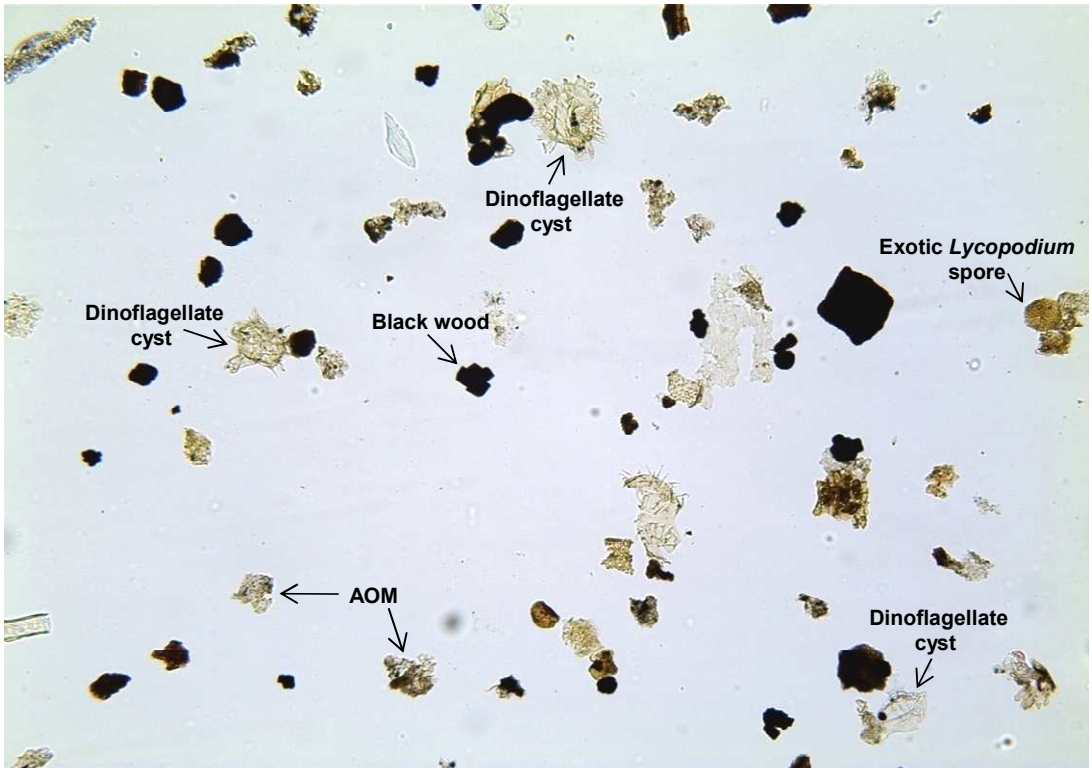

Figure 6.17 PF-1 showing the strong terrestrial influx and influence of of the marine incursion, sample 11a (5180 ft) at x250 magnification, the Abu BB80-1 borehole, Gulf of Suez area, Egypt.

The dinoflagellate cysts are dominated by the restricted shallow marine genus *Subtilisphaera* and with a low concentration of the genus *Senegalinium*.

The chorate cysts are the second morphotype that dominate the dinoflagellate cysts assemblage and are mainly represented by the genus *Florentinia* with subordinate concentrations of *Coronifera*. The genera *Cribroperidinium, Trichodinium*, and *Circulodinium* are the only proximate cysts representatives in PF-1.

Lithology and changes in sedimentary facies of PF-1

Based on the responses of gamma ray and resistivity readings the studied part of the BB80-1 is described as a thick clastic interval comprising a sandstone unit, which is underlain by a shale bed and overlain by intercalations of a very few silt and shale horizons, with the whole clastic interval overlain by a two carbonate units (Fig. 6.19). These carbonate units are in turn intercalated with another sandstone unit.

It must be noted that carbonate sequences described herein have been only recognised from the original log description provided by the drilling company and from visual interpretation of the ditch cuttings samples.

Suggested depositional environment: continental to shallow marginal marine

The presence of dinoflagellate cysts in the shale horizons of PF-1 in low abundance and diversity but also with a high dominance suggests a very shallow marine origin with possible restricted (low salinity) water conditions for this part of PF-1. As is mentioned before, dinoflagellate cysts populations having low abundances and diversity but with a high species dominance have been taken to

indicate restricted shallow marine conditions, because species diversity of dinoflagellate cysts is much less in waters of below normal salinity (Batten 1983; Leckie & Singh 1991).

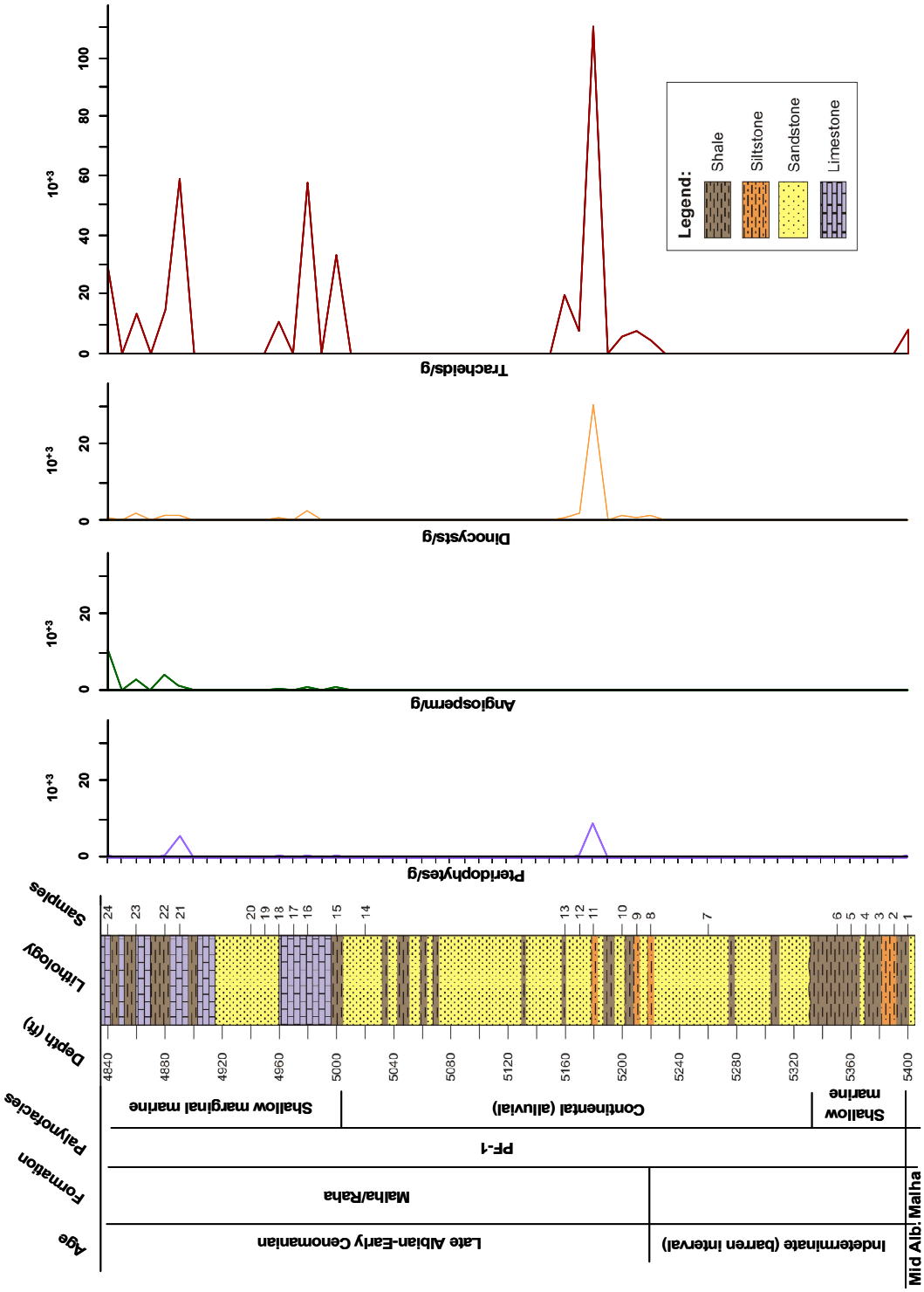

Figure 6.18 Absolute abundances (grains/g) of the recovered palynomorphs and particulate organic matter of the BB80-1 borehole, Gulf of Suez area, Egypt.

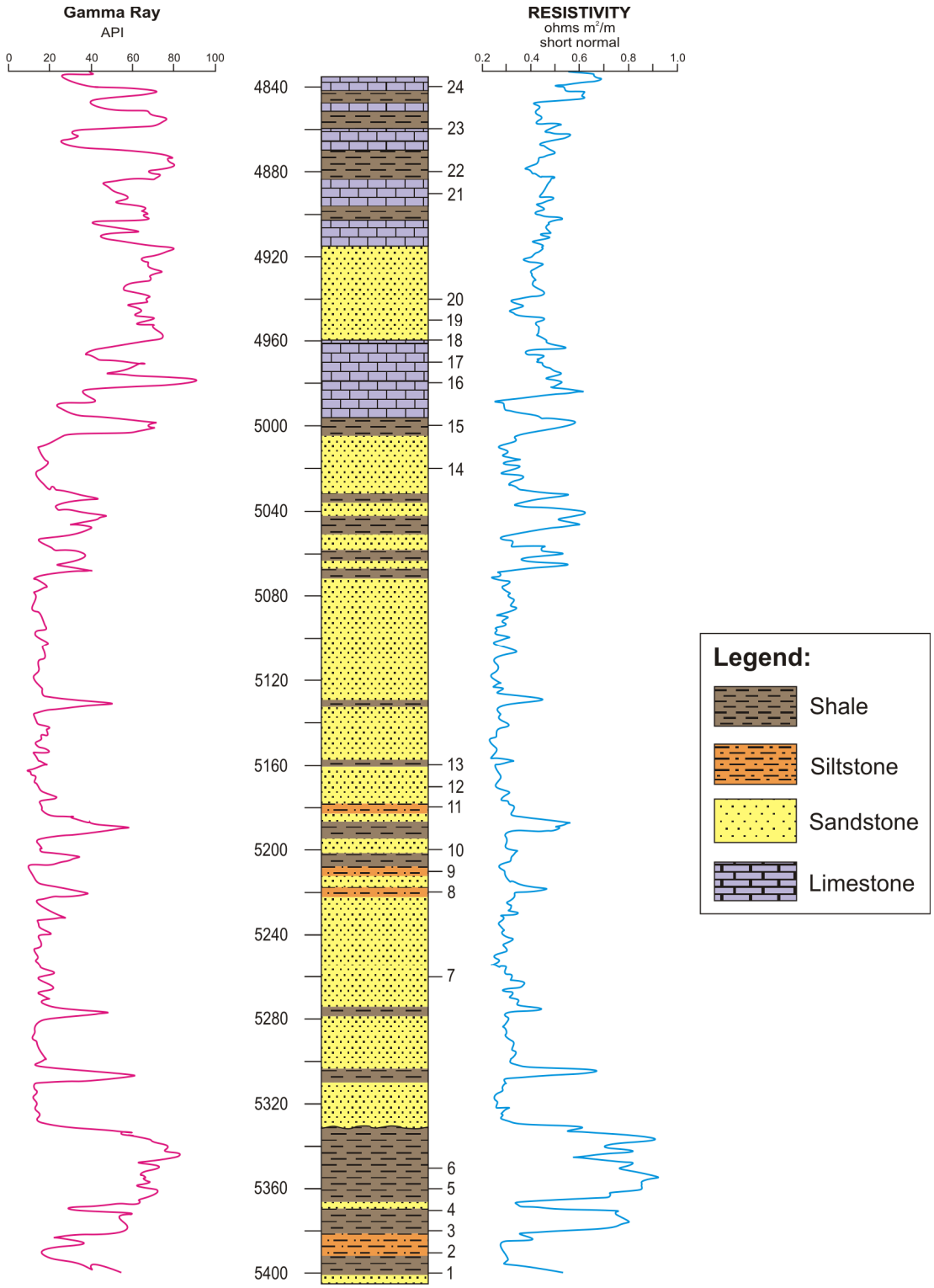

Figure 6.19 Gamma ray and resistivity data of the BB80-1 borehole showing changes in sedimentary facies.

These restricted shallow marine conditions are also supported by the dominance of the cavate peridinioid dinoflagellate cysts *Subtilisphaera*, which is known to characterise marginal marine (brackish to coastal) conditions (e.g. Davey, 1970; Piasecki, 1984; Harding, 1986; Lister & Batten, 1988). The very rare occurrences of some chorate dinoflagellate cysts in PF-1, which are know to thrive in open marine (middle shelf) conditions (e.g. Dale, 1983; Lister & Batten, 1988) do not contradict these restricted shallow marine conditions. This could be explained by occasional marine incursions that possibly reached the site of deposition of PF-1 at some time, or by transportation of these chorate cysts by marine currents and re-deposition in more nearshore settings.

The high concentrations of phytoclasts found here in shale sediments of PF-1 would also correlate with very nearshore marine environments that were close to fluvio-deltaic sources as it has been indicated in previous palynofacies types of the Abu Tunis 1x borehole (e.g. PF-1A and PF-2A). Adding to that, complete absence of oxidised wood (i.e. black wood) in PF-1, where black wood is commonly derived from the oxidation of the brown wood (e.g. Tyson, 1995), implies that brown wood have been removed from oxic conditions, and this in turn could infer development of periodically reducing conditions during deposition of shale lithology of PF-1 sediments.

Such an interpretation based on very rare concentrations of the pteridophyte spores recorded here, would tie in with the suggested shallow marginal marine conditions for the shale horizons. As spores are known to be produced in lower abundances than their associated gymnosperm-producing plants and tend to show poor transport efficiency, and thus their low concentrations are taken here to indicate relatively distal nearshore settings (e.g. Reyre, 1973; Habib, 1979; Tyson, 1989; Mutterlose & Harding, 1987; Prauss, 1989).

The very rare occurrence of the freshwater algae *Pediastrum*, *Ovoidites*, and *Botryococcus* would also indicates proximal nearshore settings of brackish conditions. As *Botryococcus* has been recorded from ancient lacustrine, fluvial, lagoonal, and deltaic to nearshore marine sediments (Reyre, 1973; Habib, 1979; Mutterlose & Harding, 1987; Batten & Lister, 1988; Prauss, 1989; Tyson, 1989). *Pediastrum* has also been found to show high abundances in low salinity lakes and also transported by fluvial systems into nearshore settings (e.g. Singh et al., 1981b; Hutton, 1988). *Ovoidites* is another algal genus when found in sediments is also taken to indicate stressed environment of below normal salinity (Batten, 1999).

The barren nature of the sandstone beds of PF-1 implies deposition in a continental possibly, alluvial environment. The latter suggestion was based not only on the lack of terrestrial organic matter (sporomorphs and phytoclasts) that would be introduced in the depositional site of PF-1 if it was close to vegetation cover, but also on the lack of marine palynomorphs, which implies isolation of the depositional site of PF-1 from any possible marine connections during the deposition of these sand beds. The deposition of the carbonate units at the top of the sequence suggests a possible deepening of depositional environment towards the end of deposition of the studied upper part of PF-1, which is may be related to the late Cenomanian global rise in sea level (Vail et al, 1977; Fig. 6.11).

Based on the data and discussion advanced above, one can suggest that sediments of PF-1 were mainly deposited in a continental, possibly alluvial environment, which has been occasionally invaded by marine incursions that resulted in deposition of marine shale under shallow marginal marine conditions, during which shale these horizons also experienced occasional reducing conditions.

6.5 Palaeovegetational cover and palaeoclimate

6.5.1 Introduction

Certain types of fossil spore and pollen grains of known botanical affinities and are known to thrive in and/or adapt to specific palaeoenvironments are used as a useful tool in palaeoenvironmental studies. These types of spore and pollen grains were not only used to indicate their depositional environments (i.e. palynofacies and palaeoenvironments analyses) in which they have been preserved, but are also used as proxy indictors of such palaeoclimate conditions that were prevailing during the life cycles of their producing-plants. From this context and for the purpose of providing an insight on the palaeoclimate prevailed during deposition of sediments of the studied boreholes; the Abu Tunis 1x and BB80-1, a summary table of some of the important spore and pollen grains of known botanical affinities and show some ecological preferences has been compiled (Tab. 6.2). The search of botanical affinities and possible ecological preferences of the taxa selected herein has been based on a survey on most of the literature that deals with Mesozoic, specifically Cretaceous and Jurassic spores and pollen grains, including Balme's (1995) in situ spores and pollen Catalogue, one of the important references.

Taxa	Botanical affinity	Palaeoclimate indication	Palaeoenvironment preference
Araucariacites	Araucariaceae (Cookson, 1947)	Local humid conditions	Relatively dry conifer vegetation
Afropollis	Winteraceae (Doyle et al., 1990)	Local costal humidity	Humid costal habitats
Aequitriradites	Liverworts	Local humid conditions	Near fluvio-lacustrine environments
Balmeiopsis	Araucariaceae (Cookson, 1947)	Local humid conditions	Relatively dry conifer vegetation
Cicatricosisporites	Schizcaeaceae (Thomson & Pflug, 1953)	Local humid conditions	Pteridophyte vegetation on wet biotopes
Classopollis	Cheirolepidiaceae	Warm dry	Costal marshes
Crybelosporites	Marsiliaceae (Dettmann, 1963); Hydropteridacean spores (Cookson & Dettmann, 1958)	Local humidity	Fresh waster environment (lakes-ponds); Swampy environment of brackish character
Deltoidospora	Matoniaceae/Cyatheaceae/ Diksoniaceae (Van Erve & Mohr, 1988)	Local wet conditions	Moist habitats near rivers and freshwater lakes and lacustrine
Elaterate	Ephedroid Crane (1988)	Local costal humidity	Humid costal conditions
Ephedripites	Ephedraceae	Hot xeric climate	
Inaperturopollenites	Taxodiaceae, Cupressaceae and other conifers (Thomson & Pflug, 1953)	Hot dry conditions	

Table 6.2 Botanical affinities and suggested ecological preferences of some selected sporomorphs and freshwater algae.

6.5.2 Palaeoclimate implications

Amongst palynomorph types that show some ecological importance and provide some inference about possible local palaeoclimate conditions are the pteridophyte spores. Pteridophyte spores are known to thrive in warm humid low lands, such as riversides and costal areas (e.g. Pelzer et al., 1992; Abbink et al., 2004) and therefore their high abundances (e.g. *Deltoidospora*, *Concavissimisporites*, and *Impardecispora*) have been suggested as a proxy for humid conditions (e.g. Abbink et al., 2004; Bornemann et al., 2005). These spores have been recorded here from sediments of the Abu Tunis 1x borehole and in very low concentrations from the BB80-1 borehole. They showed consistent occurrences through the studied Cretaceous sequence of the Abu Tunis 1x borehole, and very high abundances in intervals that corresponded to major regressive periods in marine sedimentation and lower abundances during intervals of marine transgression. This implies that these strong oscillations in their abundances are related to changes in the sedimentation trends (i.e. transgression-regression) rather than ecological parameters on land, especially that these spores show a taxonomic stability through the whole studied section. Therefore the consistent occurrence of these pteridophyte spores it is possible to suggests that local warm humid conditions were prevailing at least in the vicinity of sites of deposition of both boreholes during the studied Cretaceous interval.

Humid conditions but with coastal settings near the sites of both boreholes are also suggested to prevail during Aptian-mid Cenomanian time. This interpretation is based on the relatively high abundances of *Afropollis* a pollen grain of Winteraceaen affinity. Lower abundances of *Afropollis* have been recorded from warm and dry intracontinental basins (e.g. Doyle et al., 1982). However, higher abundances of *Afropollis* have been suggested by Doyle et al. (1982) and Schrank

(2001) to indicate humid coastal conditions, habitats in which, the authors (op. cit.) suggested the *Afropollis*-producing plants flourished and to which they were better adapted.

Regional warm and relatively dry conditions could be postulated for the studied interval of Cretaceous time. An interpretation that is perhaps supported by the presence of the coniferous pollen grain *Classopollis*. This gymnospermous pollen is known to have been produced by thermophilous, drought-resistant Cheirolepidiacean conifers and thus provides a valuable proxy indicator for palaeoclimatic conditions (e.g. Doyle et al., 1999). As high abundances of *Classopollis* have been found to be associated with evaporites, salts, and red bed deposits, and also with xeromorphic wood and leaf megafossils of Cheirolepidiacean affinity, which indicates hot dry conditions for this genus (e.g. Watson, 1988; Doyle, 1999). Adding to that, the world wide latitudinal distribution of *Classopollis* shows that this species was most abundant during Barremian-Aptian times in the hot dry palaeosubtropical latitudes (15-30° N and S of the palaeoequator), while it showed lower abundances in the hot, but slightly wetter palaeotropical region (Doyle, 1999). Doyle et al. (1982), Schrank (1990), and Brenner (1996) all suggested relatively wetter palaeoclimates for the African palaeotropics (e.g. Egypt and Sudan), based on the presence of high abundances of fern spores (indicating humidity), and lower frequencies of *Classopollis* and the cooler-temperature coniferous genus *Araucariacites* than seen in the palaeosubtropics. The gymnospermous gnetalean pollen *Ephedripites* is another xerophytic genus. Its relatively low abundance in the studied boreholes could also suggest less hot and more humid conditions, as its high abundances are taken to indicate hot and dry conditions (e.g. Doyle et al., 1982; Doyle et al., 1999). The later suggestion was based on a systematic taxonomy work of Trevisan (1980) on the fossil *Ephedripites* and on pollen produced

by the modern xerophytic gnetalean plants *Ephedra* and *Welwitschia*, where this work showed a great similarity between pollen produced by these modern xerophytic plants and *Ephedripites*. Furthermore, a macropalaeotological study on gnetalean macrofossils *Drewira* and *Eoanthus* revealed close relation between plants produced these macrofossils and modern gnetalean plants of well-known xeromorphic nature (Crane, 1988).

The hot and relatively dry palaeoclimate that is suggested to prevail during the Cretaceous over the Egyptian land area would also be compatible with such a deduction driven from the palaeolatitudinal position. During the Cretaceous, Egypt was continuously located at the palaeotropical zone for example, in the mid Aptian time, north Egypt was located at nearly latitude 10° N with the palaeoequator roughly cutting through central Egypt (Fig. 6.20). Thus, during this time Egypt and other palaeotropical countries were witnessing hot but relatively wetter conditions than that prevailed in the completely dry palaeosubtropical regions, as latitudinal regions close to the equator are known to receive the highest rainfall in comparison to that close to subtropics (Doyle et al., 1999). As the African plate moved northward towards Laurasia and by the end of the Turonian time, Egypt was positioned more northward (Fig. 6.21) with the palaeoequator nearly bordering its southern limit (Lawver et al., 2004 http://www.ig.utexas.edu/research/projects/plates/#recons), where a continuous hot but dryer palaeoclimate was developed.

Consequently, from the data and discussion advanced above, it can be assumed that sites of deposition of both Abu Tunis 1x and BB80-1 have witnessed a regional hot and relatively dry palaeoclimate that latter developed into more dryer conditions as a response to the continental break up of Western Gondwana and resultant northeast drift of the African continent. However, both boreholes could

also experienced local humid conditions that were prevailing on costal settings and near fluvio-deltaic systems.

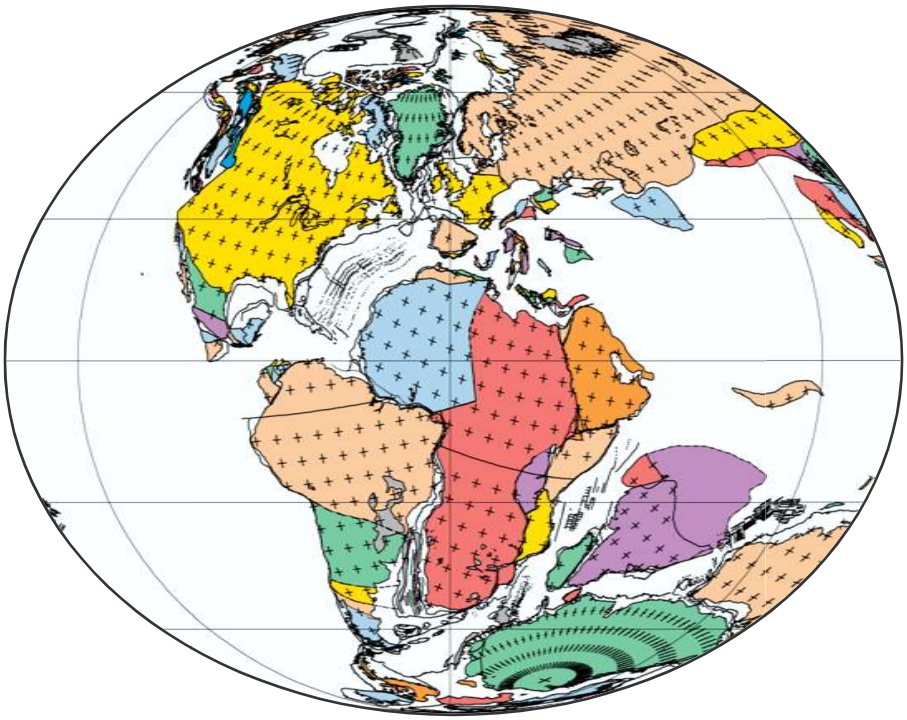

Figure 6.20 World palaeotectonic map showing the palaeogeographic position of Egypt during the Early Cretaceous (Aptian) time (after Lawver et al., 2004).

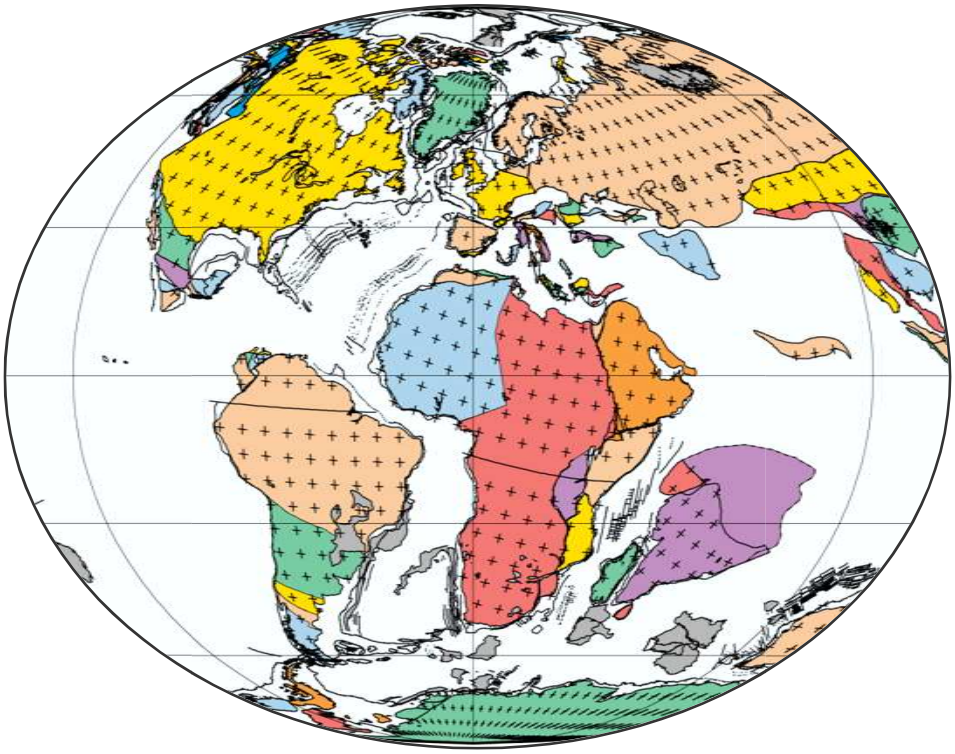

Figure 6.21 World palaeotectonic map showing the palaeogeographic position of Egypt during the Late Cretaceous (Turonian) time (after Lawver et al., 2004).

PALYNOFACIES ANALYSIS, THERMAL MATURATION, BURIAL HISTORY RECONSTRUCTION AND SOURCE ROCK EVALUATION

7.1 Introduction

Hydrocarbons are generated in sediments rich in organic matter known as source rocks, by the thermal alteration of organic matter with increasing depth of burial that increases temperature with time (Allen & Allen, 1990; Hunt, 1996).

Organic matter is biogenic material found in sediments and sedimentary rocks. Organic matter is derived from plant matter such as, lignin, cellulose, carbonised wood, spores, resin, lipids, and from animal matter such as, protein, chitin and lipids (Hunt, 1996).

Source rocks are hydrocarbon charge systems that are capable of, or have generated, released hydrocarbons (Tissot & Welte, 1984; Hunt, 1996). Lakes, deltas, and marine basins are the main depositional settings of source rocks (Allen & Allen, 1990).

The process of hydrocarbon generation was described by Hunt (1996). It involves three stages of organic matter alteration: diagenesis, catagenesis, and metagenesis (Fig. 7.1). In the diagenesis stage some of the organic matter is subjected to microbial attack and decomposition. Other organic matter components undergo chemical reactions at low temperatures (≤ 50° C), when hydrocarbon-like material is formed by the loss of nitrogen, oxygen, and sulphur. With more sediment accumulation, the source rock become more compacted, attains a deeper burial depth, and is subjected to increases in temperature as the earth's geothermal gradient increases by some 2-5°C100^{-1} meters. At this stage organic matter enters the catagenesis stage (50-200°C) and undergoes thermal and catalytic cracking

forming petroleum-range hydrocarbons. This stage is the main phase of oil generation and is referred to as the oil window (Tissot & Welte, 1984). By increasing the depth of burial and temperature, organic matter enters the metamorphism stage (>200° C), where thermal cracking of organic matter produces small amounts of methane and converts the organic matter into anthracite (coal) and 'graphite'.

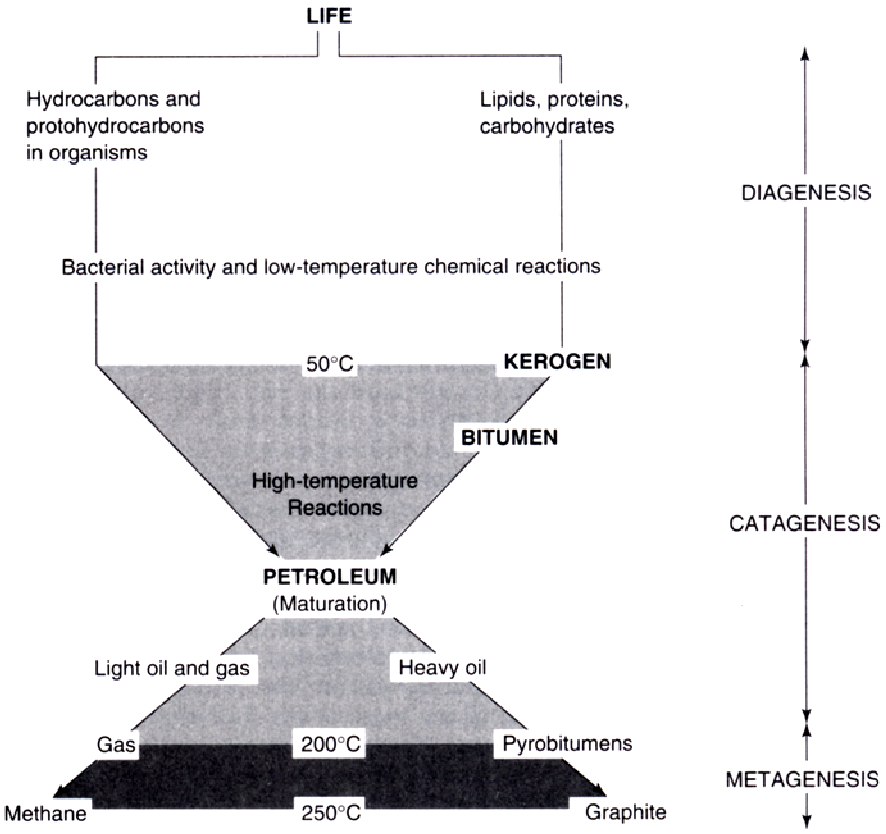

Figure 7.1 Origin of hydrocarbons and maturation processes of organic matter (after Hunt, 1996).

In a source rock evaluation for hydrocarbon potential the key analyses that have to be carried out are, the amount (i.e. total organic carbon content), type (oil-prone or gas-prone material) and the level of thermal maturation (immature or mature) of the organic matter in sediments (Tissot & Welte, 1984).

7.2 The Abu Tunis 1x borehole

The formations of the Abu Tunis 1x borehole are composed of organic-rich clastic and carbonate units, which could have potential as source rock. Therefore, the following steps of analyses have been conducted to detect and evaluate any potential source rocks.

7.2.1 Total organic carbon (TOC)

The total organic carbon content of sediment is determined by combustion of the organic carbon to CO_2 after the removal of the mineral carbonate by acid treatment. Determination of minimum values of TOC for a potential source rock is of significance. Tissot & Welte (1984) pointed out that the minimum values of TOC for a potential source rock are very important, not only because hydrocarbons in source rocks are generated from this insoluble organic matter, but also because a critical level of hydrocarbons has to be reached before expulsion (i.e. primary migration) from a source rock is possible. Brooks (1981) pointed out that there is no specific minimum amount of TOC required for a bed to act as an effective source rock and hence values must be evaluated and interpreted for different basins. However, an empirical value of about 0.5 wt % TOC is generally accepted as the lower limit required for shales before significant generation and expulsion of liquid and gas hydrocarbons take place (Ronov, 1958; Tissot & Welte, 1984; Walpes, 1985; Peters, 1986; Bordenave, 1993), with a lower limit for carbonates as a source rock of about 0.3 wt % TOC (Gehman, 1962; Brooks, 1981; Tissot & Welte, 1984).

Samples of the Masajid, Alam El Buieb, and Alamein formations are relatively rich in organic matter, and thus the deepest 29 samples were selected for total organic carbon determination (Fig. 7.3). These samples show an average total organic carbon (TOC) content value of 1.38 wt %, which is above the critical limit for

both shale and carbonate source rocks. Peters (1986) rated the generative potential of source rocks depending on their total organic carbon (TOC) content, where a source rock containing < 0.5 wt % TOC is poor, 0.5-1 wt % fair, 1-2 wt % good, and > 2 wt % very good. The total organic carbon (TOC) measured on the clastic samples 1-14, depth 10150 to 9500 ft of the Alam El Buieb Formation show minimum and maximum TOC values of 1.2 and 1.8 wt % respectively (Tab. 7.1), and an average TOC value of 1.43 wt %, which is well above the critical lower limit (0.5 wt %) for shale source rocks to generate hydrocarbons. Hence this shale sequence is regarded as of a good potential to generate hydrocarbons. The upper part of the Alam El Bueib Formation and the lower Alamein Formation are represented by samples from 15 to 29 (depths 9450-8750 ft) and are mainly composed of a significant dolostone unit intercalated with very few shale horizons. These samples show minimum and maximum TOC values of 0.93 and 1.6 wt % respectively, and an average TOC value of 1.32 wt %, which is also above the critical limit 0.3 wt % TOC for carbonate source rocks to generate hydrocarbons.

Sample	Formation	Depth (ft)	C_b	C_a	TOC	Calcite
29	Alamein Fm	8,750	1.7	1.31	1.26	3.6
28	"	8,800	2	1.5	1.43	4.8
27	"	8,850	3.04	1.45	1.23	15
26	"	8,900	5.85	1.7	1.02	40.2
25	"	8,950	4.1	1.27	0.93	26.3
24	"	9,000	1.9	1.19	1.11	6.5
23	Alamein Fm	9,050	3.41	1.46	1.19	18.4
22	"	9,100	2.11	1.33	1.23	7.3
21	"	9,150	2.23	1.61	1.51	5.9
20	"	9,200	2.35	1.37	1.24	9.2
19	Alam El Bueib Fm	9,250	2.18	1.57	1.48	5.8
18	"	9,300	2.75	1.73	1.56	9.9
17	"	9,350	2.79	1.81	1.63	9.6
16	"	9,400	2.67	1.58	1.41	10.4
15	"	9,450	2.18	1.66	1.58	5
14	"	9,500	2.08	1.53	1.45	5.2
13	Alam El Bueib Fm	9,550	2.33	1.88	1.79	4.5
12	"	9,600	1.99	1.23	1.14	7.1
11	"	9,650	2.09	1.51	1.43	5.5
10	"	9,700	1.89	1.48	1.43	3.8
9	"	9,750	1.86	1.37	1.31	4.6
8	Alam El Bueib Fm	9,800	2.73	1.95	1.8	7.7
7	"	9,850	1.93	1.67	1.63	2.5
6	"	9,900	2.09	1.93	1.62	1.6
5	"	9,950	1.59	1.43	1.41	1.4
4	"	10,000	1.99	1.27	1.18	6.7
3	"	10,050	1.9	1.24	1.16	6
2	Alam El Bueib Fm	10,100	1.47	1.23	1.2	2.2
1	Masajid Fm	10,150	2.09	1.35	1.26	6.9

Table 7.1 Total organic content for the Masajid and Alam El Bueib formations, the Abu Tunis 1x borehole, C_b = untreated samples, C_a = acid treated samples.

7.2.2 Palynofacies analysis and kerogen types

As shown in chapter 6 palynofacies analysis can be used in a palaeoenvironmental context, where the magnitude of terrestrial influx, depositional environment, and transgressive-regressive trends and characterization of depositional environment in terms of water salinity, oxic-anoxic conditions can be assessed. Alternatively, the palynofacies analysis can be also used in maturation and source rock studies (Batten, 1981; Tyson, 1993; Tyson, 1995).

The word kerogen is derived form Greek: *Kerós* = wax- or oil-forming and the root -*gen* = that which produces. According to Steuart (1912) the word kerogen was first proposed by Crum-Brown to describe the organic matter present in the Lothian (Scotland) oil shales, which when heated produced a waxy-distillate (Brooks, 1981). Kerogen is defined as the disseminated organic matter of sedimentary rocks insoluble in nonoxidizing acids, bases, and organic solvents (Brooks, 1981; Hunt, 1996). Kerogen has two sources: marine and terrestrial. Several different classifications of kerogen have been made by coal petrographers, petroleum geochemists, and palynologists.

Coal petrographers have essentially classified the kerogen based on their physical properties when seen in incident light with oil immersion objectives into three major categories; liptinite (exinite), vitrinite, inertinite (e.g. Stach et al., 1982). The word liptinite refers to a maceral group derived from organic materials that have high lipid (and fluoresce in UV light) content such as spores and pollen, phytoplanktonic algae, resin, cuticles, and bitumen. Vitrinite refers to a maceral group derived from the lignified tissues of higher plants such as trunks, branches, stems, leaves, and root of trees and plants. Inertinite is another maceral group that refers to organic material contain high carbon content and show no hydrocarbon

potential, these materials are derived from fossil charcoal and from fungal remains (Stach et al., 1982; Miles, 1994; Hunt, 1996).

Petroleum geochemists have proposed several kerogen classifications depending on chemical properties of the organic mater, for example, classification depending on the elemental analysis of the organic matter (Tissot & Welte, 1978, 1984) in terms of atomic hydrogen index (HI) *vs* Oxygen index (OI) plots (Fig. 7.2) on a Van Krevelen type diagram (Van Krevelen, 1961), which defines four kerogen types: Type I, which is commonly of lacustrine/marine origin and rich in algae (e.g. *Botryococcus*) and microbial lipids, Type II, which refers to organic matter of marine origin (MOM) such as, algae, zooplankton, and other micro organisms, which have accumulated in a reducing environment, Type III, which refers to terrestrially derived organic matter (TOM), and Type IV of Harwood (1977) equivalent to Type III-B of Barnard et al. (1981), which refers to generally inert oxidized terrestrially derived organic matter, such as wood and opaque coaly particles.

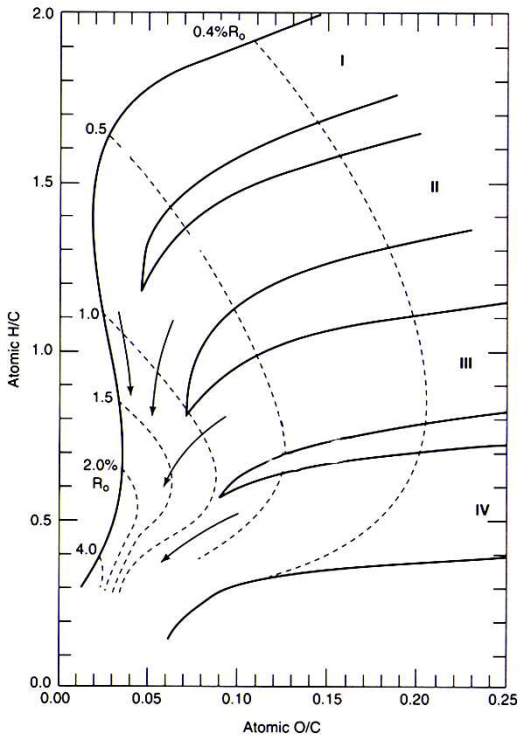

Figure 7.2 Van Krevelen type diagram showing four types of kerogen of source rock based on hydrogen and oxygen indices (after Hunt, 1996).

The palynologists as mentioned before have also proposed various kerogen classifications (e.g. Staplin, 1969; Correia, 1971; Burgess, 1974; Bujak et al., 1977; Combaz, 1980, Claret et al., 1981; Pocock, 1982; Pocock et al., 1988) based on mixed maceral terminologies of reflected light and palynological terminologies of transmitted light. Tyson (1993, 1995) has proposed a simple kerogen classification on a pure palynological basis for rapid assessment of hydrocarbon potential under transmitted light microscopy, where particulate organic matter constituents (palynomorphs, phytoclasts, and amorphous organic matter) can be placed into one of the four of the following kerogen types of (Tissot & Welte, 1984; Harwood, 1977): Type I (highly oil-prone material), Type II (oil-prone material), Type III (gas-prone material), and Type IV (inert material). Tyson's (1995) definition of each categorized kerogen constituent is as follow:

A. Palynomorphs: includes all pollen and spores, dinoflagellate cysts, acritarchs, other algal fragments, and microforaminiferal test linings (MTLs).

B. Phytoclasts: includes structured terrestrial plant debris such as wood tracheid, cuticle, and cortex tissue.

C. Opaques (black debris): includes oxidized or carbonized black coloured woody tissues including charcoal.

D. Amorphous organic matter: includes structureless organic matter such as bacterially derived AOM, resins, and more rarely humic gel of terrestrially biodegraded plant debris.

Based on Tyson's (1995) definition of the palynofacies as "a body of sediment containing a distinctive assemblage of palynological organic matter …, with a characteristic range of hydrocarbon-generating potential". Depending upon the nature of palynofacies composition, in terms of its different proportions of the

hydrocarbon-forming particulate organic matter constituents, each distinctive palynofacies can be correlated with the geochemically identified kerogen types as follow (Tyson, 1995):

1. Kerogen type I (highly oil-prone material): it includes alginitic material derived from chlorococcalean algae, prasinophyte algae, cyanobacteria, and some thiobacteria. Resins and cuticles are the only significant terrestrially-derived component belonging to this group.

2. Kerogen type II (oil-prone material): It includes amorphous organic matter, but sporopollenin palynomorphs, cuticle, and non-cellular membranous debris are also included.

3. Kerogen type III (gas-prone material): Orange or brown, translucent, phytoclast or structureless materials. Woody fragments are typical.

4. Kerogen type IV (inert material): Opaque to semi-opaque, black, or very dark brown particles, representing oxidized or carbonized phytoclasts (including charcoal). Fungal and tectin/chitinous materials are included.

In the present study, Tyson's (1995) method for visual palynofacies analysis and kerogen types determination is used, as this method is enjoying the merit of being simple, where microscopy is the only tool to be used with normal palynological slides with no additional preparation. In addition to that, it is a method that enables the study of the qualitative character of the kerogen constituents.

Absolute abundance (grains/g) of particulate organic matter particles (palynomorphs, phytoclasts, and amorphous organic matter) were determined using an Olympus (BX41) transmitted light microscope at x100x and x250 magnifications. The palynofacies and corresponding kerogen types were scored depending on changes in the average absolute abundance of particulate organic matter (POM)

constituents with no regard to formation lithologies. Each counted palynodebris constituent was classified in terms of very rare (1-10 $x10^2$), rare (11-30 $x10^2$), present (31-60 $x10^2$), common (61-100 $x10^2$), frequent (101-150 $x10^2$), abundant (151-200 $x10^2$), very abundant (200-250 $x10^2$), and extremely abundant (>250 $x10^2$). Absolute abundance of each counted palynofacies constituents are shown in Appendix 3.

The AOM-phytoclast-palynomorphs (APP) ternary kerogen plot along with its associated key to marine palynofacies of Tyson (1993, 1995) was then used to determine the oxygenation conditions that prevailed during or after the deposition of each identified palynofacies in its depositional environment, which in turn gives an insight about the kerogen quality.

A. Palynofacies PF-1 (10150-8100 ft, 3094-2469 m)

This palynofacies covers the lower part of the Abu Tunis 1x borehole section and represents the Masajid Formation (sample 1), and the Alam El Buieb and the Alamein formations (samples 2-42). This palynofacies is characterized by extremely abundant AOM (34,400 particles/g) and phytoclast (18,200 particles/g), present palynomorphs (4,400 grains/g), and rare opaque phytoclast (2,900 particles/g) concentrations (Fig. 7.3).

Kerogen of palynofacies PF-1

The extreme abundances of the brown phytoclasts and the frequent occurrence of sporomorphs could suggest a kerogen type III (gas-prone) for this interval. However, these terrestrial organic mater are accompanied with extreme abundances of AOM, therefore, this terrestrial:marine mixture would rather suggest

a kerogen type III to II (mainly gas-prone). The plot of the PF-1 in the kerogen plot (Fig. 7.4) of Tyson (1995) suggests that organic matter of the PF-1 was deposited in nearshore shelf to basin transition settings under dysoxic-suboxic conditions (Tab. 7.2), where the AOM were diluted by terrestrially derived organic matter, which were unsuitable for the preservation of a high abundance of AOM. The overall nature of the AOM-terrestrial organic matter mixture of PF-1 infers a kerogen type III to II, which is mainly gas-prone.

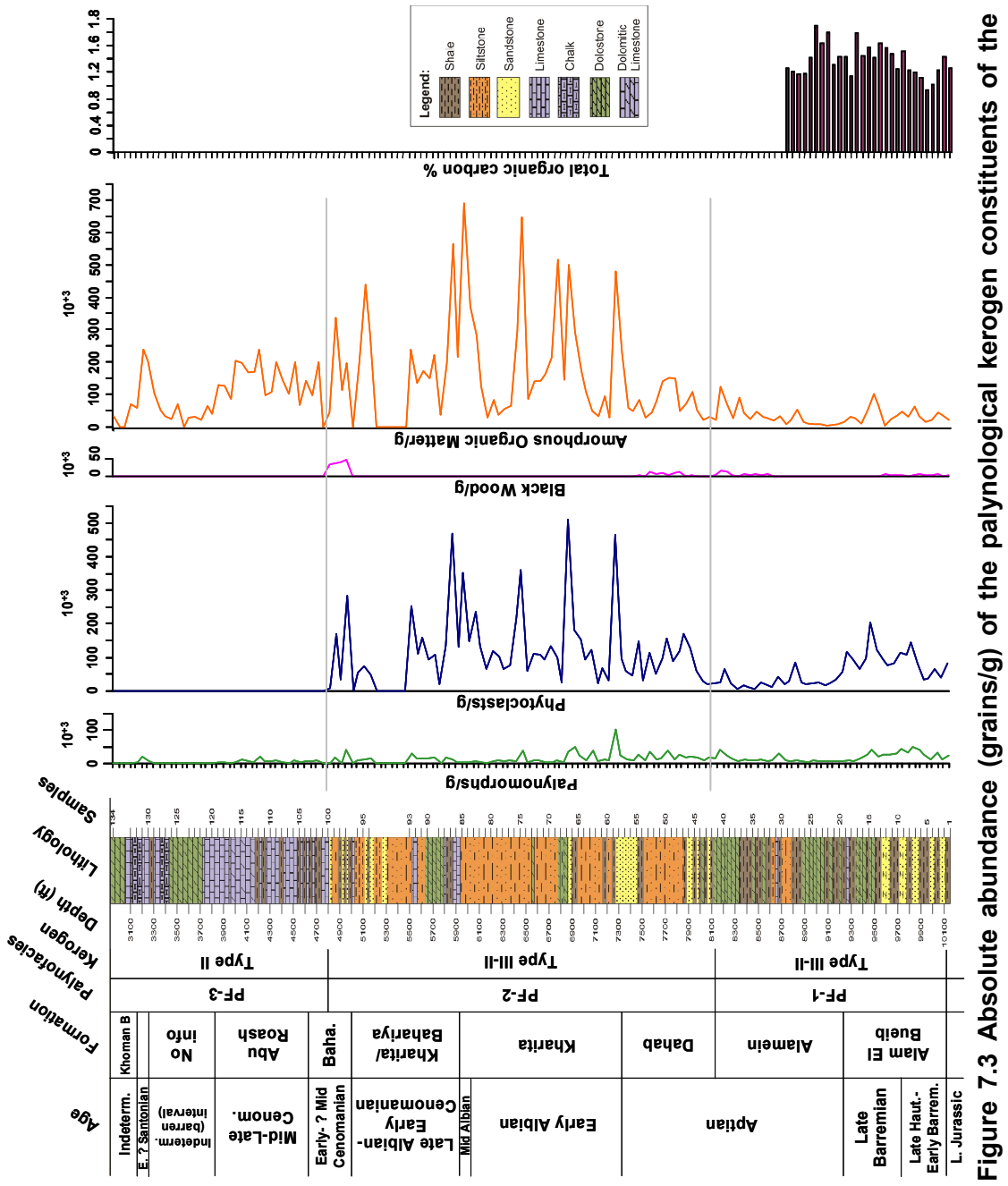

Figure 7.3 Absolute abundance (grains/g) of the palynological kerogen constituents of the Abu Tunis 1x borehole.

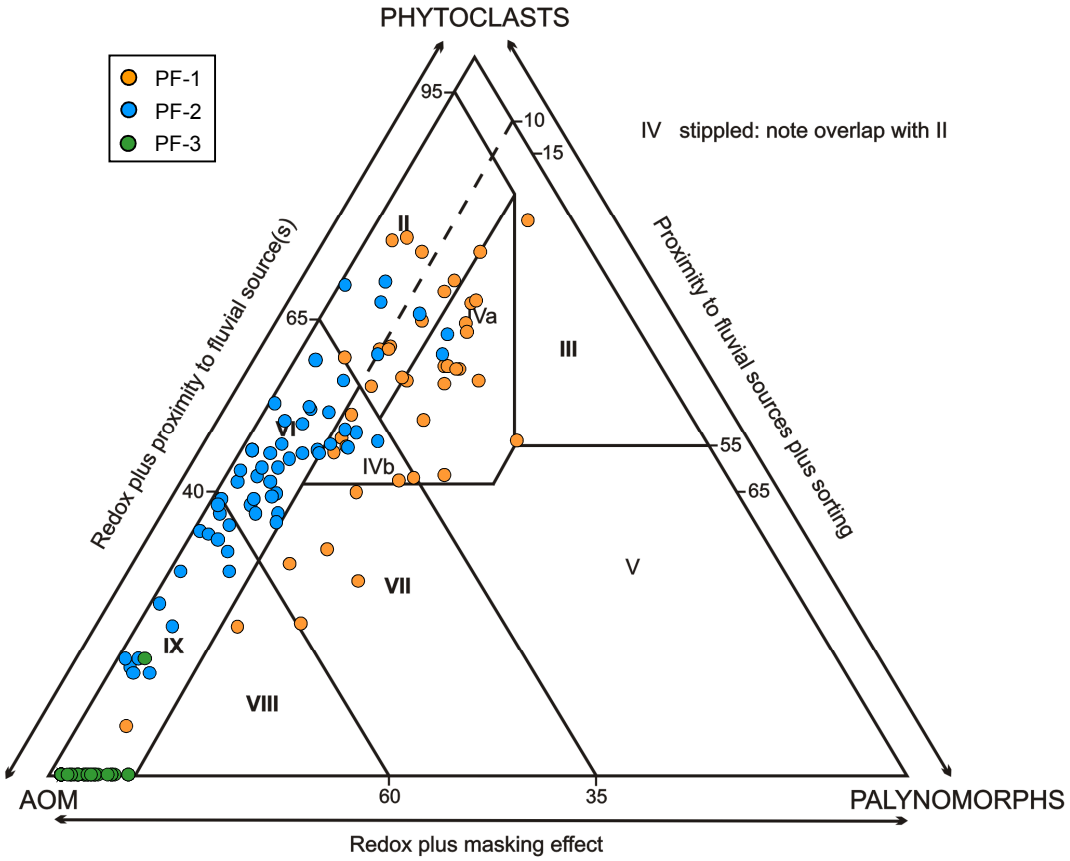

Figure 7.4 The Abu Tunis 1x palynofacies plot in the ternary kerogen plot of Tyson, 1995.

Palynofacies field	Environment	Kerogen type
I	Highly proximal shelf or basin.	III (gas prone)
II	Marginal dysoxic-anoxic basin.	III (gas prone)
III	Heterolithic oxic shelf ("proximal shelf").	III or IV (gas prone)
IV	Shelf to basin transition.	III or II (mainly gas prone)
V	Mud- dominated oxic shelf ("distal shelf").	III > IV (gas prone)
VI	Proximal suboxic-anoxic shelf.	II (oil prone)
VII	Distal dysoxic-anoxic "shelf".	II (oil prone)
VIII	Distal dysoxic-anoxic shelf.	II >> I (oil prone)
IX	Distal suboxic-anoxic basin.	II ≥ I (highly oil prone)

Table 7.2 Key to marine palynofacies fields indicated in the ternary kerogen plot (simplified from Tyson, 1995).

B. Palynofacies PF-2 (8050- 4800 ft, 2454-1463 m)

PF-2 is distinguished from the previous PF-1 by a very great increase in the AOM concentration, which is reflected in highly extreme abundances of AOM (185,500 particles/g). However, extreme abundances of phytoclasts (64,600 particles/g) also reflect a strong terrestrial influence, including concentrations of palynomorphs (5,200 grains/g) and opaque phytoclasts (5,000 particles/g).

Kerogen of palynofacies PF-2

The dominance of the AOM over terrestrially derived organic matter suggests a kerogen type II (oil-prone) for this interval. Plot of the PF-2 samples in the kerogen ternary diagram of Tyson (1995) shows that samples of the PF-2 were deposited in proximal shelf to distal basin settings under suboxic-anoxic conditions. This suggests that more oxygen depletion conditions were developed during or after the deposition of this palynofacies, which in turn, created more a reducing environment that was suitable for preservation of large amounts of AOM. These high AOM concentrations together with conditions favourable for AOM preservation support a kerogen type II, which is likely to produce oil.

C. Palynofacies PF-3 (4750-2950 ft, 1448-899 m)

PF-3 is clearly distinguished from the previous PF-1 and PF-2, where highly extreme abundances (120,900 particles/g) of AOM dominate the palynofacies composition, with minor terrestrial influence reflected in the concentration (4,200 grains/g) of palynomorphs. Phytoclasts and opaque plant debris are completely absent.

Kerogen of palynofacies PF-3

This palynofacies is almost composed of AOM, and thus an unequivocal kerogen type II (oil-prone) is assigned for the PF-3. Samples of the PF-3 plotted on the kerogen diagram of Tyson (1995), suggest that PF-3 was deposited in a distal basin setting under suboxic-anoxic conditions. Here sediments of the PF-3 were highly depleted in oxygen concentrations and lack any pronounced terrestrial influence. As a result, the PF-3 is regarded as a highly oil prone kerogen type.

7.2.3 Thermal maturation of organic matter

Thermal alteration of organic matter is generally defined as changes in the physical and chemical properties of the organic matter of a source rock during diagenesis, catagenesis, and metagenesis (Tissot & Welte, 1984).

There are several techniques, which have been used to measure organic maturation. The coal petrographers have used the vitrinite reflectance of polished surfaces to determine levels of maturation (e.g. Stach et al., 1982).

Simple geochemical methods to determine levels of maturation, include elemental analysis of organic matter in terms of the atomic H/C vs O/C plot (Van Krevelen, 1961 diagram; Tissot et al., 1979; Tissot & Welte, 1984), changes in the carbon composition in terms of C-H-O ternary diagram (Stephens, 1979) and by Rock Eval pyrolysis (Espitalié et al., 1977; Peters, 1986).

Palynologists use spores colour changes to determine levels of maturation of organic matter. For example, the thermal alteration index (TAI) of Staplin (1969), spore colour index (SCI) of Fisher et al. (1980), and thermal alteration index (TAI) of Pearson (1984). Here it was recognised that the exine colour of spores and pollen changes from light yellow to yellow orange, then brown and black, where yellow

represents immature organic matter, orange and brown represent mature organic matter, and black represents metamorphosed organic matter (Hunt, 1996). There are certain disadvantages to the visual kerogen study, i.e. the results may be biased due to caving in cuttings samples, mud contaminants, or reworking. This is in addition to the subjectivity of investigator when choosing specific colours. However, this method has many advantages, as it is an inexpensive method and provides rapid determination of maturity and assessment of hydrocarbon quality (Staplin, 1969; Correia, 1971; Raynaud & Robert, 1976; Tissot & Welte, 1984; Firth, 1993).

A. Visual spore colour and determination of thermal maturation

Here Pearson's (1984) colour chart (Fig. 7.5a) was used for visual colour determination with corresponding thermal alteration index (TAI) values following calibration with the colour scale (Fig. 7.5b) and reference slides of Fisher et al., (1980). Batten's colour scale (1980) was used to determine the maturation significance of spore colours (Tab. 7.3), where smooth thin-walled spores (e.g. *Deltoidospora, Triplanosporites, Dictyophyllidits, Cyathidites*) was chosen for colour determination, as they are most sensitive and reliable indicators of maturity (Batten, 1981). The slight and gradual change in colours observed from smooth spore exines through the studied borehole section has been found to increase with depth, and is equivalent to changes in TAI values from 2- to 3-.

Samples 1-19 (depth 10150-9250 ft) of the Alam El Buieb Formation are of marginally mature to mature organic matter, where the spores exhibit colours ranging between light brownish yellow to medium brown (Fig. 7.5). These colours correspond to TAI values of 3- to 3. Consequently, this sequence is likely to have produced hydrocarbons in fair amounts (Batten, 1981).

The lower part of the Alamein Formation (samples 20-30, depth 9200-8700 ft) is of a marginally mature organic matter, where the spores exhibit light brownish yellow colours, corresponding to TAI value of 3-. Accordingly, this sequence is likely to produce hydrocarbons, but not in a commercial amounts (Batten, 1981).

The upper part of the Alamein, the Kharita, Bahariya, Abu Roash, and Khoman B formations (samples 31-100, depth 8650-4800 ft) contain organic matter that must have undergone some chemical alterations, but is still immature. This is shown by spores from this interval, which exhibit yellow colours, which correspond to TAI values of 2. Therefore, this sequence is most unlikely to act as an active source rock.

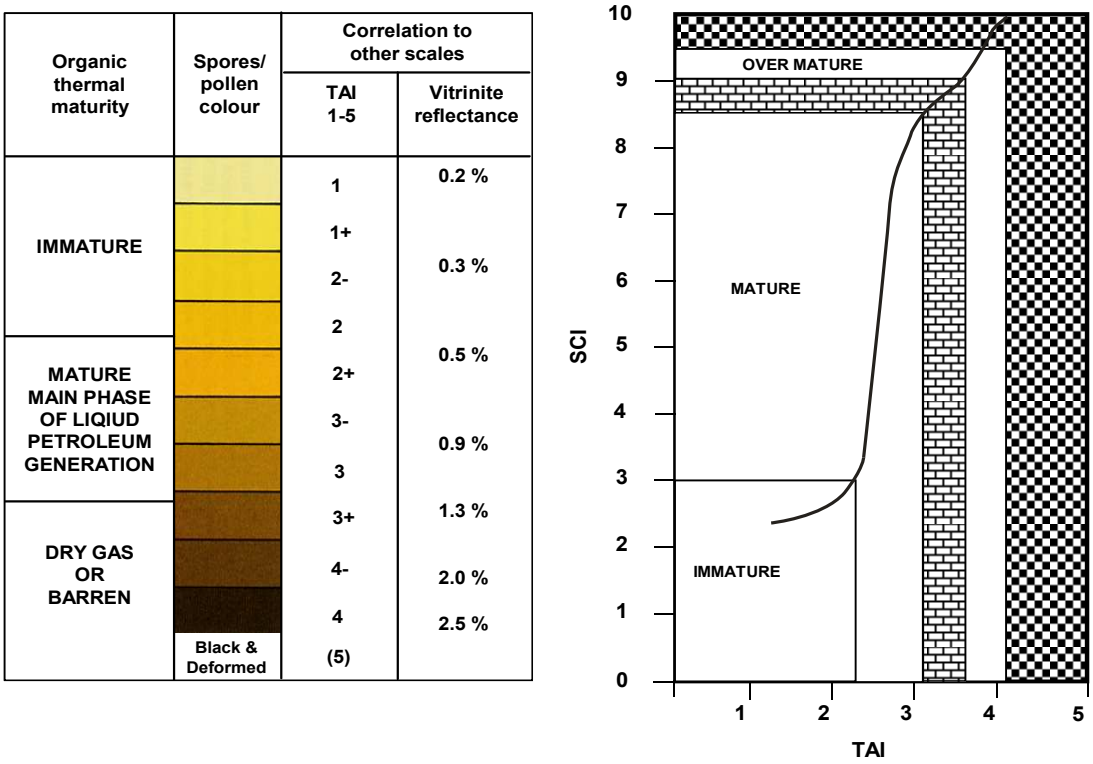

Figure 7.5 (A) Pearson's (1984) colour chart for organic thermal maturity determination correlated with thermal alteration index (TAI) and vitrinite reflectance; (B) Correlation of spore colour index (SCI) of Fisher et al., (1980) with thermal alteration index (TAI) of Staplin (1969) for organic thermal maturity determination.

B. Vitrinite reflectivity, burial history, geothermal characterisation, and thermal maturation of the Abu Tunis 1x borehole source rocks

Vitrinite is the maceral group derived from the lignified tissues of higher plants such as trunks, branches, stems, leaves, and root of trees and plants. Vitrinite is derived from the humic acid fraction of humic substances, predominately lignin and cellulose. The environment of preservation is usually weakly acidic and reducing. It has light orange to dark brown colours in transmitted white light, and grey to yellow colours in reflected light, and it does not fluoresce in UV light. In reflected light the vitrinite can be classified in to three types: unstructured vitrinite or "collinite", structured vitrinite or "telinite", and detrital vitrinite or "detrovitrinite" (Miles, 1994).

Observed spores colours	Maturation stages
1. Colourless, pale yellow, yellowish orange	Chemical change negligible; organic matter immature, having no source potential for hydrocarbon.
2. Yellow.	Some chemical change, but organic matter still immature
3. Light brownish yellow, yellowish orange	Some chemical change, marginally mature but not likely to have potential as a commercial source.
4. Light medium brown.	Mature, active volatilization, oil generation.
5. Dark brown.	Mature, production of wet gas and condensate, transition to dry gas phase.
6. Very dark brown-black.	Overmature; source potential for dry gas
7. Black (opaque).	Traces of dry gas only.

Table 7.3 Batten's palynomorph colour scale and corresponding maturation stages.

Vitrinite reflectance is a maturation indicator, where the reflectance of polished vitrinite particles increases with increasing time and/or temperature. Increases in reflectance are caused by progressive aromatization of the kerogen with accompanying loss of hydrogen (Miles, 1994). These irreversible chemical reactions have been found to increase exponentially with temperature and hence (Fig. 7.6), reflectance which measures these chemical changes also generally increases exponentially with a linear increase in temperature (Hunt, 1996).

The correlation of vitrinite reflectance with other maturation indicators and with oil and gas accumulations has resulted in an empirical definition of levels of maturation and oil and gas generation stages; where mean random (oil) vitrinite reflectance R_o value of 0.45 % is the lowest values associated with the generation of oil, R_o <0.5-0.7 % defines the "diagenesis" stage in which source rock is immature, but generally mark the beginning of commercial oil generation, 0.5-0.7 %. R_o ca. 1.3 % defines the top of the catagenesis stage "oil window", which is the main zone of oil generation, where the source rock is mature and produces commercial oil accumulations.

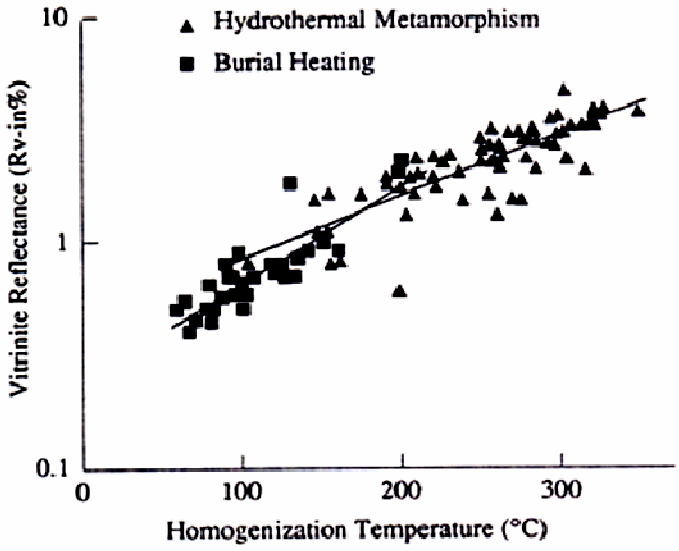

Figure 7.6 Exponential increase in vitrinite reflectance with linear increase in temperature (after Barker & Pawlewicz, 1994). Figure based on Barker & Goldstein (1990) with additional data from Aizawa (1989).

Vitrinite R_o values of 1.3-2 % defines the late catagenesis stages in which source rock is marginally over mature and wet gas (methane) and condensate generating R_o > 2 % defines the metagenesis stages in which source rock is overmature and methane gas remains as the only hydrocarbon (Tissot & Welte, 1984; Hunt, 1996). Vitrinite reflectance values only indicate levels of maturation of the source rock and cannot predict where oil or gas may be reservoired, because of the migration of the hydrocarbons.

In order to study the burial history and its relation to the geothermal regime, and hence the thermal maturation of the organic matter, modelling using *BasinMod*™ software was been carried out for the Abu Tunis 1x borehole. Vitrinite reflectivity measurements of samples that covered the whole phytoclast-rich clastic sequence of the Abu Tunis 1x borehole are shown in figure (7.8). These results showed that mean vitrinite reflectivity values decrease to stationary values in samples (AT34-AT114), which are rich in AOM (Tab. 7.4). This phenomenon was detected for example, by Marshall (1988) in the Devonian lacustrine source rock in north Scotland. This phenomenon is known as vitrinite suppression or retardation, and it was attributed by several geochemists and petrographers (e.g. Price & Barker, 1985; Hutton & Cook, 1990) to the dominance of the AOM in kerogen, where mature organic matter are adsorbed on the vitrinite particles and reduces its reflectance (Fig. 7.7).

Therefore, measured vitrinite reflectance made on samples that are phytoclast-rich have been chosen for the following thermal analyses. The measured vitrinite reflectance was compared to kinetically calculated vitrinite reflectance using the LLNL Easy % Rv developed by the Lawrence Livermore National Laboratories are included in the *BasinMod*™ (1993) burial model.

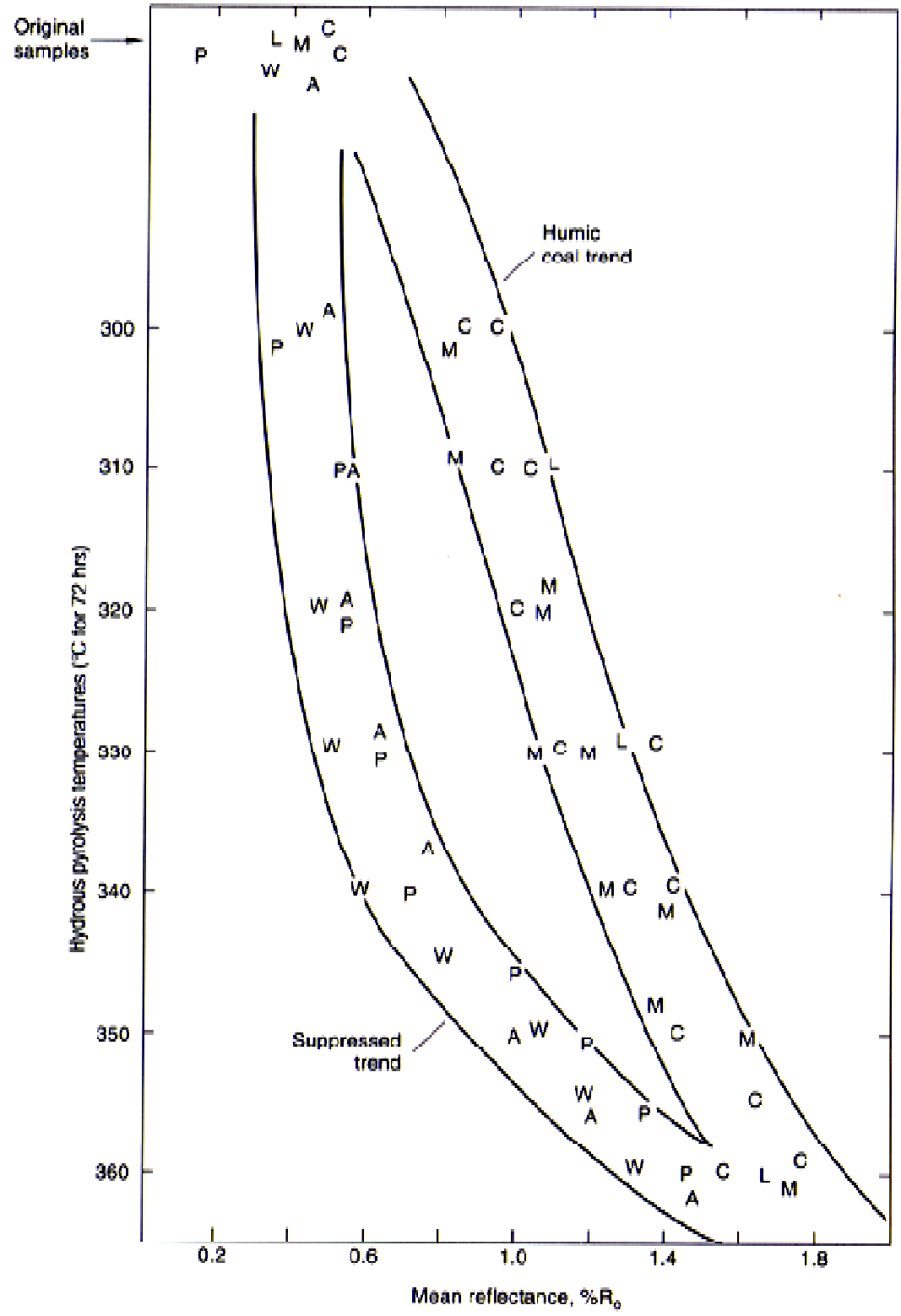

Figure 7.7 Suppressed vitrinite, mean random reflectance of vitrinite isolated from aliquots of humic coals and organic-rich shales: (C) Cretaceous coals of Wyoming plus Tertiary coals of Utah and the U. S. Gulf Coast; (L) lignite; (P) Phosphoria Shale of Wyoming; (W) Woodford Shale of Oklahoma; (A) Alum Shale of Scandinavia; (M) Mowry Shale of Wyoming. The samples were heated isothermally in water at temperatures from 300 to 360 °C, for 72 hours (after Lewan, 1993).

Kinetically calculated vitrinite reflectance (Rv %) using a Lawrence Livermore National Laboratories (LLNL) program called VITRIMAT is based on the assumption that Rv % is related to the chemical composition of kerogen. The VITRIMAT program calculates the vitrinite composition from a chemical kinetic model, in which separate reactions for the elimination of H_2O, CO_2, CH_4, and higher hydrocarbon (HC) from the coal structure are calculated. The program then calculates the vitrinite reflectance from correlations of Rv % with carbon content and with H/C and O/C ratios (Sweeney & Burnham, 1990). Profile of measured vitrinite reflectance is shown in figure (7.6).

The best acceptable match between the measured vitrinite reflectance and the kinetically calculated ones (Fig. 7.9) was achieved using a geothermal gradient of 23 ºC/km. Sedimentary basins can be classified according to the variation in geothermal gradient, where gradients of 18-20 ºC/km are cold, 25-27 ºC/km are normal, and 40-100 or up to 200 ºC/km are hot (Robert, 1988).

Sample no.	Formation	Depth (ft)	Ro %	n	sd
AT114	Abu Roash	4500	0.17	66	0.03
AT101	Bahariya	5150	0.24	52	0.05
AT88	Kharita/Bahariya	5800	0.26	48	0.04
AT82	Kharita	6100	0.34	60	0.04
AT78	Kharita	6300	0.35	55	0.04
AT71	Kharita	6650	0.36	46	0.03
AT65	Kharita	6950	0.36	57	0.03
AT59	Kharita	7250	0.37	49	0.04
AT52	Dahab	7600	0.37	61	0.05
AT46	Dahab	7900	0.38	69	0.04
AT40	Alamein	8200	0.39	44	0.07
AT34	Alamein	8500	0.39	59	0.08
AT23	Alamein	9050	0.56	65	0.07
AT15	Alam El Buieb	9450	0.55	48	0.11
AT9	Alam El Buieb	9750	0.56	48	0.11
AT3	Alam El Buieb	10050	0.58	66	0.06

Table 7.4 Vitrinite reflectivity data for the Abu Tunis (AT) 1x borehole formations.

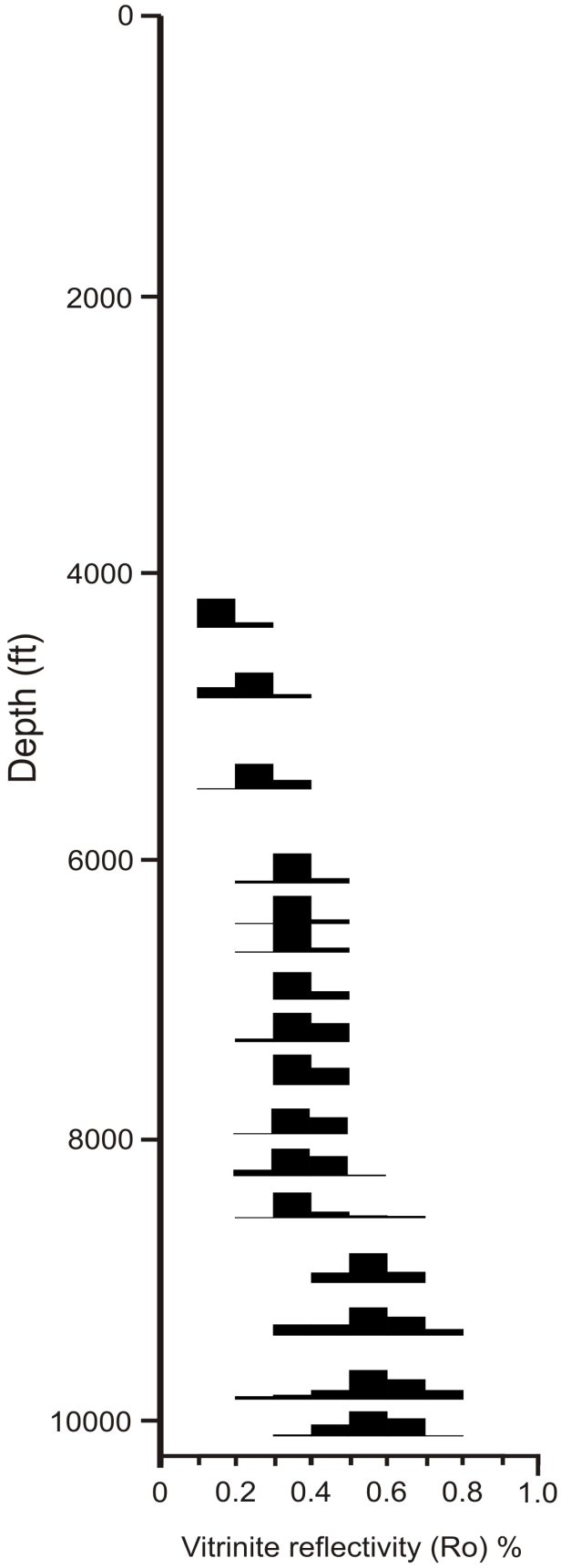

Figure 7.8 Vitrinite reflectivity profile for the different formations of the Abu Tunis 1x borehole.

The modelled geothermal gradient of 23 ºC/km used in the Abu Tunis 1x borehole, indicates that the geothermal characterisation of the underlying Jurassic sequence indicates a basin of normal geothermal gradient. The extrapolation of the modelled vitrinite reflectivity gradient (Fig. 7.9) to about 13,680 ft, which is the maximum burial depth for the lower Jurassic Wadi Natrun Formation, shows that this part of the Jurassic sequence could have reached a higher vitrinite value of > 0.7 % Rv. This in turn indicates that the lower part of the Wadi Natrun Formation will have just entered the middle stage of thermal maturation (Tissot & Welte, 1984; Hunt, 1996).

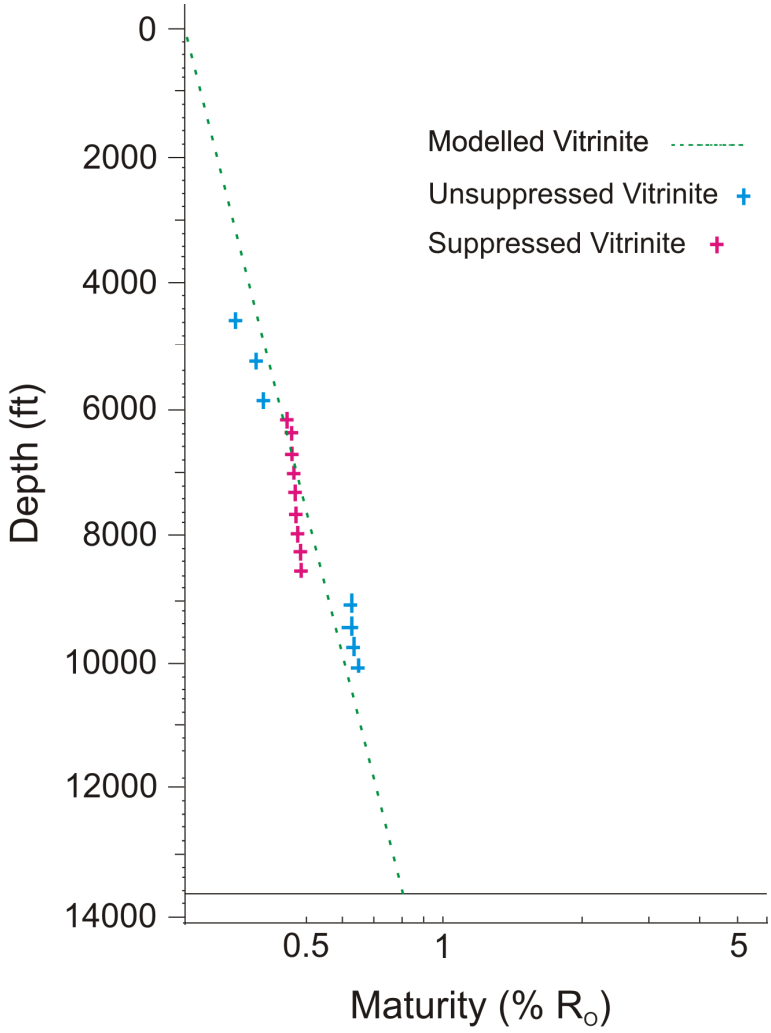

Figure 7.9 Measured vitrinite reflectivity and kinetically calculated (*BasinMod*™) vitrinite for the different formations of the Abu Tunis 1x borehole.

The burial history modelling using the *BasinMod*^{TM} software requires the entry of the thickness and the beginning age of each formation lithology. It also requires the addition of the type of the studied lithology, for which the software uses a pre-defined rock properties such as, the initial porosity, the compaction data, the density, the grain size, the thermal conductivity, and the heat capacity.

A burial history profile indicates that the Wadi Natrun Formation reached the oil window generation during the early Miocene (Fig. 7.10); whereas the lower part of the Alam El Buieb Formation entered the early mature stage of oil generation during late Oligocene and is currently still at the early mature stage.

7.2.4 Evaluation of source rock

The clastic rocks of the Alam El Buieb Formation and the overlying carbonate sequence of the Alamein Formation have average TOC values of 1.34 wt %, which is above the lower critical limit for a sedimentary rock to act as a source rock. The Alam El Buieb and Alamein formations exhibit a kerogen type III to II, which is likely to produce gas.

The visual maturity indices (i.e. TAI and SCI) along with the vitrinite maturity index (avg 0.55 %) indicate that the Alam El Buieb Formation is a source rock of very low potential as its organic matter is in the early stage of thermal maturity (Fig. 7.11). Thus it is not able to generate and expel hydrocarbons in appreciable amounts. Therefore, the Alam El Buieb Formation is considered as a non-commercial marginally mature to mature mainly gas-prone source rock.

The thick sandstones sediments of the Kharita and the lower Bahariya formations exhibit type II kerogens, which is likely to produce oil. Visual maturity indices and the extrapolated modelled vitrinite (avg 0.4 %), show that this clastic body is of immature organic matter. However, their immature organic matter shows this siltstone sequence as an inactive, immature rock of no potential to generate and expel hydrocarbon. The upper Bahariya, the Abu Roash, and the lower Khoman (B) formations, exhibits highly oil-prone kerogen type II. Visual thermal maturity index and extrapolated modelled vitrinite (avg 0.25 %) indicate that this carbonate sequence is immature, and therefore, is regarded as immature and with no potential to act as a source rock in the Abu Tunis borehole.

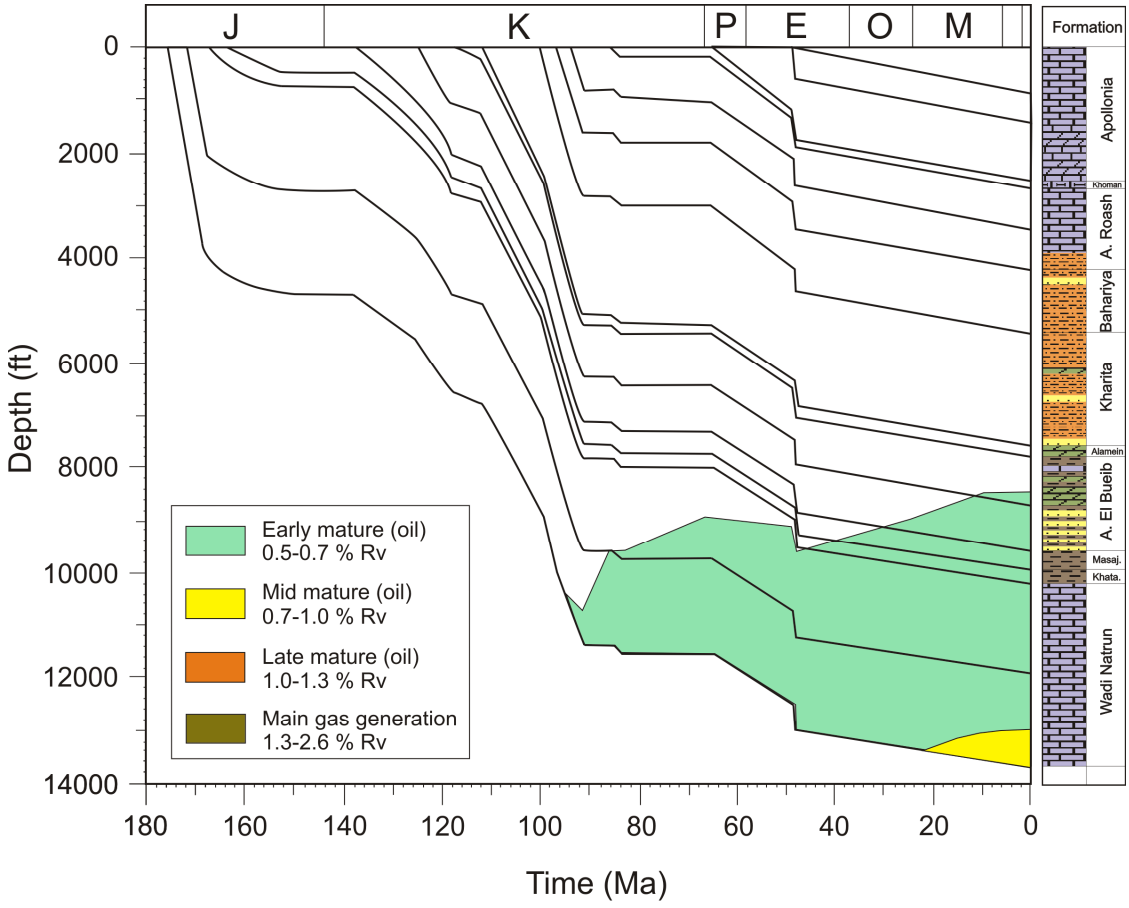

Figure 7.10 Kinetically modelled (*BasinMod*^{TM}) position of the hydrocarbon generative interval and maturity windows.

In summary, the sediments the Abu Tunis 1x borehole contains a non-commercial marginally mature to mature gas-prone source rock represented by the lower and middle Alam El Buieb Formation.

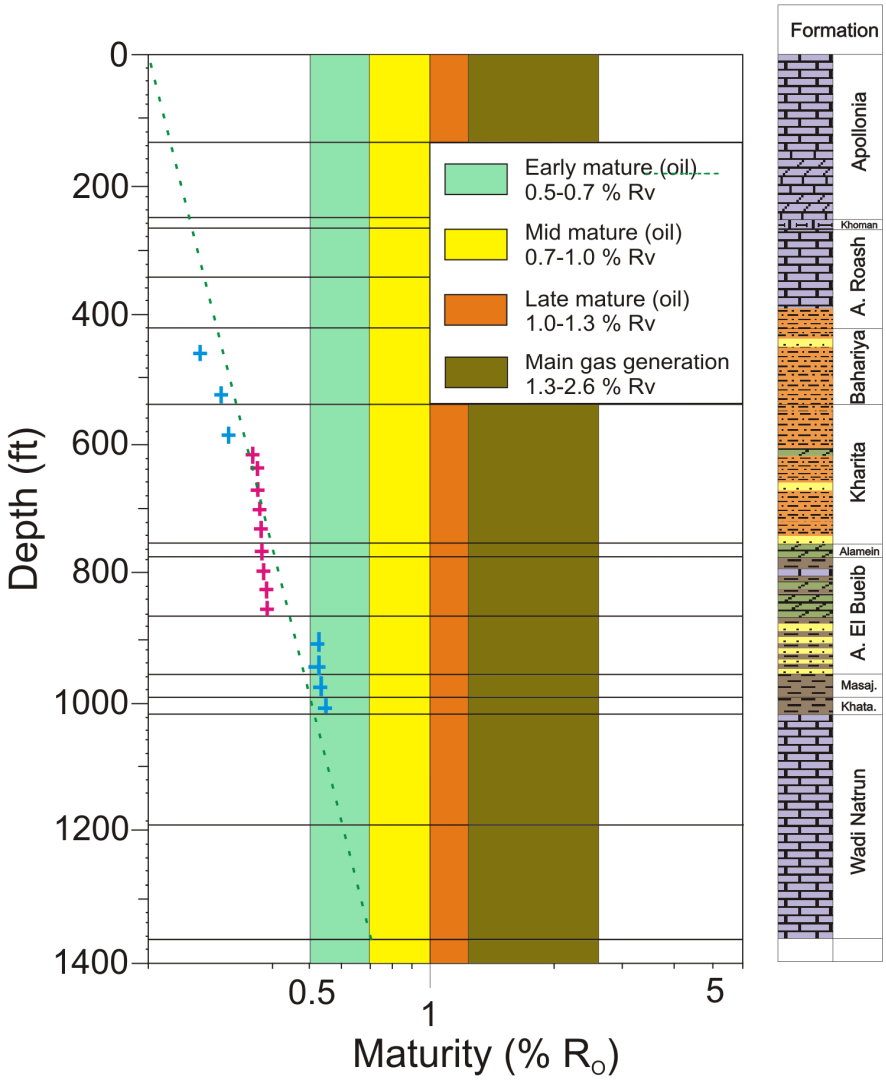

Figure 7.11 Measured vitrinite reflectivity as a maturity indicator for the Alam El Bueib source rock, and the maturity windows.

7.3 The BB80-1 borehole

The Malha and Raha formations of the BB80-1 borehole are mainly composed of thick barren sandstone units with a very few shale horizons overlain by two carbonate units that are relatively rich in terrestrial but poor in marine organic matter (Fig. 7.12). This sandstone lithology of the possible alluvial origin with its generally poor indigenous organic matter nature could be a potential hydrocarbon reservoir.

A reservoir is defined as a sedimentary body that is porous enough to act as a container for hydrocarbon accumulations within a trap, with its pores are sufficiently interconnected to allow the fluid hydrocarbons to flow and migrate through the hosting rocks. Clastic (sandstones) and carbonate rocks are typical types of hydrocarbon reservoirs (Allen & Allen, 1990).

Determination of hydrocarbon reservoir involves the integration of sedimentary facies interpretations from subsurface samples, depositional modelling, and wireline geophysical well data (Rider, 1986; Allen & Allen, 1990).

7.3.1 Depositional environment of the BB80-1 borehole

As mentioned before in chapter 6, the clastic sediments of the BB80-1 borehole are interpreted as being deposited in an alluvial environment with an occasional very shallow marine influence represented by marine shale horizons and carbonate rocks at the top of the sandstone body. This interpretation was generally based on the barren nature of the sandstone unit, proportions of terrestrial and marine palynomorphs and particulate organic matter in shale and carbonate samples, and the sedimentary facies interpretations derived from the wireline geophysical (gamma ray and resistivity) data.

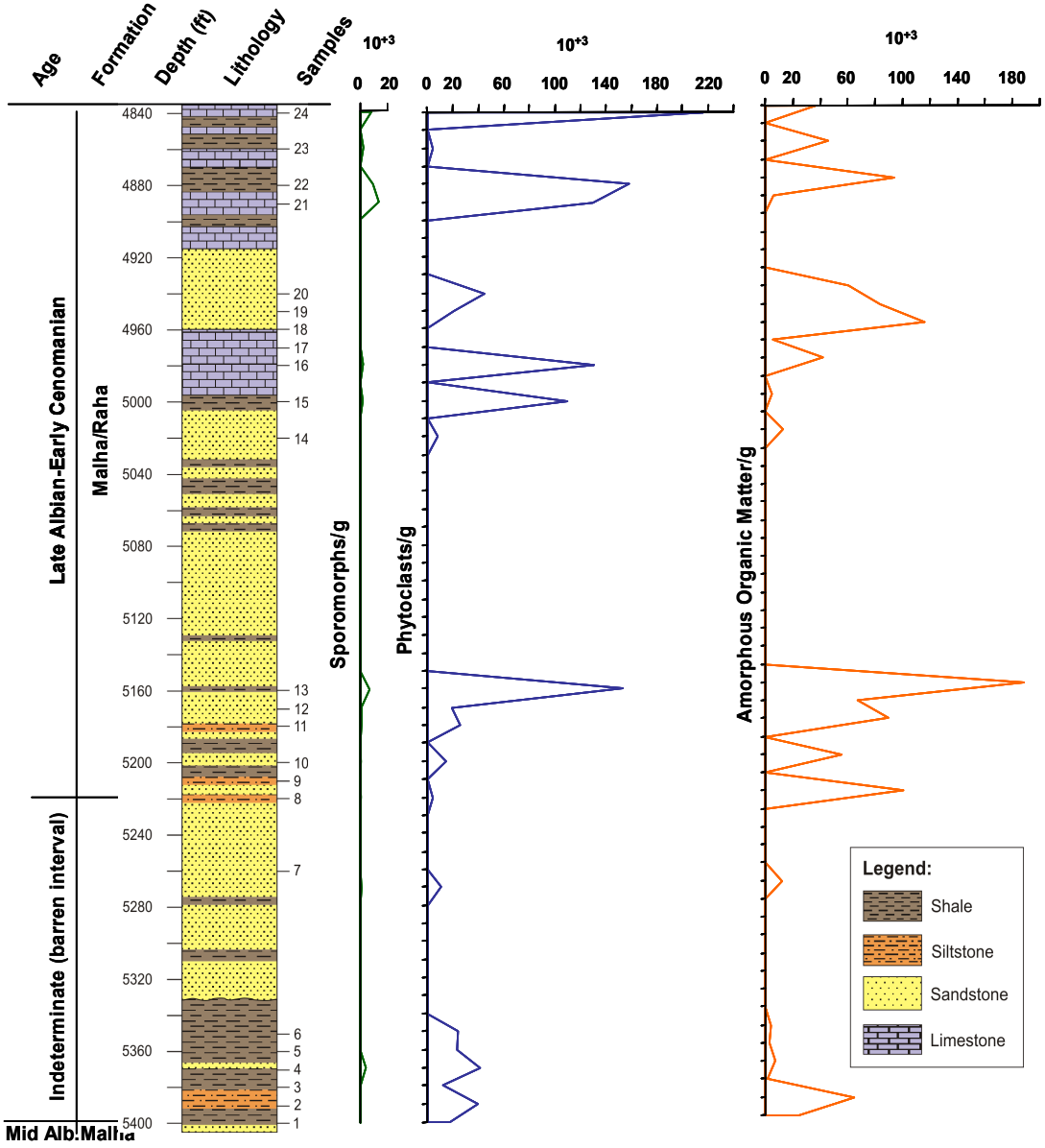

Figure 7.12 Absolute abundance (grains/g) of the palynological kerogen constituents of the BB80-1 borehole.

7.3.2 Sedimentary facies from gamma ray and resistivity data

The wireline data profile of the BB80-1 borehole (Fig. 7.13) indicates a shale unit at the base of the borehole section, based on high gamma ray values. Low resistivity and gamma values are indicative of a thick sandstone unit of the Malha and Raha formations, which is also supported by testing the cutting samples lithologies of this sequence. The identifications of the carbonate lithology from the ditch cutting samples and the resistivity profile are in agreement, as carbonate rocks of vuggy porosity are known to have moderate resistivity (Rider, 1986).

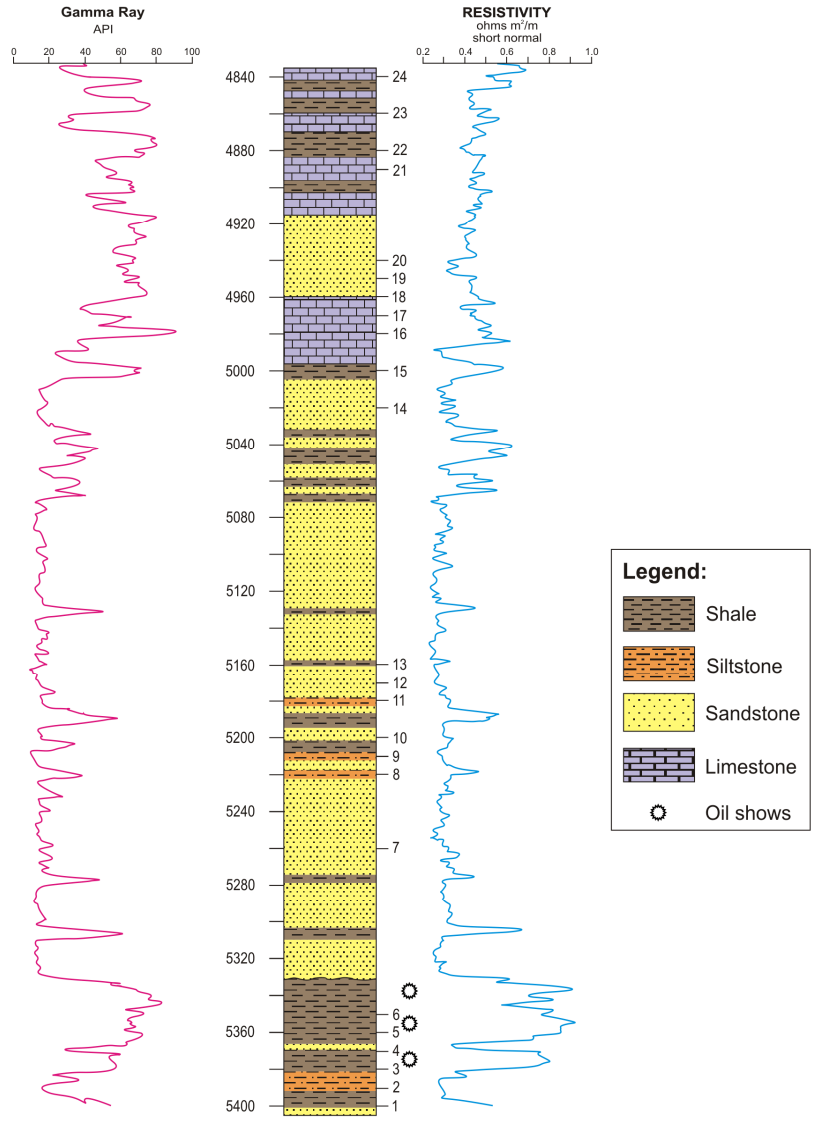

Figure 7.13 Gamma ray and resistivity data of the BB80-1 borehole showing changes in sedimentary facies and hydrocarbon shows.

7.3.3 Evaluation of the Malha and Raha formations sandstone

Porous sandstones rich in fluid hydrocarbons (in contrast to clean sandstones with saline formation waters), show a high resistivity as hydrocarbons are electrical insulators (e.g. Rider, 1986). This phenomenon was the principle to use resistivity data in detecting oil shows in reservoirs and source rocks. Very high resistivities of the shale unit at the base of the BB80-1 borehole section and in other shale horizons throughout the section, indicates the presence of some hydrocarbons (Fig. 7.13). This is supported by the thermal maturation investigation (TAI and SCI), where spores exhibit light medium brown colours, which correspond to TAI values of 3- to 3. This indicates that the organic matter of the shale beds could have generated some hydrocarbons (Batten, 1981).

A sandstone lithology that is poor in indigenous organic matter. The porous nature of this sandstone unit and indications of some hydrocarbon shows suggests that this sandstone lithology might have acted at some time as a hydrocarbon reservoir, however, due to lack in such supporting information for example, seismic data or basin analysis data; therefore no such interpretation can be made.

SUMMARY AND CONCLUSION

Ditch cutting samples have been palynologically processed from two Egyptian subsurface stratigraphic Cretaceous sections the Abu Tunis 1x borehole in the northern Western Desert and the BB80-1 borehole in the Gulf of Suez. The results show that the sediments of the Abu Tunis 1x borehole are rich in fine disseminated organic matter whilst the samples from the BB80-1 are lean in their organic matter content but of sufficient quality for simple palynological investigation. Therefore, a palynological investigation has been carried on both borehole samples. Integrated quantitative and qualitative data determined from the different organic matter constituents of the samples of both boreholes not only provides important information on the regional and intercontinental biostratigraphic framework of sediments and their possible depositional environments, but also provides an insight into palaeoclimate conditions prevailed during sedimentation. Furthermore, palynological, simple petrographic and chemical analyses of the organic matter, in addition to a burial history modelling of the Abu Tunis 1x sequence have contributed an understanding of the geothermal history of part of the Faghur Basin.

- The vertical distribution of recovered palynomorphs exhibited taxa of biostratigraphic importance and enabled the recognition of several Cretaceous biostratigraphic units that have not been recognised and/or studied in detail by the original operating drilling companies. In addition, the units originally designated by the same companies as “no information” have been revised, with eight palynologically identified biozones in the Abu Tunis 1x borehole but only two biozones in the generally organic-poor BB80-1 borehole. All palynozones have been largely identified by first appearance datum (FAD) of index taxa as follows:

A. The Abu Tunis 1x borehole

- Palynozone 1 of late Hauterivian-early Barremian age identified by total range of the African endemic gymnosperm pollen *Dicheiropollis etruscus*.
- Palynozone 2 of late Barremian age identified from the first appearance datum of angiosperm pollen grains *Retimonocolpites matruhensis, Retimonocolpites matruhensis-ghazaii complex*, *Retimonocolpites pennyi*, *Tucanopollis*, and marine phytoplankton genus *Pseudoceratium retusum* to just below the first appearance datum of the angiosperm pollen *Afropollis zonatus,* and marine phytoplankton *Florentinia mantellii* and *Pseudoceratium securigerum*.
- Palynozone 3 of Aptian age identified from the first appearance datum of *Afropollis zonatus, Florentinia mantellii,* and *Pseudoceratium securigerum* and just below the first appearance datum of marine phytoplankton *Palaeoperidinium cretaceum* to just below the first appearance datum of *Afropollis jardinus*.
- Palynozone 4 of early-mid Albian age identified from the first appearance datum of *Afropollis jardinus* to just below the first appearance datum of elaterate ephedroid pollen grains *Sofrepites legouxiae* and *Elaterosporites verrucatus*.
- Palynozone 5 of late Albian-early Cenomanian age identified by the total range of *Sofrepites legouxiae*.
- Palynozone 6 of early-? mid Cenomanian age, identified from the last appearance datum of *Sofrepites legouxiae* to just below the first appearance datum of the triporate angiosperm pollen *Proteacidites* cf. *africaensis*.
- Palynozone 7 of mid-late Cenomanian age identified by the total range of *Proteacidites* cf. *africaensis*.

- Palynozone 8 of early ? Santonian age identified by the total range of marine phytoplankton *Canningia senonica*.

B. The BB80-1 borehole

- Palynozone 1 of mid Albian age identified by the first appearance datum of *Afropollis jardinus* and *Elaterosporites klaszii*.
- Palynozone 2 of late Albian-early Cenomanian age identified from the first appearance datum of *Elaterocolpites castelainii, Elaterosporites africaensis* and *Afropollis kharamanensis* to the top of sequence.

❖ Correlation of the studied Egyptian Cretaceous sequences of the Abu Tunis 1x borehole with their contemporaneous regional and intercontinental equavalents, revealed a similarity in the biostratigraphic range (late Hauterivian) of the African-North South American endemic pollen index grain *Dicheiropollis etruscus* in Egypt with that of other countries which were confined to the same palaeotropics during the early Cretaceous such as Libya, Senegal and the Ivory Coast, with an earlier (Berriasian) questionable biostratigraphic appearance of *Dicheiropollis etruscus* recorded from West and NW African palaeosubtropical countries (e.g. Gabon and Morocco). This earlier appearance is suggested here to be less likely due to a diachroneity between the sedimentary sequences of both NE and West Africa and because as yet there is no (bio)- or litho-stratigraphic evidence for this. By comparing *Dicheiropollis etruscus* with the thermophilous drought resistant gymnosperm *Classopollis* (of close botanical affinity to *D. etruscus*) and of well know ecological and palaeoclimatic preference, it is suggested here that this discrepancy in the biostratigraphic appearances of *D. etruscus* could be due to palaeolatitudinal position (i.e. dry palaeosubtropical of West African countries *versus* relatively wetter

palaeotropical countries of NE Africa), where a dry palaeoclimate is suggested here to be the trigger of this earlier appearance.

Another phenomenon that is recognised is a similarity in acme events of the Winteraceaen angiosperm pollen *Afropollis* in the geologic record of both Egypt and Senegal. The upward persistent occurrence of *Afropollis zonatus* and *Afropollis operculatus* into the late Aptian of Senegal in contrast to an early Aptian only last appearance of the same species in Gabon has been attributed by Doyle et al. (1982) to a more favourable wetter palaeoclimate in Senegal that caused the upward continuation of the latter species. A similar event was recorded in Egypt by Schrank & Ibrahim, (1995) and is recorded here in Playnozone 3 of the Abu Tunis 1x borehole. It is suggest here that biostratigraphic units of Egypt and Senegal were actually synchronous, as both countries were confined to the same palaeolatitude (i.e. same palaeoclimate) and was both bordered by vast marine bodies namely; the Tethyan and Southern Atlantic Oceans for Egypt and Senegal respectively, where oceans are well know as the main driver for global (palaeo)- climate.

A synchronicity between the North and West African late Cretaceous biostratigraphic units is suggested here, in contrast to an argument made by Schrank & Ibrahim (1995), who proposed a diachroneity between latter areas based on a foraminiferally dated Egyptian downward range (late Turonian) of the gymnosperm index pollen *Droseridites senonicus* in contrast to an assumed – by Schrank & Ibrahim (op. cit.) - restriction of this species to the early Santonian of West Africa. However, it has been explained here that this downward extension has been recorded before in West Africa, and thus there is no evidence for this diachroneity, especially since other foraminifera-dated gymnosperm and angiosperm index forms have been recorded from similar stratigraphic horizons in both North and West Africa. The synchronicity proposed here was based on the continuous north-northeast African plate movement towards Laurasia as a response

to the breakup of Western Gondwana, where North and West African countries have been brought to a similar palaeosubtropical position and thus under similar palaeoclimate, whereby these regions should have similar palaeovegetation covers.

Palynoflora recovered from both the Abu Tunis 1x and BB80-1 exhibit characters of Cretaceous Phytogeographic Provinces of North African-North South America, which can be summarized as follows:

A. Egyptian pre-Albian palynofloral characters from the present study

The palynoflora recorded from the late Hauterivian-Aptian of the Abu Tunis 1x borehole shows a great similarity to that of the pre-Albian *Dicheiropollis*/*Afropollis* Phytogeographic Province of equatorial Africa. This palynoflora is characterised by high abundances and great diversity of smooth trilete spores (e.g. *Deltoidospora* and *Concavisporites*), the appearance of *Dicheiropollis*, low Barremian abundances and later Aptian diversification of *Ephedripites*, and an absence of bi- and tri-saccate pollen grains. The low abundances of *Exesipollenites* and *Araucariacites*, slightly more common occurrences of *Tucanopollis*, and finally the appearance and diversification of *Afropollis*, are also diagnostic features for this phytogeographic province.

B. Egyptian Albian-Cenomanian palynofloral characters from the present study

The palynoflora of the Abu Tunis 1x and the BB80-1 boreholes exhibits a remarkable similarity to that of the Albian-Cenomanian Elaterate Phytogeographic Province, which is represented here by the appearance of *Afropollis jardinus*, present occurrences of *Crybelosporites*, the appearance and diversification of gymnospermous elaterate pollen grains (e.g. *Elaterosporites*, *Elaterocolpites*, *Elateroplicites*, *Galeacornea*, and *Sofrepites*), presence of *Cretacaeiporites*, and

diversification of angiosperm pollen grains (e.g. *Tricolpites*, *Tricolporites*, and *Triporites*). A diminishing abundance and diversity of smooth trilete spores, absence of bi- and tri-saccate pollen grains, and the disappearance of *Classopollis* in the mid-late Cenomanian, also characterises the palynoflora recorded from the Abu Tunis 1x and the BB80-1 boreholes.

C. Egyptian Senonian palynofloral characters from the present study

The early Santonian palynoflora of the Abu Tunis 1x borehole is exclusively represented by marine phytoplankton and completely lacks any terrestrial palynomorphs that would be representative for the Senonian Palmae Province.

- Quantitative palynological data in terms of palynofacies analyses integrated with data derived from wireline logs along with lithological interpretations made from ditch cutting samples enabled interpretations of possible depositional environments from the Abu Tunis 1x and BB80-1 boreholes. The quantitative distribution of certain spores and pollen grains of known botanical affinity and ecological preferences were used as proxy indicators for the prevailing palaeoclimate during deposition of the investigated sedimentary sequences of both boreholes the Abu Tunis 1x and BB80-1. The quantitative vertical distributions in terms of grains or particles per gram of different terrestrial organic matter as represented by sporomorphs and associated plant debris and marine phytoplankton (largely represented by dinoflagellate cysts) plus the very minor microforaminifera test lining concentrations have been clustered at a high level using similarity analysis to produce recognizable groups of samples. These clusters to a great extent conform to the lithological units with vertical changes in overall organic matter concentrations reflecting changes in the depositional environments in term of transgression-

regression trends. These clusters of samples are referred here to as different palynofacies types, which in Abu Tunis 1x are represented by three palynofacies types with two sub-facies recognised. In the organic matter-poor samples of the BB80-1 borehole there is one palynofacies type with no such statistical analysis. The palynofacies types identified are as follows:

A. The Abu Tunis 1x borehole

Palynofacies PF-1A represents a lower clastic (shale and sandstones) unit of the Alam El Buieb Formation at the base of the sedimentary sequence of the Abu Tunis 1x. It is interpreted as being deposited during a regressive marine cycle, in a deltaic, possibly sub-aqueous delta-front to delta-top sub-environment, with the delta-front sub-environment experienced some periodic anoxic pore-water conditions.

Palynofacies PF-1B represents mixed shale and dolostone intercalations of the upper Alam El Bueib Formation and a significant mainly dolostone unit of the Alamein Formation. The included clastic and carbonate units are collectively believed to be deposited in inner shallow marine conditions during a relatively high water stand, which corresponded to the global late Barremian-Aptian transgression cycle, when reducing (anoxic) conditions prevailed during the deposition of the PF-1B sediments.

Palynofacies PF-2A represents another clastic unit that is mainly made of fine silts with some shale intercalations of the Dahab and Kharita formations. These sediments are suggested as being deposited during another regression period that was dominated by strong terrestrial fluvio-deltaic influence, possibly represented here by deltaic channel sedimentation that prograded for some time over prodelta

sediments as a response to sea level fall. Occasional short-lived local anoxic conditions are believed to have prevailed during this time.

Palynofacies PF-2B represents another clastic (fine silts and few shale horizons) unit of the Kharita Formation and the lower Bahariya Formation with a dolostone unit at the base of the Kharita Formation, where more distal but still nearshore conditions occurred. Here a partially marine isolated-brackish lagoonal setting of suboxic-anoxic conditions developed as a response to another second incoming but minor rise in sea level exemplified by general slight increases in marine phytoplankton in comparison to the preceding delta channel environment. This lagoonal setting is believed to have witnessed some occasional marine incursions, possibly during occasional connections to open marine waters or due to marine storms, which was reflected in more open marine phytoplankton concentration.

Palynofacies PF-3 represents a carbonate (limestone and dolostone) unit with some minor shale horizons of the lower Bahariya Formation and Abu Roash Formation. This sequence is interpreted as being deposited during the continued marine transgression that started to show in the preceding lagoonal environment of PF-2B, whereas outer shallow marine settings with basinal suboxic-anoxic conditions are suggested as being responsible for this distal carbonate sedimentation.

B. The BB80-1 borehole

Palynofacies PF-1 represents clastic sediments of the Malha and Raha formations, with very minor shale intercalations and a carbonate unit at the top of PF-1 rock sequence. The Malha clastics were mainly deposited in a nearly marine-isolated, far from source vegetation, continental basin. The environment was

possibly alluvial, and was invaded occasionally by marine incursions that resulted in deposition of marine shale under shallow marginal marine conditions. During the latter conditions the shale horizons experienced some occasional reducing (suboxic-anoxic) conditions, with a deepening in the marine conditions responsible for deposition of the carbonate unit of the Raha Formation.

- Investigation of the hydrocarbon potential of the Abu Tunis 1x and BB80-1 boreholes shows that sediments of the first borehole could have some potential. However, the BB80-1 has shown no potential as a hydrocarbon generator on account of both its organic poor-clastic part and the very few oil-shale horizons present in the sequence. For the Abu Tunis 1x borehole, the hydrocarbon investigation included a palynofacies analysis for kerogen type identification accompanied by spore colour determination of the thermal maturation. Elemental analysis of borehole samples for total organic carbon content was used for evaluating potential generative source rocks, with vitrinite reflectivity measurements used to determine thermal maturation and the geothermal history of the Faghur Basin through the Abu Tunis 1x borehole, and to identify the oil window of such potential source rock. Burial history modelling was also applied to the whole sedimentary sequence of the Abu Tunis 1x borehole to understand the geothermal history, locate generative rock sequences, and determine the timing of possible hydrocarbon generation within the Faghur Basin. The whole investigation can be summarised as follows:

A. The Abu Tunis 1x borehole

For the Abu Tunis 1x borehole sequence, three palynofacies types have been identified for kerogen determination, with the lower part of the borehole sequence equated as palynofacies PF-1 which corresponds to the uppermost part of the Masajid Formation, the Alam El Buieb and Alamein formations. Here terrestrially dominated organic matter with less AOM revealed a kerogen type III to II, which is mainly gas prone. Palynofacies PF-2 represents a major clastic unit of the Dahab, Kharita and the lower Bahariya formations that consist of fine silts and a few organic rich-shale horizons that are relatively dominated by AOM but still with a substantial terrestrial organic matter, which gives an overall kerogen type II, which is oil prone. Carbonate rocks of the upper Bahariya and Abu Roash formations, exhibit a highly oil prone kerogen type II, as the organic matter of PF-3 is entirely composed of AOM. The overall evaluation of the Abu Tunis 1x borehole sediments can be summarised as follows:

The clastic rocks of the Alam El Buieb Formation and the overlying carbonate sequence of the Alamein Formation have average TOC above the lower critical limit for a sedimentary rock to act as a source rock. The Alam El Buieb and Alamein formations exhibit a kerogen type III to II, which is likely to produce gas. The visual maturity indices (i.e. TAI and SCI) along with the vitrinite maturity index indicate that the Alam El Buieb Formation is a source rock of very low potential as its organic matter is still in the early stage of thermal maturity. Thus it is not able to generate and expel hydrocarbons in appreciable amounts. Therefore, the Alam El Buieb Formation is considered as a non-commercial marginally mature to mature mainly gas-prone source rock.

The thick siltstone sediments of the Dahab, Kharita and the lower Bahariya formations exhibit type II kerogens, which are likely to produce oil. Visual maturity indices and the vitrinite reflectance, show that this clastic body contains immature

organic matter. This is despite the fact that these clastic sediments contain high proportions of AOM.

The upper Bahariya, the Abu Roash, and the lower Khoman (B) formations, exhibits highly oil-prone kerogen type II. Visual thermal maturity index and vitrinite index indicate that this carbonate sequence is immature, and therefore, is regarded as immature and with no potential to act as a source rock in the Abu Tunis 1x borehole.

B. The BB80-1 borehole

In terms of visual thermal maturation (i.e. TAI and SCI), only palynological investigations on some oil-shale horizons have been applied to the hydrocarbon potential of the BB80-1 borehole. These have been integrated with geophysical data and sedimentological characters deduced from the porous nature of its sandstone lithology, which is poor in organic matter. This sandstone lithology could be regarded as a hydrocarbon reservoir, however, there is no supporting information to support such a conclusion.

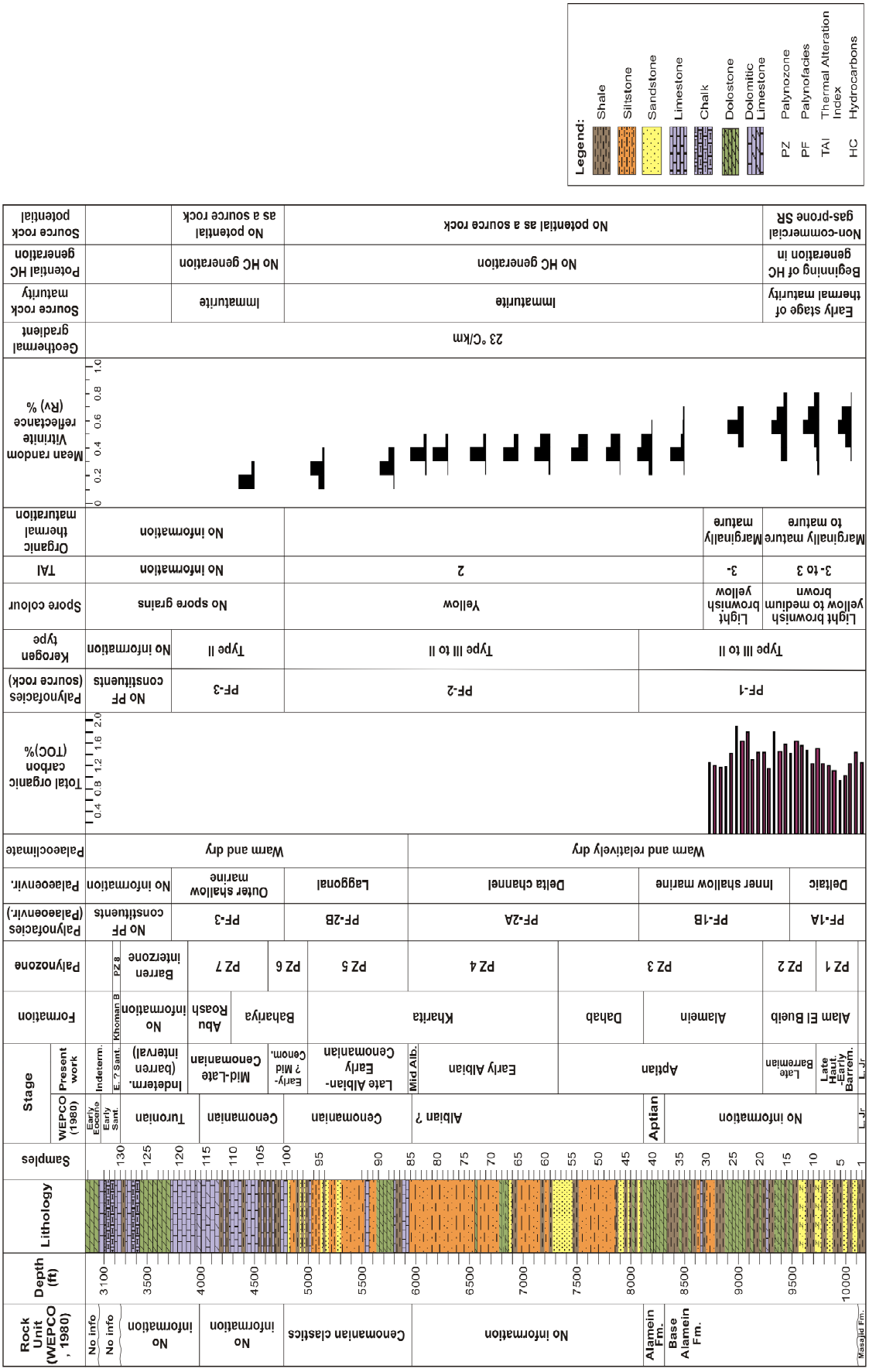

Table 8.1 Summary of age assessment, palaeoenvironmental and palaeoclimatic interpretations, and hydrocarbon evaluation of the Abu Tunis 1x borehole, northern Western Desert, Egypt.

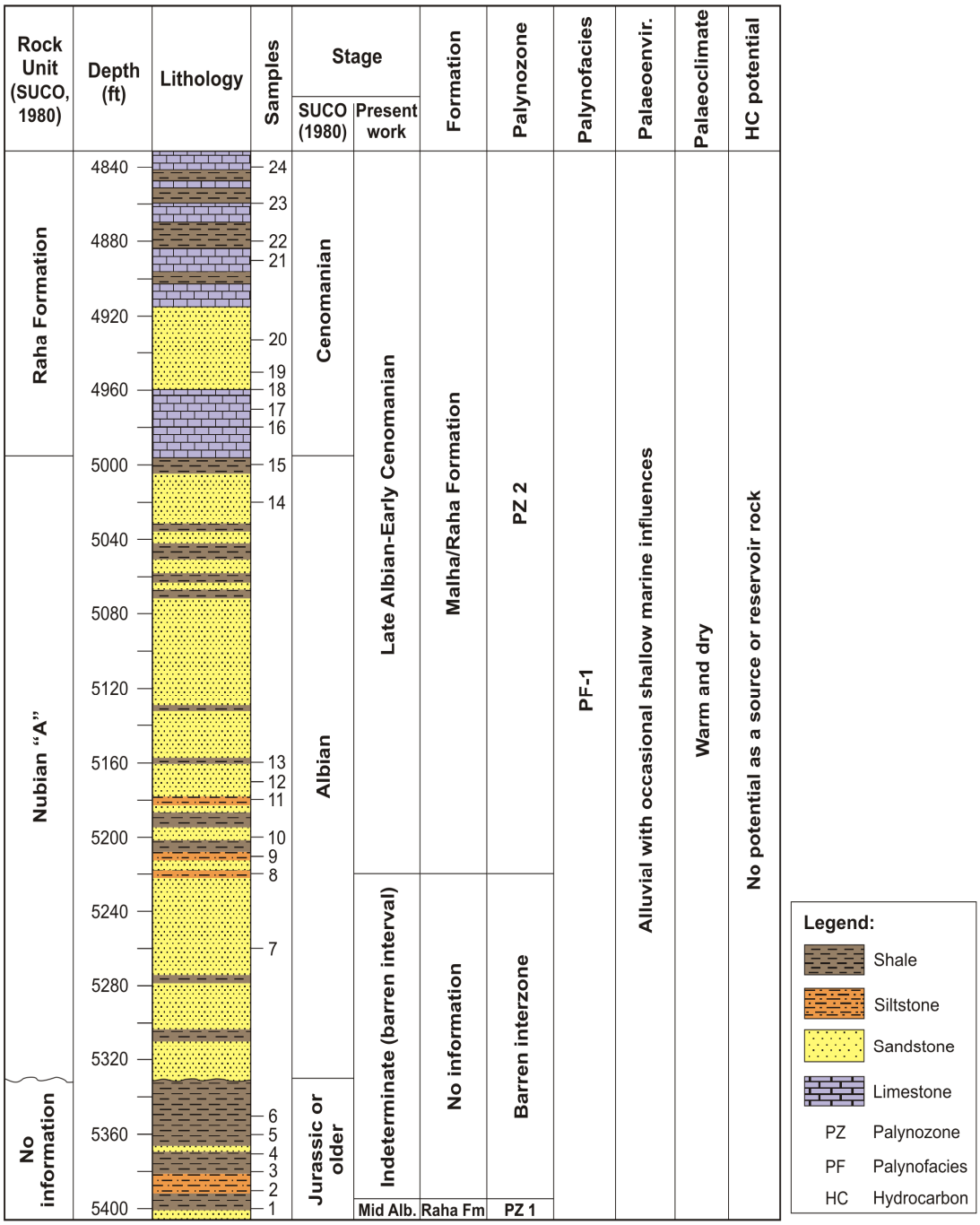

Table 8.2 Summary of age assessment, palaeoenvironmental and palaeoclimatic interpretations, and hydrocarbon evaluation of the BB80-1 borehole, Gulf of Suez, Egypt.

APPENDIX 1

List of palynological samples from the Abu Tunis 1x borehole and total recovery of palynomorphs in terms of grains/gram of sediments.

Sample number	Depth feet (meter)	Palynological status and total recovery of palynomorphs (grains/gram)	Sample number2	Depth feet (meter)2	Palynological status and total recovery of palynomorphs (grains/gram)2	Sample number3	Depth feet (meter)3	Palynological status and total recovery of palynomorphs (grains/gram)3
1	10,150 (3,094)	productive (9038)	46	7,900 (2,408)	productive (19003)	91	5,650 (1,722)	productive (10432)
2	10,100 (3,078)	productive (5131)	47	7,850 (2,393)	productive (11613)	92	5,600 (1,707)	productive (11148)
3	10,050 (3,063)	productive (6940)	48	7,800 (2,377)	productive (12296)	93	5,550 (1,692)	productive (14574)
4	10,000 (3,048)	productive (5175)	49	7,750 (2,362)	productive (19003)	94	5,500 (1,676)	productive (9914)
5	9,950 (3,033)	productive (10604)	50	7,700 (2,347)	productive (9088)	95	5,450 (1,661)	productive (5142)
6	9,900 (3,018)	productive (27772)	51	7,650 (2,332)	productive (9088)	96	5,400 (1,646)	productive (6334)
7	9,850 (3,002)	productive (10284)	52	7,600 (2,316)	productive (11334)	97	5,350 (1,631)	productive (13117)
8	9,800 (2,987)	productive (9022)	53	7,550 (2,301)	productive (11002)	98	5,300 (1,615)	barren
9	9,750 (2,972)	productive (9909)	54	7,500 (2,286)	productive (16079)	99	5,250 (1,600)	productive (5268)
10	9,700 (2,957)	productive (6190)	55	7,450 (2,271)	productive (4861)	100	5,200 (1,585)	barren
11	9,650 (2,941)	productive (5227)	56	7,400 (2,256)	productive (10452)	101	5,150 (1,570)	barren
12	9,600 (2,926)	productive (7805)	57	7,350 (2,240)	productive (7397)	102	5,100(1,554)	productive (951)
13	9,550 (2,911)	productive (5759)	58	7,300 (2,225)	productive (16079)	103	5,050 (1,539)	productive (2131)
14	9,500 (2,896)	productive (8038)	59	7,250 (2,210)	productive (8361)	104	5,000 (1,524)	productive (520)
15	9,450 (2,880)	productive (5274)	60	7,200 (2,195)	productive (10665)	105	4,950 (1,509)	productive (104)
16	9,400 (2,865)	productive (2448)	61	7,150 (2,179)	productive (18177)	106	4,900 (1,494)	productive (913)
17	9,350 (2,850)	productive (2828)	62	7,100 (2,164)	productive (17419)	107	4,850 (1,478)	productive (1596)
18	9,300 (2,835)	productive (4843)	63	7,050 (2,149)	productive (31672)	108	4,800 (1,463)	productive (2488)
19	9,250 (2,819)	productive (3816)	64	7,000 (2,134)	productive (19003)	109	4,750 (1,448)	productive (2714)
20	9,200 (2,804)	productive (2469)	65	6,950 (2,1180	productive (52258)	110	4,700 (1,433)	productive (5973)
21	9,150 (2,789)	productive (3470)	66	6,900 (2,103)	productive (17350)	111	4,650 (1,417)	productive (4430)
22	9,100 (2,774)	productive (3738)	67	6,850 (2,088)	barren	112	4,600 (1,402)	productive (4645)
23	9,050 (2,758)	productive (4185)	68	6,800 (2,073)	productive (9502)	113	4,550 (1,387)	barren
24	9,000 (2,743)	productive (2070)	69	6,750 (2,057)	productive (29862)	114	4,500 (1,372)	productive (1136)
25	8,950 (2,728)	productive (3234)	70	6,700 (2,042)	productive (20099)	115	4,450 (1,356)	productive (1728)
26	8,900 (2,713)	productive (3077)	71	6,650 (2,027)	productive (12394)	116	4,400 (1,341)	productive (1215)
27	8,850 (2,697)	productive (3440)	72	6,600 (2,012)	productive (13936)	117	4,350 (1,326)	productive (843)
28	8,800 (2,682)	productive (3670)	73	6,550 (1,996)	productive (4645)	118	4,300 (1,311)	productive (674)
29	8,750 (2,667)	productive (8418)	74	6,500 (1,981)	productive (8361)	119	4,250 (1,295)	productive (893)
30	8,700 (2,652)	productive (5028)	75	6,450 (1,966)	productive (6148)	120	4,200 (1,280)	barren
31	8,650 (2,637)	productive (4646)	76	6,400 (1,951)	productive (9954)	121	4,150 (1,265)	barren
32	8,600 (2,621)	productive (3944)	77	6,350 (1,935)	productive (4751)	122	4,100 (1,250)	barren
33	8,550 (2,606)	productive (8395)	78	6,300 (1,920)	productive (5807)	123	4,050 (1,234)	barren
34	8,500 (2,591)	productive (5359)	79	6,250 (1,905)	barren	124	4,000 (1,219)	barren
35	8,450 (2,576)	productive (2582)	80	6,200 (1,890)	barren	125	3,950 (1,204)	barren
36	8,400 (2,560)	productive (3609)	81	6,150 (1,875)	barren	126	3,900 (1,189)	barren
37	8,350 (2,545)	productive (2070)	82	6,100 (1,859)	productive (5627)	127	3,850 (1,173)	barren
38	8,300 (2,530)	productive (7406)	83	6,050 (1,844)	productive (3266)	128	3,800 (1,158)	barren
39	8,250 (2,515)	productive (8261)	84	6,000 (1,829)	productive (3266)	129	3,750 (1,143)	barren
40	8,200 (2,499)	productive (6716)	85	5,950 (1,814)	productive (2944)	130	3,700 (1,128)	productive (1720)
41	8,150 (2,484)	productive (7685)	86	5,900 (1,798)	productive (5226)	131	3,650 (1,113)	productive (1060)
42	8,100 (2,469)	productive (7716)	87	5,850 (1,783)	productive (7159)	132	3,600 (1,097)	barren
43	8,050 (2,454)	productive (5680)	88	5,800 (1,768)	productive (6334)	133	3,550 (1,082)	barren
44	8,000 (2,438)	productive (4803)	89	5,750 (1,753)	productive (8710)	134	3,500 (1,067)	Barren
45	7,950 (2,423)	productive (10326)	90	5,700 (1,737)	productive (7742)			

List of palynological samples from the BB80-1 borehole and total recovery of palynomorphs in terms of grains/gram of sediments.

Sample number	Depth feet (meter)	Palynological status and total recovery of palynomorphs (grains/gram)	Sample number2	Depth feet (meter)	Palynological status and total recovery of palynomorphs (grains/gram)3
1	5,400-10 (1,646-49)	productive (504)	**40**	4,530-40 (1,381-84)	barren
2	5,390-00 (1,643-46)	barren	**41**	4,500-10 (1,372-75)	barren
3	5,380-90 (1,640-43)	barren	**42**	4,490-00 (1,369-72)	barren
4	5,370-80 (1,637-40)	barren	**43**	4,470-80 (1,362-66)	barren
5	5,360-70 (1,634-37)	barren	**44**	4,450-60 (1,356-59)	barren
6	5,350-60 (1,631-34)	barren	**45**	4,410-20 (1,344-47)	barren
7	5,260-70 (1,603-06)	barren	**46**	4,400-10 (1,341-44)	barren
8	5,220-30 (1,591-94)	productive (508)	**47**	4,360-70 (1,329-32)	barren
9	5,210-20 (1,588-91)	productive (391)	**48**	4,350-60 (1,326-29)	barren
10	5,200-10 (1,585-88)	productive (1375)	**49**	4,310-20 (1,314-17)	barren
11	5,180-90 (1,579-82)	productive (2551)	**50**	4,300-10 (1,311-14)	barren
12	5,170-80 (1,576-79)	productive (909)	**51**	4,290-00 (1,308-11)	barren
13	5,160-70 (1,573-76)	productive (1340)	**52**	4,280-90 (1,305-08)	barren
14	5,020-30 (1,530-33)	barren	**53**	4,260-70 (1,298-01)	barren
15	5,000-10 (1,524-27)	productive (1340)	**54**	4,250-60 (1,295-98)	barren
16	4,980-90 (1,518-21)	productive (2903)	**55**	4,230-40 (1,289-92)	barren
17	4,970-80 (1,515-18)	barren	**56**	4,220-30 (1,286-89)	barren
18	4,960-70 (1,512-15)	productive (1340)	**57**	4,190-00 (1,277-80)	barren
19	4,950-60 (1,509-12)	barren	**58**	4,160-70 (1,268-71)	barren
20	4,940-50 (1,506-09)	barren	**59**	4,150-60 (1,265-68)	barren
21	4,890-00 (1,490-94)	productive (13936)	**60**	4,140-50 (1,262-65)	barren
22	4,880-90 (1,487-90)	productive (5139)	**61**	4,130-40 (1,259-62)	barren
23	4,860-70 (1,481-84)	productive (2224)	**62**	4,120-30 (1,256-59)	barren
24	4,840-50 (1,475-78)	productive (13936)	**63**	4,100-10 (1,250-53)	barren
25	4,830-40 (1,472-75)	barren	**64**	4,090-00 (1,247-50)	barren
26	4,790-00 (1,460-63)	barren	**65**	4,070-80 (1,241-44)	barren
27	4,780-90 (1,457-60)	barren	**66**	4,040-50 (1,231-34)	barren
28	4,760-70 (1,451-54)	barren	**67**	4,030-40 (1,228-31)	barren
29	4,750-60 (1,448-51)	barren	**68**	4,010-20 (1,222-25)	barren
30	4,740-50 (1,445-48)	barren	**69**	4,000-10 (1,219-22)	barren
31	4,730-40 (1,442-45)	barren	**70**	3,980-90 (1,213-16)	barren
32	4,670-80 (1,423-26)	barren	**71**	3,970-80 (1,210-13)	barren
33	4,660-70 (1,420-23)	barren	**72**	3,950-60 (1,204-07)	barren
34	4,640-50 (1,414-17)	barren	**73**	3,940-50 (1,201-04)	barren
35	4,630-40 (1,411-14)	barren	**74**	3,920-30 (1,195-98)	barren
36	4,600-10 (1,402-05)	barren	**75**	3,900-10 (1,189-92)	barren
37	4,570-80 (1,393-96)	barren	**76**	3,890-00 (1,186-89)	barren
38	4,550-60 (1,387-90)	barren	**77**	3,880-90 (1,183-86)	barren
39	4,540-50 (1,384-87)	barren	**78**	3,850-60 (1,173-77)	barren

APPENDIX 2

List of absolute abundance (grains/gram of sediments) of different palynofacies constituents of the Abu Tunis 1x borehole used in the palynofacies analysis and palaeoenvironmental interpretations.

Sample no.	Depth ft	Depth m	Sample wt (g)	Total Count	Lycopodium spores counted	Pteridophytes/g	Schizaeaceae/g	Saccate pollen/g	*Classopollis*/g	*Ephedripites*/g	Angiosperms/g	Dinocysts/g	MTL-s/g	Black Wood/g	Tracheids/g	Cuticles/g	Membranous Tissue/g	Sum (grains/g)
1	10150	2914	3	250	7	24487	0	597	0	0	0	597	597	41209	78835	1792	1194	149310
2	10100	2899	3	250	16	10452	0	0	0	0	0	784	0	13587	39455	784	261	65323
3	10050	2884	3	250	19	4621	0	0	0	0	0	220	0	13202	27944	8801	220	55009
4	10000	2868	3	250	33	5067	0	127	0	0	0	127	0	10135	15456	633	127	31672
5	9950	2853	3	250	35	10404	116	0	231	0	0	578	0	5317	10981	1156	116	28899
6	9900	2838	3	250	7	32475	0	560	2240	0	0	1680	0	40314	61030	1680	0	139978
7	9850	2823	3	250	13	11256	0	0	643	0	0	0	0	28300	36983	3216	0	80397
8	9800	2808	3	250	8	8361	0	0	2090	0	0	523	0	21426	96155	2090	0	130646
9	9750	2792	3	250	13	18009	322	0	965	0	0	965	0	19617	37948	2573	0	80397
10	9700	2777	3	250	18	11613	0	0	1161	232	0	697	0	10916	32516	929	0	58065
11	9650	2762	3	250	30	4041	0	0	279	0	0	836	0	6132	22436	557	557	34839
12	9600	2747	3	250	12	7316	348	0	2090	0	0	1045	0	20555	52258	2439	1045	87097
13	9550	2731	3	250	40	4912	0	0	314	209	0	314	0	6898	11392	1881	209	26129
14	9500	2716	3	250	22	5131	190	0	1520	0	190	950	0	9882	25084	3801	760	47508
15	9450	2701	3	250	32	5226	261	131	523	131	131	653	131	5226	14371	4965	915	32661
16	9400	2686	5	250	53	1562	237	0	237	0	142	331	0	3313	4354	1420	237	11832
17	9350	2670	5	250	16	1411	784	0	157	470	157	157	0	8152	23046	3449	1411	39194
18	9300	2655	5	250	19	1452	132	132	132	264	264	396	0	6865	19407	2112	1848	33005
19	9250	2640	5	250	16	2822	470	0	784	627	314	1254	0	8623	17088	2508	4703	39194
20	9200	2625	5	250	27	1486	186	0	465	186	93	929	0	1022	13750	2323	2787	23226
21	9150	2609	3	250	57	1247	147	0	220	0	220	1100	73	2640	9535	1834	1320	18336
22	9100	2594	5	250	35	1290	502	0	72	215	143	2150	0	2867	7167	2150	1362	17917
23	9050	2579	5	250	25	1505	301	0	0	100	100	903	0	3913	14248	2007	2007	25084
24	9000	2564	5	250	35	1577	215	0	72	143	215	2508	0	2150	8887	1577	573	17917
25	8950	2548	5	250	45	1282	334	0	557	167	223	1839	0	1839	5296	1282	1115	13936
26	8900	2533	5	250	39	1222	193	0	386	64	64	965	0	1415	9326	1801	643	16079
27	8850	2518	3	250	39	1286	214	0	107	322	322	1608	0	3966	15008	3002	965	26799
28	8800	2503	3	250	53	1656	316	0	79	316	158	1420	0	3707	9387	1656	1025	19720
29	8750	2487	5	250	35	2867	215	0	143	72	287	2723	72	3583	6450	645	860	17917
30	8700	2472	2	250	330	1007	133	0	95	38	114	684	0	475	1558	361	285	4751
31	8650	2457	3	250	30	2090	0	279	1951	0	557	5574	418	3484	15608	3484	1394	34839
32	8600	2442	3	250	30	2090	0	975	279	0	279	3902	0	5574	14911	4877	1951	34839
33	8550	2427	3	250	17	2951	0	246	1967	0	738	7378	0	12296	28527	3689	3689	61480
34	8500	2411	3	250	20	6271	0	0	1672	209	2090	0	0	10452	20067	6271	5226	52258
35	8450	2396	3	250	30	2787	0	418	1394	0	0	4877	279	6271	14632	2090	2090	34839
36	8400	2381	3	250	20	2717	0	0	3763	0	1045	8361	0	10452	20694	3136	2090	52258
37	8350	2366	3	250	50	1505	251	0	669	0	1254	1254	0	7107	6773	836	1254	20903
38	8300	2350	3	250	15	2787	0	279	2508	0	4181	1115	0	5574	46266	4181	2787	69678
39	8250	2335	3	250	15	2787	0	0	4181	836	836	0	0	2787	48496	5574	4181	69678
40	8200	2320	3	250	20	5226	418	836	7316	0	836	0	0	7316	27174	2090	1045	52258
41	8150	2305	3	250	40	2613	0	0	3658	209	732	0	0	523	13692	1568	3136	26129
42	8100	2289	3	250	20	3136	0	836	2926	627	0	627	0	3136	40971	0	0	52258
43	8050	2274	3	250	16	1045	0	784	3919	1045	261	1306	0	0	50429	3919	2613	65323
44	8000	2259	3	250	15	4738	0	2508	2508	0	1394	0	0	4181	51562	2787	0	69678
45	7950	2244	3	250	5	7525	836	2508	2508	0	5853	0	0	12542	168899	8361	0	209033
46	7900	2228	3	250	3	20903	0	0	0	0	9755	2787	0	0	314944	0	0	348389
47	7850	2213	3	250	2	31355	0	4181	2090	2090	14632	0	0	0	468235	0	0	522583
48	7800	2198	3	250	2	25084	0	0	4181	0	8361	4181	0	0	438970	41807	0	522583
49	7750	2183	3	250	2	20903	0	2090	2090	0	8361	2090	0	0	487048	0	0	522583
50	7700	2167	3	250	7	6570	597	1194	0	0	1194	0	0	0	131392	8361	0	149310
51	7650	2152	3	250	10	6271	418	418	418	836	836	836	418	0	89884	4181	0	104517
52	7600	2137	3	250	4	31355	1045	0	3136	0	2090	0	0	0	202762	20903	0	261292
53	7550	2122	3	250	9	16258	465	0	1394	0	0	0	0	0	98013	0	0	116130
54	7500	2106	3	250	7	11348	0	597	1194	0	0	0	0	0	130198	5972	0	149310
55	7450	2091	3	250	7	7167	0	1792	1194	0	597	0	0	0	123628	14931	0	149310
56	7400	2076	3	250	10	6271	418	836	0	0	0	0	0	0	88630	8361	0	104517
57	7350	2061	3	250	15	5574	0	836	557	0	0	0	0	0	54906	7804	0	69678
58	7300	2046	3	250	4	19858	0	3136	2090	0	0	2090	0	0	218440	15678	0	261292
59	7250	2030	3	250	12	6968	0	5226	1394	697	0	0	0	0	72813	0	0	87097
60	7200	2015	3	250	10	4181	0	0	2090	836	0	418	0	0	76088	16723	4181	104517
61	7150	2000	3	250	25	7525	0	1505	0	0	334	669	0	1171	28930	1672	0	41807
62	7100	1985	3	250	5	37626	0	2508	836	0	0	836	0	0	163882	3345	0	209033
63	7050	1969	3	250	7	8959	0	1194	0	0	0	597	0	0	126614	11945	0	149310
64	7000	1954	3	250	4	20903	0	3136	1045	0	1045	0	0	0	198582	36581	0	261292
65	6950	1939	3	250	2	94065	4181	4181	4181	0	2090	2090	0	0	328182	62710	20903	522583
66	6900	1924	3	250	3	25084	0	1394	0	0	0	0	0	0	296827	20903	4181	348389
67	6850	1908	3	250	35	836	0	239	119	0	0	0	0	0	28548	119	0	29862
68	6800	1893	1	250	50	5017	251	1505	0	0	251	251	0	0	51924	2508	1003	62710
69	6750	1878	3	250	2	31355	0	10452	0	2090	2090	0	0	0	476596	0	0	522583
70	6690	1860	3	250	10	4181	418	2926	0	0	0	418	0	0	96573	0	0	104517

APPENDIX 2

(continued).

Sample no.	Depth ft	Depth m	Sample wt (g)	Total Count	Lycopodium spores counted	Pteridophytes/g	Schizaeacean/g	Saccate pollen/g	*Classopollis*/g	*Ephedripites*/g	Angiosperms/g	Dinocysts/g	MTLs/g	Black Wood/g	Tracheids/g	Cuticles/g	Membranous Tissue/g	Sum (grains/g)
71	6650	1847	3	250	2	25084	4181	0	2090	0	2090	2090	0	0	487048	0	0	522583
72	6550	1817	3	250	4	10452	0	2090	2090	0	0	0	0	0	246659	0	0	261292
73	6550	1817	3	250	17	2459	0	738	0	246	0	0	0	0	48201	7378	2459	61480
74	6500	1802	3	250	3	18116	0	2787	4181	0	1394	0	0	0	314944	6968	0	348389
75	6450	1786	3	250	5	6689	0	2508	1672	0	0	1672	0	0	188130	8361	0	209033
76	6400	1771	3	250	7	4778	0	1194	597	0	2389	1792	0	0	138559	0	0	149310
77	6350	1756	3	250	10	4181	0	418	418	0	2090	1672	0	0	95737	0	0	104517
78	6300	1741	3	250	7	5972	0	0	0	597	1792	597	0	0	138559	1792	0	149310
79	6250	1725	3	250	5	8361	0	0	0	0	1672	0	0	0	194819	4181	0	209033
80	6200	1710	3	250	15	1951	0	836	0	0	0	279	0	0	65218	1394	0	69678
81	6150	1695	3	250	7	1194	0	597	0	0	0	597	0	0	146921	0	0	149310
82	6100	1680	3	250	4	4181	0	1045	0	0	1045	0	0	0	255021	0	0	261292
83	6050	1665	3	250	3	2787	0	1394	1394	0	2787	1394	1394	0	337240	0	0	348389
84	6000	1649	3	250	15	836	279	836	0	0	557	0	0	0	67169	0	0	69678
85	5950	1634	3	250	6	1394	0	0	0	0	0	0	0	0	172801	0	0	174194
86	5900	1619	3	250	4	3136	0	0	0	0	2090	1045	1045	10452	227846	10452	5226	261292
87	5850	1604	3	250	9	4181	1394	0	0	0	3716	465	0	0	97549	6968	1858	116130
88	5800	1588	3	250	30	557	0	0	0	0	697	557	0	0	30519	2090	418	34839
89	5750	1573	3	250	10	1254	0	418	418	0	6271	1672	0	0	79851	12542	2090	104517
90	5650	1543	3	250	10	4181	0	0	0	0	5853	836	0	0	93647	0	0	104517
91	5600	1527	3	250	5	7525	0	836	0	836	3345	2508	836	0	191475	1672	0	209033
92	5550	1512	3	250	9	3716	0	0	929	0	3252	465	0	0	104517	2787	0	115665
93	5500	1497	3	250	7	5972	0	1792	0	597	4181	1792	597	0	126614	4778	1792	148115
94	5150	1390	3	250	7	5375	0	597	0	0	7167	1792	0	0	110489	14931	8959	149310
95	5100	1375	3	250	3	5574	0	1394	0	0	5574	4181	0	0	0	34839	27871	79433
96	5050	1360	3	250	7	60321	1792	0	0	0	4181	2389	0	0	62710	17917	0	149310
97	4950	1329	3	250	10	5435	0	418	0	0	5017	4181	0	0	89466	0	0	104517
98	4900	1314	3	250	30	0	0	0	0	0	0	139	0	0	27732	4181	2787	34839
99	4850	1299	3	250	10	4181	0	0	0	0	1254	3763	0	0	72326	18813	4181	104517
100	4800	1284	3	250	110	0	0	0	0	0	114	380	0	0	6727	1710	570	9502
101	4750	1268	0	0	0	0	0	0	0	0	0	0	0	0	0	0	0	0
102	4700	1253	3	250	1110	38	4	11	0	4	109	260	166	23	113	132	75	934
103	4650	1238	3	250	475	26	0	0	0	0	176	854	1144	0	0	0	0	2200
104	4600	1223	3	250	2000	15	0	0	0	4	29	155	316	0	0	0	0	518
105	4550	1207	3	250	1000	8	0	0	0	0	0	443	594	0	0	0	0	1045
106	4500	1192	3	250	1150	0	0	0	0	0	4	494	411	0	0	0	0	909
107	4450	1177	3	250	655	0	0	0	0	0	0	364	1232	0	0	0	0	1596
108	4400	1162	3	250	420	0	0	0	0	0	0	498	1991	0	0	0	0	2488
109	4350	1146	3	250	385	0	0	0	0	0	0	1520	1194	0	0	0	0	2715
110	4300	1131	3	250	175	0	0	0	0	0	764	3727	1481	0	0	0	0	5972
111	4250	1116	3	250	235	0	0	0	0	0	0	2669	1779	0	0	0	0	4448
112	4200	1101	3	250	225	0	0	0	0	0	0	4051	595	0	0	0	0	4645
113	4150	1085	3	0	0	0	0	0	0	0	0	0	0	0	0	0	0	0
114	4100	1070	3	250	920	9	0	0	5	0	5	59	1059	0	0	0	0	1136
115	4050	1055	3	250	605	55	0	0	0	0	0	304	1368	0	0	0	0	1728
116	4000	1040	3	250	860	0	0	0	0	0	0	136	1079	0	0	0	0	1215
117	3950	1024	3	250	1240	0	0	0	0	0	0	246	597	0	0	0	0	843
118	3900	1009	3	250	1550	0	0	0	0	0	0	105	569	0	0	0	0	674
119	3850	994	3	250	1170	0	0	0	0	0	0	25	868	0	0	0	0	893
120	3800	979	3	0	0	0	0	0	0	0	0	0	0	0	0	0	0	0
121	3750	963	3	0	0	0	0	0	0	0	0	0	0	0	0	0	0	0
122	3700	948	3	0	0	0	0	0	0	0	0	0	0	0	0	0	0	0
123	3650	933	3	0	0	0	0	0	0	0	0	0	0	0	0	0	0	0
124	3600	918	3	0	0	0	0	0	0	0	0	0	0	0	0	0	0	0
125	3500	887	3	0	0	0	0	0	0	0	0	0	0	0	0	0	0	0
126	3450	872	3	0	0	0	0	0	0	0	0	0	0	0	0	0	0	0
127	3400	857	3	0	0	0	0	0	0	0	0	0	0	0	0	0	0	0
128	3350	842	3	0	0	0	0	0	0	0	0	0	0	0	0	0	0	0
129	3300	826	3	0	0	0	0	0	0	0	0	0	0	0	0	0	0	0
130	3250	811	3	0	0	0	0	0	0	0	0	0	0	0	0	0	0	0
131	3200	796	3	250	1020	0	0	0	0	0	0	709	316	0	0	0	0	1025
132	3150	781	3	0	0	0	0	0	0	0	0	0	0	0	0	0	0	0
133	3100	765	3	0	0	0	0	0	0	0	0	0	0	0	0	0	0	0
134	2950	720	3	0	0	32475	348	597	2240	232	0	0	0	0	0	0	154	36046

List of absolute abundance (grains/gram of sediments) of different palynofacies constituents of the BB80-1 borehole used in the palynofacies analysis and palaeoenvironmental interpretations.

Sample no.	Depth ft	Depth m	Sample wt (g)	Total Count	Lycopodium spores counted	Pteridophytes/g	Schizaeacean/g	Saccate pollen/g	*Classopollis* /g	*Ephedripites* /g	Elaterates/g	Angiosperms/g	Dinocysts/g	MTLs/g	Tracheids/g
1	5400	1466	3	250	115	12	0	0	0	1	7	0	5	0	225
2	5390	1463	3	250	0	0	0	0	0	0	0	0	0	0	0
3	5380	1460	3	250	0	0	0	0	0	0	0	0	0	0	0
4	5370	1457	3	250	0	0	0	0	0	0	0	0	0	0	0
5	5360	1454	3	250	0	0	0	0	0	0	0	0	0	0	0
6	5350	1451	3	250	0	0	0	0	0	0	0	0	0	0	0
7	5260	1424	3	250	0	0	0	0	0	0	0	0	0	0	0
8	5220	1412	3	250	165	5	3	3	0	0	10	5	35	12	177
9	5210	1408	3	250	120	3	1	1	0	0	2	0	15	2	226
10	5200	1405	3	250	130	5	0	0	0	0	0	4	40	20	181
11	5180	1399	3	250	7	15	0	0	0	0	0	0	50	0	185
12	5170	1396	3	250	105	8	0	0	0	0	0	0	50	3	189
13	5160	1393	3	250	50	2	0	0	0	0	0	0	10	0	238
14	5020	1351	3	250	0	0	0	0	0	0	0	0	0	0	0
15	5000	1344	3	250	30	4	0	0	1	0	0	5	0	0	240
16	4980	1338	3	250	17	2	0	0	0	0	0	4	10	0	234
17	4970	1335	3	250		0	0	0	0	0	0	0	0	0	0
18	4960	1332	3	250	85	5	0	0	0	0	4	6	10	3	222
19	4950	1329	3	250	0	0	0	0	0	0	0	0	0	0	0
20	4940	1326	3	250	0	0	0	0	0	0	0	0	0	0	0
21	4890	1311	3	250	15	20	0	0	0	0	9	5	5	0	211
22	4880	1308	3	250	45	4	0	0	0	0	25	45	15	0	161
23	4860	1302	3	250	55	2	0	0	0	0	15	35	23	0	175
24	4840	1296	3	250	24	3	0	0	0	0	18	60	2	0	167

APPENDIX 3

List of absolute abundance (grains/gram of sediments) of different palynofacies constituents of the Abu Tunis 1x borehole used in the palynofacies analysis and kerogen determination.

Sample no.	Depth (ft)	Depth (m)	Sample wt (g)	TotalCount	Lycopodium spores counted	Spores/g	Pollen grains/g	Dinocyst/g	MTLs/g	Black Wood/g	Tracheids/g	Cuticles/g	Membranous Tissue/g	AOM/g	Sum
1	10150	2914	3	250	8	15678	6794	1045	0	3136	73684	8361	0	21949	130646
2	10100	2899	3	250	12	5574	4181	348	0	1394	35187	3832	0	36581	87097
3	10050	2884	3	250	7	22695	5972	1194	597	7167	59724	5972	0	45987	149310
4	10000	2868	3	250	14	8660	2986	0	0	3583	31355	5375	299	22396	74655
5	9950	2853	3	250	13	21785	2490	1556	0	3112	31433	1245	0	16183	77804
6	9900	2838	3	250	6	33968	5879	0	0	7839	80347	653	0	34621	163307
7	9850	2823	3	250	4	41807	7316	1045	0	3136	141098	1045	2090	63755	261292
8	9800	2808	3	250	6	25781	6968	0	0	1394	104517	2787	0	32749	174194
9	9750	2792	3	250	5	35118	9197	0	0	4181	108697	4181	0	47660	209033
10	9700	2777	3	250	7	24487	3583	1194	0	2986	77641	3583	0	35834	149310
11	9650	2762	3	250	8	18813	5748	1045	0	4703	72117	2090	1045	25084	130646
12	9600	2747	3	250	8	18290	5748	1045	0	7316	91452	1568	0	5226	130646
13	9550	2731	3	250	5	16723	3345	836	0	836	117059	5017	0	65218	209033
14	9500	2716	3	250	3	25084	12542	1394	0	1394	202066	1394	1394	103123	348389
15	9450	2701	3	250	6	20903	4877	0	0	0	94065	1394	0	52955	174194
16	9400	2686	5	250	7	11467	2508	0	0	0	62710	1433	717	10750	89586
17	9350	2670	5	250	5	3010	2007	0	0	0	88296	3010	1505	27592	125420
18	9300	2655	5	250	4	5017	3136	627	0	627	111624	1254	3136	31355	156775
19	9250	2640	5	250	8	4390	1881	314	0	0	54871	941	941	15050	78388
20	9200	2625	5	250	13	3859	1351	1544	193	0	31644	1351	0	8297	48238
21	9150	2609	3	250	30	2787	557	1533	0	139	21182	836	1115	6689	34839
22	9100	2594	5	250	25	2709	602	1304	0	0	14549	401	1505	4013	25084
23	9050	2579	5	250	16	2665	1097	1411	0	0	23516	1097	0	9407	39194
24	9000	2564	5	250	15	3846	2341	2341	167	669	19900	1672	1171	9699	41807
25	8950	2548	5	250	18	2369	418	1115	0	0	18952	836	697	10452	34839
26	8900	2533	5	250	13	4245	579	579	193	386	23154	1351	965	16787	48238
27	8850	2518	3	250	7	4181	597	4778	0	0	83613	1194	1194	53751	149310
28	8800	2503	3	250	18	3252	1394	1858	0	232	27639	929	0	22761	58065
29	8750	2487	5	250	17	3689	885	2951	0	0	17706	1476	738	9443	36888
30	8700	2472	2	250	15	16723	5435	5435	418	1254	35536	4181	2090	33445	104517
31	8650	2457	3	250	25	4181	2676	3010	0	669	9699	669	0	20903	41807
32	8600	2442	3	250	17	4181	246	2705	0	7378	19920	0	0	27051	61480
33	8550	2427	3	250	14	6570	3285	2986	0	2090	26876	0	0	32848	74655
34	8500	2411	3	250	15	3345	2230	2508	279	6968	6968	0	0	47381	69678
35	8450	2396	3	250	22	4561	2470	1330	0	3801	10452	380	0	24514	47508
36	8400	2381	3	250	14	1792	5077	3583	0	5375	14931	896	299	42703	74655
37	8350	2366	3	250	10	2090	1672	1672	0	1254	4181	1672	0	91975	104517
38	8300	2350	3	250	15	8361	6410	279	0	5017	22297	836	0	26478	69678
39	8250	2335	3	250	6	13936	8361	0	0	13239	59923	2090	3484	73162	174194
40	8200	2320	3	250	5	17559	20067	3345	0	16723	23412	1672	836	125420	209033
41	8150	2305	3	250	17	7869	6394	0	0	3689	20411	246	738	22133	61480
42	8100	2289	3	250	15	5574	5296	7525	0	0	5574	279	13378	32052	69678
43	8050	2274	3	250	17	1967	6886	984	0	492	27543	246	0	23363	61480
44	8000	2259	3	250	8	4703	12019	0	0	1045	59575	1045	0	52258	130646
45	7950	2244	3	250	4	9407	11497	0	0	2090	125420	1045	2090	109743	261292
46	7900	2228	3	250	4	12542	5226	0	0	0	170362	0	0	73162	261292
47	7850	2213	3	250	5	18395	7525	0	0	12542	113714	3345	3345	50168	209033
48	7800	2198	3	250	4	9407	3136	0	0	10452	86749	0	0	151549	261292
49	7750	2183	3	250	3	26478	9755	0	0	4181	146323	1394	6968	153291	348389
50	7700	2167	3	250	4	12542	2090	0	0	10452	80478	7316	7316	141098	261292
51	7650	2152	3	250	7	4778	5375	0	597	5972	51362	597	0	80627	149310
52	7600	2137	3	250	5	25084	8361	2508	0	12542	111206	3345	0	45987	209033
53	7550	2122	3	250	15	6968	1951	0	0	836	28986	836	836	29265	69678
54	7500	2106	3	250	4	21949	4181	0	0	3136	142143	3136	3136	83613	261292
55	7450	2091	3	250	10	4599	2090	1254	0	0	44733	418	1254	50168	104517
56	7400	2076	3	250	8	7839	3136	1045	0	0	53304	2613	2613	60097	130646
57	7350	2061	3	250	3	15329	4181	4181	0	0	97549	0	0	227150	348389
58	7300	2046	3	250	1	75252	16723	8361	0	0	464054	0	0	480777	1045167
59	7250	2030	3	250	15	3623	4181	0	0	1394	31773	0	0	28707	69678
60	7200	2015	3	250	6	5574	4877	1394	0	0	62710	2090	2090	95459	174194
61	7150	2000	3	250	17	3689	984	738	0	0	22133	0	0	33937	61480
62	7100	1985	3	250	5	33445	3345	836	0	0	119567	1672	0	50168	209033
63	7050	1969	3	250	5	4181	1672	1672	0	0	91975	836	0	108697	209033
64	7000	1954	3	250	3	20903	1394	0	0	0	147717	4181	0	174194	348389
65	6950	1939	3	250	2	37626	10452	0	0	0	154685	18813	8361	292647	522583
66	6900	1924	3	250	1	29265	4181	0	0	0	510041	0	0	501680	1045167
67	6850	1908	3	250	6	0	2090	0	0	0	25084	697	0	146323	174194
68	6800	1893	1	250	5	10034	0	0	0	0	100336	0	0	516730	627100
69	6750	1878	3	250	3	1394	1394	0	0	0	132388	0	0	213214	348389
70	6690	1860	3	250	4	2090	2090	0	0	0	94065	0	0	163046	261292

APPENDIX 3

(continued).

Sample no.	Depth (ft)	Depth (m)	Sample wt (g)	Total Count	Lycopodium spores counted	Spores/g	Pollen grains/g	Dinocyst/g	MTLs/g	Black Wood/g	Tracheids/g	Cuticles/g	Membranous Tisuue/g	AOM/g	Sum
71	6650	1847	3	250	4	5226	3136	1045	0	0	107652	0	0	144233	261292
72	6550	1817	3	250	4	6271	3136	0	0	0	110788	0	0	141098	261292
73	6550	1817	3	250	7	1792	597	0	0	0	60321	0	0	86600	149310
74	6500	1802	3	250	1	29265	8361	0	0	0	296827	0	62710	648003	1045167
75	6450	1786	3	250	2	2090	2090	2090	0	0	219485	0	0	296827	522583
76	6400	1771	3	250	7	4181	2389	1792	0	0	75252	0	0	65696	149310
77	6350	1756	3	250	8	4703	523	1568	0	0	66368	0	0	57484	130646
78	6300	1741	3	250	7	5972	2389	597	0	0	101530	0	0	38820	149310
79	6250	1725	3	250	5	5853	0	0	0	0	119567	0	0	83613	209033
80	6200	1710	3	250	11	760	0	380	0	0	64230	0	0	29645	95015
81	6150	1695	3	250	4	1045	0	1045	0	0	133781	0	0	125420	261292
82	6100	1680	3	250	2	4181	2090	0	0	0	234117	0	0	282195	522583
83	6050	1665	3	250	2	4181	0	0	0	0	146323	0	0	372079	522583
84	6000	1649	3	250	1	4181	0	0	0	0	351176	0	0	689810	1045167
85	5950	1634	3	250	3	2787	0	0	0	0	129601	0	0	216001	348389
86	5900	1619	3	250	1	8361	0	4181	0	0	468235	0	0	564390	1045167
87	5850	1604	3	250	3	8361	6968	1394	0	0	132388	0	0	199278	348389
88	5800	1588	3	250	18	0	697	232	0	0	16258	2323	697	37858	58065
89	5750	1573	3	250	3	2787	9755	5574	0	0	107304	0	0	222969	348389
90	5650	1543	3	250	4	7316	6271	2090	0	0	94065	0	0	151549	261292
91	5600	1527	3	250	3	6968	5574	2787	0	0	149110	9755	0	174194	348389
92	5550	1512	3	250	4	7316	6271	1045	0	0	107652	3136	0	135872	261292
93	5500	1497	3	250	2	14632	8361	4181	2090	0	236208	10452	6271	240388	522583
94	5150	1390	3	250	3	1394	12542	0	0	0	48774	0	0	285679	348389
95	5100	1375	3	250	2	2090	8361	0	0	0	73162	0	0	438970	522583
96	5050	1360	3	250	4	4181	2090	3136	0	0	32400	20903	0	198582	261292
97	4950	1329	3	250	2	10452	20903	8361	0	0	234117	31355	18813	198582	522583
98	4900	1314	3	250	7	0	0	597	0	0	35237	0	0	113475	149310
99	4850	1299	3	250	2	8361	4181	4181	0	0	125420	43897	0	336544	522583
100	4800	1284	3	250	19	0	0	0	0	0	8801	0	0	46207	55009
101	4750	1268	3	250	20	0	0	0	0	0	0	0	0	42852	42852
102	4700	1253	3	250	5	0	0	8361	0	0	0	0	0	200672	209033
103	4650	1238	3	250	10	0	0	5017	1672	0	0	0	0	97828	104517
104	4600	1223	3	250	7	0	0	4778	1792	0	0	0	0	142740	149310
105	4550	1207	3	250	15	0	0	2230	0	0	0	0	0	67448	69678
106	4500	1192	3	250	5	0	0	7525	0	0	0	0	0	201508	209033
107	4450	1177	3	250	10	0	0	1254	0	0	0	0	0	103262	104517
108	4400	1162	3	250	7	0	0	2986	1194	0	0	0	0	145129	149310
109	4350	1146	3	250	5	0	0	7525	836	0	0	0	0	200672	209033
110	4300	1131	3	250	9	0	929	6039	0	0	0	0	0	109162	116130
111	4250	1116	3	250	10	0	0	6271	0	0	0	0	0	98246	104517
112	4200	1101	3	250	4	0	0	20903	0	0	0	0	0	240388	261292
113	4150	1085	3	250	6	0	0	3484	0	0	0	0	0	170711	174194
114	4100	1070	3	250	6	0	0	3484	1394	0	0	0	0	169317	174194
115	4050	1055	3	250	5	0	0	11706	0	0	0	0	0	197327	209033
116	4000	1040	3	250	5	0	0	4181	0	0	0	0	0	204853	209033
117	3950	1024	3	250	12	0	0	1394	0	0	0	0	0	85704	87097
118	3900	1009	3	250	8	0	0	2090	523	0	0	0	0	128033	130646
119	3850	994	3	250	8	0	0	1045	523	0	0	0	0	129078	130646
120	3800	979	3	250	25	0	0	0	0	0	0	0	0	41807	41807
121	3750	963	3	250	16	0	0	0	0	0	0	0	0	65323	65323
122	3700	948	3	250	45	0	0	0	0	0	0	0	0	23226	23226
123	3650	933	3	250	32	0	0	0	0	0	0	0	0	32661	32661
124	3600	918	3	250	35	0	0	0	0	0	0	0	0	29862	29862
125	3500	887	3	250	15	0	0	0	0	0	0	0	0	69678	69678
126	3450	872	3	250	40	0	0	0	0	0	0	0	0	26129	26129
127	3400	857	3	250	30	0	0	0	0	0	0	0	0	34839	34839
128	3350	842	3	250	20	0	0	0	0	0	0	0	0	52258	52258
129	3300	826	3	250	10	0	0	0	0	0	0	0	0	104517	104517
130	3250	811	3	250	5	0	0	4181	2508	0	0	0	0	202344	209033
131	3200	796	3	250	4	0	0	20903	0	0	0	0	0	240388	261292
132	3150	781	3	250	17	0	0	1721	492	0	0	0	0	59267	61480
133	3100	765	3	250	15	0	0	0	0	0	0	0	0	69678	69678
134	2950	720	3	250	30	0	0	279	0	0	0	0	0	34560	34839

List of absolute abundance (grains/gram of sediments) of different palynofacies constituents of the BB80-1 borehole used in the palynofacies analysis and kerogen determination.

Sample no.	Depth ft	Depth m	Sample wt (g)	Total Count	Lycopodium spores counted	Spores/g	Polen grains/g	Dinocysts	MTLs/g	Black Wood/g	Tracheids/g	AOM/g	Sum
1	5400	1466	3	250	25	0	167	0	0	0	17392	24248	41807
2	5390	1463	3	250	10	0	0	0	0	0	39716	64800	104517
3	5380	1460	3	250	75	167	0	56	0	0	12040	1672	13936
4	5370	1457	3	250	20	0	0	4181	0	0	40762	7316	52258
5	5360	1454	3	250	40	0	0	0	0	0	22994	3136	26129
6	5350	1451	3	0	40	0	0	0	0	0	24039	4181	28220
7	5260	1424	3	250	45	0	279	465	186	0	10219	12077	23226
8	5220	1412	3	250	10	0	418	0	0	0	3763	100336	104517
9	5210	1408	3	0	15	0	0	0	0	0	0	0	0
10	5200	1405	3	250	15	279	0	279	0	0	13936	55185	69678
11	5180	1399	3	250	9	465	0	465	0	0	25549	89652	116130
12	5170	1396	3	250	12	0	0	697	348	0	19161	66891	87097
13	5160	1393	3	250	3	1394	1394	2787	1394	0	153291	188130	348389
14	5020	1351	3	250	50	167	0	0	0	0	8194	12542	20903
15	5000	1344	3	250	9	465	1394	0	0	0	109626	4645	116130
16	4980	1338	3	250	6	0	697	1394	0	0	130297	41807	174194
17	4970	1335	3	250	80	0	0	0	0	7577	0	5487	13065
18	4960	1332	3	250	9	0	0	0	0	0	0	116130	116130
19	4950	1329	3	250	10	0	0	0	0	0	20903	83613	104517
20	4940	1326	3	250	10	0	0	0	0	0	43897	60620	104517
21	4890	1311	3	250	7	8959	4778	0	0	0	129601	5972	149310
22	4880	1308	3	250	4	9407	0	0	0	0	157820	94065	261292
23	4860	1302	3	250	20	0	1463	836	0	0	4181	45778	52258
24	4840	1296	3	250	4	1045	5226	2090	0	0	216350	36581	261292

REFERENCES

A.S.T.M. (1978) Standard method of preparing coal samples for microscopical analysis by reflected light. *American Society for Testing and Materials, Annual Book of Standards D2797-72***,** pt. 26, 384389.

ABBINK, O. A., VAN KONIJNENBURG-VAN CITTERT, J. H. A. & VISSCHER, H. (2004) A sporomorph ecogroup model for the Northwest European Jurassic-Cretaceous: concepts and framework. *Netherlands Journal of Geosciences - Geologie En Mijnbouw,* 83**,** 17-38.

ABDALLAH, A. M., ADINDANI, A. & FAHMY, N. (1963) Stratigraphy of lower Mesozoic rocks, western side of Gulf of Suez, Egypt. *Geologic Survey of Egypt Paper,* 27**,** 23.

ABDEL-KIREEM, M. R., SCHRANK, E., SAMIR, A. M. & IBRAHIM, M. I. A. (1996) Cretaceous palaeoecology, palaeogeography and palaeoclimatology of the northern Western Desert, Egypt. *Journal of African Earth Sciences,* 22**,** 93-112.

ABDELMALIK, W. M., ABOUL ELA, N. A. & EL-SHAMMA, A. G. (1981) Upper Jurassic-lower Cretaceous microflora from the north Western Desert, Egypt. *Neues Jahrbuch für Geologie und Paläontologie - Abhandlungen,* 162**,** 244-263.

ABOU KHADRAH, A. M. & KHALED, K. A. (1978) Origin and diagenesis of the Aptian Alamein Dolomite in Razzak oil field, northern Western Desert, Egypt. *Chemie der Erde,* 37**,** 154-164.

ABOUL ELA, N. M. & MAHROUS, H. A. R. (1992) Albian-Cenomanian miospores from the subsurface of the north Western Desert, Egypt. *Neues Jahrbuch für Geologie und Paläontologie Monatschefte,* 10**,** 595-613.

ABUBAKAR, M. B., OBAJE, N. G., LUTERBACHER, H. P., DIKE, E. F. C. & ASHRAF, A. R. (2006) A report on the occurrence of Albian-Cenomanian elater-bearing pollen in Nasara-1 well, Upper Benue Trough, Nigeria: Biostratigraphic and palaeoclimatological implications. *Journal of African Earth Sciences,* 45**,** 347-354.

AIZAWA, J. (1989) Relationship between vitrinite reflectivity and paleotemperature based on fluid inclusions in the southwestern coal fields of Japan. *International Conference on Coal Science.* Tokyo, Japan.

AKKAD, S. E. & ISSAWI, B. (1963) Geology and iron ore deposits of Bahariya Oasis. *Geologic Survey of Egypt Paper,* 18**,** 300.

AL-AMERI, T. K., AL-KHAFAJI, A. J. & ZUMBERGE, J. (2009) Petroleum system analysis of the Mishrif reservoir in the Ratawi, Zubair, North and South Rumaila oil fields, southern Iraq. *GeoArabia,* 14**,** 91-108.

AL-AMERI, T. K., AL-MUSAWI, F. S. & BATTEN, D. J. (1999) Palynofacies indications of depositional environments and source potential for hydrocarbons: uppermost Jurassic-basal Cretaceous Sulaiy Formation, southern Iraq. *Cretaceous Research,* 20**,** 359-363.

ALLEMANN, F. & REMANE, J. (1979) Les faunes de calpionelles du Berriasien supérieur/Valanginien. IN BUSNARDO, R., THIEULOY, J.-P. & MOULLADE, M. (Eds.) *Hypostratotype mésogeen de l'étage Valanginien (Sud-Est de la France).* CNRS ed., Les stratotypes français.

ALLEN, P. A. & ALLEN, J. R. (1990) *Basin Analysis: Principles and Applications,* Oxford, Blackwell Science.

ARAI, M., HASHIMOTO, A. T. & UESUGUI, N. (1989) Significado cronoestratigráfico da associação microflorística do Cretáceo Inferior do Brasil. *Boletim de Geociências da PETROBRAS,* 3**,** 87-103.

ÅRHUS, N., KELLY, S. R. A., COLLINS, J. S. H. & SANDY, M. R. (1990) Systematic palaeontology and biostratigraphy of two Early Cretaceous condensed sections from the Barents Sea. *Polar Research,* 8**,** 165-194.

ARMSTRONG, H. A. & BRASIER, M. D. (2005) *Microfossils,* Oxford, Blackwell Publishing.

ATTA-PETERS, D. & SALAMI, M. B. (2006) Aptian-Maastrichtian palynomorphs from the offshore Tano Basin, western Ghana. *Journal of African Earth Sciences,* 46**,** 379-394.

AWAD, M. Z. (1994) Stratigraphic, palynological and palaeoecological studies in the east-central Sudan (Khartoum and Kosti Basins), late Jurassic to mid-Tertiary. *Berliner Geowissenschaftliche Abhandlungen - Reihe A,* 161**,** 1-163.

B.S.I (1982) Petrographic analysis of bituminous coal and anthracite: Methods of preparing coal samples for petrographic analysis. *British Standards Institute, British Standard,* 6127, pt. 2, 1-5.

BAIRD, J. G. (1992) Palynofacies of the eastern margin of Gippsland Basin. *Energy, Economics, and Enviroment, Proceeding of the Gippsland Basin Symposium, Melbourne June 1992* Australian Institute of Mining and Metallurgy.

BALCH, W. M., REID, P. C. & SURREY-GENT, S. C. (1983) Spatial and temporal variability of dinoflagellate cyst abundance in a tidal estuary. *Canadian journal of Fisheries and Aquatic Sciences, Supplement,* 40**,** 244-261.

BALME, B. E. (1995) Fossils in situ spores and pollen grains: an annotated catalogues. *Review of Palaeobotany and Palynology,* 87**,** 81-323.

BARKER, C. E. & GLODSTEIN, R. H. (1990) Fluid inclusion technique for determining maximum temperature in calcite and its comparison to the vitrinite reflectance geothermometer. *Geology,* 18**,** 1003-1006.

BARKER, C. E. & PAWLEWICZ, M. J. (1994) Calculation of vitrinite reflectance from thermal histories and peak temperatures: a comparison of methods. IN MUKHOPADHYAY, P. K. & DOW, W. G. (Eds.) *Vitrinite Reflectance as a Maturity Parameter: Applications and Limitations.* Washington, DC, American Chemical Society.

BARNARD, P. C., COLLINS, A. G. & COOPER, B. S. (1981) Identification and distribution of kerogen facies in a source rock horizon – examples from the North Sea Basin. IN BROOKS, J. (Ed.) *Organic Maturation Studies and Fossil Fuel Exploration.* London, Academic Press.

BARNARD, P. C. & COOPER, B. S. (1981) Oils and source rocks of the North Sea area. IN ILLING, L. V. & HOBSON, G. D. (Eds.) *Petroleum Geology of the Continental Shelf of North-West Europe.* London, Heyden.

BASKIN, D. K. (1979) A method of preparing phytoclasts for vitrinite reflectance analysis. *Journal of Sedimentary Petrology,* 49**,** 633-635.

BATTEN, D. J. (1973) Use of palynological assemblage-types in Wealden correlation. *Palaeontology,* 16**,** 1-40.

BATTEN, D. J. (1974) Wealden palaeoecology from the distribution of plant fossils. *Proceedings of the Geologists Association,* 85**,** 433-58.

BATTEN, D. J. (1981) Palynofacies, organic maturation and source potential for petroleum. *Organic Maturation Studies and Fossil Fuel Exploration.* London, Academic Press.

BATTEN, D. J. (1983) Identification of amorphous sedimentary organic matter by transmitted light. IN BROOKS, J. (Ed.) *Petroleum Geochemistry and Exploration of Europe.* Geological Society of London Special Publication.

BATTEN, D. J. (1998) Palaeoenvironmental implications of plant, insect and other organic-walled microfossils in the Weald Clay Formation (Lower Cretaceous) of southeast England. *Cretaceous Research,* 19**,** 279-315.

BATTEN, D. J. (1999) Palynofacies analysis. IN JONES, N. P. & ROWE, N. P. (Eds.) *Fossil Plants and Spores: Modern Techniques.* London, Geological Society of London.

BATTEN, D. J. & LISTER, J. K. (1988) Evidence of freshwater dinoflagellates and other algae in the English Wealden (Early Cretaceous). *Cretaceous Research,* 9**,** 171-179.

BATTEN, D. J. & UWINS, P. J. R. (1985) Early-late Cretaceous (Aptian-Cenomanian) palynomorphs. *Journal of Micropalaeontology,* 1**,** 151-168.

BEADNELL, H. J. L. (1902) The Cretaceous region of Abu Roash, near the Pyramids of Giza. *Report.* Giza, Egyptian Survey Department.

BELOW, R. (1981) Dinoflagellaten-Zysten aus dem oberen Hauterive bis unteren Cenoman Süd-West Marokkos. *Palaeontographica Abteilung B,* 176**,** 1-145.

BELOW, R. (1982a) Dinoflagellate cysts from Valanginian to lower Hauterivian sections near Ait Hamouch, Morocco. *Revista Española de Micropaleontologia,* 14**,** 23-52.

BELOW, R. (1982b) Scolochorate Zysten der Gonyaulacaceae (Dinophyceae) aus der Unterkreide Marokkos. *Palaeontographica Abteilung B,* 182**,** 1-51.

BELOW, R. (1984) Aptian to Cenomanian dinoflagellate cysts from the Mazagan Plateau, northwest Africa (Site 545 and Site 547, Deep Sea Drilling Project Leg 79). *Initial Reports of the Deep Sea Drilling Project,* 79**,** 621-649.

BERTRAND, R., BERUBÉ, J.-C., HÉROUX, Y. & ACHAB, A. (1985) Pétrographie du kérogène dans le paléozoïque inférieur: méthode de préparation et exemple d'application. *Revue de l'Institut Français du Pétrole,* 40**,** 155-167.

BETTAR, I. & COURTINAT, B. (1987) Palynologie de la série grésocarbonatée d`Imi n`Tanout (Cretacé inférieur, zone synclinale d`Essaouira, Maroc). *Bulletin de l' Institut scientifique - Rabat,* 11**,** 103-108.

BETTAR, I. & MÉON, H. (2001) Palynological study of the middle/upper Albian transition in the Tarfaya Basin (southwest of Morocco) and some new data about the African-South American Province. *Revue de Micropaléontologie,* 44**,** 107-123.

BETTAR, I. & MÉON, H. (2006) La palynoflore continentale de l'Albien du Bassin d'Agadir-Essaouira (Maroc). *Revue de Paléobiologie,* 25**,** 593-631.

BINT, A. N. (1986) Fossil Ceratiaceae: a restudy and new taxa from the mid-Cretaceous of the Western Interior, U.S.A. *Palynology,* 10**,** 135-180.

BOGGS, J. S. (1987) *Principles of Sedimentology and Stratigraphy,* Columbus, Merrill Publishing Company.

BOLKHOVITINA, N. A. (1961) Fossil and Recent spores of the family Schizaeaceae. *Trudy Geologicheskogo Instituta. Akademiya nauk SSSR,* 40**,** 1-218 (in Russian).

BORDENAVE, M. L. (1993) *Applied Petroleum Geochemistry,* Paris, Edition Technip.

BORNEMANN, A., PROSS, J., REICHELT, K., JO., H., HEMLEBEN, C. & MUTTERLOSE, J. (2005) Reconstruction of short-term palaeoceanographic changes during the formation of the Late Albian "Niveau Breistroffer" black shale (Oceanic Anoxic Event 1d, SE France). *Journal of Geological Society,* 162**,** 623-639.

BOSTICK, N. H. & ALPERN, B. (1977) Principles of sampling and constituents selection for microphotometry in measurements of maturation of sedimentary organic matter. *Journal of Microscopy,* 109**,** 41-47.

BOSWORTH, W. (1985) Geometry of propagating continental rifts. *Nature,* 316**,** 625-627.

BOSWORTH, W. (1994) A model for the 3-dimensional evolution of continental rift basins, north-east Africa. *Geologische Rundschau,* 83**,** 671-688.

BOSWORTH, W., HUCHON, P. & MCCLAY, K. (2005) The Red Sea and Gulf of Aden basins. *Journal of African Earth Sciences,* 43**,** 334-378.

BOSWORTH, W. & MCCLAY, K. (2001) Structural and stratigraphic evolution of the Gulf of Suez rift, Egypt: a synthesis. IN ZIEGLER, P. A., CAVAZZA, W., ROBERTSON, A. H. F. & CRASQUIN-SOLEAU, S. (Eds.) *Peri-Tethys*

Memoir 6: Peri-Tethyan Rift/Wrench Basins and Passive Margins. Paris, Mémoires du Muséum National d'Histoire Naturelle.

BRAY, J. R. & CURTIS, J. T. (1957) An ordination of the upland forest communities of Southern Wisconsin. *Ecological Monographs,* 27**,** 325-349.

BRENNER, G. J. (1968) Middle Cretaceous spores and from north-eastern Peru. *Pollen et Spores,* 10**,** 341-382.

BRENNER, G. J. (1976) Middle Cretaceous floral provinces and early migrations of angiosperms. IN BECK, C. B. (Ed.) *Origin and Early Evolution of Angiosperms.* New York, Colombia University Press.

BRENNER, G. J. (1996) Evidence for the earliest stage of angiosperm pollen evolution: a paleoequarorial section from Israel. IN TAYLOR, D. W. & HICKEY, L. J. (Eds.) *Flowering Plant Origin, Evolution & Phylogeny* New York, Chapman & Hall.

BROOKS, J. (1981) Organic maturation of sedimentary organic matter and petroleum exploration. IN BROOKS, J. (Ed.) *Organic maturation studies and fossil fuel exploration.* London, Academic Press.

BUJAK, J. P., BARSS, M. S. & WILLIAMS, G. L. (1977) Offshore east Canada's organic type and color and hydrocarbon potential. *The Oil and Gas Journal,* 75**,** 198-201.

BUJAK, J. P. & WILLIAMS, G. L. (1979) Dinoflagellate Diversity through Time. *Marine Micropaleontology,* 4**,** 1-12.

BUMBY, A. J. & GUIRAUD, R. (2005) The geodynamic setting of the Phanerozoic basins of Africa. *Journal of African Earth Sciences,* 43**,** 1-12.

BURGER, D. (1980) Palynology of the Lower Cretaceous of the Surat Basin. *Bureau of Mineral Resources, Geology and Geophysics Australia, Bulletin,* 189**,** 106.

BURGESS, J. D. (1974) Microscopic examination of kerogen (dispersed organic matter) in petroleum exploration. *Geological Society of America Special Paper* 153**,** 19-30.

CANE, R. F. (1976) The origin and formation of oil shale. IN YEN, T. F. & CHILINGARIAN, G. V. (Eds.) *Develpoments in Pertoleum Science.* Amsterdam, Elsevier.

CARATINI, C., BELLET, J. & TISSOT, C. (1983) Les palynofacès: représentation graphique, interêt de leur étude pour les reconstitutions paléogéographique. *Géochimie Organique des Sédiments Marine d'ORGON À MISEDOR.* Éditions du Centre National de la Recherche Scientifique, Paris.

CLARET, J., JARDINE, S. & ROBERT, P. (1981) La diversité des roches mères pétrolières: aspects gèologiques et implication èconomiques à partir de quatre exemples *Bulletin des Centres de Recherches Exploration-Production Elf Aquitaine,* 5**,** 383-417.

CLARKE, K. R. & GORLEY, M. A. (2006) PRIMER. 6 ed. Plymouth, UK, PRIMER-E Limited.

CLARKE, K. R. & WARWICK, R. M. (2001) Changes in Marine Communities: An Approach to Statistical Anallysis and Interpretation. 2nd ed., Primer-E Ltd.

CLARKE, R. F. A. & VERDIER, J.-P. (1967) An investigation of microplankton assemblages from the chalk of the Isle of Wight, England. *Verhandelingen der Koninklijke Nederlandse Akademie van Wetenschappen, Afdeeling Natuurkunde, Eerste Reeks,* 24**,** 1-96.

COFFIELD, D. Q. & SCHAMEL, S. (1989) Surface expression of an accommodation zone within the Gulf of Suez rift, Egypt. *Geology,* 17**,** 76-79.

COMBAZ, A. (1964) Les palynofaciès. *Revue de Micropaléontologie,* 7**,** 205-218.

COMBAZ, A. (1980) Les kérogènes vus au microscope. IN DURAND, B. (Ed.) *Kerogen: Insoluble Organic Matter From Sedimentary Rocks.* Paris, Éditions Technip.

COOKSON, I. C. & EISENACK, A. (1970a) Cretaceous microplankton from the Eucla Basin, Western Australia. *Proceedings of the Royal Society of Victoria,* 83**,** 137-157.

CORNET, B. & TRAVERSE, A. (1975) Palynological contributions to the chronology and stratigraphy of the Hartford Basin in Connecticut and Massachusetts. *Geoscience and Man,* 11**,** 1-33.

CORREIA, M. (1971) Diagenesis of sporopollenin and other comparable organic substances: application to hydrocarbon research. IN BROOKS, J., GRANT, P., MURI, M. D., SHAW, G. & VAN GIJZEL, P. (Eds.) *Sporopollenin.* London, Academic Press.

COUPER, R. A. (1953) Upper Mesozoic and Cainozoic spores and pollen grains from New Zealand. *New Zealand Geological Survey Palaeontological Bulletin,* 22**,** 1-77.

CRANE, P. R. (1988) Major clades and relationships in the "higher" gymnosperms. IN BECK, C. B. (Ed.) *Origin and Evolution of Gymnosperms.* New York, Columbia University

CRANE, P. R. (1996) The fossil history of the Gnetales. *International Journal of Plant Sciences,* 6 supplement**,** S50-S57.

DALE, B. (1983) Dinoflagellate resting cysts: “benthic plankton” IN FRYXELL, G. A. (Ed.) *Survival Strategies of the Algae.* Cambridge University Press.

DANZÉ-CORSIN, P. & LAVEINE, J. P. (1963) Microflore. IN BRICHE, P., DANZÉ-CORSIN, P. & LAVEINE, J. P. (Eds.) *Flore Infraliasique du Boulonnais.* Memoirs de la Societe Geologique du Nord.

DARWISH, M. & EL ARABY, A. (1993) Petrography and diagenetic aspects of some siliciclastic hydrocarbon reservoirs in relation to rifting of the Gulf of Suez, Egypt. *Geodynamics and Sedimentation of the Red Sea-Gulf of Aden Rift System.* Giza, Geologic Survey of Egypt.

DAVEY, R. J. (1970) Non-calcareous miroplankton from the Cenomnain of England , northern France, and North America, Part II. *Bulletins of the British Museum (Natural History), Geology,* 18**,** 333-397.

DAVEY, R. J. & ROGERS, J. (1975) Palynomorph distribution in Recent offshore sediments along two traverses off South West Africa. *Marine Geology,* 18**,** 213-225.

DAVEY, R. J. & VERDIER, J. P. (1973) An investigation of microplankton assemblages from latest Albian (Vraconian) sediments. *Revista Española de Micropaleontologia,* 5**,** 173-212.

DAVEY, R. J. & VERDIER, J. P. (1974) Dinoflagellate cysts from the Aptian type sections at Gargas and la Bédoule, France. *Palaeontology,* 17**,** 623-653.

DAVIES, E. H. & AVERY, M. P. (1984) A system for vitrinite reflectance analysis on dispersed organic matter for offshore eastern Canada. *Current Research, Geological Survey of Canada,* Paper 84-1A**,** 367-372.

DE VERNAL, A., BILODEAU, G., HILLAIRE-MARCEL, C. & KASSOU, N. (1992) Quantitative assessment of carbonate dissolution in marine sediments from

foraminifera linings *vs* shell ratio: Davis Strait, northwest North Atalntic. *Geology,* 20**,** 527-530.

DE VERNAL, A. & GIROUX, L. (1991) Distribution of organic-walled microfossils in Recent sedimentsfrom the Estuary anf Gulf of St. Lawrence: some aspects of the organic matter fluxes. *Canadian Journal of Fisheries and Aquatic Sciences, Special Publication,* 113**,** 189-199.

DEGENS, E. T. & MOPPER, K. (1976) Factors controlling the distribution and early diagenesis of organiv material in marine sediments. IN RILEY, J. P. & CHESTER, R. (Eds.) *Chemical Oceanography.* 2nd ed. London, Academic Press.

DEJAX, J. (1987) Sur la présence de grains de pollen à sculpture crotonoide dans le Crétacé inférieur du Congo. *Association des Palynologues de Langue Francais; Symposium 9.* Montpellier, France.

DELCOURT, A. F., DETTMANN, M. E. & HUGHES, N. F. (1963) Revision on some Lower Cretaceous microspores from Belgium. *Palaeontology,* 6**,** 282-292.

DETTMANN, M. E. (1963) Upper Mesozoic microfloras from south-eastern Australia. *Proceedings of the Royal Society of Victoria,* 77**,** 1-148.

DINO, R., POCKNALL, D. T. & DETTMANN, M. E. (1999) Morphology and ultrastructure of elater-bearing pollen from the Albian to Cenomanian of Brazil and Ecuador: implications for botanical affinity. *Review of Palaeobotany and Palynology,* 105**,** 201-235.

DOMINICK, W. (1985) Stratigraphie und sedimentologie (geochemie, schwermineralanayse) der oberkreide von Bahariya und ihre korrelation zum Dakhla Becken (Western Desert, Ägypten). *Berliner Geowissenschaftliche Abhandlungen - Reihe A,* 62**,** 1-173.

DOUKAGA, M. (1980) Etude palynologique dans le Crétacé moyen du bassin sedimentaire du Gabon. Lille, Université des Sciences et Technologies de Lille.

DOW, W. G. & PEARSON, D. B. (1975) Organic matter in Gulf coastal sediments. *Offshore Technology Conference, Dallas, 1975.*

DOWNIE, C., HUSSAIN, M. A. & WILLIAMS, G. L. (1971) Dinoflagellate cysts and acritarchs association in the Paleogene of southeast England. *Geoscience and Man,* 3**,** 29-35.

DOYLE, J. A. (1992) Revised palynological correlations of the lower Potomac Group (USA) and the Cocobeach sequence of Gabon (Barremian-Aptian). *Cretaceous Research,* 13**,** 337-349.

DOYLE, J. A. (1999) The rise of angiosperms as seen in the African Cretaceous pollen record. IN HEINE, K. (Ed.) *Third Conference on African Palynology.* Johannesburg 14-19 September, 1997, Balkema, Rotterdam.

DOYLE, J. A., BIENS, P., DOERENKAMP, A. & JARDINÉ, S. (1977) Angiosperm pollen from the pre-Albian lower Cretaceous of equatorial Africa. *Bulletin des Centres de Recherches Exploration-Production Elf-Aquitaine,* 1**,** 451-473.

DOYLE, J. A., JARDINÉ, S. & DOERENKAMP, A. (1982) *Afropollis*, a new genus of early angiosperm pollen, with notes on the Cretaceous palynostratigraphy and paleoenvironments of northern Gondwana. *Bulletin des Centres de Recherches Exploration-Production Elf Aquitaine,* 6**,** 39-117.

DOYLE, J. A., VAN CAMPO, M. & LUGARDON, B. (1975) Observation on exine structure of *Eucommiidites* and lower Cretaceous angiosperm pollen. *Pollen et Spores,* 17**,** 429-486.

DURINGER, P. & DOUBINGER, J. (1985) La palynologie: un outil de characterisation des facies marins et continentaux a la limit Muschelkalk Supérieur - Lettenkohle. *Science Géologie Bulletin, Strasbourg,* 38**,** 19-34.

DUXBURY, S. (1980) Barremian phytoplankton from Speeton, east Yorshire. *Palaeontographica Abteilung B,* 173**,** 107-146.

DUXBURY, S. (1983) A study of dinoflagellate cysts and acritarchs from the Lower Greensand (Aptian to Lower Albian) of the Isle of Wight, southern England. *Palaeontographica, Abteilung B,* 186**,** 18-80.

DYBKJAER, K. (1991) Palynological zonation and palynofacies investigation of the Fjerritslev Formation (Lower Jurassic - basal Middle Jurassic) in the Danish Subbasin. *Danmarks Geologiske Undersogelse serie A,* 30**,** 150.

EL-BEIALY, S. Y. (1993) Mid-Cretaceous palynomorphs from the Bardawil-1 borehole, north Sinai, Egypt. *Cretaceous Research,* 14**,** 49-58.

EL-BEIALY, S. Y. (1994a) Palynological evidence for the age and depositional environment of the Cretaceous Bahariya Formation, north Western Desert, Egypt. *Sciences Géologiques - Bulletin,* 47**,** 51-65.

EL-BEIALY, S. Y. (1994b) Early Cretaceous dinoflagellate cysts and miospores from the Mersa Matruh 1 borehole, north West Desert, Egypt. *Qatar University Science Journal,* 14**,** 148-200.

EL-BEIALY, S. Y. (1994c) Palynological investigations of Cretaceous sediments in the Abu El Gharadig oil field, Western Desert, Egypt. *Newsletters on Stratigraphy,* 31**,** 71-84.

EL-BEIALY, S. Y. & AL-HITMI, H. H. (1994) Micropalaeontology and palynology of the lower and middle Cretaceous Thamama and Wasia Groups, DK-C well, Dukhan oil field, Western Qatar. *Bulletin de la Société Géologique de France,* 47**,** 67-95.

EL-BEIALY, S. Y., AYYAD, S. N. & KHOLEIF, S. E. (1990) Mesozoic-Tertiary palynomorphs and planktonic foraminifera of the subsurface section of the Sindy-1 well eastern Nile Delta, Egypt. *Newsletters on Stratigraphy,* 22**,** 71-86.

ERBA, E., CHANNELL, J. E. T., CLAPS, M., JONES, C., LARSON, R., OPDYKE, B., PREMOLI SILVA, I., RIVA, A., SALVINI, G. & TORRICELLI, S. (1999) Integrated stratigraphy of the Cismon Apticore (Southern Alps, Italy): a "reference" section for the Barremian-Aptian interval at low latitudes *Journal of Foraminiferal Research,* 29**,** 371-391.

ESPITALIÉ, J., LAPORTE, J. L., MADEC, M., MARQUIS, F., LEPLAT, P., PAULET, J. & BOUTEFEU, A. (1977) Méthode rapide de caracterisation des roches mères de leur potentiel pétrolier et de leur degré d`évolution. *Revue de l'Institut Français du Pétrole,* 32**,** 23-42.

ETTER, W. (1999) Community analysis. IN HARPER, D. A. T. (Ed.) *Numerical Palaeobiology: Computer-based Modelling and Analysis of Fossils and their Distributions.* Chichester, John Wiley and Sons Ltd.

EVITT, W. R. (1985) *Sporopollenin Dinoflagellate Cysts: Their Morphology and Interpretation,* Dallas, Texas, American Association of Straigraphic Playnologists Foundation.

FEDEROVA, V. A. (1977) The significance of the combined use of microphytoplankton, spores, and pollen for differentiation of multi-facies sediments IN SAMOILOVICH, S. R. & TIMOSHINA, N. A. (Eds.) *Questions*

of Phytostratigraphy. Leningrad, Trudy Neftyanoi nauchno-issledovatelskii geologorazvedochnyi Institute (VNIGRI).

FENSOME, R. A., GOCHT, H. & WILLIAMS, G. L. (1995) The Eisenack Catalog of Fossil Dinoflagellates. *New Series.* Stuttgart, Germany, E. Schweizerbart'sche Verlagsbuchhandlung.

FENSOME, R. A., GOCHT, H. & WILLIAMS, G. L. (1996) The Eisenack Catalog of Fossil Dinoflagellates. *New Series.* Stuttgart, Germany, E. Schweizerbart'sche Verlagsbuchhandlung.

FENSOME, R. A., MACRAE, R. A. & WILLIAMS, G. L. (2008) DINOFLAJ2, Version 1. American Association of Stratigraphic Palynologists.

FENSOME, R. A., TAYLOR, F. J. R., NORRIS, G., SARJEANT, W. A. S., WHARTON, D. I. & WILLIAMS, G. L. (1993) *A classification of fossil and living dinoflagellates*, Micropaleontology Press Special Paper.

FENSOME, R. A. & WILLIAMS, G. L. (2004) The Lentin and Williams Index of Fossil Dinoflagellates. *Contributions Series No. 42.* American Association of Stratigraphic Palynologists Foundation.

FIRTH, J. V. (1993) Palynofacies and thermal maturation analysis of sediments from the Nankai Trough. *Proceedings of the Ocean Drilling Project, Scientific Results,* 131**,** 57-69.

FISHER, M. J. (1980) Kerogen distribution and depositional environments in the Middle Jurassic of Yorkshire U.K. IN C., B. D., SINGH, H. P. & TIWARI, R. S. (Eds.) *4th International Palynological Conference, Lucknow 1976-1977.*

FISHER, M. J., BARNARD, P. C. & COOPER, B. S. (1980) Organic maturation and hydrocarbon generation in the Mesozoic sediments of the Sverdrup Basin, Arctic Canada. *4th International Palynololigical Conference, Lucknow (1976-1977).* Lucknow.

FOUCHER, J.-C., PONS, D., MAMI, L. & BELLIER, J.-P. (1994) Premier inventaire de la microflore crétacée (dinokystes, spores et pollen) du Sud-Est constantinois (Algérie): conséquences biostratigraphiques. *Compte rendu hebdomadaire des seances de l'Academie des Sciences Paris,* 318**,** 1563-1570.

FUNKHOUSER, J. W. (1969) Factors that affect sample reliability. IN TSCHUDY, R. & SCOTT, R. (Eds.) *Aspects of Palynology.* Wiley-Interscience, New York.

GARFUNKEL, Z. & BARTOV, Y. (1977) The tectonics of the Suez rift. *Geological Survey of Israel Bulletin,* 71**,** 44.

GEHMAN, H. M. J. (1962) Organic matter in limestones. Geochem. *Geochimica et Cosmochimica Acta* 26**,** 885-897.

GHORAB, M. A. (1961) Abnormal stratigraphic features in Ras Gharib oil field. *Third Arabian Petroleum Congress.* Alexandria, Egypt.

GHORAB, M. A., EBEID, Z. & TAWFIK, N. (1971) On the stratigraphy of the north-eastern corner of the Western Desert. *Ninth Annual Meeting of the Geological Society of Egypt.* Giza, Egypt.

GOODMAN, D. K. (1979) Dinoflagellate 'communities' from the Lower Eocene Nanjemoy Formation of Maryland, USA. *Palynology,* 3**,** 169-190.

GOODMAN, D. K. (1987) Dinoflagellate cysts in ancient and modern sediments. IN TAYLOR, F. J. R. (Ed.) *The Biology of Dinoflagellates.* Botanical Monographs.

GORIN, G. & MONTEIL, E. (1990) Preliminary note on the organic facies, thermal maturity, and dinoflagellate cysts of the upper Maastrichtian Wang Formation in the northern Subalpine Massifs (western Alps, France). *Eclogae Geologicae Helvetiae,* 83**,** 265-85.

GREEN, O. R. (2001) A Manual of Practical Laboratory and Field Techniques in Palaeobiology, Dordrecht, Kluwer Academic Publishers.

GRUAS-CAVAGNETTO, C. (1978) Étude palynologique de l'Éocene du Bassin anglo-parisien. *Mémoire de la Société Géologique de France, Nouvelle Série,* 56**,** 1-64.

GÜBELI, A. A., HOCHULI, P. A. & WILDI, W. (1984) Lower Cretaceous turbiditic sediments from the Rif Chain (northern Morocco): palynology, stratigraphy and paleogeographic settings. *Geologische Rundschau,* 73**,** 1018-1114.

GUIRAUD, R. & BOSWORTH, W. (1997) Senonian basin inversion and rejuvenation of rifting in Africa and Arabia: synthesis and implications to plate-scale tectonics. *Tectonophysics,* 282**,** 39-82.

GUIRAUD, R. & BOSWORTH, W. (1999) Phanerozoic geodynamic evolution of north-eastern Africa and the north-western Arabian platform. *Tectonophysics,* 315**,** 73-108.

GUIRAUD, R., BOSWORTH, W., THIERRY, J. & DELPLANQUE, A. (2005) Phanerozoic geological evolution of Northern and Central Africa: an overview. *Journal of African Earth Sciences,* 43**,** 83-143.

GUIRAUD, R., ISSAWI, B. & BOSWORTH, W. (2001) Phanerozoic history of Egypt and surrounding areas. IN ZIEGLER, P. A., CAVAZZA, W., ROBERTSON, A. H. F. & CRASQUIN-SOLEAU, S. (Eds.) *Peri-Tethys Memoir 6: Peri-Tethyan Rift/Wrench Basins and Passive Margins.* Paris, Mémoires du Muséum National d'Histoire Naturelle.

HABIB, D. (1975) Neocomian dinoflagellate zonation in the western North Atlantic. *Micropaleontology,* 21**,** 373-392.

HABIB, D. (1977) Comparison of lower and middle Cretaceous palynostratigraphic zonation in the western North Atlantic. IN SWAIN, F. M. (Ed.) *Stratigraphic Micropaleontology of Atlantic Basin and Borderlands.* New York, Elsevier.

HABIB, D. (1979) Sedimentology of palynomorphs and palynodebris in Cretaceous carbonaceous facies south of Vigo Seamount. *Initial Reports of the Deep Sea Drilling Project,* 47**,** 451-467.

HABIB, D. (1982) Sedimentary supply origin of Cretaceous black shales. IN SCHLANGER, S. O. & CITA, M. B. (Eds.) *Nature and Origin of Cretaceous Carbon-Rich Facies.* London, Academic Press.

HABIB, D. (1983) Sedimentation-Rate-Dependent Distribution of Organic-Matter in the North-Atlantic Jurassic-Cretaceous. *Initial Reports of the Deep Sea Drilling Project,* 76**,** 781-794.

HABIB, D. & DRUGG, W. S. (1983) Dinoflagellate Age of Middle Jurassic-Early Cretaceous Sediments in the Blake-Bahama Basin. *Initial Reports of the Deep Sea Drilling Project,* 76**,** 623-638.

HABIB, D., MOSHKOVITZ, S. & KRAMER, C. (1992) Dinoflagellate and calcareous nannofossils response to sea level change in Cretaecous-Tertiary boundary section. *Geology,* 20**,** 165-168.

HANTAR, G. (1990) North Western Desert. IN SAID, R. (Ed.) *The Geology of Egypt.* Rotterdam, Balkema.

HARDING, I. C. (1986b) An Early Cretaceous dinocyst assemblage from the Wealden of southern England. *Palaeontology Special Paper,* 35**,** 95-109.

HARDING, I. C. (1996a) Taxonomic stabilization of dinoflagellate cyst taxa, as exemplified by two morphologically complex Early Cretaceous species. *Review of Palaeobotany and Palynology,* 92**,** 351-366.

HARWOOD, R. J. (1977) Oil and gas generation by laboratory pyrolysis of kerogen. *American Association of Petroleum Geologists Bulletin,* 61**,** 2082-2102.

HAY, W. W., DECONTO, R., WOLD, C. N., WILSON, K. M., VOIGT, S., SCHULZ, M., WOLD-ROSSBY, A., DULLO, W.-C., RONOV, A. B., BALUKHOVSKY, A. N. & SOEDING, E. (1999) Alternative global Cretaceous paleogeography. IN BARRERA, E. & JOHNSON, C. (Eds.) *The Evolution of Cretaceous Ocean/Climate Systems.* Geological Society of America Special Paper.

HERNGREEN, G. F. W. (1973) Palynology of Albian-Cenomanian strata of borehole 1-QS-1-MA, State of Maranhão, Brazil. *Pollen et Spores,* 15**,** 515-555.

HERNGREEN, G. F. W. (1974a) Middle Cretaceous palynomorphs from north-eastern Brazil. *Sciences Géologiques Bulletin,* 27**,** 101-116.

HERNGREEN, G. F. W. (1974b) Palynology of Albian-Cenomanian strata of borehole 1-QS-1-MA, State of Maranhão, Brazil. *Pollen et Spores,* 15**,** 515-555.

HERNGREEN, G. F. W. (1975) Palynology of middle and upper Cretaceous strata in Brazil. *Mededelingen Rijks Geologische Dienst, N.S.,* 26**,** 39-91.

HERNGREEN, G. F. W. (1980) Cretaceous microfloral provinces. *Berliner Geowissenschaftliche Abhandlungen Reihe A,* 19**,** 79-82.

HERNGREEN, G. F. W. & CHLONOVA, A. F. (1981) Cretaceous microfloral provinces. *Pollen et Spores,* 23**,** 441-555.

HERNGREEN, G. F. W. & JIMENEZ, H. D. (1990) Dating of the Cretaceous Une Formation, Colombia and the relationship with the Albian-Cenomanian African-South American microfloral province. *Review of Palaeobotany and Palynology,* 66**,** 345-359.

HERNGREEN, G. F. W., KEDVES, M., ROVNINA, L. V. & SMIRNOVA, S. B. (1996) Cretaceous palynofloral provinces: a review. IN JANSONIUS, J. & MCGREGOR, D. C. (Eds.) *Palynology: Principles and Applications.* Texas, American Association of Stratigraphic Palynologists Foundation.

HILLER, S. J. & MARSHALL, J. E. A. (1988) A rapid technique to make polished thin section of sedimentary organic matter concentrates. *Journal of Sedimentary Petrology,* 58**,** 754-755.

HOCHULI, P. A. (1981) North Gondwanan floral elements in lower to middle Cretaceous sediments of the southern Alps (southern Switzerland, northern Italy). *Review of Palaeobotany and Palynology,* 35**,** 337-358.

HOCHULI, P. A. & KELTS, K. (1980) Palynology of middle Cretaceous black clay facies from Deep Sea Drilling Project Sites 417 and 418 of the western North Atlantic. *Initial Reports of the Deep Sea Drilling Project,* 51-53**,** 897-935.

HOEDEMAEKER, P. J. & LEEREVELD, H. (1995) Biostratigraphy and sequence stratigraphy of the Berriasian-lowest Aptian (lower Cretaceous) of the Rio-Argos succession, Caravaca, SE Spain. *Cretaceous Research,* 16**,** 195-230.

HUGHES, N. F. (1994) *The enigma of angiosperm origins,* Cambridge, Cambridge University Press.

HUGHES, N. F., DREWRY, G. E. & LAING, J. F. (1979) Barremian earliest angiosperm pollen. *Palaeontology,* 22**,** 513-535.

HUGHES, N. F. & MOODY-STUART, J. C. (1967) Palynological facies and correlation in the English Wealden. *Review of Palaeobotany and Palynology,* 1**,** 259-268.

HUNT, J. M. (1996) The source rock. IN HUNT, J. M. (Ed.) *Petroleum Geochemistry and Geology.* San Francisco, W. H. Freeman & Company.

HUTTON, A. C. (1988) The lacustrine Condor oil Rocks. IN FLEET, A. J., KELTS, K. & TALBOT, M. R. (Eds.) *Lacustrine Petroleum Source Rocks.* Geological Society of London Special Publication.

HUTTON, A. C. & COOK, A. C. (1990) Influence of alginite on reflectance of vitrinite from Joadja, NSW, and some other coals and oil shales containing alginite. *Fuel,* 59**,** 711-714.

IBRAHIM, M. I. A. (1996) Aptian-Turonian palynology of the Ghazalat-1 well (GTX-1), Qattara Depression, Egypt. *Review of Palaeobotany and Palynology,* 94**,** 137-168.

IBRAHIM, M. I. A. (2002a) New angiosperm pollen from the upper Barremian-Aptian of the Western Desert, Egypt. *Palynology,* 26**,** 107-133.

IBRAHIM, M. I. A. (2002b) Late Albian-middle Cenomanian palynofacies and palynostratigraphy, Abu Gharadig-5 well, Western Desert, Egypt. *Cretaceous Research,* 23**,** 775-788.

IBRAHIM, M. I. A. & ABDEL-KIREEM, M. R. (1997) Late Cretaceous palynofloras and foraminifera from Ain El-Wadi area, Farafra Oasis, Egypt. *Cretaceous Research,* 18**,** 633-660.

IBRAHIM, M. I. A., ABOUL ELA, N. M. & KHOLEIF, S. E. (1997) Paleoecology, palynofacies, thermal maturation and hydrocarbon source rock potential of the Jurassic-lower Cretaceous sequence in the subsurface of the north Eastern Desert, Egypt. *Qatar University Science Journal,* 17**,** 153-172.

IBRAHIM, M. I. A., AL-HITMI, H. H. & KHOLEIF, S. E. (2000) Albian-Cenomanian palynology, paleoecology and organic thermal maturity of well DK-B in the Dukhan oil field of western Qatar. *GeoArabia,* 5**,** 483-508.

IBRAHIM, M. I. A. & EL-BEIALY, S. Y. (1995) Kimmeridgian-Barremian palynostratigraphy of the Malha-1 well, northern Sinai, Egypt. *Sciences Géologiques - Bulletin,* 48**,** 187-209.

IBRAHIM, M. I. A., ELA, N. M. A. & KHOLEIF, S. E. (2002) Dinoflagellate cyst biostratigraphy of Jurassic-Lower Cretaceous formations of the North Eastern Desert, Egypt. *Neues Jahrbuch für Geologie und Paläontologie - Abhandlungen,* 224**,** 255-319.

IBRAHIM, M. I. A. & SCHRANK, E. (1996) Palynological studies on the late Jurassic-early Cretaceous of the Kahraman-1 well, northern Western Desert, Egypt. *Géologie de l'Afrique et de l'Atlantique Sud: Actes Colloques Angers 1994.* Pau, Elf Aquitaine.

INCORPORATION, P. R. A. (1993) BasinMod^{R} 1-D for Windows^{TM}: Basin Modelling System. 4.0 ed. Denver, USA, Platte River Association Incorporation.

IVERSEN, J. & TROEL-SMITH, J. (1950) Pollenmorfologiske definitioner og typer. *Danmarks Geologiske Undersogelse,* 3**,** 441-555.

JAIN, K. P. & MILLEPIED, P. (1973) Cretaceous microplankton from Senegal Basin, NW Africa. 1. Some new genera, species and combinations of dinoflagellates. *The Palaeobotanist,* 20**,** 22-32.

JAN DU CHÊNE, R., DE KLASZ, I. & ARCHIBONG, E. E. (1978) Biostratigraphic study of the borehole OJO-1, SW Nigeria, with special emphasis on the Cretaceous microflora. *Revue de Micropaléontologie,* 2**,** 123-139.

JANSONIUS, J. & HILLS, L. V. (1976) Genera File of Fossil Spores. Special Publication ed. Calgary, Geology Department, University of Calgary, Canada.

JARDINÉ, S. (1967) Spores à expansions en forme d`elateres du Crétacé moyen d`Afrique occidentale. *Review of Palaeobotany and Palynology,* 1**,** 235-258.

JARDINÉ, S., BIENS, P. & DOERENKAMP, A. (1974) *Dicheiropollis etruscus*, un pollen caractéristique du Crétacé inférieur Afro-Sudamericain. Conséquences pour l`évaluation des unités climatiques et implication dans la dérive des continents. *Sciences Géologiques - Bulletin,* 27**,** 87-100.

JARDINÉ, S. & MAGLOIRE, L. (1965) Palynologie et stratigraphie du Crétacé, des bassins de Sénégal et d` Côte De`Ivoire. *Mémoire Bureau Recherche Géologie et Minéralogie,* 32**,** 187-245.

JARRIGE, J. J., DESTEVOU, P. O., BUROLLET, P. F., THIRIET, J. P., ICART, J. C., RICHERT, J. P., SEHANS, P., MONTENAT, C. & PRAT, P. (1986) Inherited discontinuities and Neogene structure - the Gulf of Suez and the north-western edge of the Red-Sea. *Philosophical Transactions of the Royal Society of London Series a Mathematical Physical and Engineering Sciences,* 317**,** 129-139.

KASKA, H. V. (1989) A spore and pollen zonation of early Cretaceous to Tertiary non-marine sediments of central Sudan. *Palynology,* 13**,** 79-90.

KEDVES, M. (1998) Upper Cretaceous pollen grains from Egypt II. *Plant Cell Biology and Development,* 9**,** 8-27.

KEDVES, M. (1999) Upper Cretaceous pollen grains from Egypt III. *Plant Cell Biology and Development,* 10**,** 14-29.

KERDANY, M. T. & CHERIF, O. H. (1990) Mesozoic. IN SAID, R. (Ed.) *The Geology of Egypt.* Rotterdam, Balkema.

KHALIL, S. M. (1998) Tectonic evolution of the eastern margin of the Gulf of Suez, Egypt. London, Royal Holloway, University of London.

KHALIL, S. M. & MCCLAY, K. (1998) Structural architecture of the eastern margin of the Gulf of Suez: feild studies and analogue modelling results. *Fourteenth Exploration Conference.* Cairo, Egypt.

KLAUS, W. (1960) Sporen der Karnischen Stufe der ostalpinen Trias. *Jahrbuch der Geologischen Bundesanstalt,* 5**,** 107-184.

KRUTZSCH, W. (1959) Mikropalaontologische (sporenpalaontologische) Untersuchungen in der Braunkohle des Geiseltales. *Geologie,* 8**,** 1-425.

LANGENHEIM, R. L. J. (1965) Collecting amber. IN KUMMEL, B. & RAUP, D. (Eds.) *Handbook of Paleontological Techniques* San Francisco, Freeman.

LANJOUW, J. (1961) International Code of Botanical Nomenclature (1959). *The Ninth International Botanical Congress Montreal, 1959.* Montreal, Canada, Regnum Vegetabile.

LARSSON, S. G. (1978) *Baltic amber - a palaeobiological study,* Klampenborg, Denmark, Scandinavian Science Press.

LAWAL, O. & MOULLADE, M. (1986) Palynological biostratigraphy of Cretaceous sediments in the Upper Benue Basin, NE Nigeria. *Revue de Micropaléontologie,* 29**,** 61-83.

LAWVER, L. A., DALZIEL, I. W. D., GAHAGAN, L. M., KYGAR, R. M. & HERBER, B. D. (2004) Atlas of Plate Reconstructions (750 Ma to Present Day). University of Texas Institute for Geophysics.

LECKIE, D. A. & SINGH, C. (1991) Estuarine deposits of the Albian Paddy Member (Peace River Formation) and lowermost Shaftesbury Formation, Alberta, Canada. *Journal of Sedimentary Petrology,* 61**,** 825-849.

LEEREVELD, H. (1997a) Upper Tithonian-Valanginian (upper Jurassic-lower Cretaceous) dinoflagellate cyst stratigraphy of the western Mediterranean. *Cretaceous Research,* 18**,** 385-420.

LEEREVELD, H. (1997b) Hauterivian-Barremian (lower Cretaceous) dinoflagellate cyst stratigraphy of the western Mediterranean. *Cretaceous Research,* 18**,** 421-456.

LENTIN, J. K. & WILLIAMS, G. L. (1976) A monograph of fossil peridinioid dinoflagellate cysts. *Bedford Institute of Oceanography, Report Series,* BI-R-75-16**,** 1-237.

LEWAN, M. D. (1993) Identifying and understanding suppressed vitrinite reflectance through hydrous pyrolsis experiments. *Abstract, 10th Annual Meeting of the Society for Organic Petrology.* Norman, Oklahoma.

LISTER, J. K. & BATTEN, D. J. (1988) Stratigraphic and paleoenvironmental distribution of early Cretaceous dinoflagellate cysts in the Hurlands Farm Borehole, West Sussex, England. *Palaeontographica Abteilung B,* 210**,** 8-89.

LUND, J. J. & PEDERSEN, R. K. (1985) Palynology of the marine Jurassic formations in the Vardekloft Ravine, Jameson Land, East Greenland. *Bulletin of the Geological Society of Denmark,* 33**,** 371-399.

MAHMOUD, M. S. (2003) Palynology and palaeoenvironment of the Quseir Formation (Campanian) from central Egypt. *Journal of African Earth Sciences,* 36**,** 135-148.

MAHMOUD, M. S. & DEAF, A. S. (2007) Cretaceous palynology (spores, pollen and dinoflagellate cysts) of the Siqeifa 1-X borehole, northern Egypt. *Rivista Italiana di Paleontologia e Stratigrafia,* 113**,** 203-221.

MAHMOUD, M. S. & MOAWAD, A. M. M. (2002) Cretaceous palynology of the Sanhur-1X borehole, northern western Egypt. *Revista Española de Micropaleontologia,* 34**,** 129-143.

MAHMOUD, M. S., OMRAN, A. M. & ATAA, S. A. S. (1999) Stratigraphy of the upper Jurassic-lower Cretaceous sequences from three boreholes, northern Egypt: palynological evidence. *Newsletters on Stratigraphy,* 37**,** 141-161.

MAHMOUD, M. S., SOLIMAN, H. A. & DEAF, A. S. (2007) Early Cretaceous (Aptian-Albian) palynology of the Kabrit-1 borehole, onshore northern Gulf of Suez, Egypt. *Revista Española de Micropaleontología,* 39**,** 169-187.

MARSHALL, J. E. A. (1988) The recognition of multiple hydrocarbon generation episodes: an example from Devonian lacustrine sedimentary rocks in the Inner Moray Firth, Scotland. *Journal of the Geological society, London,* 155**,** 335-352.

MAY, F. E. (1980) Dinoflagellate cysts of the Gymnodiniaceae, Peridiniaceae, and Gonyaulacaceae from the upper Cretaceous Monmouth Group, Atlantic Highlands, New Jersey. *Palaeontographica Abteilung B,* 172**,** 10-116.

MCCLAY, K., NICHOLS, G. J., KHALIL, S., DARWISH, M. & BOSWORTH, W. (1998) Extensional tectonics and sedimentation, eastern Gulf of Suez, Egypt.

IN PURSER, B. H. & BOSENCE, D. W. J. (Eds.) *Sedimentation and Tectonics of Rift Basins: Red Sea-Gulf of Aden.* London, Chapman & Hall.

MCNEILL, J., BARRIE, F. R., BURDET, H. M., DEMOULIN, V., HAWKSWORTH, D. L., MARHOLD, K., NICOLSON, D. H., PRADO, J., SILVA, P. C., SKOG, J. E., WIERSEMA, J. H. & TURLAND, N. J. (2006) International Code of Botanical Nomenclature (Vienna Code). *Regnum Vegetabile,* 146**,** 1-568.

MESHREF, W. M. (1990) Tectonic framework. IN SAID, R. (Ed.) *The Geology of Egypt.* Rotterdam, Balkema.

METWALLI, M. H. & ABD EL-HADY, Y. E. (1975) Petrographic characteristics of oil-bearing rocks in Alamein oil field; significance in source-reservoir relations in northern Western Desert, Egypt. *American Association of Petroleum Geologists Bulletin,* 59**,** 510-523.

MILES, J. (1994) Illustrated Glossary of Petroleum Geochemistry. Oxford, Clarendon Press.

MILLIOUD, M. E. (1967) Playnological study of the type localities at Valangin and Hauterive. *Review of Palaeobotany and Palynology,* 5**,** 155-167.

MILLIOUD, M. E. (1969) Dinoflagellates and acritarchs from Western European lower Cretaceous type localities. IN BRONNIMANN, P. & RENZ, H. H. (Eds.) *First International Conference on Planktonic Microfossils.* Geneva, Switzerland.

MINER, E. L. (1935) Paleobotaical examination of Cretaceous and Tertiary coals. *American Midland Naturalist,* 16**,** 585-625.

MONTEIL, E. (1991b) Morphology and systematics of the ceratioid group: a new morphographic approach. Revision and emendation of the genus Muderongia Cookson and Eisenack 1958. *Bulletin des Centres de Recherches Exploration-Production Elf-Aquitaine,* 15**,** 461-505.

MORGAN, P. (1990) Egypt in the framework of global tectonics. IN SAID, R. (Ed.) *The Geology of Egypt.* Rotterdam, Balkema.

MORGAN, R. (1978) Albian to Senonian palynology of site 364, Angola Basin. *Initial Reports of the Deep Sea Drilling Project,* 40**,** 915-951.

MOUSTAFA, A. R. (1976) Block faulting of the Gulf of Suez. *Unpublished Report.* Cairo, Egyptian General Petroleum Company.

MOUSTAFA, A. R. (1993) Structural characteristics and tectonic evolution of the east-margin blocks of the Suez rift. *Tectonophysics,* 223**,** 381-399.

MOUSTAFA, A. R. & KHALIL, M. H. (1995) Superposed deformation in the northern Suez rift, Egypt: relevance to hydrocarbons exploration. *Journal of Petroleum Geology,* 18**,** 245-266.

MÜLLER, J. (1959) Palynology of Recent Orinoco Delta and shelf sediments: reports of the Orinoco Shelf expedition; volume 5. *Micropaleontology,* 5**,** 1-2.

MÜLLER, J. (1966) Montane pollen from the Tertiary of NW Borneo. *Blumea,* 4**,** 231-235.

MUSTAFA, A. A. & TYSON, R. V. (2002) Organic facies of Early Cretaceous synrift lacustrine source rocks from the Muglad Basin, Sudan. *Journal of Petroleum Geology,* 25**,** 351-365.

MUTTERLOSE, J. & HARDING, I. (1987) Phytoplankton from the anoxic sediments of the Barremian (lower Cretaceous) of north-west Germany. *Abhandlungen der Geologischen Bundesanstalt (Vienna),* 39**,** 177-215.

NAGY, J., DYPVIK, H. & BJAERKE, T. (1984) Sedimentological and paleontological analyses of Jurassic North Sea deposits from deltaic environments. *Journal of Petroleum Geology,* 7**,** 169-188.

NAUMOVA, S. N. (1939) Spores and pollen of the coals of the U.S.S.R. *17th International Geological Congress.* Moscow.

NORTON, P. (1967) Rock stratigraphic nomenclature of the Western Desert. *Internal Report.* Cairo, Pan-American Oil Company.

OMRAN, A. M., SOLIMAN, H. A. & MAHMOUD, M. S. (1990) Early Cretaceous palynology of three boreholes from northern Western Desert (Egypt). *Review of Palaeobotany and Palynology,* 66**,** 293-312.

PAPROTH, E. & STREEL, M. (1970) Correlations biostratigraphiques pres de la limite Devonien/Carbonifere entre les facies littoraux ardennais et les facies bathyaux rhenans. IN STREEL, M. & WAGNER, R. H. (Eds.) *Colloque sur la Stratigraphie du Carbonifere, Liege, April 1969.* Les Congres et Colloques de l'Universite de Liege.

PARRY, C. C., WHITLEY, P. K. J. & SIMPSON, R. D. H. (1981) Integration of palynological and sedimentological methods in facies analysis of the Brent

Formation IN ILLING, L. V. & HOBSON, G. D. (Eds.) *Petroleum Geology of the Continental Shef of North West Europe* Londn, Heyden.

PATTON, T. L., MOUSTAFA, A. R., NELSON, R. A. & ABDINE, S. A. (1994) Tectonic evolution and structural setting of the Suez rift. IN LANDON, S. M. (Ed.) *Interior Rift Basins.* Tulsa, American Association of Petroleum Geologists Memoir.

PEARSON, D. L. (1984) Pollen/spore color "standard". Phillips Petroleum Company Geological Branch.

PELZER, G., RIEGEL, W. & WILDE, V. (1992) Depositional control on the lower Cretaceous Wealden coals of Northwest Germany. *Geological Society of America Special Paper,* 267**,** 227-243.

PENNY, J. H. J. (1986) An early Cretaceous angiosperm pollen assemblages from Egypt. IN BATTEN, D. J. & BRIGGS, D. E. G. (Eds.) *Studies in Palaeobotany and Palynology in Honour of N. F. Hughes.* London, Special Papers in Palaeontology.

PENNY, J. H. J. (1988a) Early Cretaceous acolumellate semitectate pollen from Egypt. *Palaeontology,* 31**,** 373-418.

PENNY, J. H. J. (1988b) Early Cretaceous striate tricolpate pollen from the Borehole Mersa Matruh 1, North West Desert, Egypt. *Journal of Micropalaeontology,* 7**,** 201-215.

PENNY, J. H. J. (1989) New early Cretaceous forms of the angiosperm pollen genus *Afropollis* from England and Egypt. *Review of Palaeobotany and Palynology,* 58**,** 289-299.

PENNY, J. H. J. (1991) Early Cretaceous angiosperm pollen from the borehole Mersa Matruh-1, north West Desert, Egypt. *Palaeontographica Abteilung B,* 222**,** 31-88.

PENNY, J. H. J. (1992) The relevance of the early Cretaceous angiosperm palynology of Egypt to biostratigraphy and reconstruction of angiosperm palaeolatitudinal migrations. *Cretaceous Research,* 13**,** 369-378.

PETERS, K. E. (1986) Guidelines for evaluating petroleum source rock using programmed pyrolysis. *American Association of Petroleum Geologists Bulletin,* 70**,** 318-329.

PHIPPS, D. & PLAYFORD, G. (1984) Laboratory techniques for extraction of palynomorphs from sediments. *Papers, Deptartment of Geology, University of Queensland,* 11**,** 1-23.

PIASECKI, S. (1984) Dinoflagellate cysts stratigraphy of the Lower Cretaceous Jydegard Formation, Bornholm, Denmark. *Bulletin of the Geological Society of Denmark,* 32**,** 145-161.

PIASECKI, S. (1986) Palynological analysis of the organic debris in the Lower Cretaceous Jydegard Formation, Bornholm, Denmark. *Grana,* 25**,** 119-129.

POCKLINGTON, R. & LEONARD, J. D. (1979) Terrigenous organic mattter in sediments of the St. Lawrence Estuary and the Saguenay Fjord. *Journal of the Fisheries Research Board of Canada,* 36**,** 1250-1255.

POCOCK, S. A. J. (1961a) Microflora of the genus *Murospora*. Spores from Mesozoic strata of Western Canada and Australia. *Journal of Paleontology,* 35**,** 1231-1234.

POCOCK, S. A. J. (1970) Palynology of the Jurassic sediments of Western Canada. Part 1 (continued). Terrestrial species. *Palaeontographica Abteilung B,* 130**,** 73-136.

POCOCK, S. A. J. (1982) Identification and recording of particulate sedimentary organic matter. IN STAPLIN, D. J., DOW, W. G., MILNER, C. W. D., O'CONNOR, D. I., POCOCK, S. A. J., VAN GIJZEL, P., WELTE, D. H. & YUKLER, M. A. (Eds.) *How to Assess Maturation and Paleotemperatures.* Society of Economic Paleontologists and Mineralogists, Short Course.

POCOCK, S. A. J., VASANTHY, G. & VENKATACHALA, B. S. (1988) Introduction to the study of particulate organic materials and ecological perspectives. *Journal of Palynology,* 23-24**,** 167-188.

POTONIÉ, R. (1956) Synopsis der Gattungen der Sporae dispersae. I. Teil: Sporites. *Beihefte zum Geologischen Jahrbuch,* 23**,** 1-103.

POTONIÉ, R. (1958) Synopsis der Gattungen der Sporae dispersae. II. Teil: Sporites (Nachtage), Saccites, Aletes, Praecolpates, Polyplicates, Monocolpates. *Beihefte zum Geologischen Jahrbuch,* 31**,** 1-114

POTONIÉ, R. & KREMP, G. O. W. (1954) Die Gattungen der palaozoischen Sporae dispersae und ihre Stratigraphie. *Geologisches Jahrbuch,* 69**,** 111-194.

POWELL, A. J., DODGE, J. D. & LEWIS, J. (1990) Late Neogene to Pleistocene palynological facies of the Peruvian continental margin upwelling, Leg 112. *Proceedings of the Ocean Drilling Project, Scientific Results,* 112**,** 297-321.

PRAUSS, M. (1989) Dinozysten-stratigraphie und palynofazies im oberen Lias und Dogger von NW-Deutschland. *Palaeontographica Abteilung B,* 214**,** 1-124.

PRICE, L. C. & BARKER, C. E. (1985) Suppression of vitrinite reflectance in amorphous rich kerogen - a major unrecognised problem *Journal of Petroleum Geology,* 8**,** 59-84.

PUNT, W., HOEN, P. P., BLACKMORE, S., NILSSON, S. & LE THOMAS, A. (2007) Glossary of pollen and spore terminology. *Review of Palaeobotany and Palynology,* 143**,** 1–81.

QUATTROCCHIO, M. E., MARTINEZ, M. A., CARPINELLI PAVISICH, A. & VOLKHEIMER, W. (2006) Early Cretaceous palynostratigraphy, palynofacies and palaeoenvironments of well sections in northeastern Tierra del Fuego, Argentina. *Cretaceous Research,* 27**,** 584-602.

RAVN, R. L. (1998) TAXON: an electronic internet database. American Association of Stratigraphic Palynologists.

RAYNAUD, J. F. & ROBERT, P. (1976) Les méthodes d`étude optique de la matiere organique. *Bulletin Centre*.

REGALI, M. S. P. (1989) Evolucao da paleoflora no Cretaceo das margens equatorial de nordest do Brazil. *Revista Escola de Minas,* 42**,** 17-33.

REGALI, M. S. P., UESUGUI, N. & SANTOS, A. S. (1974) Palinologia dos sedimentos Meso-Cenozoicos do Brasil (I & II). *Boletim Tecnico da PETROBRAS,* 17**,** 177-191, 263-301.

REGALI, M. S. P. & VIANA, C. F. (1989) Late Jurassic-early Cretaceous in Brazilian sedimentary basins: correlation with the international standard scale. *Report.* PETROBRAS, Rio de Janeiro.

REYMENT, R. A. & TAIT, E. A. (1972) Biostratigraphical dating of the early history of the South Atlantic Ocean. *Philosophical Transactions of the Royal Society of London, B. Biological Sciences,* 264**,** 55-95.

REYRE, Y. (1973) Palynologie du Mésozoique Saharien. *Mémoris du Muséum National d'Histoire Naturelle,* 27**,** 1-284.

RIDER, M. H. (1986) *The Geological Interpretation of Well Logs,* Glasgow, Blackie - Halsted Press.

RIDING, J. B., POULSEN, N. E. & BAILEY, D. A. (2001) A taxonomic study of the dinoflagellate cyst Muderongia simplex Alberti 1961 and related species. *Palynology,* 24**,** 21-35.

RIDING, J. B., WALTON, W. & SHAW, D. (1991) Toarcian to Bathonian (Jurassic) palynology of the Inner Hebrides, northwest Scotland. *Palynology,* 15**,** 115-180.

ROBERT, P. (1988) Methods and means of paleogeothermal analysis. IN ROBERT, P. (Ed.) *Organic metamorphism and geothermal history.* Dordercht, Elf-Aquitaine & D. Reidel.

RONOV, A. B. (1958) Organic carbon in sedimentary rocks (in relation to the presence of petroleum). *Geochemistry,* 5**,** 497-509.

SAAD, S. I. (1978) Palynological studies in the Egyptian Western Desert, Umbarka 1X borehole. *Pollen et Spores,* 20**,** 261-301.

SAID, R. (1962) Tectonic framework of Egypt. IN SAID, R. (Ed.) *The Geology of Egypt.* Amsterdam, Elsevier.

SAID, R. (1971) Explanatory notes to accompany the geological map of Egypt. *Geological Survey of Egypt,* 56**,** 123pp.

SAID, R. (1990) Cretaceous paleogeographic maps. IN SAID, R. (Ed.) *The Geology of Egypt.* Rotterdam, Balkema.

SALARD-CHEBOLDAEFF, M. (1990) Intertropical African palynostratigraphy from Cretaceous to Quaternary times. *Journal of African Earth Sciences,* 11**,** 1-24.

SCHRANK, E. (1982) Kretazische Pollen und Sporen aus dem “Nubischen Sandstein” des Dakhla-Beckens (Egypt). *Berliner Geowissenschaftliche Abhandlungen - Reihe A,* 40**,** 87-109.

SCHRANK, E. (1983) Scanning electron and light microscopic investigations of angiosperm pollen from the lower Cretaceous of Egypt. *Pollen et Spores,* 25**,** 213-242.

SCHRANK, E. (1984a-a) Oragic-geochemical and palynological studies of a Dakhla Shale profile (Late Cretyaceous) in southeast Egypt. *Berliner Geowissenschaftliche Abhandlungen - Reihe A,* 50**,** 177-187.

SCHRANK, E. (1984a-b) Paleozoic and Mesozoic palynomorphs from the Foram 1 well (Western Desert, Egypt). *Neues Jahrbuch für Geologie und Paläontologie Monatschefte,* 2**,** 95-112.

SCHRANK, E. (1990) Palynology of the clastic Cretaceous sediments between Dongola and Wadi Muqaddam, northern Sudan. *Berliner Geowissenschaftliche Abhandlungen - Reihe A,* 120**,** 149-168.

SCHRANK, E. (1991) Mesozoic palynology and continental sediments in NE Africa (Egypt and Sudan) - a review. *Journal of African Earth Sciences,* 12**,** 363-373.

SCHRANK, E. (1992) Nonmarine Cretaceous correlations in Egypt and northern Sudan; palynological and palaeobotanical evidence. *Cretaceous Research,* 13**,** 351-368.

SCHRANK, E. (2001) Paleoecological aspects pf *Afropollis/*elaterate peaks (Albian-Cenomanian pollen) in the Cretaceous of Northern Sudan and Egypt. IN GOODMAN, D. K. & CLARKE, R. T. (Eds.) *Proceeding of the IX International Palynological Congress, Houston, Texas, 1996.* American Association of Stratigraphic Palynologists Foundation.

SCHRANK, E. & IBRAHIM, M. I. A. (1995) Cretaceous (Aptian-Maastrichtian) palynology of foraminifera-dated wells (KRM-1, AG-18) in north-western, Egypt. *Berliner Geowissenschaftliche Abhandlungen - Reihe A,* 177**,** 1-44.

SCHRANK, E. & MAHMOUD, M. S. (1998) Palynology (pollen, spores and dinoflagellates) and Cretaceous stratigraphy of the Dakhla Oasis, central Egypt. *Journal of African Earth Sciences,* 26**,** 167-193.

SCHRANK, E. & MAHMOUD, M. S. (2000) New taxa of angiosperm pollen, miospores and associated palynomorphs from the early Late Cretaceous of Egypt (Maghrabi Formation, Kharga Oasis). *Review of Palaeobotany and Palynology,* 112**,** 167-188.

SCHRANK, E. & MAHMOUD, M. S. (2002) Barremian angiosperm pollen and associated palynomorphs from the Dakhla Oasis area, Egypt. *Palaeontology,* 45**,** 33-56.

SCHÜTZ, K. I. (1994) Structure and stratigraphy of the Gulf of Suez, Egypt. IN LANDON, S. M. (Ed.) *Interior Rift Basins* Tulsa, American Association of Petroleum Geologists Memoir.

SIMPSON, E. H. (1949) Measurement of diversity. *Nature,* 163**,** 688.

SINGH, C. (1964) Microflora of the Lower Cretaceous Mannville Group, east-central Alberta. *Research Council of Alberta Bulletin,* 15**,** 1-238

SINGH, C. (1971) Lower Cretaceous microflora of the Peace River area, north-western Alberta. *Research Council of Alberta Bulletin,* 28**,** 542.

SINGH, G., OPDYKE, N. D. & BOWLER, J. M. (1981) Late Cainozoic stratigraphy, palaeomagnetic chronology and vegetational history from Lake George, N.S.W. *Journal of the Geological Society of Australia,* 28.

SKOG, J. E. (2005) Report of the Committee for Fossil Plants:6. *Taxon,* 54**,** 827.

SMELROR, M. & LEEREVELD, H. (1989) Dinoflagellate cyst and acritarch assemblages from the Late Bathonian-Early Oxfordian of Montange Crussol, Rhône Valley, southern France. *Palynology,* 13**,** 121-141.

SMYTH, M., JIAN, F. X. & WARD, C. R. (1992) Potential petroleum source rocks in Triassic lacustrine-delta sediments of the Gunnedah Basin, Eastern Australia. *Journal of Petroleum Geology,* 15**,** 435-450.

SOLIMAN, S. M. & AMER, K. M. (1972) Cretaceous sedimentation in Eastern Desert, Egypt, and evaluation for petroleum prospecting. *Eighth Arab Petroleum Congress.* Algiers, Algiers.

SRIVASTAVA, S. K. (1977) Microspores from the Fredericksburg Group (Albian) of the southern United States. *Paleobiologie Continentale,* 6**,** 1-119.

SRIVASTAVA, S. K. (1978) Cretaceous spore-pollen floras: a global evaluation. *Biofogical Memoirs,* 3**,** 1-130.

SRIVASTAVA, S. K. (1981) Evolution of upper Cretaceous phytogeoprovinces and their pollen flora. *Review of Palaeobotany and Palynology,* 35**,** 155-173.

SRIVASTAVA, S. K. (1984) A new elater-bearing late Albian pollen species from offshore eastern Saudi Arabia. *Botanical Journal of the Linnean Society,* 89**,** 231-238.

STACH, E., MACKOWSKY, M.-T., TEICHMÜLLER, M., TAYLOR, G. H., CHANDRA, D. & TEICHMÜLLER, R. (1975) *Stach's Textbook of Coal Petrology,* Berlin, Gebrüder Borntraeger.

STACH, E., MACKOWSKY, M.-T., TEICHMÜLLER, M., TAYLOR, G. H., CHANDRA, D. & TEICHMÜLLER, R. (1982) *Stach's Textbook of Coal Petrology,* Berlin, Gebrüder Borntraeger.

STAMPFLI, G. M. & BOREL, G. D. (2002) A plate tectonic model for the Paleozoic and Mesozoic constrained by dynamic plate boundaries and restored synthetic oceanic isochrons. *Earth and Planetary Science Letters,* 196**,** 17-33.

STANCLIFFE, R. P. W. (1989) Microforaminiferal linings: their classification, biostratigraphy and paleoecology, with special reference to specimens from British Oxfordian sediments. 35**,** 337-352.

STAPLIN, F. L. (1969) Sedimentary organic matter, organic metamorphism, and oil and gas occurrence. *Bulletin of Canadian Petroleum Geology,* 17**,** 47-66.

STEPHENS, J. F. (1979) Coal as a C-H-O ternary system. *Geochemistry Fuel,* 58**,** 489-494.

STEUERT, D. R. (1912) The chemistry of the oil shales. *Oil Shales of the Lothians.* Memoirs of the Geological Survey of Scotland.

STOCKMARR, J. (1971) Tablets with spores used in absolute pollen analysis. *Pollen et Spores,* 13**,** 616-621.

STOUT, J. D., GOH, K. M. & RAFTER, T. A. (1981) Chemistry and turnover of naturally occuring resistant organic compounds in soil. *Soil Biochemistry,* 5**,** 1-73.

STOVER, L. E. (1963) Some middle Cretaceous palynomorphs from West Africa. *Journal of Micropalaeontology,* 9**,** 85-94.

SUCO (1980) Final report and composite log of the BB 80-1 borehole. *Report.* Cairo, Suez Oil Company.

SULTAN, I. Z. (1986) Palynostratigraphy of the Lower Cretaceous sediments in the Nile Delta region. *Revista Española de Micropaleontología,* 18**,** 55-70.

SULTAN, I. Z. & ALY, S. M. (1986) Palynological zonation of Albian-Cenomanian sediments in the northern part of the Western Desert, Egypt. *Bulletin of the Faculty of Science, Alexandria University,* 26**,** 80-101.

SUMMERHAYES, C. P. (1983) Sedimentation of organic matter in upwelling regimes. IN THIEDE, J. & SUESS, E. (Eds.) *Coastal Upwelling: Its*

Sediments Record Part B: Sedimentary Records of Ancient Coastal Upwelling New York, Plenum Press.

SWEENEY, J. J. & BURNHAM, A. K. (1990) Evaluation of a simple model of vitrinite reflectance based on chemical kinetics. *American Association of Petroleum Geologists Bulletin,* 64**,** 1559-1570.

THUSU, B. & VAN DER EEM, J. G. L. A. (1985) Early Cretaceous (Neocomian-Cenomanian) palynomorphs. *Journal of Micropalaeontology,* 4**,** 131-150.

THUSU, B., VAN DER EEM, J. G. L. A., EL-MEHDAWI, A. & BU-ARGOUB, F. (1988) Jurassic-early Cretaceous palynostratigraphy in north-east Libya. IN EL-ARANUTI, A., OWENS, B. & THUSU, B. (Eds.) *Subsurface Palynostratigraphy of NE Libya.* Benghazi, Garyounis University Publications.

TISSOT, B. & PELET, R. (1981) *Sources and fate of organic matter in ancient sediments*, Oceanologica Acta, Special Issue.

TISSOT, B. P., DEROO, G. & HERBIN, J. P. (1979) Organic matter in Cretaceous sediments of the North Atlantic: contribution to sedimentology and paleogeography. IN TALWIAN, M., HAY, W. & RYAN, W. B. F. (Eds.) *Deep Drilling Results in the Atlantic Ocean: Continental Margins and Paleoenvironment.* the American Geophysical Union.

TISSOT, B. P. & WELTE, D. H. (1978) *Petroleum Formation and Occurrence,* Berlin, Springer.

TISSOT, B. P. & WELTE, D. H. (1984) *Petroleum Formation and Occurrence,* Berlin, Springer-Verlag.

TORRICELLI, S. (2000) Lower Cretaceous dinoflagellate cyst and acritarch stratigraphy of the Cismon APTICORE (Southern Alps, Italy). *Review of Palaeobotany and Palynology,* 108**,** 213-266.

TORRICELLI, S. (2001) Dinoflagellate cyst stratigraphy of the lower Cretaceous Monte Soro Flysch in Sicily (S Italy). *Rivista Italiana di Paleontologia e Stratigrafia,* 107**,** 79-105.

TORRICELLI, S. (2006) Dinoflagellate cyst stratigraphy of the Scisti a Fucoidi Formation (early Cretaceous) from Piobbico, central Italy: calibrated events for the Albian of the Tethyan Realm. *Rivista Italiana di Paleontologia e Stratigrafia,* 112**,** 95-111.

TORRICELLI, S. & AMORE, M. R. (2003) Dinoflagellate cysts and calcareous nannofossils from the upper Cretaceous Saraceno Formation (Calabria, Italy): implications about the history of the Liguride complex. *Rivista Italiana di Paleontologia e Stratigrafia,* 109**,** 499-516.

TRAVERSE, A. (2004) Proposal to conserve the fossil pollen morphogeneric name *Classopollis* against *Corollina* and *Circulina*. *Taxon,* 53**,** 847-848.

TRAVERSE, A. (2007) *Paleopalynology,* Dordrecht, Springer.

TREVISAN, L. (1972) *Dicheiropollis*, a pollen type from lower Cretaceous sediments of Southern Tuscany (Italy). *Pollen et Spores,* 22**,** 85-132.

TREVISAN, L. (1980) Ultrastructure notes and considerations on *Ephedripites, Eucommiidites* and *Monosulcites* pollen grains from Lower Cretaceous sediments of southern Tuscany (Italy). *Pollen et Spores,* 22**,** 85-132.

TROFIMOV, V. S. (1979) Amber concentrates in the shore zones of Recent and ancient seas and oceans. *Lithology and Mineral Resources,* 13**,** 307-313.

TSCHUDY, R. H. (1969) Applied palynology. IN TSCHUDY, R. & SCOTT, R. (Eds.) *Aspects of palynology.* New York, Wiley-Interscience.

TYLER, M. A., COATS, D. W. & ANDERSON, D. M. (1982) Encystment in a dynamic environment: deposition of dinofalgellate cysts by a frontal convergence. *Marine Ecology Progress,* Series 7**,** 163-178.

TYSON, R. V. (1984) Palynofacies investigation of Callovian (Middle Jurassic) sediments from DSDP Site 534, Black-Bahama Basin, Western Central Atlantic. *Marine and Petroleum Geology,* 1**,** 3-13.

TYSON, R. V. (1989) Late Jurassic palynofacies trends, Piper and Kimmeridge Clay Formations, UK onshore and offshore. IN BATTER, D. J. & KEEN, M. C. (Eds.) *Northwest European Microplaeontology and Palynology.* Chichester, British Micropalaeontological Society Series, Ellis Horwood.

TYSON, R. V. (1993) Palynofacies analysis. IN JENKINS, D. G. (Ed.) *Applied Micropaleontology.* Dordrecht, Kluwer.

TYSON, R. V. (1995) Sedimentary Organic Matter: Organic Facies and Palynofacies, London, Chapman & Hall.

UWINS, P. J. R. & BATTEN, D. J. (1988) Early to mid-Cretaceous palynology of north-east Libya. IN EL-ARANUTI, A., OWENS, B. & THUSU, B. (Eds.)

Subsurface Palynostratigraphy of NE Libya. Benghazi, Garyounis University Publications.

VAIL, P. R., MITCHUM, J. R. M. & THOMPSON, S. (1977) Seismic stratigraphy and global changes of sea level, Part 4: Global cycles of relative changes of sea level. *Seismic Stratigraphy - Application to Hdrocarbon Exploration.* American Association of Petroleum Geologists, Memoirs.

VAN DER ZWAN, C. J. (1990) Palynostratigraphy and palynofacies reconstruction of the Upper Jurassic to lowermost Cretaceous of the Draugen Field, offshore mid Norway. *Review of Palaeobotany and Palynology,* 62**,** 157-186.

VAN HOUTEN, F. B., BHATTACHARYA, D. P. & MANSOUR, S. E. I. (1984) Cretaceous Nubia Formation and correlative deposits, eastern Egypt: major regressive-transgressive complex. *Geological Society of America Bulletin,* 95**,** 397-405.

VAN KREVELEN, D. W. (1961) Coal: Typology-Chemistry-Physics-Constitution. Amsterdam, Elsevier Science.

VIANA, C. F. (1968) Correspondencia entre os Ostracodes das serie Cocobeach (Gabao) e Bahia (Brasil). *Boletim Tecnico da PETROBRAS,* 9**,** 367-382.

WALL, D., DALE, B., LOHMANN, G. P. & SMITH, W. K. (1977) The environmental and climatic distribution of dinoflagellate cysts in modern marine sediments from regions in the North and South Atlantic Oceans and adjacent seas. *Marine Micropaleontology,* 2**,** 121-200.

WALPES, D. W. (1985) Geochemistry in petroleum exploration. Boston, International Human Resources Development Corporation.

WARD, J. V. (1986) Early Cretaceous angiosperm pollen from the Cheyenne and Kiowa Formations (Albian) of Kansas, U.S.A. *Palaeontographica Abteilung B,* 202**,** 1-81.

WATSON, J. (1988) The Cheirolepidiaceae. IN BECK, C. B. (Ed.) *Origin and Evolution of Gymnosperms.* Nwe York, Columbia University Press.

WEPCO (1968) Final report and composite log of the Abu Tunis 1x borehole. *Report.* Cairo, Western Desert Operating Petroleum Company.

WEVER, H. E. (2000) Petroleum and source rock characterization based on C7 star plot results: examples from Egypt. *American Association of Petroleum Geologists Bulletin,* 84**,** 1041-1054.

WILKINSON, J. J. (1991) Volatile production during contact metamorphism: the role of organic matter in pelites. *Journal of the Geological Society,* 148**,** 731-736.

WILLIAMS, G. L. (1992) Palynology as a palaeoenvironmental indicator in the Brent Group, northern North Sea. IN MORTON, A. C., HASZELDINE, R. S., GILES, M. R. & BROWN, S. (Eds.) *Geology of the Brent Group.* Geolological Society of London Special Publication.

WILPSHAAR, M. (1995) Direct stratigraphic correlation of the Vercors carbonate platform in SE France with the Barremian stratotype by means of dinoflagellate cysts. *Cretaceous Research,* 16**,** 273-281.

WILSON, L. R. (1959) A method of determining a useful microfossil assemblage for correlation. *Oklahoma Geology Notes.*

WOOD, G. D., GABRIEL, A. M. & LAWSON, J. C. (1996) Palynological techniques, processing and microscopy. IN JANSONIUS, J. & MCGREGOR, D. C. (Eds.) *Palynology: Principles and Applications.* Tulsa, American Association of Stratigraphic Palynologists Foundation.